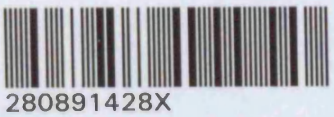

UNIVERSITY OF LONDON THESIS

Degree PhD Year 2006 Name of Author FOLEY, Aidan Eugene

THE USE AND DEVELOPMENT OF SOME GROUNDWATER TRACING TECHNIQUES FOR WELLHEAD PROTECTION: STUDIES FROM THE CORALLIAN LIMESTONE OF YORKSHIRE.

By

Aidan Eugene Foley

Department of Earth Sciences
University College London

2006

A thesis submitted as partial fulfilment of the requirements for the degree of Doctor of Philosophy of the University of London

ProQuest LLC
789 East Eisenhower Parkway
P.O. Box 1346
Ann Arbor, MI 48106-1346

ABSTRACT

The research was driven by questions pertaining to the vulnerability and protection of public water supply wells in fissured and karstic aquifers. The requirement of the industrial and research communities for highly detectable and non-toxic ground water tracers was addressed through the development of Sulphur Hexafluoride (SF_6) for this purpose. This dissolved gas tracer exhibits similar physico-chemical properties to the chlorofluorocarbons (CFCs), and these hydrologic tracers were examined together in their respective capacities as *applied* (i.e. injected) and *environmental* (already present) groundwater tracers. Public water supply wells in the Corallian limestone of Yorkshire, England, were used to test the application of SF_6. A hydrogeological conceptualisation of the system prior to use of the experimental technique was built from the results of geophysical borehole logging, single-borehole dilution tests and forced and non-forced gradient (dye) tracer tests. The novel tracer SF_6 was injected into a karst swallet draining the River Derwent and was tracked for 44 days to a dilution 2×10^8 times smaller than the injected concentration, and still 100 times above background. The SF_6 results enabled specific elements of the conceptual model to be stated theoretically and compared directly with data for the purposes of discriminating between different processes potentially operative within the aquifer. These comparisons included an analysis of breakthrough curve (BTC) tailing as a function of a geohydrological dipole, hydrodynamic dispersion as a function of tracer transport along multiple pathways (fissures and karstic conduits), and the effects of double-porosity diffusion. Paradoxical observations between rates of tracer transport and apparent groundwater ages obtained by applying simple piston-flow models to measured CFC concentrations indicated additional processes within the aquifer. The Corallian CFC survey was supported by a detailed examination of the largest local source of CFC contamination in the area, an operational landfill site situated above the aquifer.

For Mum and Dad

ACKNOWLEDGEMENTS

This work would not have happened at all without the help and guidance of the following people; thank you:

Tim Atkinson, John Barker, Tony Osborne, Sarah Houghton, Yuan Zhao, Celine Ahmed, Ron Dudman, Belinda Hewett, Fergus Willmore, Gerd Cachandt, Danuta Kaminski, Richard Rabe, Jeff Pacey.

And I would also like to thank the following folk for help in the field, with secondary data collection and general assistance:

Sal Watson, Gerd van den Daele, Pat Mottram, Nick Woodman, Simon Quinn, Peter Ring, Martin Ziegler, Katja Zimmerman, Rita Pietschmann, Helen Blyth, Isabel Cardenas (Pio!), Pete Rawson, John Stanbridge, Steve Shipley, Kevin Freer and the Irton crew, Matilda Beatty, Bethany Atkinson, Jenny Morris, Andy Sarney, McCains Ltd., Yorwaste Ltd., Yorkshire Water Services Ltd. and the Environment Agency (York Office).

For help with diagrams:

Jelly and Isabel.

For funding:

The Natural Environment Research Council for their provision of CASE studentship no. NER/S/A/2001/06506; Yorkshire Water Services Ltd. for participating as the industrial partners in the CASE studentship and for providing personnel, workspace and data; and to the Environment Agency, for providing willing assistance, data and additional funding.

Further acknowledgements:

All Crown copyright material is reproduced with the permission of the Controller of HMSO. Ordnance Survey maps are reproduced with permission. The BGS 1:50 000 Solid and Drift Geology map is reproduced with permission and remains Copyright NERC 1998.

TABLE OF CONTENTS

LIST OF FIGURES

LIST OF PLATES

LIST OF TABLES

CHAPTER 1

INTRODUCTION

1.1 BACKGROUND AND DEVELOPMENT OF RESEARCH OBJECTIVES

UK legislation demands that water undertakings supply clean, potable water to consumers, while EU Water Framework Directive (2000/60/EC) legislation requires member states to ensure the ecological health of natural water bodies at the surface. There is no EU Framework Directive specifically for groundwater yet, but this is under development. The requirements that surface waters be of good ecological health, when these are often fed by groundwater, and that water supplies be pure and potable, when about one third of public supplies in England and Wales derive from groundwater, together have led to a situation in which the Environment Agency and water undertakings have a mutual interest in assessing the vulnerability to contamination of groundwaters in general and water abstractions in particular.

Contamination might arise from infiltration of man-made chemicals from diffuse sources, or from point sources. However, the concept of vulnerability is broader than the types of contaminants and the nature of their sources: for aquifers, vulnerability includes the ability of groundwater flow to transport and attenuate contaminants. For specific sources, vulnerability also arises from the peculiar circumstances that exist in the catchment area or recharge zone feeding the abstraction. Certain types of aquifer are known to be particularly vulnerable either because they have low attenuation capacity or because groundwater travels very swiftly within them, or both. Karst aquifers are an outstanding case in point, as solutional development of voids within them leads to channelled groundwater flow that may travel at speeds of kilometres per day, with attenuation produced by local dilution and limited dispersion. However, most previous research on karst aquifers in Britain has focused on upland regions of Carboniferous Limestone that have long been known to be cavernous, whereas very little work has examined manifestly karstic limestone aquifers in lowland settings. There has been comparatively little work on the development and influence of karst features in any of the limestone aquifers that are major sources of water supplies – the Chalk and certain Permian and Jurassic Limestones in England, of which the Corallian Limestone of east Yorkshire is one. This aquifer underlies the lowland area of the Vale of Pickering, and outcrops on the dip slope of the cuesta forming the hills to the north of the Vale. The aquifer is known to be karstic, exhibiting the classic karst features of sinking rivers and large springs, and water tracing tests have demonstrated very rapid

speeds of groundwater flow, suggesting that these features may be linked by solution conduits, or by networks of open fissures.

The Corallian is, moreover, used extensively for water supply. In its eastern part it forms the gathering grounds of water supplies for Scarborough, which are abstracted from a well at Irton (Figure 1.1) which provides a prolific yield, and from two other wells located further to the east (Cayton Carr and Cayton Station Road). The Irton well has been the subject of several previous water tracing investigations and it was established as early as 1909 (Richardson, 1934) that it is fed in part by water from the River Derwent that infiltrates into discrete swallets shortly after it flows from the north onto the Corallian limestone outcrop (allogenic recharge). This situation renders the Irton source particularly vulnerable to accidental contamination from both point and diffuse pollution sources anywhere in the Derwent's 600 km^2 catchment area upstream of the swallets. The results of a series of tracer tests carried out since 1995 by the Environment Agency and RKL Arup Ltd. (on behalf of Yorkshire Water Services Ltd.) have confirmed that water flows in only a few hours from the Derwent swallow-holes to the Irton source and that contaminants might also subsequently remain in the aquifer for a period of weeks at least, possibly longer (ARUP, 2000). Thus, the east Yorkshire Corallian aquifer epitomises the vulnerability of water supplies from lowland karst aquifers, which makes it an ideal case for further study.

One of the aims of the research described in this thesis was to obtain a fuller understanding of the nature of groundwater flow in the east Yorkshire Corallian aquifer, and the vulnerability of the water abstractions within it to contamination, by means of further tracer investigations. Artificial tracers were introduced and their migration studied in groundwater at a very local scale, in single boreholes, and also across the whole area of the Corallian aquifer east of the River Derwent. In addition, man-made chlorofluorocarbon (CFC) compounds were studied as environmental tracers across the whole east Yorkshire aquifer, providing information on groundwater residence times and on local sources of contamination by these compounds. Aspects of the work required the development of novel artificial tracers that could be used to find out how long contaminants might remain at very low levels within parts of the aquifer, and this led to the employment of sulphur hexafluoride (SF_6) as an introduced tracer, the first time it has been successfully used for this purpose in any British aquifer. The results of these investigations, combined with other methods of hydrogeological assessment, enabled previous concepts of groundwater flow and contaminant migration within the East Yorkshire aquifer to be refined, and implications for the vulnerability of the Irton and other wells to be assessed.

In short, the central objectives of the research were:

1) To improve the characterisation of the eastern Corallian in terms of a hydrogeological conceptual model by providing a solid framework of data through the use of established groundwater investigation techniques. These were, in particular, single-borehole dilution tests, tracer tests, geophysical logging and a review of existing work in the area. The objective of improved conceptualisation and strengthening of data was adopted for the purposes of managing the aquifer

in the event of significant pollution, as well as to supplement and interpret the results from CFC measurements and from use of the novel tracer SF_6.

2) To develop a novel tracer methodology using the dissolved gas tracer SF_6. The purpose of developing this method was to provide (for the hydrogeological community) a non-toxic and highly detectable tracer for use in groundwater tracing toward public supply wells. The detectability and low background levels of SF_6 were fundamental in the selection of this tracer as these are the characteristics permitting breakthrough curve tailing to be quantified at lower levels than is possible using more established tracers such as fluorescent dyes. Quantification of extended breakthrough curve tailing permitted the construction and testing of particular analytical models for discriminating between potential processes affecting the observed form of mass transport in the aquifer.

3) To conduct a CFC survey of the eastern Corallian aquifer for the purpose of understanding groundwater age distributions and residence times, and thereby to elucidate flow mechanisms and processes occurring in the aquifer and to identify potentially polluted groundwaters.

4) To further develop the method of characterising landfill impacts on surface and groundwater bodies through the use of CFC analyses. This objective was also considered necessary due to the potential influence that the local landfill site could have had on the CFC survey of the Corallian.

The research was funded predominantly by the UK Natural Environment Research Council (NERC) under their programme of 'Co-operative Awards in Science and Engineering' (CASE). This programme was designed to promote closer relations between academia and industry. Within the field of hydrogeology, closer academic/industrial relations translate into research designed to meet both immediate industrial requirements and the academic research agenda. In this particular instance co-operation was between University College London (UCL) and Yorkshire Water Services Ltd. (YWS). The industrial requirement was investigation into the pollution vulnerability of some YWS-operated water wells, in particular that at Irton, as described above. The academic research agenda included a continuing need within the hydrogeological community for new tracer testing methodologies as well as requirements for understanding the roles of fractures and karst conduits on subsurface mass transport, groundwater vulnerability and wellhead protection in porous media, and a broader understanding of the properties of lowland karst aquifers. Several more specific objectives were defined on the basis of a previous groundwater tracing experiment conducted by Professor T.C. Atkinson of UCL (ARUP, 2000), who was instrumental in setting up and supervising the CASE studentship. In the early part of the studentship a number of lines of inquiry were considered to be potentially rewarding. These included a regional study of the extent of karstic development throughout the Corallian aquifer, the general contaminant transport characteristics of the aquifer, the use of the easternmost part of the aquifer as a natural tracer laboratory for the development of new tracers, and the development of computer programs describing conduit flow within a porous matrix.

In deciding between these possible avenues of investigation it was necessary to consider the resources available at UCL for the conduct of the research. Obviously a framework of understanding of the aquifer could be largely achieved with the help of established and reliable techniques. Moreover, it was also necessary to prove to YWS and the Environment Agency (EA) that it was possible to safely conduct tracer tests using routine methods before attempting anything more ambitious. The Groundwater Tracing Unit (GTU) laboratory at UCL was well-equipped with a Perkin-Elmer Luminescence Spectrometer, so that routine fluorescent dye studies were an obvious choice. In addition, concurrent with the first few months of the CASE studentship (which began in October 2001) was the final part of a UCL project examining the potential for CFCs to be used as indicators of groundwater contaminated by landfill leachate and gases. As this project was drawing to a close, and as the instrumentation (a gas chromatograph with an electron capture detector, or GC-ECD) had been installed in the GTU laboratory, it was decided that some knowledge of the CFC distribution in the Corallian would be useful for understanding groundwater flow and, potentially, the vulnerability of the aquifer to pollution. This approach was also attractive as the GC-ECD is one of the most commonly used analytical instruments employed for the detection of halogenated organic compounds in the environment, many of which are harmful and include pesticides, herbicides and industrial solvents (most halogenated organic compounds are priority controlled (List 1) substances under the European Commission Groundwater Directive 80/68/EEC).

The choice to use the GC-ECD subsequently played a pivotal role in the development of a novel tracer technique as, during the time spent learning how to use the equipment and taking preliminary samples, an investigation into possible new tracer substances found that SF_6 was a legally permitted tracer of leaks within *post-treatment* drinking water distribution systems (UK Drinking Water Inspectorate, 2002). The ARUP (2000) experiment had established that tracer breakthrough curve tailing (measurable persistence) using fluorescent dyes at Irton was severely compromised by both high background levels of natural fluorescence and regulatory limitations on maximum dye concentrations at public water-supply wells (Ward *et al.*, 1998). SF_6, by contrast, has no such toxicity consideration, being almost completely inert at STP, and has a very, very low background concentration in natural waters. Furthermore, SF_6 is widely noted in the oceanographic and groundwater research literature (e.g. Watson and Liddicoat, 1985; Busenberg and Plummer, 1997) as a highly-detectable, atmospherically-derived (already present or environmental) hydrologic tracer. However, it is not widely noted for its use as an introduced (or applied or artificial) groundwater tracer. From this position it was realised that, as the same analytical technique could be applied to both CFCs and to SF_6 (the GC-ECD being sensitive to halogenated compounds), it would be possible to structure tracer-oriented research in the direction of simultaneous analysis of both environmental (naturally present[1] - CFCs) and applied (SF_6) groundwater tracers. This approach was thus adopted to examine groundwater flow and aquifer response to dissolved contaminants in the Corallian limestone.

[1] The term 'natural' does not denote a natural source, as virtually all CFCs are anthropogenic. It simply refers to their largely uniform abundance in the atmosphere and modern atmospherically-equilibrated waters.

Once all of the data had been collected and reviewed it was necessary to discriminate between processes potentially controlling the form of tracer breakthrough curves, and in particular breakthrough curve tailing. These processes ranged from simple advective control over tracer transport distributed among different flowpaths, to dispersion within individual karst conduits and double-porosity diffusion. Part of the research therefore focussed upon the implementation of established and experimental analytical models capable of providing discriminatory power over different conceptualisations of tracer transport in the aquifer. One further necessary consideration was the potential influence on groundwater of the largest local source of CFCs, the Seamer Carr landfill. This also dovetailed well with the only British CFC landfill studies that at the time had been conducted at the University of East Anglia (Bateman, 1998) and at UCL (Atkinson, 2002). Therefore a more localised and detailed survey of the Seamer Carr landfill was undertaken in conjunction with the EA who recognised the potential sensitivity of a CFC-based method (in comparison to standard hydrochemical analyses) for identifying the impacts of landfill-sourced contamination on nearby ground and surface water bodies, and who provided additional funding for this purpose.

1.2 THESIS OUTLINE

From the above discussion regarding the background and objectives of the thesis may be drawn a narrative regarding the development of ideas and circumstances culminating in this thesis. Obviously the choice of instrumentation was important in determining what type of tracer was to be developed, and this choice would not have been made were it not for the prior work on CFCs in groundwater of Bateman (1998) and Atkinson (2002). Furthermore, the existence of a willingness to provide experimental facilities by both YWS and the EA stemmed from an open-mindedness regarding tracer testing that had been inculcated in the Yorkshire area from the time of Chadha (1968). Darminder Chadha was Principal Hydrogeologist in the Environment Agency, and in the Yorkshire Water Authority which preceded it, from 1972 to 2002. He was a key figure in the management of the Corallian aquifer and well placed to encourage workers in the region to follow a tradition of scientific experimentation with respect to putting tracers into the ground, as evidenced by the appetite of several EA and YWS staff for this type of work. Such narrative, based upon the ideas, philosophies and achievements of previous workers, may in fact be traced back to William Smith 'The Father of English Geology' who in the earlier part of the 19th Century spent several years working in and around the Scarborough area, and in particular on the town's water supply from Corallian springs. He even invented a piezometer to gauge how much additional storage had been created in the rocks due to engineering works undertaken at his direction. Details of his work are really peripheral to the main thesis and will not be followed further here, but this brief mention is sufficient to highlight additional strands of narrative present in the background to the thesis. A review of his work, as part of a general history of water supply to Scarborough, is given more fully in Appendix 1.

Returning to the main themes of the thesis, presented in the opening chapters are reviews of the geology and hydrogeology of the Corallian as developed from existing sources (Chapter 2), reviews of the use of CFCs and SF_6 as tracers of various parts of the hydrological cycle (Chapter 3), and a

methods chapter (Chapter 4). Together these chapters reflect the immediate background to the research as described above, namely the circumstances leading to the CASE studentship and the methodological choices made. However, the main results chapters, Chapters 5, 6 and 7, describe the development of a conceptual model of the aquifer starting at the local and leading to the regional scale, that is, as one moves from the review chapters to the results, the narrative grows from one of history to become one of scale. This approach was necessitated by the degree of prior knowledge required to develop interpretations of particular results. Thus, the single-borehole dilution tests and geophysical logging do not require a regional picture in order to be understood, whereas conceptualisations of aquifer processes at intermediate (from tens to a few thousands of metres) and regional or sub-regional (aquifer-wide) scales *do* require that local evidence be accounted for. In this way the results and analyses of local scale experiments and measurements are presented before the intermediate scale, which is presented before the regional scale. This explains why geophysical logging and single borehole dilution tests are presented in Chapter 5, tracer tests in Chapter 6 and CFC results in Chapter 7.

The general principle of the borehole dilution test is to inject a tracer uniformly into a well or borehole and to measure its rate of dilution, which may then be related to the specific discharge of the aquifer at that point. In contrast to the complex injection and analysis of SF_6, the borehole dilution tests were conducted using common salt and a hand-lowered electrical conductivity probe. Such experiments provide very local information on flow characteristics within an aquifer, so that these experiments formed the bottom-end of the scale of experimentation. Several fluorescent dye tracer tests, also simple in comparison to the SF_6 tracer test, further contributed to an understanding of the aquifer that proved essential in constraining a hydrogeological conceptualisation and explaining the form of the SF_6 results at the intermediate scale. Together, the geophysics, the borehole dilution tests and the fluorescent dye and SF_6 tracer tests provide a strong framework within which to interpret the often noisy CFC results, which are presented subsequently and reflect processes occurring on an aquifer-wide basis. The analysis of tracer tests conducted as part of this research also draws heavily upon results obtained from previous tracer testing, particularly that of ARUP (2000). Whilst the Seamer Carr landfill study forms an important aspect of the regional CFC study, being the characterisation of a large contaminant source, it is presented as a stand-alone study in Chapter 8 as it formed the basis of a consultancy report prepared for the Environment Agency.

On the whole, the structure of the thesis reflects a logical progression in the development of knowledge and ideas regarding the hydrogeology of the Corallian, that is to say, a form of scientific narrative that provides a unifying theme throughout the thesis and which ensures that it is more than simply the sum of its individual parts. Nevertheless, an understanding of those individual parts is essential for an appreciation of the narrative, and for understanding what to expect from the thesis, so that these will be described more fully in the following section.

1.3 SYNOPSIS OF CHAPTERS

Following this Introduction, Chapter 2 provides a detailed review of the geology and hydrogeology of the Vale of Pickering as obtained from various existing sources. It begins with a regional perspective examining the main structural elements and controls on sedimentation leading to the deposition of Mesozoic sediments, including the Corallian limestone, in what is now north-eastern England. It continues with a more detailed picture of the limestone itself, focussing on lithological differences within the limestone, and between the limestone and what are now associated aquitards. The review continues with an examination of the geomorphology and climate of the region and then narrows to the hydrology and hydrogeology of the eastern part of the aquifer in which the field experiments were performed. This encompasses description of groundwater catchments, groundwater levels, karst features, hydrochemistry and so on. As there are significant Quaternary deposits in the field area the hydrogeology of these is described toward the end of the chapter. The chapter concludes with a short overview of groundwater protection practices in the eastern Corallian. Chapter 2 is intended to give a broad appreciation of the geology and hydrogeology of the field area as it is presented in the literature, and to provide the background to a thesis that is not just concerned with developing new tracer methods, but to applying existing techniques to improve understanding of the selected field area.

Chapter 3 provides a review of the application of CFCs and SF_6 as hydrological tracers, beginning with an examination of their historical production and chemistry and continuing with an overview of the principles of establishing recharge ages of groundwater with CFCs, i.e. their use as environmental tracers. The chapter continues with an exploration of the applications to which CFCs have been put in hydrology, including groundwater contamination studies, and includes a review of the use of CFCs and SF_6 as *applied* (introduced) groundwater tracers. The chapter finishes with a brief look at environmental legislation governing production of these known ozone-depleting and global-warming compounds.

Chapter 4 describes the methods and techniques adopted in pursuit of the goals of the research. This begins with an overview of the types and locations of experiments conducted during the research and continues with a closer inspection of each type of experiment, detailing materials employed and protocols observed during the experiments and whilst taking and analysing samples. This chapter therefore includes a study of the analytical precision and detection limits of the methods employed. The SF_6 tracer method is described in detail, the description including all relevant information regarding tracer preparation and injection, sampling, sample preparation and GC-ECD operation.

Chapter 5 is the first of three results chapters presented, as described above, in the order that most easily facilitates construction of a conceptual model of the system. Generally speaking this order is largely one of scale, with borehole-specific geophysical logging and borehole dilution test results (Chapter 5) providing information useful in constraining tracer test interpretations on the several-kilometre scale (Chapter 6), which are in turn useful for interpreting wider-aquifer-scale processes reflected in the CFC results from groundwater (Chapter 7). Chapter 5 begins with qualitative

descriptions of the geophysical logs and goes on to extract fissure spacing and aperture data from the logs. This is followed by presentation of the borehole dilution test results, which are again appraised qualitatively prior to being modelled in two different ways to provide information regarding fluxes of groundwater through the aquifer at specific localities. These modelling methods are described in full and compared to one another to draw broader conclusions regarding flow in the aquifer.

Chapter 6 deals with the intermediate scale and covers tracer tests conducted over distances of between 20 metres and several kilometres. In doing so it offers the weightiest set of results and analysis in the thesis, drawing upon both the previous chapter and previous work on the aquifer to develop and test a variety of conceptual models of groundwater flow and mass transport. The chapter begins with a short review of the statistical properties of tracer breakthrough curves before presenting specific results from various tracer tests, describing these both qualitatively and according to the statistical properties reviewed. Following presentation of these results is an initial system conceptualisation and detailing of the empirical evidence for which any model of the easternmost part of the aquifer must account. This is immediately followed by a review of processes potentially affecting tracer transport in the aquifer, such as dispersion, sorption, double-porosity diffusion etc. and an introduction to the methods adopted to discriminate between different processes. The most likely processes are then stated mathematically and compared to the data individually, leading to refinement of the conceptualisation of the aquifer. The chapter concludes with a discussion of the relationship between well performance and tracer behaviour.

Chapter 7 presents and discusses the results from the CFC survey of the eastern Corallian and also the River Derwent. Supporting measurements are reported, as are problems regarding CFC contamination of the analytical equipment. Different methods of interpreting the CFC data are presented and the most suitable models of interpretation (e.g. piston-flow versus mixing models) discussed. Non-conservative processes affecting CFC tracer concentrations are evaluated on the basis of the evidence and the chapter concludes with some further discussion of CFC apparent ages and the degree of mixing of different-aged waters likely to be occurring in the aquifer. Chapter 7 also sets the scene for the following chapter, the CFC survey of Seamer Carr landfill.

Chapter 8, as mentioned, is presented as a stand-alone piece of work due to its funding as a consultancy project for the EA and its consequent prior existence as a report. The chapter begins with a review of previous work performed at Seamer Carr and continues with a site description covering topography, hydrology, geology and hydrogeology. The sampling locations are presented followed by the results of the CFC survey and supporting measurements, all of which encompass the major surface waters on or near the site as well as groundwater, leachate and landfill gas measurements. The findings are summarised in terms of a renewed conceptualisation of the interaction between the landfill, the subsurface (superficial deposits, aquitards and the Corallian) and nearby water bodies. The implication of these findings for continued work on the site, and the broader implications of the study in terms of the use of the CFC method to characterise landfills, are discussed toward the end of the chapter.

Chapter 9 is the concluding chapter of the thesis and summarises the main findings of the research. In concluding, the main findings are discussed with relevance to the objectives of the research, as outlined above, and are separated into a number of categories in which this thesis contributes to the advancement of hydrogeological research.

CHAPTER TWO

THE GEOLOGY AND HYDROGEOLOGY OF THE VALE OF PICKERING

"(Kirkdale Cave)...formed at the junction of the Chemnitzia limestones with the more earthy limestones above[2]; the upper surface of the Chemnitzia – limestones throughout this region is very hummocky, and is known to the quarrymen of Pickering and Hutton by the name of 'hilly and holey'; on this irregular surface repose the more earthy limestones above with soft marly partings, which are easily worked away, and form a series of hollows that is the cave line throughout the district. It is at this horizon in the limestone that the numerous 'swallows' or underground channels are formed, in which most of the streams of the neighbourhood lose a part or all of their water; and if the denudation of these valleys was carried 100 ft lower, it is probable that a fine series of caves would be exposed in the region."

Fox-Strangways (1892)
The Jurassic rocks of Britain, Vol.1: Yorkshire

2.1 INTRODUCTION

Much of the following account of the geology and hydrogeology of the Vale of Pickering, with particular respect to the Corallian limestone, is derived from the Institute of Geological Sciences regional guide to eastern England (IGS, 1980), the Eastern and Central England edition of the series 'Geomorphology of the British Isles' (Straw and Clayton, 1979) and Harrison's 1973 Ph.D. thesis 'The hydrogeology of the Vale of Pickering' (Harrison, 1973). Additional material regarding the hydrogeology of the eastern part of the Vale of Pickering is taken from Chadha's 1968 M.Sc. thesis and a number of unpublished reports held by Yorkshire Water Services Ltd. (formerly the Yorkshire Water Authority) and the Environment Agency (formerly the National Rivers Authority). There are virtually no published works relating specifically to the hydrogeology of the Vale of Pickering, Tate *et al.* (1969), Reeves *et al.* (1978) and Carey and Chadha (1998) being, to the author's knowledge, the

[2] At the junction of the upper oolites and the Coral Rag, see below.

only exceptions. The Solid and Drift Geology map (Sheet 54, 1:50 000, Scarborough, BGS (1998)) has been much relied upon.

By way of background to the rest of the thesis, this chapter begins with a discussion of the regional geology and general structure, narrows in focus to more local features, and continues by highlighting those factors exerting greatest control over the present day hydrogeology.

2.2 THE GEOLOGY OF THE VALE OF PICKERING AND THE CORALLIAN LIMESTONE

2.2.1 REGIONAL GEOLOGY

The region may be discussed in some holistic sense by first identifying a sensible boundary, as has been done in Figure 2.1. This boundary roughly corresponds, at least in the north and the west, to outcrops of nothing older than Triassic rocks. This is satisfactory insofar as the rocks of prime consideration herein are of a younger age, and therefore fall within the boundary. However, the arbitrariness of such a procedure is clear if one considers that both rocks and earth movements of preceding Periods play central roles in determining later depositional history (the Mesozoic being confined almost exclusively to sedimentary rocks). With this in mind, the regional geology may now be discussed in terms of controlling structural elements, in particular the 'block and trough' development caused by epeirogenic movements in the Lower Carboniferous (Figure 2.2). The blocks and troughs of greatest importance to the region defined are:

1) The Market Weighton Block
2) The East Midlands Shelf
3) The Cleveland Basin

The Market Weighton Block is considered to be the northernmost part of the East Midlands Shelf (IGS, 1980). However, the distinction is necessary as the block (some 20 km from north to south) has displayed considerably greater stability than the shelf itself (and more still than the Cleveland Basin), since at least the Upper Triassic. This is important because the stability of the block, relative to episodic subsidence and uplift of the other two elements, is the controlling influence on the thickness and nature of Jurassic deposition, including that of the Corallian, as one moves from south to north. South of the block, subsidence over the East Midlands Shelf was more uniform and shallower than it was within the Cleveland Basin. The transition from the Market Weighton Block to the Cleveland Basin is much steeper than that from the Block to the Shelf, as can be seen in Figure 2.3, and is marked by considerable faulting (the Howardian Hills Fault Belt). Nonetheless, it is necessary to emphasise the similarity in situation, as this illustrates the relationship between the Corallian (north of block) and Lincolnshire (south of block) limestones. The hydrogeology of the latter has received much greater attention than that of the former, but is in several respects analogous.

The Cleveland Basin underwent subsidence during the Lower Carboniferous and the Jurassic, but was uplifted toward the end of the Carboniferous, and inverted (in stages) in the Upper Cretaceous (IGS, 1980). This inversion imparted a major east-west trending anticline (the Cleveland anticline, Fig 2.2), with several secondary dome features (e.g. the Robin Hood's Bay and Lockton domes), which now form the North Yorkshire Moors. The basin was not completely inverted, however, and retains its synclinal (if faulted) structure beneath the Vale of Pickering.

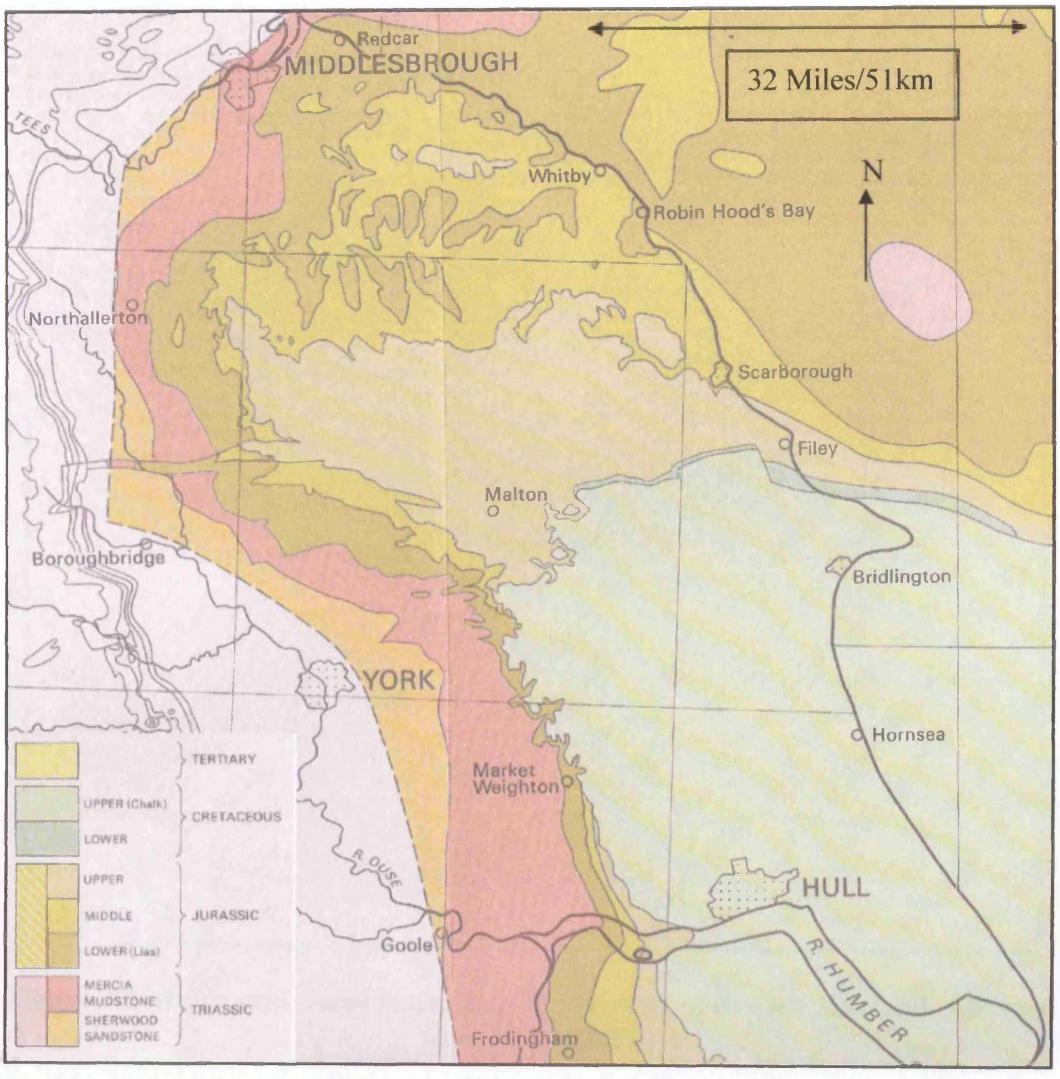

Figure 2.1 Solid geology of eastern North Yorkshire, including offshore Only Triassic rocks and younger are shown in colour. After IGS (1980). Crown copyright, reproduced with permission.

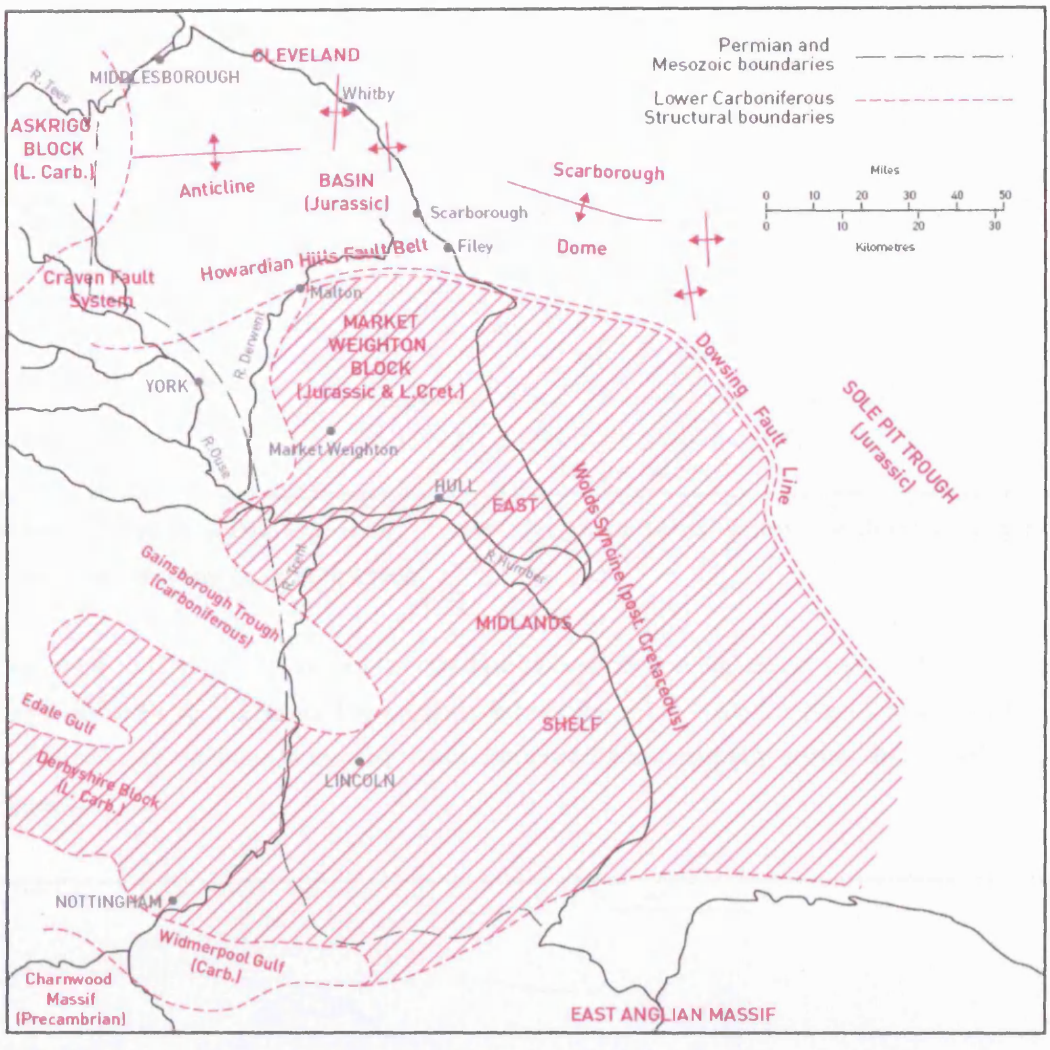

Figure 2.2 Major structural features of the geology of eastern England. Adapted from IGS (1980).

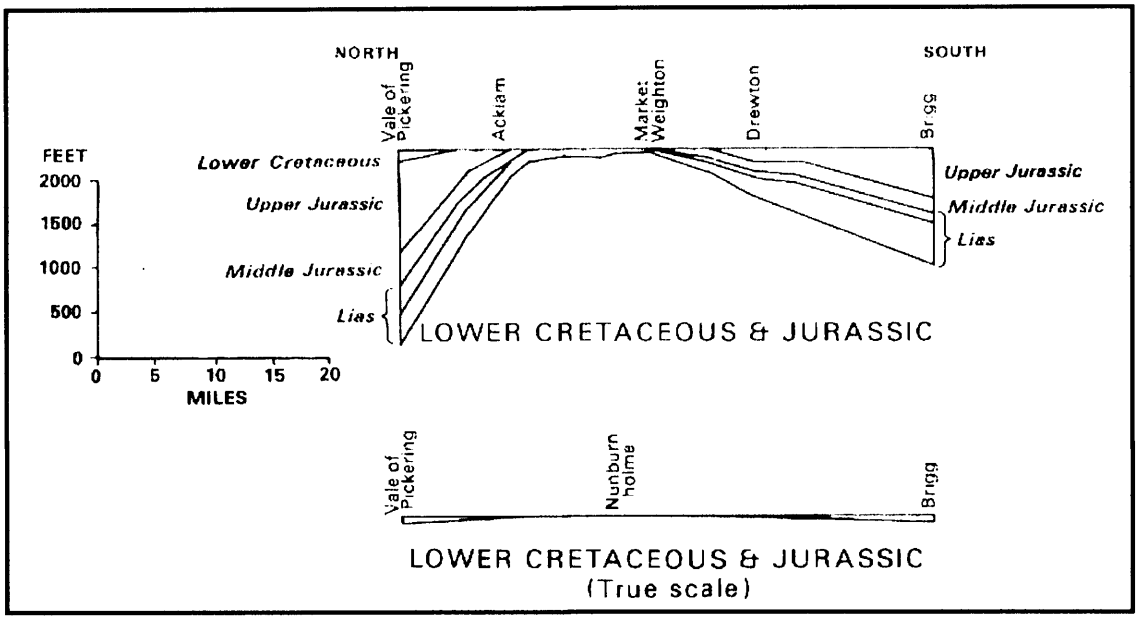

Figure 2.3 Cross-section across the Market Weighton block during the Jurassic and Lower Cretaceous (adapted from IGS, 1980).

It should be added that the three elements listed above form a significant part of the south-eastern margin of the North Sea Basin. The extensive subsidence of this basin has played an important role in the formation of north-south trending faults that intersect and partially control the modern coastline (Figure 2.4).

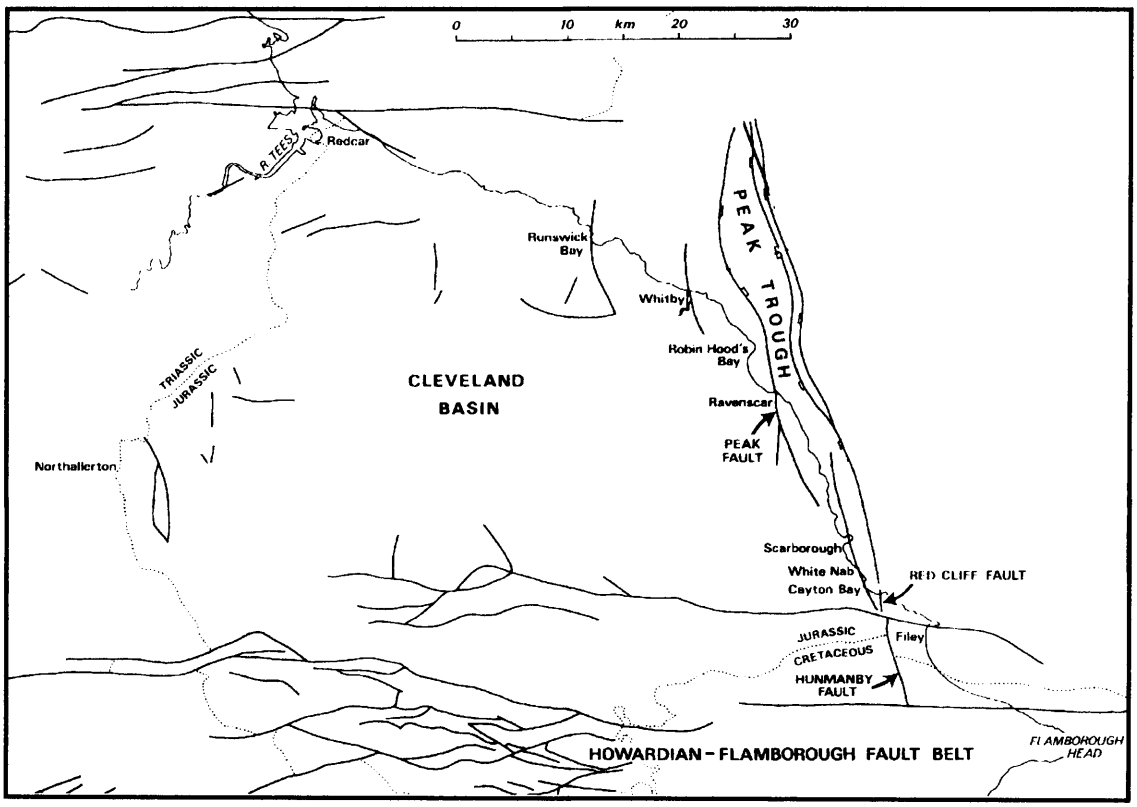

Figure 2.4 Major fault systems extending through the Jurassic in the Cleveland Basin (adapted from Milsom and Rawson, 1989).

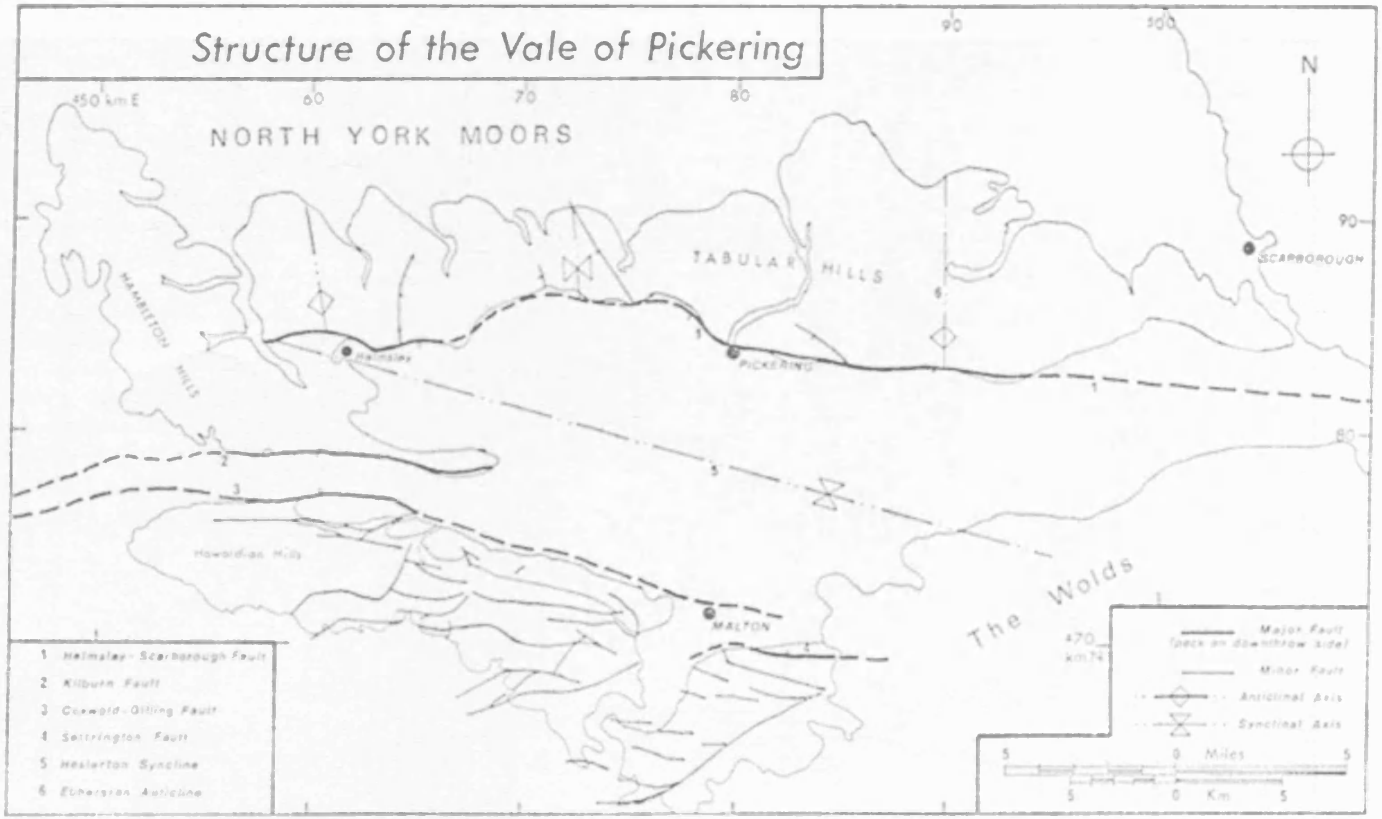

Figure 2.5 Structure of the Vale of Pickering (adapted from Harrison, 1973).

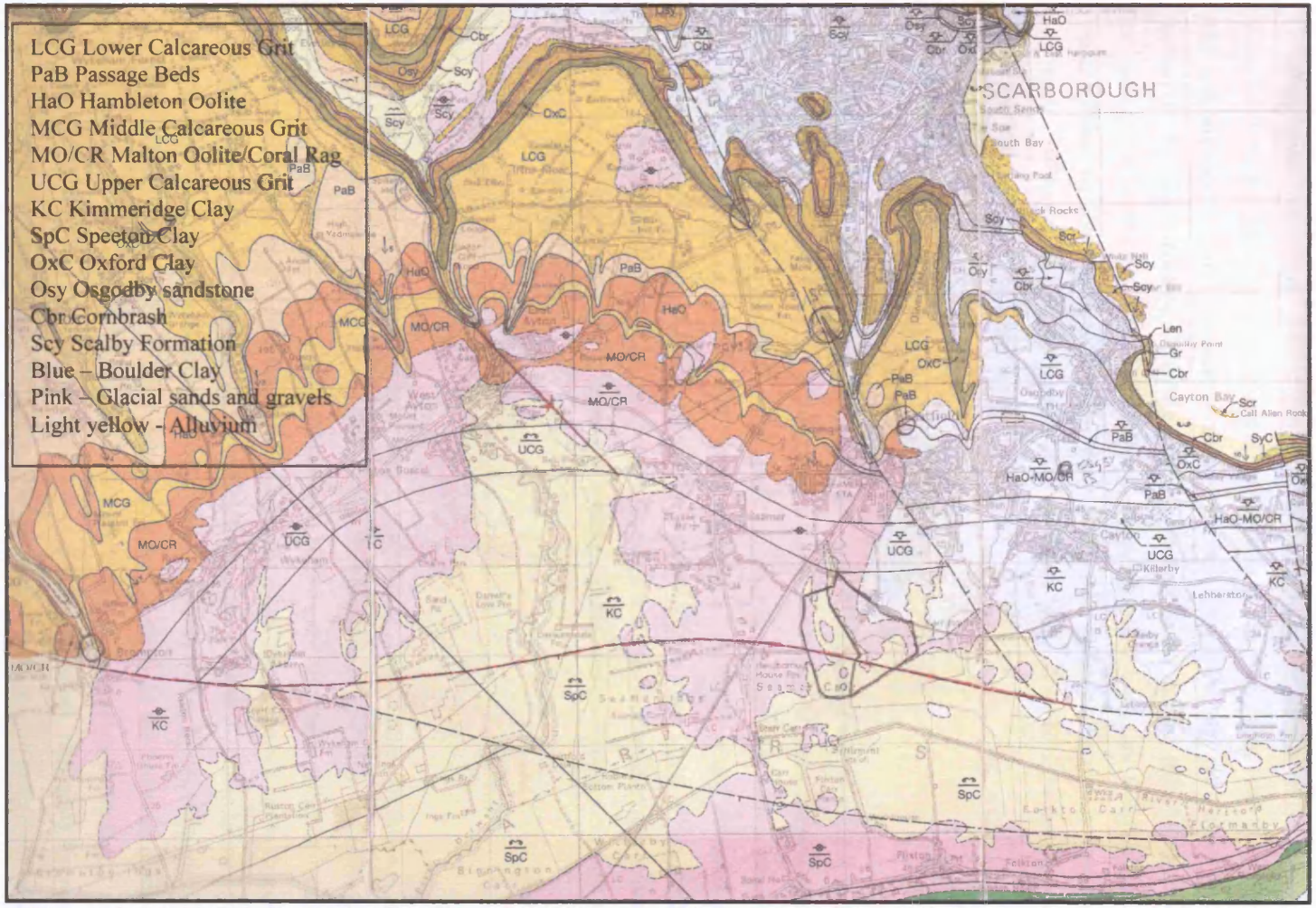

Figure 2.6 1:50 000 Geological (Solid and Drift) map of the eastern Vale of Pickering. Part of Sheet 54 (BGS, 1998). Copyright NERC, reproduced with permission. Grid squares 1 km, orientation north.

2.2.2 STRUCTURE, FOLDING, FAULTING AND JOINTING.

2.2.2.1 Outline of structure

The axial trace of the syncline dominating the Vale of Pickering extends east-south-east from Helmsley to the coast (Figure 2.5). It is bounded to the north by the Tabular Hills (the northern limb), to the south by the Yorkshire Wolds, and the south-west by the Howardian Hills (the southern limb). The syncline closes to the west-north-west in the Hambleton Hills, and the Vale is blocked at its eastern end by glacial moraine. Generally speaking, the beds in the Tabular Hills (north) dip south, and the beds in the south (and beneath the Wolds), dip north. The Yorkshire Wolds are comprised of Upper Cretaceous Chalk that lies unconformably on the older sediments beneath it. This unconformity is a result of a major marine transgression over the entire area, where hitherto the Market Weighton Block had been at or just below sea-level.

2.2.2.2 Folding

As mentioned above, the late Cretaceous inversion of the Cleveland Basin took place in stages. The resultant differential doming produced non-uniform dip and strike of the rocks comprising the Tabular Hills. Minor folding is thus evident, and in particular there are minor folds with north-south axes at Ebberston (the Ebberston Anticline) and Sinnington (Figure 2.5). Of these, the Ebberston anticline is sufficiently strongly folded to abut Oxford Clay against Kimmeridge Clay, at the junction of the Helmsley-Filey fault (see Figure 2.6 and below). The dips in the area of interest (the northern limb of the syncline) are between 1.5° and 5° and predominantly to the south and south-east, from the Tabular Hills to the Vale of Pickering.

2.2.2.3 Faulting

The faults are central to an understanding of the hydrogeology. They control, for instance, spring lines at the southern boundary of the Tabular Hills (along the Helmsley-Filey Fault). Collectively, the faults marking the boundary of the Cleveland basin and the Market Weighton Block are known as the Howardian Hills fault belt. These are responsible for the small graben, known as the Coxwold-Gilling Gap, which separates the Hambleton from the Howardian Hills (Figure 2.7). The latter are extensively faulted and broken up into much smaller blocks than the corresponding (more northerly) Tabular and Hambleton Hills. The fault of greatest significance to this study is the Helmsley-Filey fault, also known as the Ebberston-Filey fault, which is considered to be the most northerly fault of the Howardian Hills fault belt. This normal fault, thrown down to the south, runs along the southern edge of the Tabular Hills until reaching Brompton, whereupon it cuts across the eastern end of the Vale to Filey (Figure 2.6). Along much of its length it brings the Corallian of the Tabular Hills into contact with the Kimmeridge Clay. Its throw increases toward the east, and as it approaches the coast is understood to be intersected by a series of north-north-west to south-south-east trending normal faults

(with minor transcurrent movement) representing the easternmost expression of North Sea Basin subsidence in the area (Figures 2.4 and 2.6).

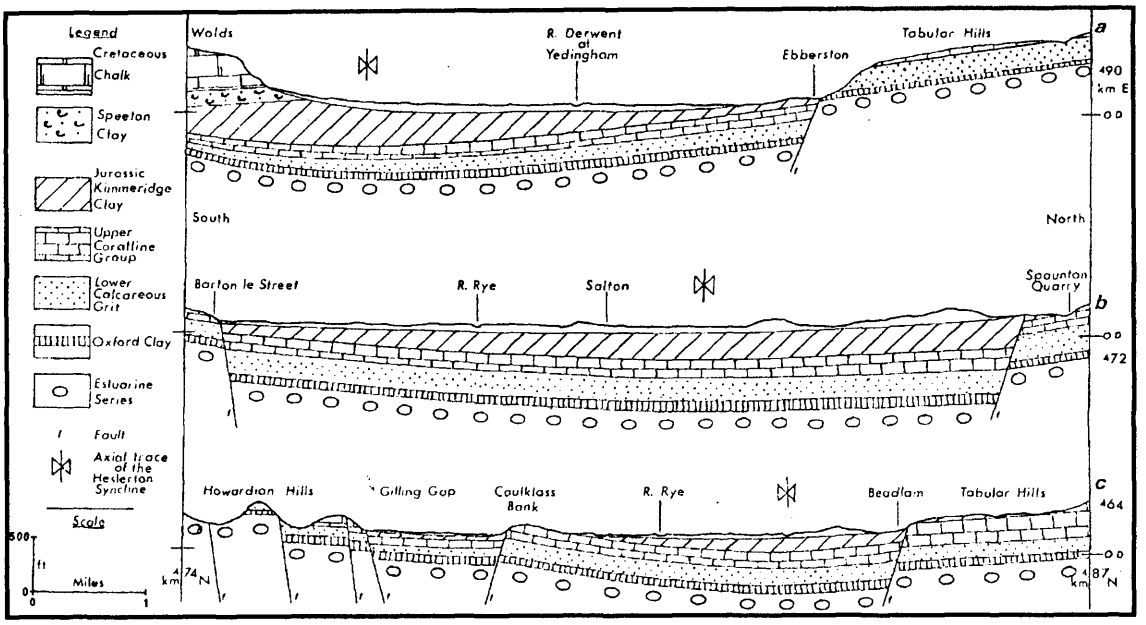

Figure 2.7 Successive sections across the Vale of Pickering, reproduced from Harrison (1973). Note that the topmost section is in the east, moving successively west (Eastings given on right-hand side of diagram).

2.2.2.4 Jointing

Harrison (1973) identifies four types of jointing within the Corallian in the Tabular Hills, stating that much of it is strongly dependent upon the minor folding present, and that although the joint pattern may not be universal throughout the Corallian, the joints are systematic with respect to the fold axes. His rose diagram is reproduced below to illustrate the point (Figure 2.8). The four types are:

1. Release joints parallel to the land surface, caused by erosion of overburden
2. Cross joints (ac joints)
3. Longitudinal joints (bc joints)
4. Oblique (shear) joints

(Please note that the terms ac and bc are standard structural geology reporting terms (e.g. Park, 1982)).

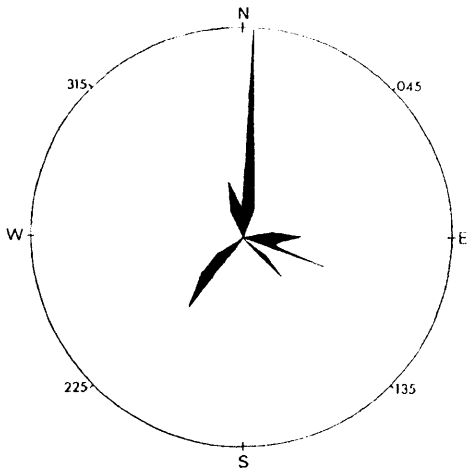

Figure 2.8 Orientation of joints in the Tabular Hills (after Harrison, 1973). Unknown number of measurements.

From the rose diagram it may be seen that the major joints lie parallel to the predominant axes of folding (north-south) in the Tabular Hills. These longitudinal joints range in direction between 330° to 016° and are supplemented by cross joints, trending between 85° and 105°, which lie parallel to the dip of the limbs of the minor folds. There are two sets of oblique (or shear) joints trending at 45° to the primary joint sets, at 135° to 140° and at c. 225°.

There is no reported data on the spacing of joint sets in any of the literature reviewed, although observations at outcrop indicate that joint frequency is highly variable, ranging from intensely fractured individual beds (joint spacings of a few centimetres), through spacing on the meter scale, up to spacing occurring over hundreds of meters (see Plates 2.1 to 2.4). Judging from the geological map (Figure 2.6) major joints seem to repeat on a 500 – 750 m interval. This is on the basis that minor dry valleys across the outcrop have both this spacing and are oriented in the same directions as major, obvious, and mapped joints. For example the north-easternmost cuesta shown on Figure 2.6 is clearly fault controlled. Furthermore, it runs parallel with the north-eastern facing cuesta north of Forge Valley. Following this series westward, at about a similar spacing we encounter Bee Dale, the most developed dale in Wykeham Forest, and at a little greater than equal spacing westward again, we have Brompton Dale. Between these more significant features are smaller dales, parallel to one another until Forge Valley, where the orientation changes. The orientation of the dry valleys on Irton Moor appears to be largely perpendicular to the north-eastern cuesta, whereas on Wykeham Moor they are parallel to it. The spacing of the minor dry valleys on the southern side of Irton Moor is about 500 m. On Wykeham Moor this has expanded to 750 m. The regularity of this spacing and orientation is likely to be due to the joint structure in the underlying Corallian. Larger joints presumably also control the north-west facing section of the cuesta.

Plate 2.1 (top left) A major vertical (longitudinal) joint (a single joint in 200m of exposure) and associated intense fracturing of adjacent beds, Hambleton Oolite, Wykeham Quarry (SE 960 844).

Plate 2.2 (top right) Hambleton Oolite showing fracturing on the scale of several centimeters.

Plate 2.3 (bottom) Malton Oolite at Brompton Springs exhibiting vertical joint spacing on the sub-metre scale (lighter-coloured bed in centre of photo c. 80 cm thick).

Plate 2.4 The Malton Oolite in Forge Valley.

The release joints to which Harrison refers are typically along bedding plane partings and create those fissures through which groundwater flow predominantly occurs (see Section 2.3 and results chapters). The spacing of these joints measured as part of this research is about 1.5 m in the oolitic limestones and 3 m in the calcareous grit members of the Corallian (following section and Chapter 6). Although the spacing of smaller joint sets is unknown, this approach indicates that the scales of fissuring in the aquifer are different on vertical and horizontal scales, however, this aspect of the research has not been followed more closely than this.

2.2.3 THE CORALLIAN GROUP

2.2.3.1 Introduction to the Corallian Group

In the Lower and Middle Jurassic the Cleveland basin had received much deltaic and freshwater sediment (a paralic basin). By the Upper Jurassic this pattern had changed to one of predominantly marine (albeit shallow) deposition, with continuing subsidence (IGS, 1980). It was in this environment that the three formations of the Corallian were formed; the Lower Calcareous Grit, the Coralline Oolite, and the Upper Calcareous Grit. As these show significant lateral variability and thickness (Figure 2.9), and as they are central to this thesis, they will be described in more detail. A generalised section, covering the entire Yorkshire Corallian, is given by Harrison (1973):

Formation	Member	Thickness
Upper Calcareous Grit		9 – 24 m
Coralline Oolite	Malton Oolite	15 – 27 m
	Middle Calcareous Grit	0 – 24 m
	Hambleton Oolite	0 – 36 m
Lower Calcareous Grit		21 – 61 m

Table 2.1 Idealised section of Corallian Group

And at Irton, the public water supply well of greatest importance to the people of Scarborough, the section is as follows:

Formation	Member	Thickness
Drift		*15.8 m*
Kimmeridge Clay		*13.1 m*
Upper Calcareous Grit		11.3 m
Coralline Oolite	Coral Rag	6.1 m
	Malton Oolite	16.6 m
	Middle Calcareous Grit	0.3 m
	Hambleton Oolite	22.2 m
	Passage Beds	4.1 m
Lower Calcareous Grit		35.1 m
Oxford Clay		*c. 48m*
	Total thickness of Corallian:	**95.7 m**

Table 2.2. Irton borehole section (New Well) after Wilson (1930-31) (Cited in Tate, Robertson and Gray, 1970).

Briefly, before further description, it should be noted that because of lateral facies variations and attempts to correlate the Yorkshire Jurassic with that of the Jurassic in other parts of the country, there has been a great deal of shifting in the nomenclature and division of the group. For this thesis the BGS divisions of 1998, as given on the 1:50 000 map of the Solid and Drift Geology (Sheet 54, Scarborough, BGS 1998), have been used. IGS (1980) details the divisions as presented by previous workers.

2.2.3.2 The Lower Calcareous Grit Formation

The Lower Calcareous Grit exhibits a gradual transition from the muds of the Oxford Clay to a 'thickly bedded hard buff grit with a siliceous cement', grading into a 'hard grey siliceous grit' and further into a 'very ferruginous sandstone containing large gritty fossiliferous limestone doggers' (all quotes from

IGS, 1980). The grit is described by Harrison (1973) as a 'fairly massively bedded (1-2 m beds) grey calcarenite but with bands of purer limestone or sandstone interspersed'. From these descriptions it can be seen that the formation is neither a true grit nor a true limestone, but overall a fine-grained calcareous sandstone (IGS, 1980). In hand-specimen the rock is 'composed of sand grains (<2 mm in diameter) in a calcareous cement but with numerous ooliths and intraclasts together with *Rhaxella* spicules up to 4 mm in length' (Ibid.).

2.2.3.3 The Coralline Oolite Formation

The Coralline Oolite Formation is quite variable throughout the extent of the Corallian Group. Because of this some of the thinner or less extensive members do not appear in Table 2.1, the generalised section. These include the Passage Beds (calcareous sandstones, shelly limestones and thin-bedded sandy limestones, just above the Lower Calcareous Grit), the Birdsall Calcareous Grit (buff calcareous sandstone grading into the Middle Calcareous Grit) and the Coral Rag (coral beds sitting atop the Malton Oolite). On the coast and in the Tabular Hills, the Malton (upper) and Hambleton (lower) Oolite members are clearly separated by the Middle Calcareous Grit, although this member is sometimes thin (e.g. only 30 cm thick in the Irton old well) or not present. The full thickness of 24 m given in Table 2.1 represents the combination of the Middle and Birdsall Calcareous Grits that occurs in the west.

The Hambleton Oolite is a cream-grey oolitic limestone exhibiting large variations in lithology and fauna (IGS, 1980). It is thin to thick bedded, but not as fossiliferous as overlying beds. It contains a high proportion of silica derived from *Rhaxella* spicules and occasional coral masses, which contributes to its relative hardness and persistence. The Hambleton Oolite typically grades into the Middle Calcareous Grit and thence into the Malton Oolite, which is the most persistent member of the Coralline Oolite Formation (Ibid.). The Malton Oolite is thick to massively bedded and may be up to 25 m thick (e.g. at Cayton Carr). This member is more uniformly oolitic than the Hambleton Oolite and represents the peak of oolith production in the area (Ibid.). The Malton Oolite at Pickering is described in thin-section by Harrison (1973), who notes that ooliths are typically 0.1 – 1.0 mm in diameter and that there is an abundance of fossil fragments up to 5mm in length. He goes on to say that interstices between ooliths and shell fragments are filled with recrystallised pseudospar that 'leaves the Oolite with a very low intrinsic permeability' (Ibid.). In places the Coral Rag forms the top of the Malton Oolite and is notable for its exceptionally fossiliferous nature. It consists of reef limestones and reef detritus (IGS, 1980), which in Forge Valley achieve 7 m in thickness.

2.2.3.4 The Upper Calcareous Grit Formation

The uppermost formation of the Coralline Group is the Upper Calcareous Grit. It is a fine grained sandstone grading to calcareous mudstones and limestones that may reach 17 m in thickness. It is 11.3 m thick in the Irton borehole, but does not crop out on the eastern Tabular Hills having been largely removed by erosion.

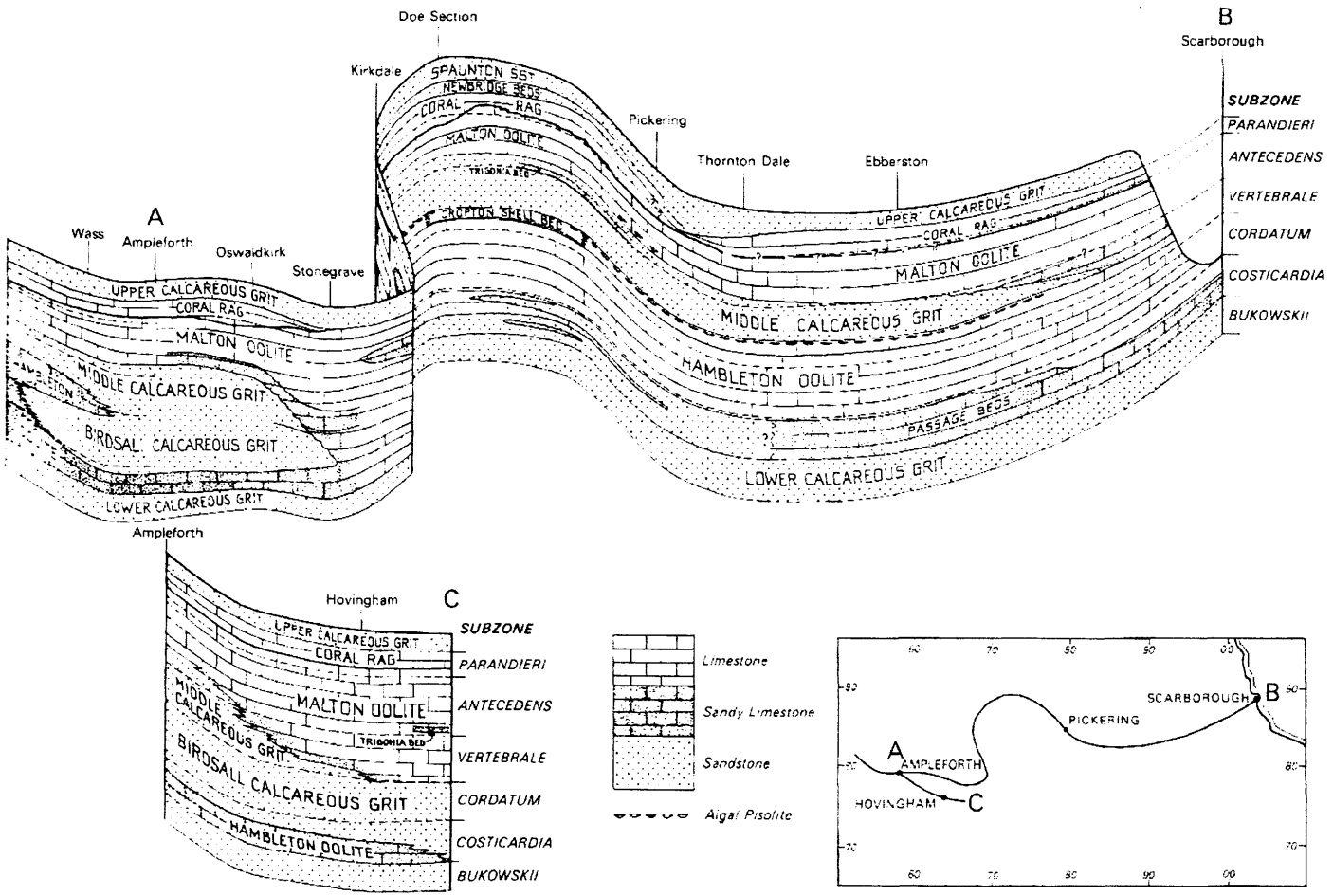

Figure 2.9 Corallian Ribbon diagram after IGS (1980). Crown copyright, reproduced with permission.

2.2.4 THE OXFORD AND KIMMERIDGE CLAYS

The Oxford and Kimmeridge clays are grouped together here as they are the major aquitards associated with the hydrogeology of the Corallian, representing its lower and upper boundaries respectively.

2.2.4.1 The Oxford Clay

The Oxford Clay, a grey-green mudstone immediately beneath the Corallian, exhibits cyclic deposition of shell beds and fine mud and a gradual transition to the Lower Calcareous Grit in its upper part (IGS, 1980). It varies in thickness between 36 and 76 m, but is 48 m thick in Irton Observation Borehole 7 (OBH7) on Irton Moor, (European Geophysical Services, 2002). Harrison (1973) notes that it contains some sandy shale beds permeable enough to transmit water, although as these layers are thin and horizontal the formation acts as an aquitard. The formation crops out beneath the Corallian on the escarpment and in the upper reaches of Forge Valley, as well as at Ebberston where it is exposed by the throw of the Ebberston-Filey fault.

2.2.4.2 The Kimmeridge Clay

The Kimmeridge clay exhibits its full thickness of over 400 m in the Vale of Pickering to the south of the Ebberston-Filey fault. To the north of the fault, however, it has been substantially eroded so that, in the Irton New Well it is only 13m thick and, within one kilometre north of Irton, thins to nothing. In substance it comprises of

> "...small scale rhythms each 0.3 to 2.5 m thick, consisting of soft mudstones, shelly mudstones, calcareous mudstones and relatively rare thin argillaceous limestones or lines of cementstone nodules. Oil shales of varying richness occur at many horizons."
>
> IGS (1980) pg. 76.

The presence of the blue-grey Kimmeridge marks the difference between the unconfined (northern) and confined (southern) parts of the Corallian (except where the division is marked by boulder clay in the east).

2.2.5 GEOMORPHOLOGY

The solid geology plays a defining role in the geomorphology and topography of the region, in that it provides the landscape upon which geomorphic agents operate. Elements of the solid geology such as, for example, the elevation of the Corallian scarp, the position of folds and structural weaknesses throughout the outcrop area, major fault lines and the differences in mechanical strength between the limestones and the mudstones (in particular the Kimmeridge Clay), are all factors influencing the modern landscape of the Vale of Pickering. However, as comprehensive geomorphological description of the Tabular, Hambleton and Howardian Hills, the Vale of Pickering and the northern Yorkshire

Wolds is highly complex (and in parts controversial), it is beyond the scope of this thesis. Therefore, the following account will incorporate an overview of the regional situation into an examination of those elements considered most relevant to the hydrogeological context. These elements are, chiefly, the glacial emplacement of boulder clays and other glacial drift features (e.g. outwash fans and kame terraces), and the incision of glacial meltwater through the Corallian cuesta to form Lake Pickering and its associated alluvial deposits.

The glacial features referred to above are connected exclusively to the last glaciation, the little evidence remaining from earlier glacial stages being confined to "...a few small outcrops of till, sand and gravel..." (p. 119 IGS, 1980) in the western Vale of Pickering and some erratics on the moors. Interglacial sea levels are considered to have caused planation of the Tabular hills, which is still evident on the highest parts of Irton Moor (Figure 1.1) as well as further to the west (Straw and Clayton, 1979). However, in the Scarborough area, two main Devensian stages are identifiable.

During the first of these an ice sheet, extending down the east coast, came inland along the Vale of Pickering and emplaced a kame terrace at Wykeham (see Figures 2.11 and 2.12). This kame terrace is taken to represent the maximum extent of the ice at this time. During this 'Wykeham' stage the ice did not overrun the Corallian high ground, but did block drainage of the Esk Valley to the north, leading to the creation (by ice-damming) of a pro-glacial Lake Esk, and subsequently a pro-glacial Lake Hackness. It was these that led eventually to the overtopping and formation of meltwater channels through the Corallian escarpment.

Forge Valley, (Figures 2.6, 1.1, 2.11 & 2.12) was not the only point at which the Corallian escarpment was breached by glacially dammed meltwaters to the north. Only 6 km to the east, just prior to the coast, a northward jutting salient of the escarpment (Oliver's Mount, Figures 2.6 & 1.1) was formed between a subglacial meltwater channel (on the west side) and a 'direct' meltwater channel on the east (Straw and Clayton, 1979). This channel was not such an important discharge route as Forge Valley, but was instrumental in depositing some of the material which was later to underlie Seamer Carr landfill (Chapter 8). A further channel (now Newtondale) was cut north of Pickering which now stands on the resultant depositional fan, but as the study area does not extend so far west, it will not be considered further. Forge Valley, however, due to its hydrogeological importance (to follow) deserves greater consideration.

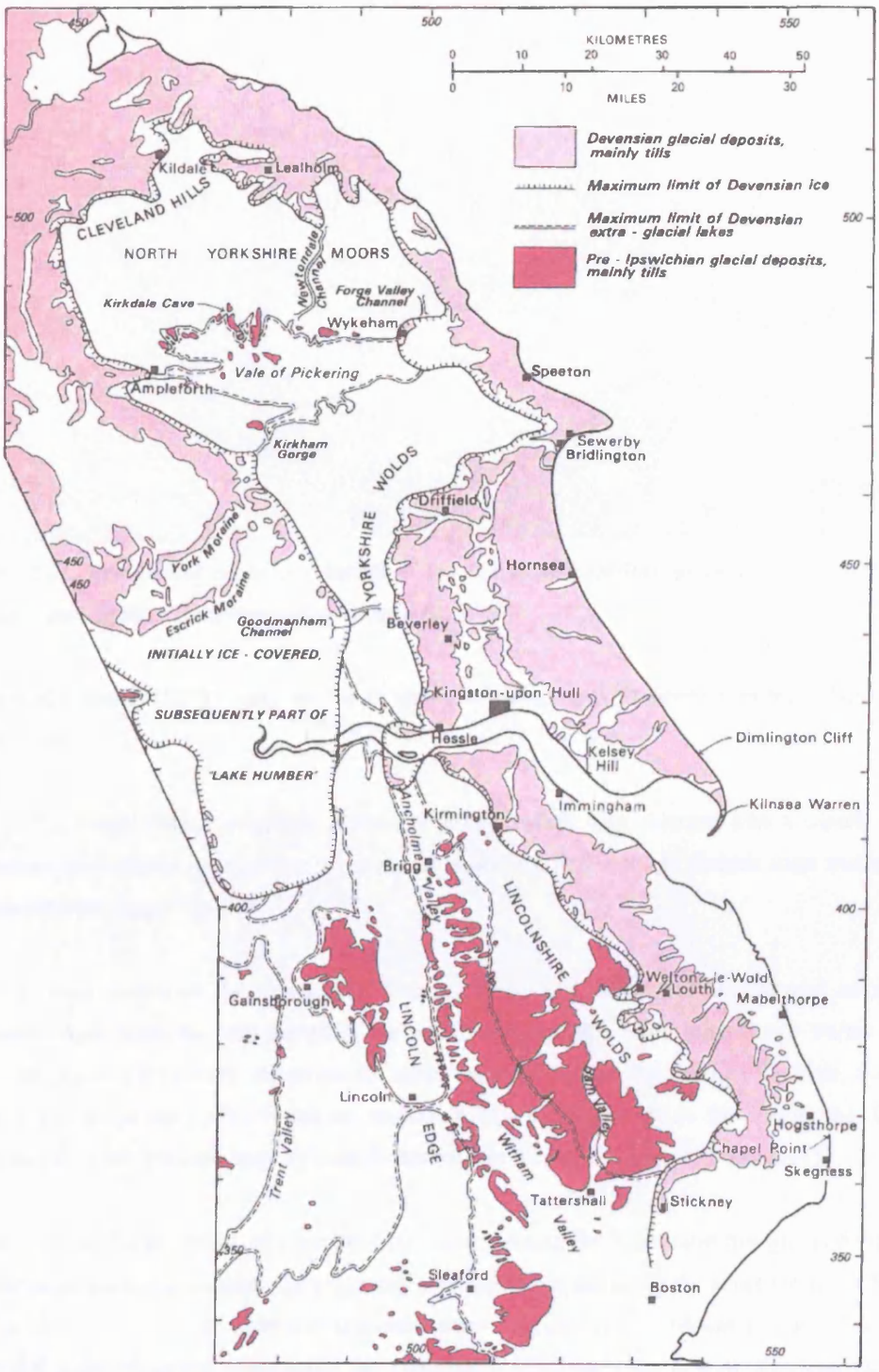

Figure 2.10 Regional Geomorphology of north-eastern England. After IGS (1980). Crown copyright, reproduced with permission.

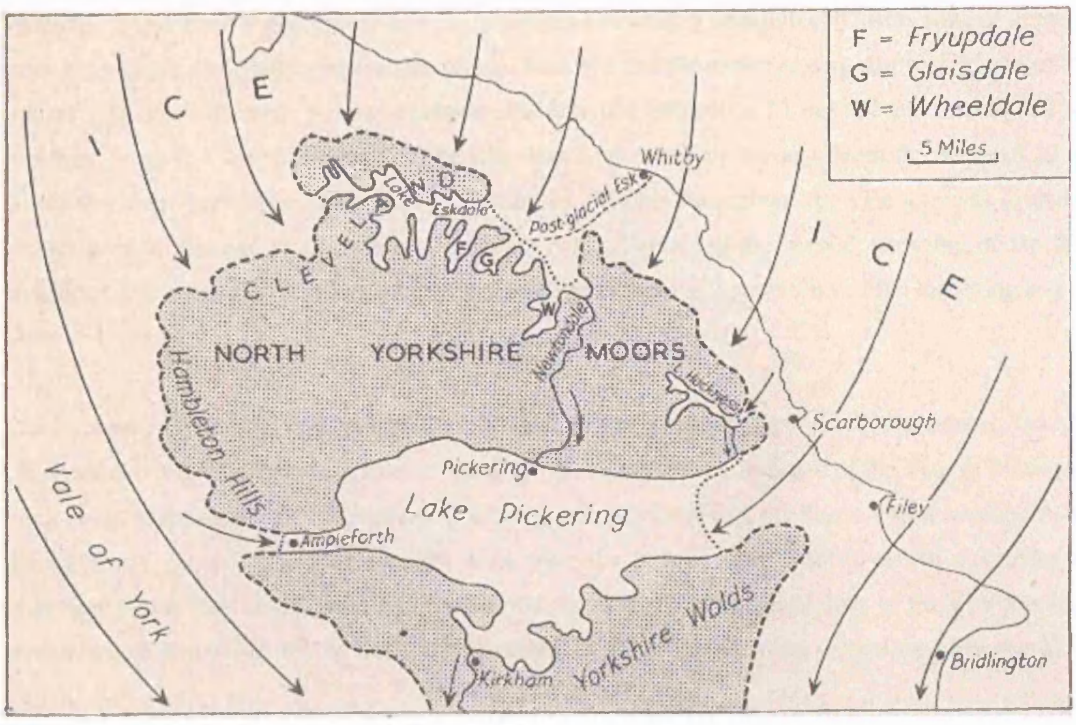

Figure 2.11. Pro-glacial lakes in relation to ice sheets and ice-free ground in the north-east of England during the Devensian (after Gresswell, 1958).

Straw and Clayton (1979) state, on the evidence of valley gravels grading between Hackness and Ayton, that:

"...Forge Valley, originally a small dipslope valley, was enlarged into a superb gorge by meltwaters that utilised it on at least two separate occasions, first at the Wykeham stage and later at the Cayton-Speeton stage." (p. 26)

From an examination of the topography it seems likely that Seavegate Gill formed an additional meltwater route from the escarpment to the south, although this route joins Forge Valley before it enters the Vale of Pickering. Whatever the route, once the waters had reached the Vale, their egress was blocked to the east by North Sea ice, to the south by the Wolds and to the west by the Howardian Hills, and thus the first (and largest) Lake Pickering was formed (Figures 2.10 and 2.11).

To the south of Forge Valley, where meltwaters were entering the Vale, extensive gravel deposits were laid down on top of the boulder clays that had been emplaced alongside the kame terrace at Wykeham and the deposits from the meltwater channels either side of Oliver's Mount (Figures 2.6 and 1.1). However, Lake Pickering overtopped the Howardian Hills (at what is now Kirkham Gorge) and drained to the west, completely emptying itself, before a second cold stage (the Cayton-Speeton stage) recreated the influent conditions that had led to the original. During this stage Forge Valley was further enlarged and boulder clays firmly emplaced along the entire eastern end of the vale. The levels of Lake

Pickering 1 and Lake Pickering 2 were 75 maOD and 45 maOD respectively[3], with alluvial deposits from both stages contributing to the flat alluvial lake bed that forms the present day topography of the central vale. The difference in height between the lake bed (at approx 23 maOD) and the edge of the Kirkham gorge (c.45 m) indicates that the lake would have had an average depth in excess of 22 m. Given that there are approximately 15 m of alluvial deposits throughout the vale this was probably greater prior to the end of deposition (Harrison, 1973). Following the second emptying of the lake significant thicknesses of peat formed due to the poorly drained soil conditions of the low-lying central Vale.

The thickness of the alluvium, the position and nature of the outwash gravels, kame terrace, boulder clays and tills are all important factors in the hydrogeology of the eastern end of the Vale of Pickering. For a study of groundwater flow and tracer behaviour in the Corallian, the Forge Valley swallow holes are obviously central. The drift deposits underlying the Seamer Carr landfill, which comprises an important part of this study, form a minor aquifer that a regional understanding of the hydrogeology cannot ignore, and which will be dealt with in greater detail in the following section (and Chapter 8).

2.2.6 SUMMARISING GEOLOGICAL SCHEMATIC

The main parts of the geological information relevant to the field area presented above have been summarised in a basic schematic diagram that will be used later in the thesis for the purposes of describing experimental and sampling locations and presenting data. It is given in Figure 2.12 below.

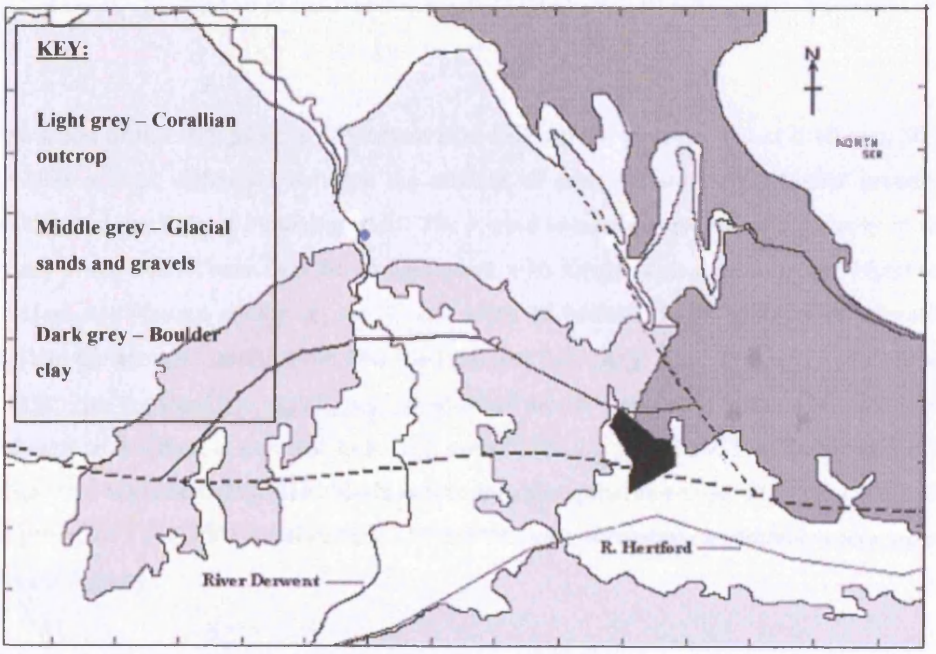

Figure 2.12 Simple geological schematic summarising main elements of solid and drift geology. Note that the blue dot identifies the Forge Valley swallowholes and the black shape represents Seamer Carr landfill.

[3] On the evidence of varying raised shoreline deposits on the Vale margins.

2.3 HYDROLOGY AND HYDROGEOLOGY OF THE EASTERN VALE OF PICKERING.

The eastern Vale of Pickering is taken to be that area between Ebberston and the coast (see Figure 1.1). However, as many hydrological and hydrogeological data for the region have their focus only on the larger area west of Ebberston, these data have been included where relevant.

2.3.1 REGIONAL CLIMATE AND HYDROLOGY

2.3.1.1 Precipitation

The average annual rainfall in the Scarborough area between 1975 and 1992 is given in the following table:

Location	NGR	Avg. annual ppt. 1975-1992
Irton	TA005 840	659 mm
Wykeham	SE947 863	802 mm
Scarborough	TA031 883	660 mm
Filey	TA114 807	640 mm

Table 2.3. Average precipitation for selected stations from 1975 to 1992, after Aspinwall & Co. (1994).

As the elevation of the rain gauge at Wykeham is c. 150 maOD, whereas that at Irton is c. 30 maOD, we may infer a clear difference between the amount of precipitation on the higher ground of the Tabular Hills and the Vale of Pickering itself. The coastal values are also low and broadly in line with those found in the vale. These data are in agreement with longer term data from the Meteorological Office's High Mowthorpe station on the Wolds south of Malton (NGR SE887 688, elevation 145 maOD). Here the average rainfall from 1961 to 1990 was 740 $mmyr^{-1}$ and from 1971 to 2000 was 729 $mmyr^{-1}$ (http://www.metoffice.com/climate/uk/ accessed 11-10-2004). The average rainfall for the east and north-east of England is reported to be 755 $mmyr^{-1}$ for the period 1971 – 2000 (Op. Cit.). More recent data from Wykeham indicates a slight decrease in precipitation compared to the 1975-1992 data, with the years 2002 and 2003 experiencing 747 and 745 mm of rainfall respectively (pers. comm. UK Environment Agency).

2.3.1.2 Temperature

Long term temperature data is also available for the east and north-east of England (http://www.metoffice.com/climate/uk/ accessed 11-10-2004) and is presented in the following table:

Month	Max. Temp. *(deg. C)*	Min. Temp. *(deg. C)*	Avg. Temp. *(deg. C)*
Jan	5.8	0.4	3.1
Feb	6.3	0.5	3.4
Mar	8.6	1.8	5.2
Apr	10.8	3	6.9
May	14.3	5.5	9.9
Jun	17.1	8.4	12.8
Jul	19.7	10.6	15.2
Aug	19.5	10.5	15
Sep	16.6	8.6	12.6
Oct	12.8	5.9	9.4
Nov	8.7	2.8	5.8
Dec	6.6	1.2	3.9
Year	**12.3**	**5**	**8.7**

Table 2.4. Average monthly and annual temperatures for north and north-eastern England in the period 1971 – 2000 (http://www.metoffice.com/climate/uk/).

From this table it may be seen that the average yearly temperature is 8.7°C.

2.3.1.3 Recharge

Based on evapotranspiration, land use, root constant and wilting point data for a variety of vegetation, effective rainfall (recharge) data is calculated by Aspinwall & Co. (1994) and summarised below.

Land use	Effective Rainfall (avg. 1975 – 1992) Irton	Wykeham
Grass	266 $mmyr^{-1}$	388 $mmyr^{-1}$
Cereals	217 $mmyr^{-1}$	348 $mmyr^{-1}$
Root Crops	252 $mmyr^{-1}$	375 $mmyr^{-1}$
Woodland	200 $mmyr^{-1}$	337 $mmyr^{-1}$

Table 2.5. Effective rainfall (recharge) to the Corallian for the southern and northern areas of the outcrop zone (as represented by Irton and Wykeham respectively). After Aspinwall & Co. (1994).

2.3.1.4 Surface hydrology and land drainage

The Tabular, Hambleton and Howardian Hills and the Vale of Pickering are drained by two main river systems, that of the Rye, in the west, and the Derwent, which begins in the east.

The Derwent actually rises on Fylingdales Moor to the north of the Corallian and flows southward into the Vale through the now-oversized Forge Valley. Just prior to entering Forge Valley, some flow is diverted along the 'Sea Cut', which runs eastward to the coast. Upon leaving Forge Valley, due to glacial tills blocking drainage to the coast, the Derwent runs a short distance south before turning west to capture the Hertford and the Rye on its journey to Kirkham gorge and the Vale of York. In contrast, the Rye rises on the Cleveland hills to the north of the Corallian and cuts through the escarpment to enter the Vale at Helmsley, and then flows eastward to join the Derwent at Ryemouth. These two main rivers capture the drainage of several smaller north-south running streams and rivers that dissect the Corallian into more-or-less discrete blocks (Figure 2.13). To the west the rivers Riccal, Dove and Seven, and Hodge Beck, are tributary to the Rye, with the Pickering, Thornton, Sawdon and Bedale Becks (and numerous smaller streams) tributary to the Derwent.

Due to the flat topography of the Vale itself, the Rivers Derwent and Rye have well-developed meanders, except for those parts where they (in particular the Derwent) have been channelised. This channelisation reflects the need for agricultural drainage of the flat, low lying and poorly (naturally) drained 'Carr' lands of the central Vale. There is thus a very extensive network of subsurface land drains and drainage ditches, dating back centuries, feeding the main watercourses.

2.3.2 OVERVIEW OF HYDROGEOLOGY

The geological map (Figure 2.6) shows the major geological units relevant to the hydrogeology of the eastern Vale. The two main aquifers are the Corallian limestone and the Quaternary sands and gravels, which will be discussed in more detail in the following sections. Table 2.6 provides a summary of their UK Environment Agency groundwater classifications.

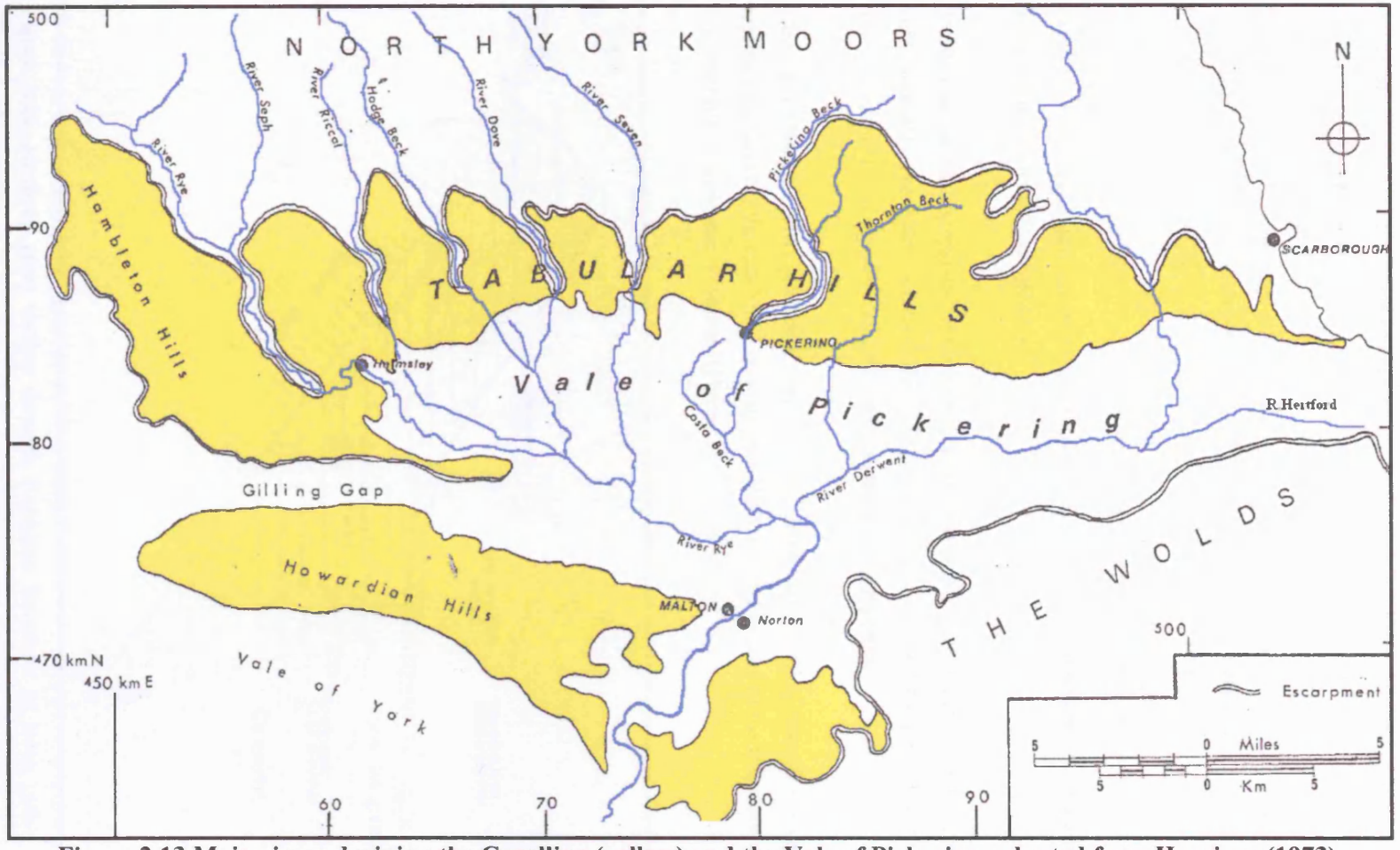

Figure 2.13 Main rivers draining the Corallian (yellow) and the Vale of Pickering, adapted from Harrison (1973).

Period	Unit	UK Env. Agency Classification
Quaternary	Peat	Low perm. drift deposit
Quaternary	Glacial sands and gravels	Minor aquifer
Quaternary	Boulder clay	Non-aquifer
Cretaceous	Speeton clay	Non-aquifer
U. Jurassic	Kimmeridge clay	Non-aquifer
U. Jurassic	Corallian limestone	Major aquifer
U. Jurassic	Oxford clay	Non-aquifer
M. Jurassic	Osgodby formation (sandstone)	Minor aquifer

Table 2.6. Hydrogeological classification of geological strata in and around the Vale of Pickering (pers.comm Environment Agency).

For the purpose of conceptualising the hydrogeology, the words 'non-aquifer' may be replaced by the word 'aquitard'. The table is given as these classifications are important for groundwater vulnerability concepts as well as for broadly classifying water-transmitting properties.

Carey and Chadha (1998) provide a useful north – south cross section through the aquifer in the eastern Vale showing the relative location of Irton PWS and importance of the Ebberston – Filey fault in controlling groundwater movement (Figure 2.14).

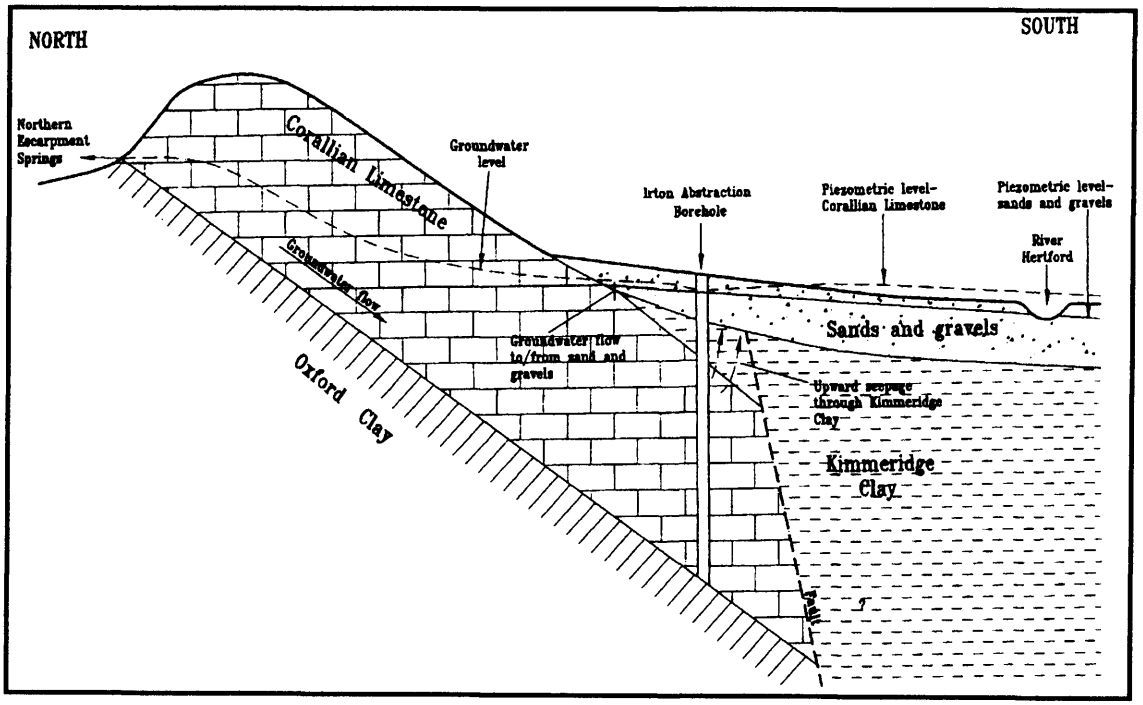

Figure 2.14. Idealised cross section through Corallian limestone at Irton (after Carey and Chadha, 1998).

From this diagram it can be seen that the Kimmeridge clay, emplaced against the Corallian, acts essentially as a large groundwater dam, blocking escape of water to the south, creating storage, and redistributing flow both upward and along the fault to feed springs and the sand and gravel deposits. These, in turn, drain to the network of land drains, ditches and rivers at the surface.

The full thickness of the Corallian is not necessarily realised at the fault boundary (as shown), as the fault increases in throw to the east (see Section 2.2.2). At Brompton the Upper Calcareous Grit and Coral Rag have been eroded away and the fault is at the junction of the outcrop and the Vale, not beneath the Vale as shown here (i.e. it is further north). Furthermore, it is likely that the Ebberston – Filey fault is not a single clean break as illustrated, but a series of en-echelon normal faults (Harrison, 1973). At Brompton (hydrograph and tracer results to be discussed in Chapter 7) the measured dip of the strata at the Mill Pond spring is 1° to the north (Mottram, 2003), which may indicate a small faulted block south of the main outcrop. Reeves (1978) depicts numerous en-echelon faults along the northern boundary of the Vale of Pickering, using the structure to help explain differences in groundwater chemistry.

2.3.3 THE CORALLIAN LIMESTONE

2.3.3.1 Hydrogeological properties

It is generally agreed (Harrison, 1973; Chadha *et al.*, 1977; Kendrick, 1979; Barker and Courchee, 1981; Waters-Marsh, 1984; Carey and Chadha, 1998) that the majority of flow in the Corallian limestone is through dip-aligned bedding-plane and vertical fissures[4]. However, the non-uniform development of the fissure system, as well as the variably saturated thickness of the aquifer, mean that the macroscopic hydrogeological properties of transmissivity and storage exhibit considerable spatial variation. Table 2.7 is illustrative of this point.

Although none of Harrison's (1973) data have been included in this table, it is still apparent that sites in the unconfined zone of the aquifer (Seavegate Gill, Swallowholes BH and West Ayton Quarry) display a reduced transmissivity (35 – 1400 m^2d^{-1}) compared to those in the confined zone (3000 – 40,000 m^2d^{-1}) (see Figure 2.15). Data from boreholes to the west strongly confirm this tendency (Harrison, 1973), which is primarily due to the limited saturated thickness of the aquifer in the unconfined zone.

The storage values cited are derived from a combination of pumping tests (confined zone boreholes) and an examination of borehole response to rainfall events (unconfined zone boreholes). Barker and Courchee (1981) state that the latter method consistently gives a storage value of between 0.02 and

[4] For the purpose of this thesis, the term 'fissure' is used to represent any largely planar fracture, joint, bedding-plane opening etc. that is potentially capable of transmitting water. It does not mean that the feature *is* transmitting water, nor does it imply any particular process involved in the genesis of such a feature.

0.03 when applied to boreholes in Forge Valley, and they accept a storage value of 0.02 as representative of unconfined zone storage (although this may represent enhanced fissure capacity due to the proximity of the swallowholes). Carey and Chadha (1998) give a value for unconfined storage of 1 – 2%. Values from pumping tests in the confined zone give expectedly lower values (0.0006 – 0.0014). The elevation of the storage coefficient at McCains (0.01) is probably due to only partial confinement by leaky boulder clay in contact with overlying silts, sands and gravels, as there is no Kimmeridge Clay at this point.

Hydraulic conductivity values cited in Harrison (1973) are from Corallian cores of unspecified location. That cited in Kendrick (1979) is from a single core from an unspecified limestone horizon on Spaunton Moor to the west of Pickering. The matrix permeability values given for the limestones are all within an order of magnitude of each other, and four or five orders of magnitude lower than macroscopic (field) hydraulic conductivities derived from a consideration of transmissivity and saturated aquifer thickness. The conductivity value representing the calcareous grits is obviously much higher, and therefore a more significant proportion of flow may be expected to occur in the grit horizons, although one must be cautious of generalising from this single value. The same applies to the single value for matrix porosity of 11% for the limestones. Nonetheless, this is a significant figure as it indicates the potential dual porosity nature of the aquifer, an important consideration in contaminant and tracer studies (Chapters 5, 6, 7, & 8). With this in mind, it is appropriate to review the karst features and fissure-flow mechanisms mentioned above.

2.3.3.2 Karst features and fissure-flow in the Corallian

The most important karst features in the eastern Corallian, in terms of water supply, are the swallowholes in Forge Valley that drain the river Derwent and recharge the aquifer. Here dissolution, operating on bedding planes in the upper Malton Oolite, has led to fissure development on the order of 15 cm at least (Barker and Courchee, 1982). Whilst this is not on the same scale as the caves at Kirkdale (NGR SE 678 857) and Bogg Hall (NGR SE 4710 4866), these fissures typically supply over 70% of all the water abstracted at Irton pumping station, the main water source for approximately one hundred thousand people living in the Scarborough district.

There are several other notable swallowholes in the Corallian: on Hutton Beck (NGR 710 891), on the River Dove (NGR 708 885), on the River Rye (NGR SE 608 831) and on the River Riccal at (NGR 632 842). In all cases swallowhole development is confined to the purer, oolitic, limestone horizons. However, in contrast to the Hutton Beck and Rivers Dove, Rye and Riccal swallowholes, those in Forge Valley are developed in the Malton (Upper) Oolite, as opposed to the Hambleton (Lower) Oolite.

Site	Location (NGR)	Reference	Transmissivity (m^2/d)	Storage	Matrix K (m/d)	n porosity
Irton Old Well	TA 004 840	1,2	5640 - 6980	0.00078		
Irton New Well	TA 004 840	1,2	36500			
Irton Obs BH	TA 004 840	2	9290			
Cayton Station Road	TA 047 827	2	3558* – 12450**	0.0014		
Osgodby Pumping Stn.	TA065 840	2	3285	0.0006		
McCains	TA 050 835	2	4115* - 40349**	0.01		
Seavegate Gill	SE 989 857	1	35 – 80	0.0270		
Seavegate Farm	SE 992 854	1		0.0236		
Swallowholes BH	SE 990 853	1	800 – 1000	0.0297		
West Ayton Quarry	SE 982 852	1	1400			
Wykeham Village Hall	SE 969 836	2	200			
Tetherings Plump	SE 975 828	2	10000			
Lab. tests Calc. Grits		3			0.086	
Lab. tests Ool. Lmstn		3			6.05×10^{-6}	
Average K Cor. Lmstn		3			4.32×10^{-5}	
Lab. tests Cor. Lmstn	SE720 861	4			5.25×10^{-5}	0.11

1) Barker and Courchee (1982); 2) Aspinwall and Co. (1994 & 1995); 3) Harrison, 1973; 4) Kendrick (1979). *Pumping test early data. ** Pumping test late data.

Table 2.7. Summary of hydrogeologic properties of the Corallian limestone aquifer in the eastern Vale of Pickering (matrix permeability and porosity data from western and central Vale).

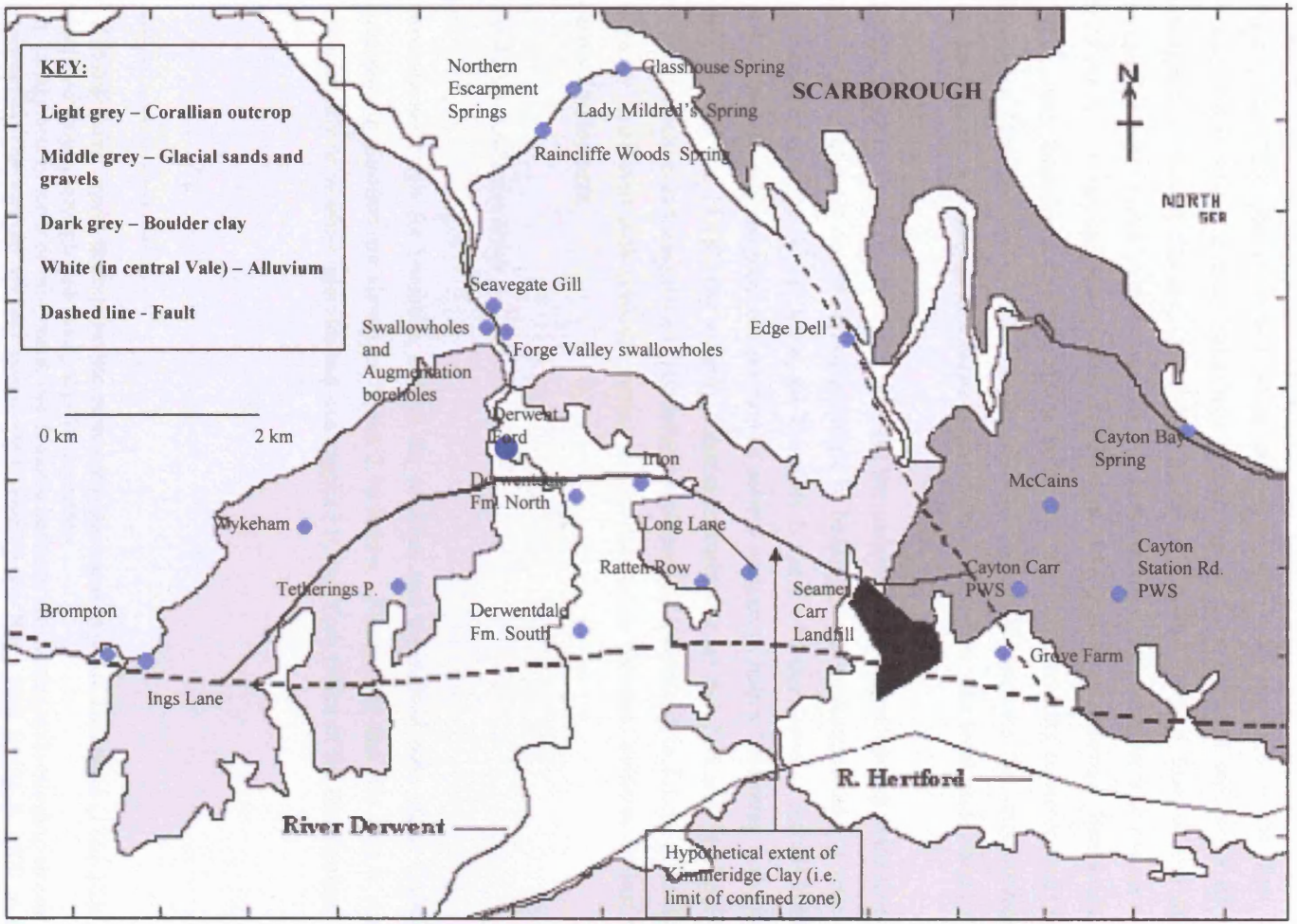

Figure 2.15 Geological schematic, borehole and spring locations, eastern Vale of Pickering. Grid squares 1 km to a side.

The Hutton Beck and River Dove swallowholes share the same resurgence: Bogg Hall spring. The cave behind the resurgence, at over 300 m long and up to 8 m wide (Scunthorpe Caving Club), is the largest known phreatic cave in the Corallian[5,6]. That the Hutton Beck and River Dove sink in the Lower and resurface in the Upper limestone is indicative of the importance of vertical fracturing in the Corallian[7]. Indeed, Harrison (1973) states that the majority of flow in the Tabular Hills is through longitudinal joints, with some 'cross-flow' (i.e. east-west) occurring through ac and shear joints (see Figure 2.8). This phenomenon is even more pronounced in the area of the Rye and Riccal swallowholes, where several faults, with throws up to 50 m, control the points of river water resurgence (Southern Science Ltd. 1994). However, although vertical flow is also an important mechanism in the Forge Valley – Irton system, here the same fissure may be followed, at a dip of 1.8°, from the river to the Old Well, where it re-appears at 56 m below the surface (Barker and Courchee, 1982). Other karst landforms in evidence in the area include several dry (underdrained) valleys (e.g. Brompton Dale and just north of Irton) and some associated sinkholes that only operate during or shortly after the very strongest recharge events (from conversation with local landowners).

From the above discussion it may be seen that the controls on karst development in the Corallian are a) the presence of purer oolitic limestone layers; b) bedding plane weaknesses; and c) vertical faulting. However, despite the factors listed, the Corallian is not a well-developed or mature karst. Harrison (1973) lists the mineralogical composition of several samples of oolitic limestone, with silica ranging between 4.62 and 11.48% (by weight), magnesium carbonate up to 6.71% and 'sideritic complexes' (iron, aluminium and magnesium carbonates, sulphates and oxides) up to 6.13%. This high level of impurity, combined with common lateral and vertical facies changes, militates against widespread karstic development.

2.3.3.3 Groundwater levels

Groundwater levels for boreholes in both the confined and unconfined zone of the Corallian east of Brompton-by-Sawdon are shown in Figure 2.16 below. Please note that this data is continuous at either weekly or monthly intervals and was supplied by the York Office of the Environment Agency.

---

[5] Kirkdale cave, made famous by the pioneering geologist William Buckland (1784-1856), and now mostly destroyed through quarrying, was 10 m shorter.

[6] In the context of karst development, the distance between the sinking and resurging stream is of some importance. The furthest sinking stream (HB) feeding the Bogg Hall spring is 1500 m distant, the closest (RD) only 1000 m. In comparison, the end of the natural flow system beginning at Forge Valley is some 8 km away at Cayton Bay. As one of the key controls on cave development is the establishment of a connection in the first place (Ford and Williams, 1980), it seems likely that, other things being equal, waters sinking at Hutton Beck and the River Dove have had considerably longer to work on the dissolution of rock than those sinking at Forge Valley.

[7] Scunthorpe Caving Club notes a diveable 40 ft (12.2 m) vertical sump, exhibiting turbulent upward flow, at the furthest end of Bogg Hall cave. This report is in a caving magazine I no longer possess so cannot give the full reference.

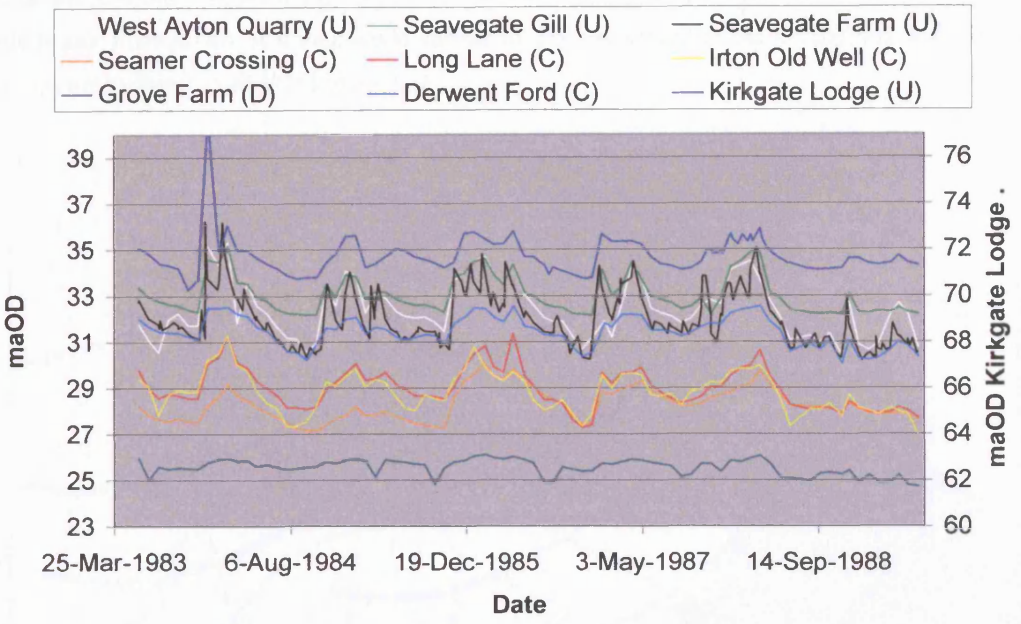

Figure 2.16 Monthly groundwater elevations in the confined (C) and unconfined (U) zones of the Corallian aquifer north and east of Brompton, 1983 to 1989. Also shown is Grove Farm, a well in the Quaternary drift aquifer (D).

One borehole (Grove Farm) screened in the drift is included as a reference (see Section 2.3.4.2). It should also be noted that as Kirkgate Lodge is at a significantly higher elevation than the other boreholes it has been plotted on a second axis to facilitate comparison.

From Figure 2.16 it can be seen that there is a general tendency for boreholes in the unconfined zone to exhibit more rapid fluctuations than their confined zone counterparts. This is particularly noticeable for the first recharge period on the graph (winter 1983), where differences between unconfined boreholes may also be observed. Kirkgate Lodge exhibits a slower recession than the other unconfined sites, which reflects its position on an interfluvial area as opposed to near a river. Those sites nearer the Derwent tend to drain more easily at times of high groundwater level.

Generally speaking, groundwater contours have been found to be strongly associated with topography (Chadha, 1968; Harrison, 1973; Barker and Courchee, 1981), and as the Tabular Hills are quite sharply incised by fluvial (and glacio-fluvial) action, the steepest gradients are adjacent to the rivers. That the base of the aquifer crops out along the river valleys and on the northern escarpment also contributes to the rapid drainage of these areas. Both Chadha (1968) and Barker and Courchee (1982) produce approximate groundwater contour maps, of which the latter is reproduced below (Figure 2.17). It should be noted that these contours only indicate relative piezometric elevations; they are largely hypothetical and must be viewed only as a guideline.

Where the Corallian is confined further to the south it typically exhibits artesian conditions and groundwater fluctuations of a magnitude similar to those observed in the unconfined zone, although with less peakedness, as seen in Figure 2.16.

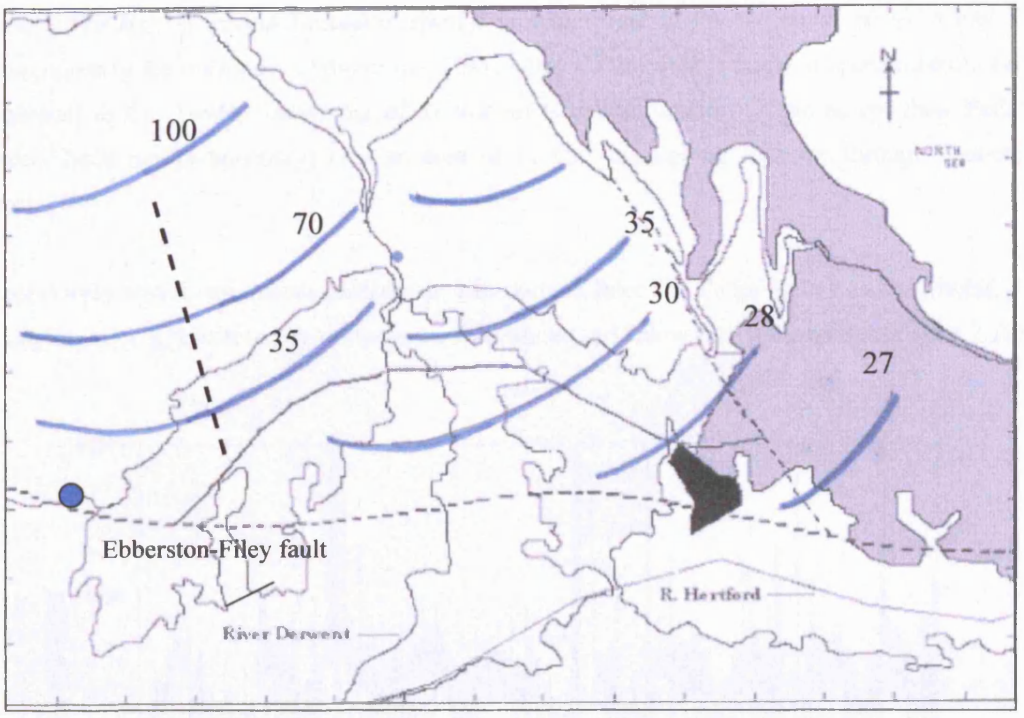

Figure 2.17 Groundwater contour map with simplified geology of the eastern Corallian and Vale of Pickering. The thicker N-S dashed line indicates the approximate position of the Sawdon anticline and the blue dot represents Brompton spring. All figures are in metres above Ordnance Datum (maOD) and grid square sizes are 1 km to a side.

2.3.3.4 Groundwater catchments and recharge areas east of Ebberston

The catchment of the Corallian limestone east of Ebberston may be divided sensibly into two parts: that area supplying Brompton Springs, and that supplying Irton pumping station and other abstraction points toward the coast, culminating at Cayton Bay spring and Filey pumping station (decommissioned).

However, no clear groundwater divide has been established between these two areas, partly due to the low levels of saturated thickness of the recharge zone in the north, but also due to the lack of monitoring wells in the outcrop zone. In their construction of a groundwater flow model for the area, Aspinwall & Co. (1994) suggested that a divide lies along a line between the Sawdon and Bedale Becks, although they were later obliged to extend the model to include Brompton springs themselves (Aspinwall & Co. 1995). A minor anticlinal fold axis (see Section 2.2.2.2 above) at Ebberston provides a more certain groundwater divide, although a smaller spring at Welldale, discharging about 25% of the Brompton flow, exists halfway between Brompton and Ebberston (Figure 1.1). The divide between Brompton and the east is still debateable, although the Irton pumping test indicates a cone of

depression extending (in the Vale) at least as far west as Charm Park (NGR SE983 832). Chadha *et al.* (1977) consider the division coincident with a minor anticline along Sawdon Beck.

From a consideration of recharge values and spring discharge (from data supplied by the Environment Agency), the area supplying Brompton springs is somewhere in the region of 30 – 35 km^2. The recharge area to the remainder of the Irton – Cayton Bay – Filey area is larger at approximately 44km^2 (Aspinwall & Co. 1994), comprising of 33 km^2 of Corallian outcrop (if we accept their Bedale - Sawdon Beck model boundary) plus an area of 11 km^2 undergoing recharge through Quaternary deposits.

As previously stated, significant recharge is also derived from the Forge Valley swallowholes. This transfer of water is monitored by weirs on the river above and below the swallowholes (Figure 2.18).

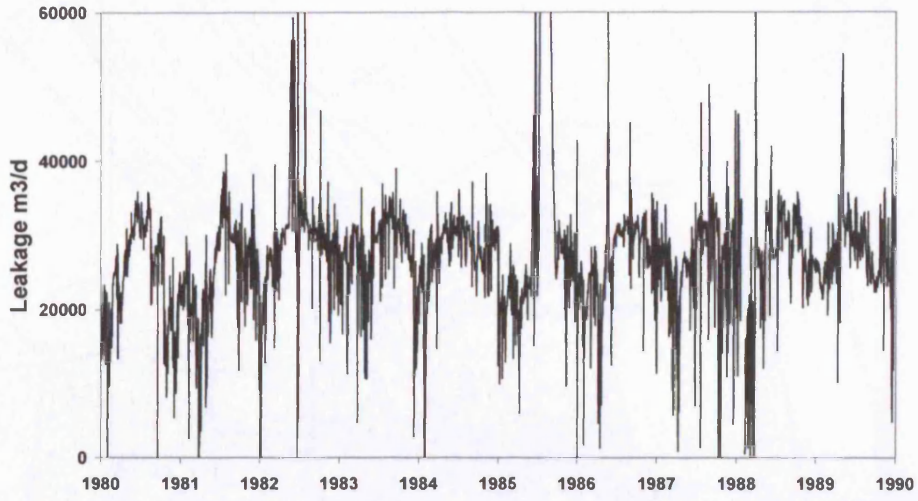

Figure 2.18 Leakage from the River Derwent at Forge Valley, 1980-1990.

Average leakage based on data from 1979 to 1997 given by Aspinwall and Co. (1994) is 28 000 m^3d^{-1}. This data is based upon the difference in flow between the Forge Valley and Ayton gauging stations positioned, respectively, above and below the swallowholes on the River Derwent. Aspinwall and Co. (1994) also state that this represents about 90% of the water pumped at the major abstractions per year (Irton, Cayton Carr, Cayton Station Road and McCains), although over the period 1983 to 1993 total abstraction was less than total leakage. However, it is very important not to confuse the rough equality between leakage and abstraction with the idea that everything that is abstracted comes from the swallowholes, as this ignores the contribution of the outcrop north of the eastern vale. It is also very important to note that, on average, the abstraction rate at Irton, the closest and most obviously affected well, is only some 60% of measured leakage. However, these are average values and at periods of low flow the river may be entirely swallowed (as in 1976, 1989, 1990 and 1991) leaving the bed dry until it is joined by the River Hertford several kilometres downstream.

2.3.3.5 A brief introduction to Brompton Springs

There are two associated springs at Brompton, one at the Mill Pond and the other at Brompton Hall School. They are situated at the very end of Brompton Dale, an under-drained dipslope valley extending up onto Wykeham Moor but truncated to the south by the presence of the Ebberston-Filey fault (see Figure 2.6). The spring locations are shown in more detail, together with the location of the Brompton Dale Shallow and Deep boreholes, on Figure 2.19.

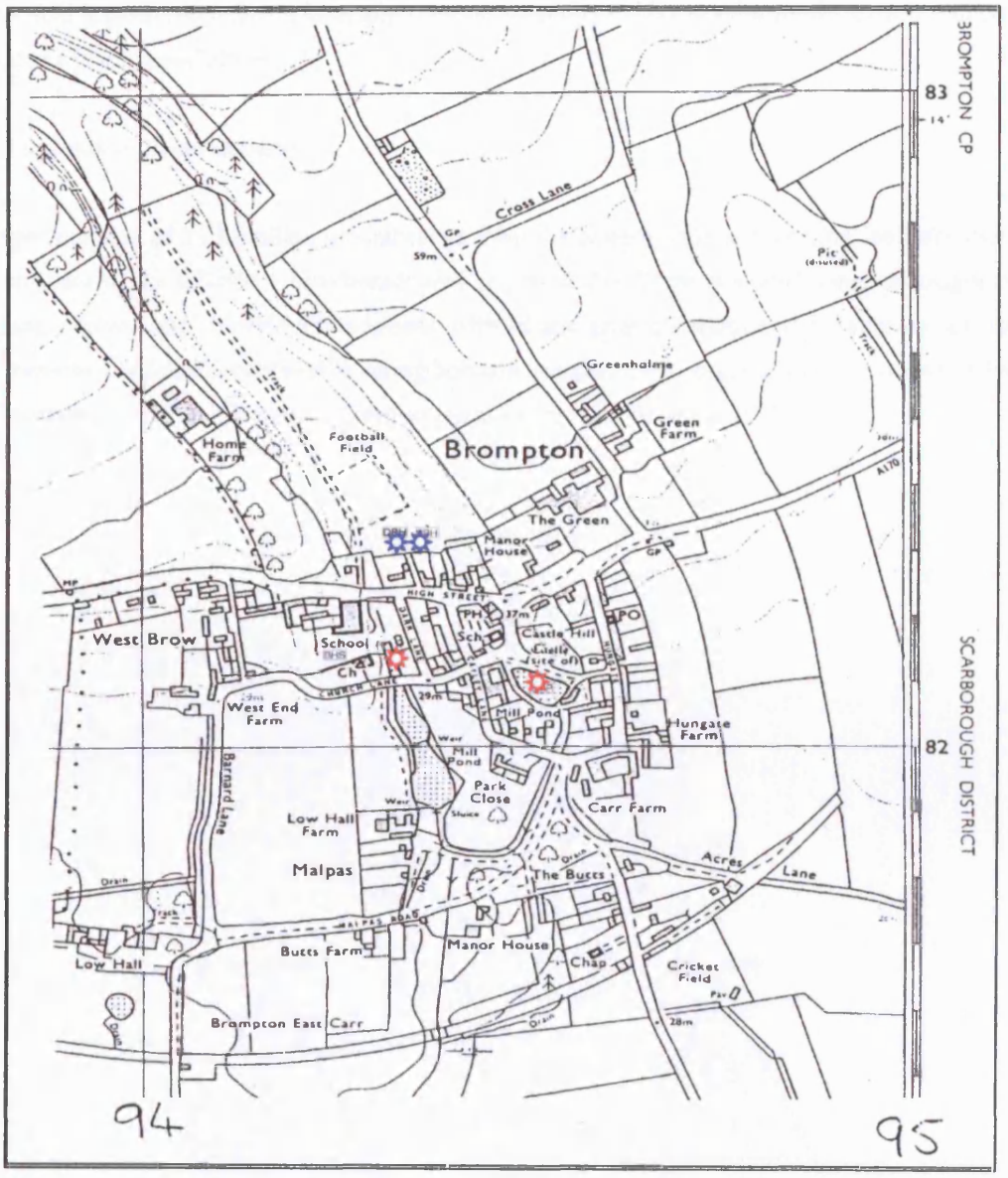

Figure 2.19 Local map of Brompton showing locations of springs (red stars) and boreholes (blue stars). The side of the square is 1 km and the map is oriented northward.

Both springs issue from fissures in the Malton Oolite. In the case of the Mill Pond Spring these fissures outcrop over some 50 m (west to east) of exposed limestone (all along the northern edge of the pond) and well up from below the bed of the pond. The level of the spring is approximately 28 maOD,

whereas the shallow and deep borehole casings are elevated to 34.5 and 35 maOD respectively. The dip of the strata at the Mill Pond is 1° to the north (Mottram, 2003) and on this basis the Malton Oolite is expected to be within 3 m of the uncased section of the shallow borehole (at 19.5 – 17.0 maOD (or 15 – 17.5 mbfl) in Brompton Dale Shallow borehole). The deep borehole is open over the interval 10.0 – 8.0 maOD (45-47mbfl) and is likely to be exclusively within the Lower Calcareous Grit (the LCG). The dip to the north is in contrast to the general dip of the Tabular Hills in this area, which is some 4° to the south. There may, therefore, be a faulted block rotated downward to the north forming part of the Ebberston-Filey fault, which dams the aquifer and causes the spring, or there may simply be a minor fold imposed onto the regional dip. It is not currently possible to offer further evidence in favour of either of these possibilities.

2.3.3.6 Corallian hydrochemistry

A Piper diagram of 21 Corallian groundwaters from the eastern Vale of Pickering indicates that the majority are of the calcium – bicarbonate type (Figure 2.20). There is a small range of magnesium, sodium, sulphate and chloride enhancement, without any great differentiation between sample types (i.e. between confined/unconfined or spring/borehole samples). The single distinctive outlier (a Forge Valley spring), with no dominant ion, reflects immaturity (Chadha *et al.*, 1977).

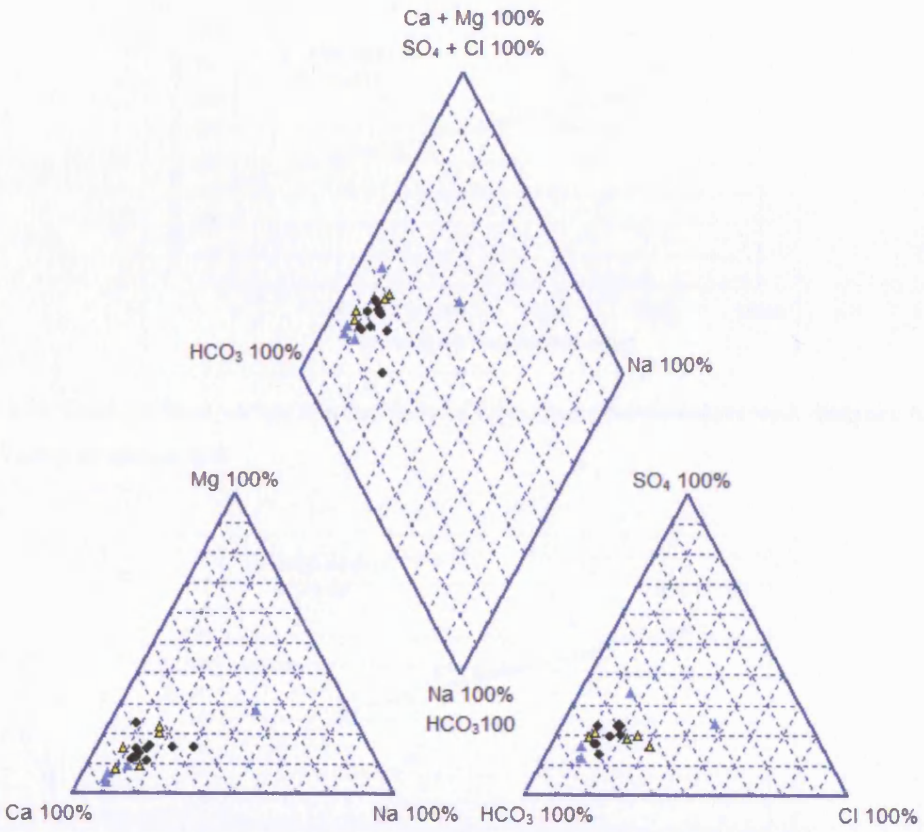

Figure 2.20 Piper plot of 21 Corallian groundwaters. Blue triangles = Springs from the unconfined zone; Yellow triangles = Unconfined zone borehole waters; Black circles = Confined zone waters (10 boreholes plus Cayton Bay spring).

Greater differences may be observed, however, in the total concentrations of the major ions and the electrical conductivity of the water. As one moves away from the Forge Valley swallowholes the dominance of river water on the groundwater chemistry is lessened through two mechanisms. Firstly, the further the river water moves from the swallowholes the longer it has to equilibrate with the aquifer, and secondly, the further it moves the more it mixes with 'true' groundwater derived from recharge on the outcrop. This pattern may be illustrated with the following series of graphs (Figures 2.21 – 2.23):

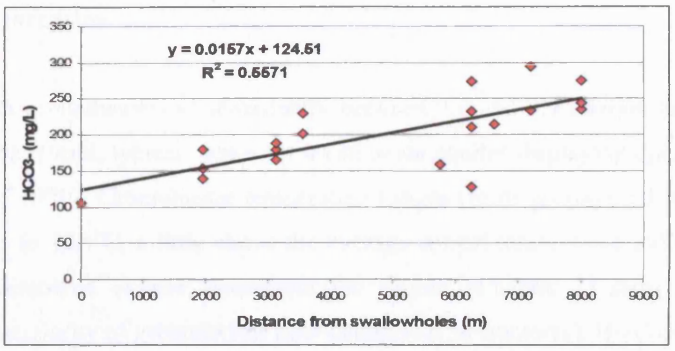

Figure 2.21 Changes in bicarbonate composition of Corallian groundwaters with distance from the Forge Valley swallowholes.

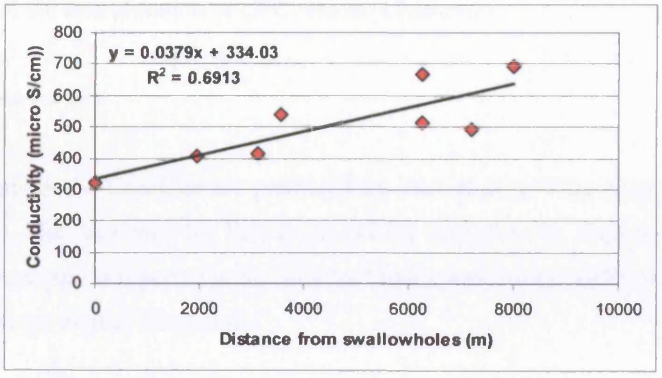

Figure 2.22 Changes in electrical conductivity of Corallian groundwaters with distance from the Forge Valley swallowholes.

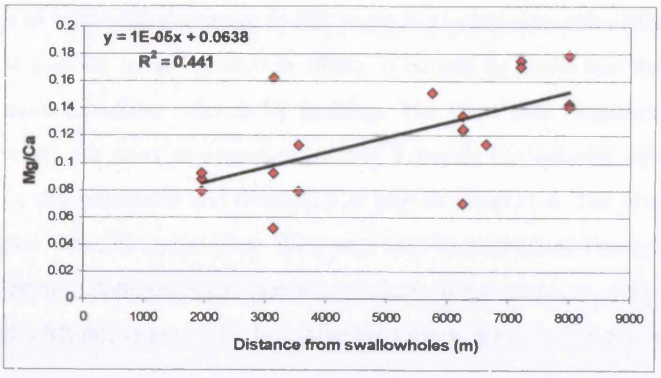

Figure 2.23 Changes in the Mg/Ca ratio of Corallian groundwaters with distance from the Forge Valley swallowholes.

The data for these diagrams are taken from Chadha *et al.* (1977), Barker and Courchee (1981), Aspinwall & Co. (1994) and Oxley (2002). The first two graphs show a general trend of increasing levels of dissolved material with distance from the swallowholes (the first data point on both of these graphs is river water). The third illustrates (albeit noisily) the progress of increasing magnesium concentration (and potentially the re-precipitation of calcite) along the groundwater flowpaths. The noise in these data is due to factors such as the proximity of the outcrop (contributing additional, more equilibrated groundwater), variations in flowpaths throughout the aquifer, and data being taken from different sampling campaigns.

The pH of Corallian groundwaters is consistently between 7.4 and 7.9 (Barker and Courchee, 1981; Oxley, 2002; Chadha, 1968), typical values for a carbonate aquifer displaying open-system conditions (Freeze and Cherry, 1979). Groundwater temperature ranges (from geophysical logging presented in Chapter 5) from 8.5 to 10.5°C, a little above the average annual temperature indicated in Table 2.4[8]. Measurements of dissolved oxygen throughout the aquifer (Chapter 7) show that the aquifer is oxidising where the majority of groundwater flow occurs (i.e. in fractures). Borehole core, on the other hand, exhibits deposition of iron-oxides associated with fracturing as well as a darker, grey colour evident in the centre of oolitic limestone beds. Although this is strongly suggestive of the persistence of anoxic conditions in the matrix blocks it is not a direct measurement, although the observation does have some bearing on the interpretation of CFC results (Chapter 7).

2.3.3.7 Tritium measurements

Tritium measurements in the Corallian are presented by Tate *et al.* (1970), Mather and Smith (1972) and Harrison (1973). The data used by Tate *et al.* (1970) was taken in 1968 by the Atomic Energy Research Establishment and is reported more fully by Mather and Smith (1972). Harrison's data refers only to wells and springs west of Ebberston.

Mather and Smith (1972) report measurements from a number of wells and springs within the Corallian. The wells include one at Seamer, the Irton Old and New Wells, and both public supply boreholes at Filey. The water sampled at Filey had zero tritium and it was thus concluded that water took at least 14 years to travel from outcrop to this point (i.e. more than the difference between major tritium inputs in 1954 and the sampling date in 1968). It should be noted that the Filey boreholes are separated from the main Corallian outcrop by faulting. The Irton data (together with measurements from the River Derwent) are used to constrain mixing between background aquifer water and river water, and this data is also presented and discussed as part of Chapter 6. The river value was 107 TU and the mixed, pumped water from the New Well was 93 TU. Individual fissures sampled within the Old Well showed varying compositions, but all of them were close to river water composition. Brompton Spring had a tritium value of 57 TU, whereas Cayton Bay Spring and Welldale Spring both

[8] Indicating either higher recharge in warmer months or local temperature deviations from those given for the whole of the north and north-east.

had values of 8 TU. The latter two springs issue from the Lower Calcareous Grit, whereas the former issues from the Malton Oolite, with differences ascribed to intergranular and fissure flow respectively.

Harrison (1973) surveys 5 wells and springs supplied by the Corallian, and finds that the most plausible explanation for the observed values is a component of high-tritium recharge passing through fissures and mixing with an older, tritium-free groundwater. This is on the basis that the measured values in groundwaters are too low to be accounted for by radioactive decay, even assuming initially low tritium values in rainfall.

2.3.4 HYDROGEOLOGY OF THE DRIFT DEPOSITS

2.3.4.1 Hydrogeological properties of the drift

The term 'drift' here covers boulder clays and tills, outwash gravels and sands, alluvial deposits (silts and fine sands) and peat. Obviously this variation is reflected in a wide range of hydrogeological properties. However, as the boulder clays are largely restricted to the very eastern end of the Vale, in terms of hydrogeology they are only really important in creating confined conditions where the Kimmeridge clay is not present above the Corallian. This is an area of only very limited extent just south of Scarborough. The tills also have some influence on the hydrogeology of Seamer Carr landfill, to be addressed in Chapter 8. For now, the drift deposits to be discussed will be limited to those of water-bearing importance, namely the sand and gravel deposits and, to a lesser extent, the alluvium.

The flow mechanism in the drift under the hydraulic gradients observed in the Vale is intergranular – laminar. Due to the variety of depositional controls, the drift deposits may be highly heterogeneous and anisotropic. The groundwater flow regime at Seamer Carr will be discussed more fully in Chapter 8, although this table is sufficient to illustrate that there will be a range of hydraulic conductivity values for the drift. A review of the (limited) literature indicates the following values (Table 2.8).

Strata	**Location**	**Reference**	**Hydraulic Conductivity**
Peat	Seamer Carr	Aspinwall & Co. (1996)	0.09 - 0.9 md^{-1}
Silty sand	Seamer Carr	Aspinwall & Co. (1996)	5 – 10 md^{-1}
Sand & gravel	Seamer Carr	Aspinwall & Co. (1996)	45 – 160 md^{-1}
Sand & gravel	Seamer Carr	Aspinwall & Co. (1994)	10 – 100 md^{-1}
Sand & gravel	Seamer Carr	Yorwaste Ltd. (1995)	9 md^{-1}
Undifferentiated	Pickering*	Harrison (1973)	0.61 md^{-1}
Undifferentiated	Wombleton**	Harrison (1973)	1.24 md^{-1}

*California Fm., Pickering, NGR SE 815 813 & **Wombleton, NGR SE 664 832

Table 2.8. Hydraulic conductivity values for drift deposits in the Vale of Pickering.

Based on values from similar deposits, Aspinwall (1994) also quotes a specific yield for the sands and gravels of 20-30%, although given the high levels of silt and clay this evaluation may be an overestimate. Furthermore, as measurements of drift thickness vary considerably, and there is no mention of pumping tests in the literature reviewed, it is only possible to estimate a transmissivity from the hydraulic conductivity values presented and an estimate of saturated thickness. For a nominal saturated aquifer thickness of 15 m, transmissivity ranges between 9 and 2400 m^2d^{-1}.

2.3.4.2 Groundwater levels in the drift

The only reliable data for groundwater levels in the drift in the eastern part of the Vale are at Seamer Carr, where several dozen boreholes are screened in the drift for the purposes of contaminant monitoring around the landfill site, and at Grove Farm, a private supply, less than a kilometre to the east (at NGR TA 044 821). The data set at Grove Farm extends from 1976 to 2002 and is the longest continuous drift monitoring data set available (Figure 2.24).

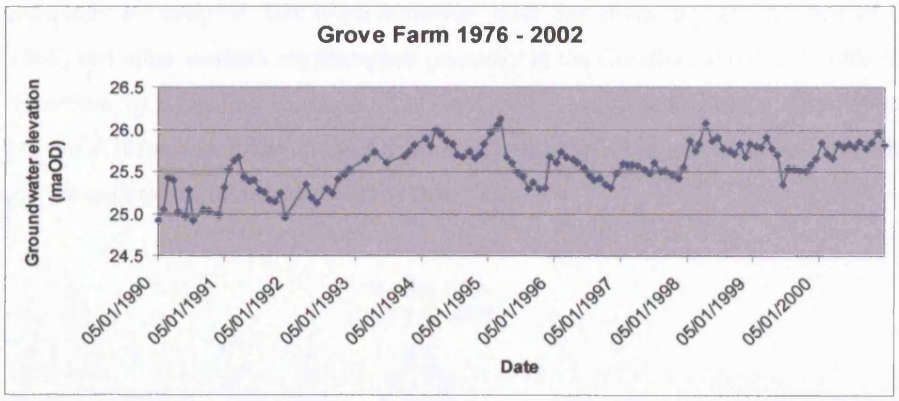

Figure 2.24 Drift water levels at Grove Farm in the eastern Vale of Pickering.

The data from Seamer Carr is less temporally extensive, although there are many boreholes (over 90). A representative selection with a north/south spread of approximately 1 km (highest groundwater levels in the north) is presented below (Figure 2.25):

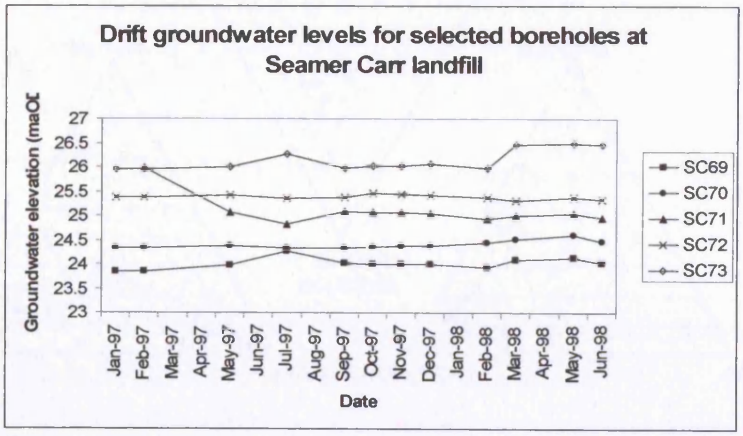

Figure 2.25 Representative drift groundwater levels at Seamer Carr (after Delaney, 2000).

From these two figures it appears that there is little seasonal fluctuation in drift water levels, with the majority of measurements showing differences of less than 0.5 m. Groundwater levels are generally at or close to the ground surface. The full Seamer Carr data set indicates decreasing head values across the (eastern) Vale from north to south (toward the river Hertford, see Chapter 8). It is also probable that, where the Kimmeridge clay is thin, i.e. north of the Ebberston Filey fault, it is leaky. As in these areas the Corallian tends to exhibit strong artesian conditions, water levels in the drift correspondingly exhibit upward hydraulic gradients. That the drift is in hydraulic contact with the Corallian is accepted by a number of workers (Chadha *et al.*, 1977; Aspinwall, 1994; Carey and Chadha, 1998). A closer examination of water levels and hydraulic gradients at Seamer Carr is made in Chapter 8.

2.3.4.3 Hydrochemistry of drift groundwaters

This section will focus in a limited way on the natural chemistry of drift groundwaters. Much of this section draws upon the work done by Harrison (1973), who gives a more complete discussion of the drift groundwaters he sampled. His work, however, does not cover any ground east of Ebberston. Chadha (1968) and other workers are interested primarily in the Corallian and devote little attention to the drift. However, by including Harrison's (1973) data it is possible to produce the following Piper diagram (Figure 2.26) which shows the major ion composition of drift groundwater from 35 boreholes and springs (the majority boreholes) throughout the Vale.

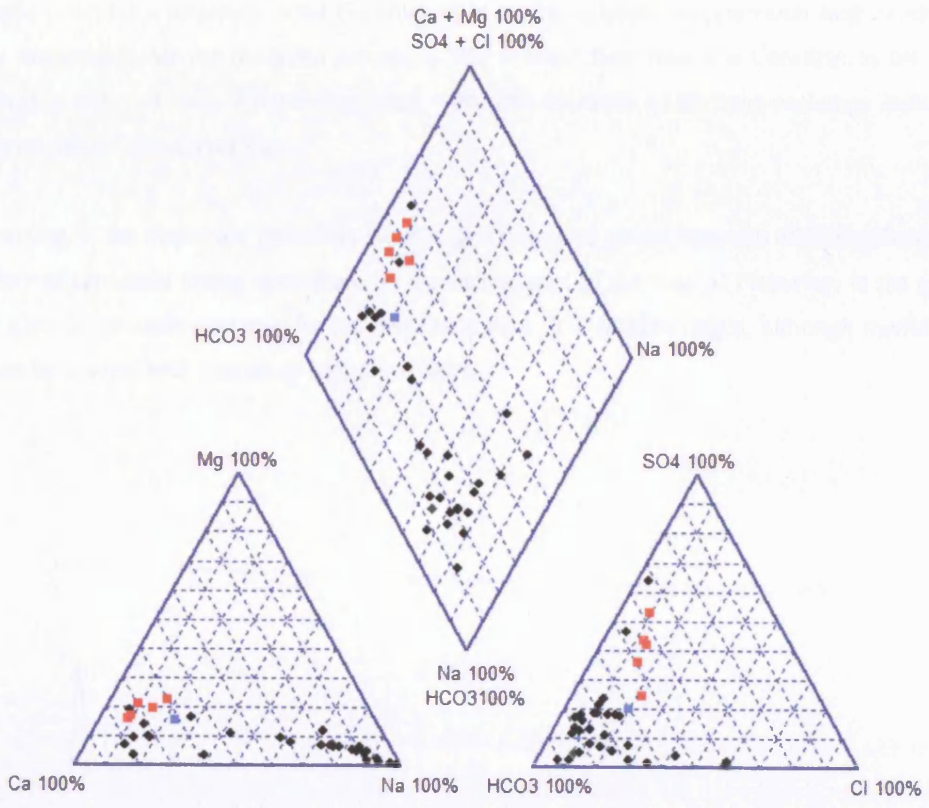

Figure 2.26 Piper plot of 35 Vale of Pickering drift groundwaters. See text for details.

Harrison (1973) data points are in black and additional data points in red are from Yorwaste Ltd. (personal communication). As these data represent the western and central Vale, and the eastern Vale, respectively, they will be discussed separately. The blue data point is Corallian groundwater sampled at Seamer Carr (also Yorwaste Ltd.).

From drift deposits in the western and central vale (black) there is a spread of cations between calcium and sodium (actually Na + K) type waters, whereas most of the anions are clustered into a bicarbonate dominated water with a roughly equal number of sulphate and chloride enhanced samples. Harrison (1973) interprets the spread in cationic composition from Ca to Na as a transition from either shallower or Corallian-influenced drift waters to wells drilled deeper into the drift. The deeper drift waters have had time to undergo cation exchange with the (predominantly alluvial) drift (i.e. uptake of Ca^{2+} in exchange for Na^{+}), with the clustering at the two end points suggesting rapid equilibration. The waters with enhanced sulphate and chloride are exclusively related to boreholes in or adjacent to the Kimmeridge clay. As this is a marine clay it may be expected to show enhanced levels of calcium and magnesium sulphates and chlorides (Harrison, 1973).

In contrast to these primarily alluvial (silty) or Kimmeridge clay influenced groundwaters, the more aquiferous deposits (sands and gravels) at the eastern end of the Vale show a calcium bicarbonate – calcium sulphate distribution, with some (although not much) magnesium enhancement. As at Seamer Carr much of the drift groundwater is derived from the stratigraphically lower Corallian, the Corallian sample provides a reference point (in blue) upon which sulphate enhancement may begin to operate. One explanation for the observed process is that upward flow from the Corallian to the drift occurs through a thin and leaky Kimmeridge clay, with little evidence of the base exchange indicative of the alluvial silts of the central Vale.

In summary, the major ion chemistry of drift groundwaters grades between differing facies due to the variety of processes acting upon them. In the eastern part of the Vale of Pickering, in the glacial sands and gravels, groundwater may be expected to reflect its Corallian origin, although modified to some extent by contact with marine or lacustrine clays.

2.4 GROUNDWATER SOURCE ZONE PROTECTION IN THE EASTERN VALE OF PICKERING

2.4.1 EARLY WORK

The first tracer tests recorded between the Forge Valley swallowholes and Irton were performed in 1908 and are referred to by Richardson (1934) as 'Colour tests' with 'colour' arriving at Irton within six hours. No comment is made regarding vulnerability. However, the protection of the well is given considerable attention in another early document entitled "Report on the protection of the water-gathering grounds contributing to the Irton, Osgodby and Cayton Bay waterworks" (Morton, 1938). This cites the same tracer test as well as increased turbidity and reduction in hardness at Irton during times of high flow in the Derwent. The connection, Morton (1938) notes, as "Perhaps the gravest source of potential pollution at the present time...", words as true now as they were then. He also considers that the best possible course of action to mitigate this risk is to acquire, by Act of Parliament, the whole of Forge Valley. He dismisses as impractical, however, gaining a similar control over the entire catchment to the river Derwent above Forge Valley, although given limitless funds this seems to Morton (1938) the most sensible course of action. He settles for the enactment of bye-laws controlling discharge to the river and advocates the outright purchase of the whole of Irton Moor, that outcrop of Corallian undoubtedly contributing to the well. However, he only suggests the latter measure after noting the abundance of fissures in the Corallian and the consequent rapidity of flow. Morton (1938) also notes that the greatest potential threats are housing development in Forge Valley, leading to potential influx of sewage to the swallowholes, and agricultural runoff from the river catchment or on the outcrop. The pollution incident record for the river Derwent given by ARUP (2000) indicate the most likely river pollutants are sewage, oil or agricultural runoff (slurries), and they cite an incident probability of 1 incident of major severity (defined as leading to extensive fish kills) every 8 years, so that little seems to be different now as when Morton wrote his report. With respect to the Osgodby and Cayton Bay waterworks (both now decommissioned) Morton (1938) suggests better building controls in terms of sewage removal on the limestone outcrop to the north of these points, as he recognises the considerable development that these areas were undergoing at the time of writing. Morton (1938) also comments upon the proposed locations of two refuse tips and a cemetery in the district, so is clearly well aware of such threats to groundwater security. In fact it should be of some credit to Mr Morton that he was so aware of these practices, as the chlorination of water at Irton had only begun ten years earlier (Debenham, 1971).

Immediately subsequent to Morton (1938) is a report by Morton and Overfield (1939) in which previous recommendations of purchase of Irton Moor are exchanged for a 'zoning' scheme in which land is divided into that set aside for development of a district and the remainder remain exclusively agricultural. From this it can be seen that the primary fears of Morton (1938) were industrial or residential development of Irton Moor. Morton and Overfield (1939) comment upon provisions made by the Town and Country Planning Act of 1932 in this respect.

So it seems that some initial groundwater protection was considered in terms of source-protection-zones for the Irton waterworks from an early stage. Morton and Overfield (1939) also comment upon similar measures having already been taken with respect to the water supplies of southern English coastal towns at this time. And in all probability the latter recommendations of Morton and Overfield (1939) were the policies adopted, for the Scarborough Water Corporation does not seem to have acquired the moor, and indeed there is little but agricultural development on it (bar an RAF radio station which may actually be significant as a source of industrial contamination).

2.4.2 LATER WORK

The National Rivers Authority (NRA; now part of the Environment Agency) published its Policy and Practice for the Protection of Groundwater in 1992 (NRA, 1992). This policy was adopted in response to the Water Resources Act of 1991 and was implemented in two ways; 1) Mapping groundwater vulnerability (NRA, 1995a); and 2) Defining groundwater source protection zones (NRA, 1995b). The latter requires definition of a 50 day travel time zone, a 400 day travel time zone, and a zone describing the catchment of the well or source. In the eastern Vale of Pickering this was implemented in 1996 with the production of a MODFLOW model of the aquifer between Brompton Springs and the coast (Aspinwall and Co., 1994 and 1995; Entec UK Ltd., 2001). This model was primarily a resource management tool for examining options for the regulation of flow in the river Derwent, which had been identified as one of the priority low-flow rivers in England and Wales (Carey and Chadha, 1998). It therefore paid particular attention to the relationship between the river and the aquifer, using zones of high permeability running eastward from the river to account for the observed losses through the bed of the river and also to account for the very high yield at Irton and the hydrochemical distribution within the aquifer (Aspinwall and Co., 1994; Carey and Chadha, 1998). Scanlon *et al.* (2003) indicate that a MODFLOW model may be used to accurately simulate spring and well discharges in a karstic limestone (the Edwards Aquifer, Texas), and that spring discharges are more susceptible to fluctuations in recharge than they are to pumping. This is borne out to some extent by the Corallian model, which did provide a reasonable representation of groundwater level fluctuations and river leakage. However, the model also served to define the source protection zones of the public water supply wells at Irton, Cayton Carr House Lane and Cayton Station Road, as well as that of the well at McCains food factory (Figure 2.27), and these proved more problematic.

The zones of high permeability, whilst sufficient to recreate observed losses and groundwater level changes, were inappropriate for modelling contaminant transport, as much of the water is travelling through a few poorly defined bedding planes, whereas the model assumes a porous medium. This was made abundantly clear in 1999 when a tracer test using two different tracers proved that water entering the Forge Valley swallowholes, just north of Ayton, arrived at McCains within 2 – 5 days, and at Cayton Carr House between 7 and 15 days, clearly much faster than the 400 days predicted (ARUP, 2000). Additionally, the Irton pumping test of 1981 (Barker and Courchee, 1982) exhibited drawdown in a well 2 km south-west of Irton (i.e. at least a kilometre outside the blue catchment zone). The model, therefore, was not a sufficiently rigorous tool for source-protection-zone purposes.

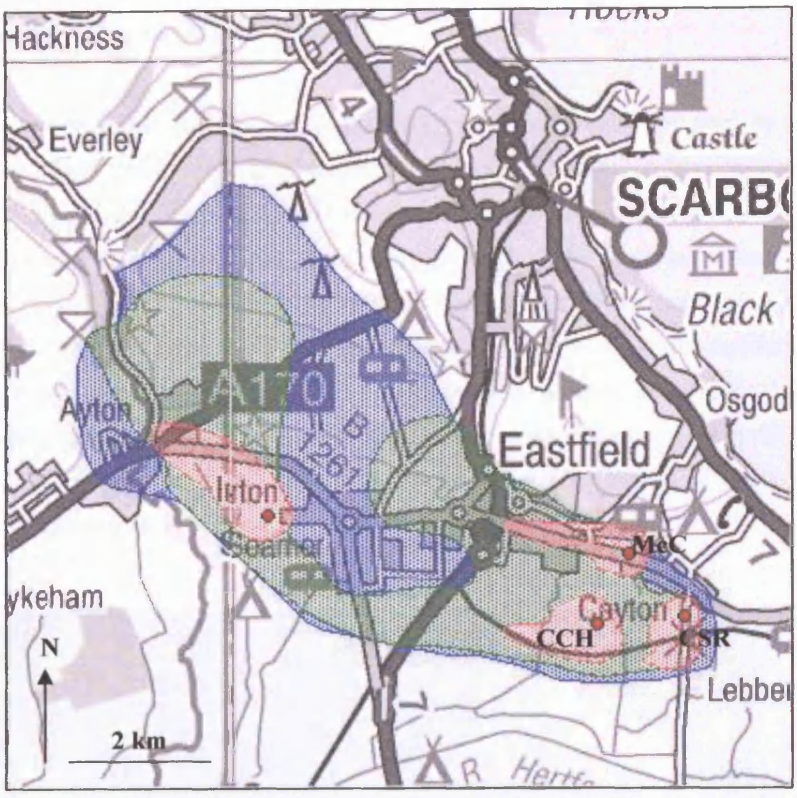

Figure 2.27 Inner, 50 day travel time zone (pink), Outer, 400 day travel time zone (green) and total catchment (blue) of the Irton, Cayton Carr House (CCH), Cayton Station Road (CSR) and McCains (McC) boreholes (after Aspinwall & Co. (1994).

Yorkshire Water Services Ltd. recognise the potential severity of pollution of the aquifer. Of the three public supply wells, Irton is by far the more important, and mitigation of the hazard, proven in 1908, has been undertaken with a number of measures. The first of these was the construction of protective housing around the main observed swallowholes. These structures, however, as Morton (1938) noted would probably be the case, cannot enclose all the multiple fissure openings and swallows in the bed and banks of the river. Another measure was the installation of pollution monitors at Irton that constantly analyse the raw water for significant changes in fluorescence. A further measure was considerably more ambitious and involved drilling a number of wells into the Osgodby sandstone, beneath the Oxford Clay (the Osgodby is between 168 and 180 mbgl at Irton) for the purposes of installing an Aquifer Storage and Recovery (ASR) scheme that would pump treated water from the water works into the Osgodby for the provision of up to 30 days supply in the event of contamination of the Corallian. The results from tracer testing to be presented in this thesis indicate how long one may expect a contaminant signal of a certain magnitude to persist in water pumped from the Corallian. They also indicate relationships between contaminant persistence and well operation. Borehole dilution tests and CFC measurements improve conceptualisation of groundwater flow from the single-borehole scale to the scale of the whole eastern part of the aquifer. These advancements are important for understanding how best to provide and protect a sustainable water supply from both the Irton New Well, the main source from the Corallian, and the ASR scheme, and for understanding how contaminant behaviour is likely to appear in the wider Corallian to the west.

2.5 SUMMARY OF CHAPTER TWO

Chapter 2 has introduced the geology and hydrogeology of the field area. The geology of the southern North Yorkshire Moors and the Vale of Pickering has been described with reference to major structural elements of the British Isles. From a regional overview encompassing climatic and geomorphic factors, the chapter narrowed in focus to highlight the hydrogeology of the Corallian limestone aquifer and associated drift deposits. This included an appraisal of hydraulic behaviour and groundwater chemistry in the eastern part of the Vale, in both the major (Corallian) and minor (drift) aquifers. The Chapter continued by reviewing the existing source-protection-zone policies and implementation, noting potential shortfalls therein, and identifying how the research undertaken is useful in the protection and management of the existing water resource. Please note that a brief history of Scarborough's water supply is given in Appendix 1.

Plate 2.5 The River Derwent at the Forge Valley swallowholes intake structure, April 2003. The geologist in the water is the author.

CHAPTER THREE

THE USE OF CFCs 11, 12 AND 113, CCl_4 AND SF_6 AS HYDROLOGIC TRACERS.

3.1 INTRODUCTION

This chapter introduces SF_6 and CFCs 11, 12 and 113 in terms of their chemistry, historical production and application, and in their capacity for use as hydrological tracers. CCl_4 is also described as it is a related compound and may be employed in a similar way to the CFCs.

The majority of hydrologic tracer studies utilising these compounds simply measure the amount already present in the environment as a result of global industrial production (natural sources being negligible). This is what is meant when CFCs are referred to as 'environmental' or 'historical' tracers. Such studies typically aim to 'date' oceanic or ground-water at depth by determining the year when the water was last in contact with the atmosphere, as either rainfall or surface water, by comparing extant concentrations with calculated historical concentrations. However, there have been a number of studies deliberately using CFCs to identify groundwater contamination (contamination being concentrations above that which may be accounted for through equilibration with the atmosphere), and these studies will be reviewed as part of this chapter.

The use of SF_6 as an 'artificial' (i.e. deliberately introduced) tracer is also well established in the Earth Sciences, although primarily in oceanography, limnology and atmospheric sciences. Examples include studies of atmosphere-ocean (and lake) gas exchange rates, the subduction of oceanic water masses, and marking oceanic iron-fertilisation experiments. CFCs have been used less in this context than SF_6. As far as artificial groundwater tracers are concerned, CFCs and SF_6 have at times been used, although a review of the literature illustrates that this is minimal. Reference is occasionally made to unpublished studies, but these often prove difficult, if not impossible, to obtain.

In this thesis SF_6 is developed as an artificial tracer method, whereas CFCs are used in their capacity as environmental tracers, both for an attempt to date Corallian groundwater and as indicators of landfill contamination of surface and groundwater. Despite this, much of the material presented in this chapter is generic to the use of CFCs/SF_6 as tracers in a variety of disciplines.

3.2 AN INTRODUCTION TO THE CHEMISTRY OF CFCS 11, 12 AND 113, CCL_4 AND SF_6

3.2.1 NOMENCLATURE (CFCS)

Also known as Freons, Frigens, Flugene (manufacturers' trade names), CFCs are based on one or more carbon atoms saturated by chlorine and fluorine atoms. The chemical names of the CFCs measured for this project are as follows: CFC 11: Trichlorofluoromethane ($CFCl_3$), CFC 12: Dichlorodifluoromethane (CF_2Cl_2) and CFC 113: Trichlorotrifluoroethane ($C_2Cl_3F_3$). The numbering convention is that of three digits, the first being carbon atoms minus one, the second being hydrogen atoms plus one and the third being the number of fluorine atoms. All other available bonds are filled by chlorine atoms. Where a compound has only one carbon atom the first digit is not given. Thus, dichlorodifluoromethane has 1 carbon atom (1-1=0), 0 hydrogen atoms (0+1=1) and 2 fluorine atoms. This gives CFC 012, the zero being ignored to leave CFC 12. Both CFCs 11 and 12 are fully halogenated methane, CFC 113 is a halogenated ethane. Carbon tetrachloride (CCl_4) is not a true CFC as it has no fluorine atom, but is methane fully substituted by chlorine atoms.

3.2.2 HISTORICAL PRODUCTION AND USES

3.2.2.1 CFCs

CFCs were first produced in the 20th Century for use as refrigerants, but have further industrial application in aerosol propellants, plastic foams, cleaning agents and solvents (Bateman, 1998). However, the production of CFCs was preceded by the production of CCl_4 (extensively manufactured from 1908), which was used as an industrial solvent and a fumigant, but is now mainly used as a chemical feedstock for CFCs 11 and 12 (Ibid.). CFC 12 production became significant in the 1930s, CFC 11 production in the 1940s and CFC 113 production only in the 1960s. Figure 3.1 charts changes in atmospheric concentration of CFCs and SF_6 throughout the last 100 years (up to 2003). The data in this graph is a combination of measurements made at Mace Head, Ireland (since 1979 for CFCs 11 and 12, since 1980 for CFC 113 and since 1984 for CCl_4) and calculated concentrations (pre-measurement) based on industrial production figures, and atmospheric lifetimes.

3.2.2.2 SF_6

Sulphur hexafluoride, first produced industrially in 1953, is a highly stable compound used primarily in electrical insulation and as a blanket-gas in the production of magnesium (Maiss and Brenninkmeijer, 1998). Maiss and Brenninkmeijer (2000) state that production peaked in 1995, subsequently falling by about 30% by 1998. This is not reflected in Fig. 3.1 as there is a lag between the fall in production and a reduction in atmospheric concentration. The SF_6 data in Fig. 3.1 is from the USGS Reston Laboratory web pages (http://water.usgs.gov/lab) and is based on measurements of flasks (pre-1992) and in-situ measurements at Niwot Ridge, Colorado (North America) (1992-2000).

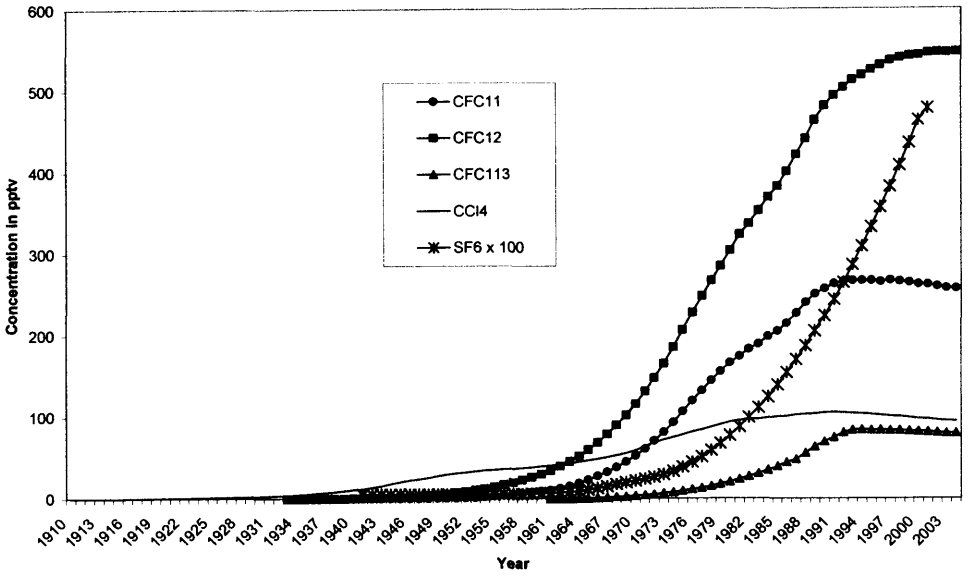

Figure 3.1 Atmospheric histories of CFCs 11, 12 and 113, CCl_4 and SF_6.

3.2.3 PHYSICO-CHEMICAL PROPERTIES, SOLUBILITY AND UNITS.

3.2.3.1 Physico-chemical properties

Table 3.1 gives the physico-chemical properties of the CFCs relevant to this study, CCl_4 and SF_6.

	CFC 11	CFC 12	CFC 113	CCl4	SF6
Chemical Formula	CCl3F	CCl2F2	CCl2FCClF2	CCl4	SF6
Relative molecular mass	137.37	120.91	187.38	153.82	146.05
Boiling point (C)	23.8	-29.8	47.6	76.8	
Melting point (C)	-111	-158	-35	-23	-50.8
Sublimation point (C)					-63.9
Density of liquid at 25 C (g/cm3)			1.565	1.587	

Table 3.1 Physico-chemical properties of the CFCs, CCl_4 and SF_6.

3.2.3.2 Solubility

Henry's Law is used to calculate equilibrium concentrations in water at a particular temperature and salinity. It may be stated as follows:

$$K_{(H)} = \frac{c}{p} \qquad (3.1)$$

Where c = concentration of dissolved gas ($molkg^{-1}$)

p = partial pressure of gas in contact with the solution (atm)

$K_{(H)}$ = the Henry's Law constant ($molkg^{-1}$ atm^{-1})

The law says that the concentration of a gas dissolved in a solvent is proportional to the pressure of the gas above the solution. Henry's Law constants are empirically derived by determining the concentrations in both the solvent and in the gaseous phase, at known temperature and salinity, once equilibrium may be assumed. Various workers have performed such experiments for the compounds in which we are interested: CFC 11 and 12 by Warner and Weiss (1985), CFC 113 by Bu and Warner (1995), CCl_4 by Hunter-Smith *et al.* (1983) and Gossett (1987), and SF_6 by Ashton *et al.* (1968), Wilhelm *et al.* (1977), Mroczek (1997), Marcus (1997) and Bullister *et al.* (2002).

Because much of the research into CFCs and SF_6 has focussed on oceanic waters, the salinity term has been important for deriving a formula for describing $K_{(H)}$. However, as this thesis is concerned only with fresh (essentially non-saline) waters, the expression governing salinity tends toward zero and may be ignored. The simplified formula thus becomes:

$$\ln K_{(H)} = a_1 + a_2\left(\frac{100}{T}\right) + a_3 \ln\left(\frac{T}{100}\right) \qquad (3.2)$$

Where T = temperature (°K)
$K_{(H)}$ = Henry's Law constant (molkg^{-1} atm^{-1})
a_1, a_2 and a_3 = constants (see Table 3.2)

The reader is referred to Warner and Weiss (1985), Bu and Warner (1995), or Bullister *et al.* (2002) for the salinity expression. For groundwater dating, Plummer and Busenberg (1999) note that for water of $10^0/_{00}$ salinity and a recharge date in the 1960s, the error from ignoring the salinity correction would be only 1 year (too old). This is negligible compared to other sources of error (see Chapters 7 and 8).

For CCl_4 the formula derived by Hunter-Smith *et al.* (1983) is preferable to that of Gossett (1987) (Bateman, 1998) and may be written:

$$\ln H = \frac{-2918}{T} + 9.77 \qquad (3.3)$$

Where H = Henry's Law constant of Hunter-Smith *et al.* (1983), a dimensionless constant that may be related to $K_{(H)}$ as follows (Warner and Weiss, 1985):

$$K_{(H)} = \frac{1}{HRT} \qquad (3.4)$$

Where $K_{(H)}$ = Henry's Law constant (molkg^{-1} atm^{-1})
H = Henry's Law constant of Hunter-Smith *et al.* (1983) (dimensionless)
R = the gas constant (0.082056 kg atm mol^{-1} K^{-1})

T = equilibrium temperature (°K)

The constants for Equation 3.2 are given in table 3.2:

	a1	a2	a3
CFC 11	136.2685	206.115	57.2805
CFC 12	124.4395	185.4299	51.6383
CFC 113	-136.129	206.475	55.8957
SF6	-98.7264	142.803	38.8746

Table 3.2. Values for the constants a_1, a_2 and a_3 used for determining $K_{(H)}$ of the CFCs and SF_6 (after Warner and Weiss (1985), Bu and Warner (1995) and Bullister *et al.* (2002)).

The Henry's Law constants ($K_{(H)}$) are given in table 4.3 and graphed in Figure 3.2:

Temp (C)	CFC 11	CFC 12	CFC 113	CCl4	SF6
8	0.023631	0.00606	0.007379	0.07968	0.0004274
10	0.021131	0.005485	0.006528	0.073525	0.0003927
12	0.01898	0.004983	0.005801	0.067918	0.0003618
14	0.01712	0.004545	0.005178	0.062805	0.0003342
16	0.015508	0.004161	0.004641	0.058138	0.0003095
18	0.014105	0.003824	0.004178	0.053871	0.0002873
20	0.01288	0.003526	0.003776	0.049967	0.0002674
22	0.011807	0.003263	0.003426	0.046392	0.0002495
24	0.010865	0.00303	0.003121	0.043113	0.0002333

Table 3.3. Variations in $K_{(H)}$ for CFCs, CCl_4 and SF_6 from temperatures between 8 and 24°C. Values in molkg^{-1} atm^{-1}.

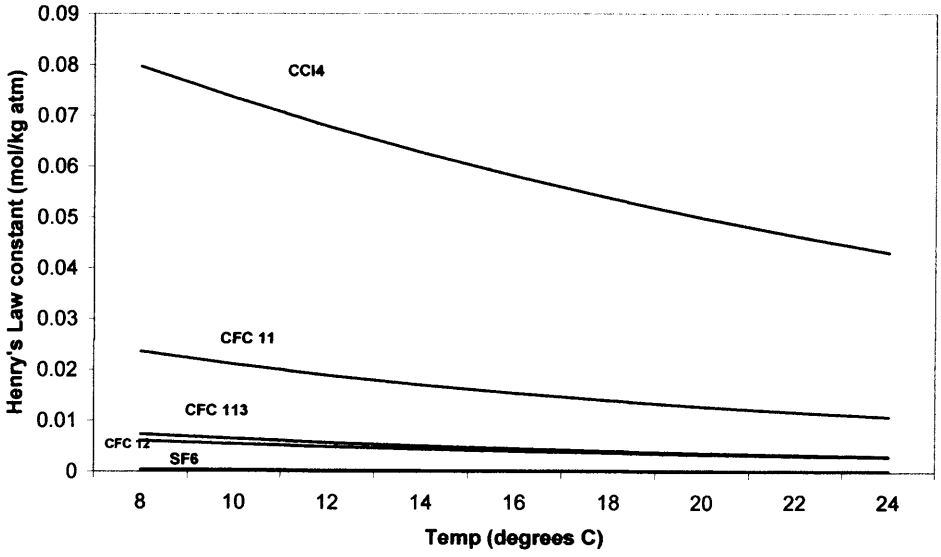

Figure 3.2. Variations in $K_{(H)}$ for CFCs, CCl_4 and SF_6 from temperatures between 8 and 24°C. Values in molkg^{-1} atm^{-1}.

As may be seen from the graph, there is generally an increase in $K_{(H)}$ (that is, an increase in solubility) with a decrease in temperature.

3.2.3.3 Units

The units used in this thesis are consistent with the majority of recent literature on the subject. For atmospheric or gaseous concentrations, figures are presented in parts per trillion by volume, or pptv. This is also known as the Atmospheric Mixing Ratio. For concentrations in water, figures are usually given in picograms per kilogram ($pgkg^{-1}$), 1 $pgkg^{-1}$ being synonymous with 1 part in every 10^{15} for pure water. Modern-day equilibrium concentrations in water ($pgkg^{-1}$) are equivalent to the atmospheric concentration (pptv) multiplied by both the molecular weight and the Henry's Law constant ($molkg^{-1}$ atm^{-1}).

3.3 BASIC PRINCIPLES OF DATING GROUNDWATER WITH CFCS AND SF_6

There are a number of assumptions associated with 'dating' groundwater using CFCs and SF_6. It should be noted that, due to susceptibility to degradation, CCl_4 is frequently omitted from CFC dating studies. The assumptions will be discussed in greater detail below, but firstly it is necessary to define what is meant by the term 'dating'.

When discussing CFCs and SF_6 (as opposed to other environmental tracers such as tritium) 'dating' groundwater refers to identifying the date at which a parcel of water became isolated from the unsaturated zone air, with which it is assumed to have been in equilibrium (Plummer and Busenberg, 1999). This means the point in time at which the parcel of water travels beneath the water table, and is also referred to as the 'recharge' age of groundwater. As the atmospheric history of CFCs and SF_6 is known, the history of recharge concentrations (based on the Henry's Law constants as described in Section 3.2), may also be calculated. It is on this basis that the dating principle operates. However, there are a number of considerations to be accounted for:

3.3.1 THE EFFECT OF THE UNSATURATED ZONE.

To reiterate, because equilibrium is assumed between unsaturated zone air and water at the surface of the water table, or water entering the water table, and because unsaturated zone air is assumed to be representative (in terms of CFCs and SF_6) of the atmosphere, Henry's Law may be used to calculate the concentration of CFCs and SF_6 in the recharging water. However, the second assumption is questionable for thick unsaturated zones (i.e. greater than a few metres). A number of studies have reported CFC concentrations at the base of thick unsaturated zones to be only a fraction of the atmospheric values at the time of sampling (Weeks *et al.*, 1982; Busenberg *et al.*, 1993; Cook and Solomon, 1995; Severinghaus *et al.*, 1997). This appears to be the case primarily for porous (i.e. non-fractured) media, where diffusion models perform well in the description of unsaturated zone profile data. Other factors of importance include porosity, pore tortuosity, sorption and the degree of water saturation of the unsaturated zone (Plummer and Busenberg, 1999).

In the case of a shallow water table and/or fractured media, the effects of 'barometric pumping' and thermal gradients result in much more rapid transport of present-day air to the water table. In these cases the assumption of unsaturated zone air being representative of the atmosphere is more likely to be valid. Plummer and Busenberg (1999) and Busenberg and Plummer (2000) state that, once water has entered the water table, CFCs and SF_6 will not significantly exchange with the unsaturated zone atmosphere because their diffusion rates in water are 5 orders of magnitude lower than they are in air.

Failure to account for the time it takes atmospheric air to travel to the water table will result in the model age (see next section) of the groundwater being too old.

3.3.2 MODEL AGE

Once the tracer has travelled beneath the water table, it then moves with the groundwater, but subject to numerous physical and chemical processes, such as dispersion, mixing, sorption and degradation. Because these processes need all be accounted for, the age of a water sample is usually stated as an 'apparent' or 'model' age. That is to say, the model used to describe the age of a groundwater is unlikely to account for all of the processes affecting transport, or at least may not describe the relevant processes accurately. A typical simplifying assumption is that of 'piston flow', whereby the water is assumed to move as a discrete plug through the aquifer. Age dating in fractured rock may be problematic because of both different concentration gradients (for different compounds) between fractures and matrix and different diffusion coefficients resulting in different rates of transport. Because of such effects, the age derived through comparison of CFC (or SF_6) concentrations with the calculated concentrations of historical recharge is only apparent. Thus 'apparent' or 'model' age of the groundwater.

In the Corallian limestone, groundwater transport is concentrated along fractures, bedding plane features and conduits of varying permeability. Some water may travel very rapidly from the point of recharge to the point of discharge, whereas some recharging water may be stored in less permeable fractures, and yet more in the (albeit low) primary porosity of the limestone. This means that water discharging at any spring or borehole is likely to be a mixture of waters of different ages.

CFC-containing groundwater may be mixtures between old (CFC free) groundwaters and young waters, or between different young (CFC containing) waters. A two-component mixture of present-day and CFC-free (pre-20th Century) groundwater will plot on the straight line in Figure 3.3. The area bounded by the curve (representing the ratio between CFC 113 and CFC 11 over time) and the straight mixing line will encapsulate any waters with a CFC composition resulting solely from atmospheric input (i.e. non-contaminated and non-degraded).

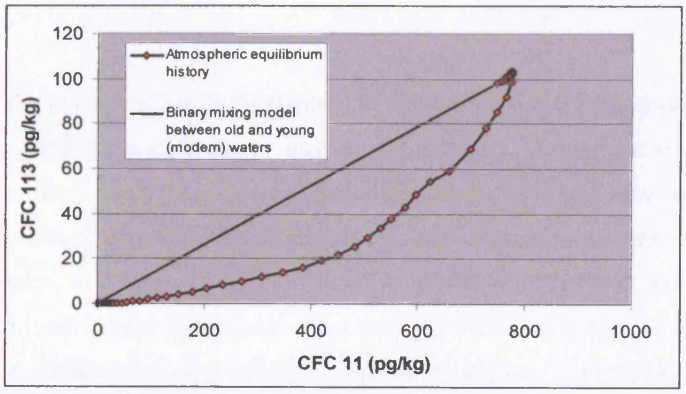

Figure 3.3. Envelope diagram of historical recharge ratios between CFC 113 and CFC 11, showing a mixing line between present-day and CFC-free groundwater end-members.

Computer models for determining groundwater age based on environmental tracers have been developed to the extent of LUMPED (Ozyurt and Bayari, 2003), which is an enhanced version of TRACER, a spreadsheet program for calculating the mean residence time of groundwater based on CFCs 11 and 12 and tritium (Bayari, 2002). TRACER employs either a piston flow, exponential mixing or linear mixing (or combination) model to simulate measured concentrations at a point. LUMPED enhances this capability with the capacity to use CFC 113, SF_6 and ^{85}Kr as environmental tracers, and also increases the number of possible models to 15. A similar spreadsheet program has been produced by the United States Geological Survey (USGS_CFC2004.xls) and is freely available at http://water.usgs.gov/lab/shared/software/USGS_CFC2004.xls. For data analysis purposes in this thesis piston-flow and binary mixing models are used to determine tentative groundwater recharge dates, and to examine the possible proportions of new and old waters mixing at springs and water wells. The appropriateness of these assumptions is discussed further in Chapter 7.

3.3.3 RECHARGE TEMPERATURE

As noted in Section 3.2, the Henry's Law constant is a function of temperature (Figure 3.2). Thus, to accurately reconstruct recharge concentration histories, the temperature (at the base of the unsaturated zone) at the time of recharge should be known. For this study a recharge temperature of 10° C is assumed on the basis of geophysical borehole logging temperature profiles (which is presented in Chapter 5). The effect of an incorrect recharge temperature of 2°C will be less than three years for a pre-1990 recharged water, and more than three years for a post-1990 recharged water (Plummer and Busenberg, 1999) (due to lesser or greater atmospheric concentrations over time).

Recharge pressure is also important, as the Henry's Law constants governing solubility have been calculated at 1 atm pressure (see section 3.1). Average barometric pressure is not usually known, but may be estimated from elevation (Ibid). Where this is less than 1000m (as in the Corallian) this effect can be ignored (Ibid).

3.3.4 EXCESS AIR

Excess air is the phenomenon of air being trapped in the unsaturated zone between recharging water and the water table, and dissolving due to increased hydrostatic pressure. It may happen either in fractures or at the capillary fringe, and can lead to the assignment of model ages that are too young (as the air entrained is younger than that already dissolved). The effect is more pronounced for post-1990 recharged groundwaters, but is usually negligible (Ibid). Wilson *et al.* (1990) (cited in Bateman, 1998) also working on the Lincolnshire Limestone, cite a value of 0.84×10^{-7} cm^3g^{-1}. If representative of the Corallian this would introduce an error of approximately 0.01% into a post-1990 water (for CFC 12 which is the most susceptible to excess air due to its lower solubility).

3.3.5 SORPTION

CFC 113 appears to be the CFC most susceptible to sorption. In column experiments with ground sand, Ciccioli *et al.* (1980) found no retardation of CFC 11, 12 or 113, but when using ground limestone they report retardation factors of 1.1, 1.0 and 1.5 respectively. Cook *et al.* (1995) found CFC 113 to be retarded in transport by 30-50% compared to CFC 12 in an aerobic silty-sand aquifer with low organic carbon. Brown (1980) (cited in Cook and Solomon, 1997) also reported retardation of CFCs 113 and (to a lesser extent) CFC 11 in column experiments with sand. Busenberg and Plummer (1993), however, found no such process operating in the Delmarva peninsular, apparent ages from CFCs 12 and 113 closely matching one another. For the unsaturated zone, Plummer *et al.* (1993) note that sorption is less likely to occur on wet sediments than dry, as CFCs compete with water molecules for absorption sites. This means that greater sorption of CFCs may be expected in unsaturated zones in arid areas.

In general, CFC 12 is reported as the CFC least susceptible to adsorption, CFC 113 the most, although not in all instances. Little literature appears to be available regarding the sorption characteristics of CCl_4, although this compound is of limited use for dating as it is degradable under oxic conditions (see next section). With respect to SF_6, however, Biggin (1991), Wilson and Mackay (1993, 1996) and Upstill-Goddard and Wilkins (1995) report that it is not retarded through sorption onto either natural organic or aquifer materials.

The effect of sorption on the apparent age of a water sample will be to make it appear older than it actually is.

3.3.6 DEGRADATION

There is an extensive literature concerning the degradation of CFCs in sediments and groundwater. Much of the work has been driven by the need to identify mechanisms for the removal of CFCs from the environment, due to their atmospheric impacts. Contributions also come from the waste management industry and it has been important to clarify CFC breakdown products, as they are often more toxic than the CFCs themselves (Hohener *et al.*, 2003).

As CFCs are recalcitrant in aerobic environments (Ibid) most research has focussed on anaerobic environments. CFC degradation pathways in nature are usually biologically mediated (Ibid.) and anaerobic environments displaying such CFC removal may be found in the oceans (e.g. Shapiro *et al.*, 1997; Lee *et al.*, 1999; Huhn *et al*, 2001), sediments (e.g. Lovley & Woodward, 1992), and groundwater (e.g. Oster *et al.*, 1996; Dunkle Shapiro *et al*, 1998; Kofod & Isenbeck-Schroter, 2000). CFCs have also been found to be degraded through reaction with zero-valent iron (Scheutz *et al.*, 2000) and in reactions involving palladium and metal carbide catalysts (Hohener *et al.*, 2003).

Khalil and Rasmussen (1989, 1990) were the first to report CFC degradation in anaerobic soils (termite mounds and rice paddies). They identify dechlorination of CFCs 11 and 12. Lesage *et al* (1990) discuss the degradation products resulting from reductive dechlorination and reductive defluorination of CFC 113. As this was the VOC of greatest concentration in their study (see also Section 3.4.2, Gloucester landfill) they collaborated with other research groups to conduct batch experiments, detailed in Lesage *et al.* (1992), and in Lesage *et al.* (1993). The latter examined CFC 113 degradation in anaerobic leachate holding tanks and anaerobic batch experiments, concluding that the half life of this compound was 18 days (for the holding tanks) and 5 days (for the batch experiments). The difference between the two values was ascribed to better environmental regulation during the batch experiments.

Denovan and Strand (1992) studied, under laboratory conditions, the microbial degradation of CFCs 11, 12 and 113. They compared degradation rates for experiments using micro-organisms taken from landfill leachate and from non-contaminated sediments, finding that the acclimated biomass degraded CFCs faster. Other laboratory experiments include the simulation of landfill conditions (Deipser and Stegman, 1997); biodegradation of CFCs, hydrofluorocarbons (HCFCs) and vinyl chloride in compost and marl (Deipser, 1998) and reduction of CFCs 11 and 12 under sulphate-reducing conditions (Lovely and Woodward, 1992).

Semprini *et al.* (1992), showed degradation of CCl_4 and CFCs 11 and 113 in a confined aquifer under artificially induced anaerobic conditions. By injecting the CFCs alongside acetate as a growth substrate and nitrate and sulphate as electron receptors, they found that CFC 11 was degraded by 3 times as much as CFC 113 (68% and 20% respectively), and CCl_4 was almost totally degraded (95%) over the ten-week test period.

Happell and Wallace (1998) demonstrate that CCl_4 can be removed under aerobic conditions in the unsaturated zone, using CFCs 11, 12 and 113 as non-reactive analogues. Happell *et al.* (2003) followed this work with an interesting study of CFC removal at the groundwater/surface water interface beneath slow-flowing surface waters in the Florida Everglades. Their study reports losses of between 50 and 90% for CFCs 11, 12 and 113 occurring within the upper 5cm of anoxic river bed sediment. Kofod and Isenbeck-Schroter (2000) (cited in Hohener *et al.*, 2003) also report a similar finding. Bauer and Yavitt (1995) find CFC 11 and 12 removals in anaerobic soils from two sites in New York State, concluding that such sites (bogs) are important sinks for the global CFC budget.

Importantly, both the Bauer and Yavitt (1995) and the Happell *et al.* (2003) studies describe a correlation between CFC reduction and an increase in methane concentration. Cook *et al.* (1995) had demonstrated CFC 12 stability under sulphate reducing conditions in an aquifer where CFC 11 was almost totally degraded, and Plummer *et al.* (1998b) demonstrate the almost complete degradation of CFC 11 and 113 within sealed ampoules of river water after 400 days, whereas they found CFC 12 not to degrade under identical conditions. Katz *et al.* (2001) note CFC 11 degradation in nitrate contaminated limestone groundwater and Shapiro *et al.* (1998) found degradation of both CFC 11 and CFC 12 under methanogenic conditions. These findings agree with the observations of Plummer and

Busenberg (1999) that methanogenesis is a prerequisite for degradation of all CFCs. Their explanation is that sulphate out-competes CFC 12 as an electron receptor, and therefore once the reducing environment has gone beyond the reduction of all sulphate (i.e. has become methanogenic), CFC 12 is degraded.

To recap, CFCs 11 and 113 are both significantly more degradable than CFC 12 in natural environments and laboratory analogues. However, all three are degradable under methanogenic conditions. Both the relative degradability and rates of degradation (half-lives) for the CFCs vary considerably between studies. CFC 11 degradation is reported between 10 (Oster *et al.*, 1996) and 600 (Shapiro *et al.*, 1997) times that of CFC 12, the differences being due to variability between individual anaerobic environments. Good agreement in dating between different CFCs is usually cited as evidence of their reliability and poor agreement, conversely, as evidence of degradation or contamination effects (although this view neglects the effects of different diffusion coefficients of the three CFCs). The best review work on CFC degradation is that of Plummer and Busenberg (1999) and Hohener *et al.* (2003). It should be noted that even though CFCs are degradeable, the second-most degradable (CFC 113) was found to be the organic compound most persistent (of 37 hazardous organic compounds) over a decadal timescale (Lesage *et al.*, 1990). The effects of CFC degradation will be that apparent ages are older than actual water ages.

In contrast to the CFCs, SF_6 degradation does not appear to occur under even methanogenic conditions (Watson *et al.*, 1991; Busenberg and Plummer, 2000), and it is noted elsewhere to be an exceptionally stable molecule in groundwater (Wilson and Mackay, 1993; 1996). Thus it is likely to provide both a good dating tool in itself, and also a good constraint on CFC dating (unfortunately this aspect is not pursued further in this study due to detection limit limitations for SF_6).

3.3.7 SUMMARY OF SECTION 3.3

This section has outlined and reviewed the main work associated with the CFC/SF_6 groundwater dating technique. Table 3.4 summarises the effects that failure to account for the above factors (Sections 3.3.1 to 3.3.6) will have on model age (adapted from Plummer and Busenberg (1999)).

Factor	Effect on model age
Thick unsaturated zone	Too old
Choice of flow model	Either too young or too old
Recharge temperature	Overestimated: Too young Underestimated: Too old
Recharge pressure	Overestimated: Too old Underestimated: Too young
Excess air	Too young
Sorption	Too old
Degradation	Too old
Contamination	Too young/Impossible to date

Table 3.4. Summary of factors affecting model groundwater ages

3.4 REVIEW OF SF_6 AND CFC APPLICATIONS IN THE HYDROLOGICAL SCIENCES.

3.4.1 CFCS, CCL_4 AND SF_6 AS ENVIRONMENTAL TRACERS

Following James Lovelock's first atmospheric measurements of CFC 11 in 1970 (Lovelock, 1971), the use of chlorofluorocarbons as hydrologic tracers was reported by a handful of workers throughout the remainder of the decade, both in the published literature (Thompson *et al.*, 1974; Schultz *et al.*, 1976; Hahne *et al.*, 1978; Thompson and Hayes, 1979;), and the unpublished (Randall and Schultz, 1976; Thompson 1976; Hayes and Thompson 1977; Randall *et al.*, 1977; Schultz, 1979 (all cited in Plummer and Busenberg, 1999)). These workers had realised that a natural water could be identified as having been in contact with the atmosphere during the 20th Century should it contain CFCs or CCl_4. However, it was Randall and Schultz (1976) who were the first of these pioneers to note that this 'dating' technique could be improved if one were to know more accurately the input-function (to be derived via Henry's Law from a reconstructed atmospheric history) of the CFCs and CCl_4 (see Sections 3.2 and 3.3).

This foundation was built upon in the 1980s as the oceanographic community refined the necessary analytical techniques (e.g. Bullister and Weiss, 1988) and developed greater understanding of the Henry's Law constants governing solubility (see Section 3.1). Up until the early 1990s much of the work was limited to field applications, as sample preservation was found to be poor, primarily due to CFC diffusion through, and sorption to, sampling materials (Plummer and Busenberg, 1999). Improvements in sampling methodology came with the application of CFC dating techniques to groundwater, Busenberg and Plummer (1992) being the first to use flame-sealed borosilicate glass ampoules to isolate samples from the atmosphere. This then opened the way for other workers, and a profusion of CFC groundwater age-dating studies followed. Significant contributions during the 1990s were made by Dunkle *et al.* (1993), Busenberg *et al.* (1993), Plummer *et al.* (1993), Ekwurzel *et al.* (1994), Reilly *et al.* (1994), Katz *et al.* (1995), Cook *et al.* (1995), Cook *et al.* (1996), Cook and Solomon (1995), Cook and Solomon (1997), Szabo *et al.* (1996), Oster *et al.* (1996), Bateman (1998), Johnston *et al.* (1998), Plummer *et al.* (1998 A & B). By 1999 the technique was sufficiently established to command the comprehensive review of Plummer and Busenberg (1999), a textbook chapter (Cook and Herczeg (eds), 1999).

These workers have studied CFC concentrations in a wide variety of groundwater settings, ranging from natural (background, non-anthropogenic) levels in volcanic springs, to anthropogenic contamination several orders of magnitude above atmospheric equilibrium. At the time of writing CFCs have become part of a standard suite of environmental tracers used for dating groundwater, often being used in conjunction with noble gases, radioactive isotopes (^{222}Rn, ^{3}H, ^{85}K), stable isotopes ($\delta^{18}O$, $\delta^{2}H$), and SF_6. Examples of such multi-tracer studies may be found in Plummer *et al.* (1998 A and B), Beyerle *et al.* (1999), Nativ *et al.* (1999), Plummer *et al.* (2000), Bauer *et al.* (2001), Zoellmann *et al.* (2001) and Cook *et al.* (2003).

SF_6 has been used as an environmental hydrologic tracer in the same manner as the CFCs once it was recognised that it too had a time-dependent input function into the atmosphere over the second half of the 20th Century (Figure 3.1). However, the first measurements of SF_6 had again been made by Lovelock (1971), who in 1970 reported the atmospheric concentration of SF_6 to be 0.03 pptv. The atmospheric histories of SF_6 and CCl_4 from 1970 to 1983 were reconstructed by Watson and Liddicoat (1985) based on oceanic depth profiles constrained by CFCs 11 and 12. This was later refined by Maiss and Levin (1994), based on production data, and then extended back to the time of first production (Maiss *et al.*, 1996; Geller *et al*, 1997; Maiss and Brenninkmeijer, 1998). The first published study to use SF_6 as a dating tool for groundwater was that of Busenberg and Plummer (1997). Later studies include Plummer and Busenberg (1999), Busenberg and Plummer (2000), Bauer *et al.* (2001), Plummer *et al.* (2001), Zoellmann *et al.* (2001) and Vollmer and Weiss (2002). Busenberg and Plummer (1997), Harnisch and Eisenhauer (1998) and Busenberg and Plummer (2000) all measure natural SF_6 concentrations in a variety of groundwaters and rock samples, concluding that volcanic activity can produce SF_6 above background atmospheric concentrations and should therefore be accounted for in dating studies.

3.4.2 GROUNDWATER CONTAMINATION STUDIES USING CFCS, CCL_4 OR SF_6

A large proportion of groundwater studies attempting to date groundwaters have reported CFC contamination of aquifers. The first of these was Thompson and Hayes (1979), who identified a CFC 11-enriched plume extending 74 km eastward along a fault in the Edwards limestone aquifer (USA). The contamination of groundwaters with CFCs is comprehensively reported by Hohener *et al.* (2003), with two-thirds of the 24 studies they review reporting contamination of samples. Typical examples of CFC contaminant studies include those of Bohlke and Denver (1995) and Dunkle Shapiro *et al.* (2004), briefly described here to illustrate the versatility of the methods.

Bohlke and Denver (1995) describe a 40 year history of halocarbon contamination of the Danube River in Hungary by examining water in an adjacent gravel aquifer. Aquifer recharge moves through the gravels away from the river and groundwater ages are constrained using ^3H and He ratios. They note peaks in halocarbon loading of the aquifer occurring in the 1960s and 1970s, coincident with episodes of major industrial expansion, but decreasing subsequently. In contrast to this study, where CFCs contamination is constrained by other environmental tracer data, Dunkle Shapiro *et al.* (2004) reconstruct halogenated volatile organic compound (HVOC) inputs to groundwater-sourced drinking water supplies in the US over last 40 years by re-examination of chromatograms archived during previous CFC sampling campaigns. Data from 413 different wells indicates an unchanging detection frequency of HVOCs, but a general increase in concentrations above atmospheric equilibrium between 1940 and 2000, sample ages being determined through CFC dating. At least three HVOCs were found in 100% of samples.

However, despite such successes on the contaminant front, only Lesage *et al.* (1990), Bateman (1998) and Atkinson (2002) have sought to characterise landfill contamination of groundwaters through the use of CFCs, although other workers have identified elevated CFC concentrations in landfill gases (Brookes and Young, 1983; Deipser and Stegmann, 1994; Foskett, 1994; Ward *et al.*, 1996). This is potentially a very important method for identifying landfill impacts, as CFCs may be detectable after considerably greater dilution (dilution factor of 4000 for CFC 12, (Bateman, 1998)) than more commonly used indicators such as chloride and ammonia (as low as a factor 10 dilution (Ibid)). This thesis develops and discusses the work of both Bateman (1998) and Atkinson (2002) through comparison and interpretation of CFC measurements made at Seamer Carr landfill, Yorkshire, UK (Chapter 8).

SF_6 has been used to constrain groundwater ages for the purpose of predicting nitrate levels in wells under certain catchment-loading conditions (Zoellmann *et al.*, 2001). Beyond this it has been used as a partitioning tracer for identifying NAPL contamination of the saturated and unsaturated zones. Although this application is beyond the scope of this review, the interested reader is referred to the following (non-exhaustive) list for more detailed information: Wilson and Mackay (1995); Annable *et al.* (1998a and b); Werner and Hohener (2002).

3.4.3 SF_6 AND CFCS AS ARTIFICIAL GROUNDWATER TRACERS

3.4.3.1 CFCs

The first (recorded) use of a CFC as an artificial tracer was contemporaneous with the first measurements of environmental levels in groundwater, and reported by the same authors (Thompson *et al.*, 1974). They injected a solution containing fluorescein and 100 $mgkg^{-1}$ CFC 11 into a sand and gravel aquifer, recording that the CFC arrived at a monitoring well in the time expected, but that fluorescein did not. However, subsequent to this, there appears to be virtually nothing in the literature covering the application of CFCs as artificial tracers. This may be due to the utility that they offer in terms of natural dating, and indeed the focus has been on this aspect. In this respect it should be noted that, with the wilful introduction of CFCs (or SF_6) to an aquifer, the possibility to date the groundwater using this method is then lost.

3.4.3.2 SF_6

Although there have been some studies, SF_6 has had only limited use as an artificial groundwater tracer. The following is a review of all of the known work that has been undertaken in this field. The review does not include work describing the use of the gas as a partitioning tracer for the identification of non-aqueous-phase liquids in the unsaturated zone, nor its application to tracing in non-groundwater environments.

The first known application of SF_6 to groundwater tracing is in an unpublished report for the UK Institute of Hydrology (Biggin, 1991). This report describes the development of an analytical technique for the analysis of SF_6, a study of the behaviour of SF_6 in batch experiments with different geological materials, a study of the degassing rate of SF_6 saturated solutions, a study of background levels in the atmosphere and groundwater, and the use of SF_6 as a tracer of groundwater in confined and unconfined gravels and in a karst conduit. This series of experiments is the most comprehensive to have been performed using SF_6 in groundwater and is described in more detail below:

The materials chosen for the batch experiments were siliceous sand, calcareous sand, powdered chalk, montmorillonite clay and peat. These were expected to show a range of adsorption characteristics. However, the results from all batches were erratic and inexplicable with reference to the geological materials chosen. It was therefore concluded that sorption to, or diffusion through, the plastic bottle caps used was the reason for the results. However, as no geologic material showed either consistent or large uptake of tracer, the experimental results were taken to indicate that sorption would not be an important process affecting SF_6 in groundwater tracing experiments.

The degassing experiment found that, in an open, straight-sided, glass beaker the concentration decreased exponentially with time, with about a 35% loss within 5 hours. 100% losses were recorded at less than 120 hours.

The results from the karst study showed that, in a vadose conduit (i.e. one with an open water surface), all of the SF_6 was lost from solution. However, the three experiments over short distances (up to 100 m) in the gravels gave better results. The first two of these experiments were in unconfined gravels and designed with the aim of testing how significantly degassing would affect tracer performance. Positive results were obtained in both experiments, with SF_6 peaks being recorded at up to 50 days (following injection) in the second experiment, thus indicating that complete degassing was not a problem under laminar flow conditions. Furthermore, the SF_6 outperformed both Rhodamine WT and iodide in terms of first arrival and recovery. However, results from these tests did show numerous and messy peaks that may be due to volatilisation and subsequent re-dissolution of tracer gas. In the confined gravel the results were similar to the second unconfined test, with much better recovery of SF_6 than Rhodamine WT, as well as better defined peaking.

Thus, Biggin (1991) successfully applied SF_6 to tracing groundwater under laminar, Darcian flow conditions in shallow, unconsolidated sediments. These experiments were augmented by studies of degassing and sorption. Biggin (1991) did not, however, examine flow through fissured or potentially dual porosity media. Instead, his karst experiment was confined to an open conduit in which a large surface area of water was present, as well as rapids and riffles, and thus degassing led to the conclusion that SF_6 was inappropriate for such systems.

Subsequent to the work of Biggin (1991) was that of Wilson and Mackay (1993), who examined two aspects of SF_6 tracer performance. The first was a column experiment comparing SF_6 transport to that

of bromide (a conservative, ionic tracer). The SF_6 behaved almost identically to the bromide, although there was greater variability in the SF_6 data. The second aspect was to test a method by which a tracer solution may be saturated with SF_6. The method was to permit the gas to diffuse through a PTFE tube into the tracer volume, which resulted in the unsatisfactory final tracer concentration of only 15% of SF_6 solubility after 18 hours (40 mgL^{-1} at STP according to Morrison & Johnstone, 1955). One important facet of SF_6 tracer use noted by the authors is that an SF_6 saturated solution should be injected only beneath the water table, as mass loss to the unsaturated zone will severely affect tracer performance (Wilson and Mackay, 1993).

The next piece of work in the literature describes 'The potential for SF_6 as a geothermal tracer' (Upstill-Goddard and Wilkins, 1994). These workers injected SF_6 and sodium fluorescein into water being pumped into the 'hot dry rock' (HDR) geothermal reservoir at Rosemanowes in south-west England. The purpose of the study was to see whether SF_6 would perform under heated conditions (<80°C). Upstill-Goddard had previous experience of SF_6 tracer use in both lakes (Upstill-Goddard *et al.*, 1990) and oceanic waters (Upstill-Goddard *et al.*, 1991). The results from the geothermal reservoir tracer test were promising, and:

"...we confidently predict that SF_6 will find increasing use as a tracer in the geo- and hydro-sciences."

(Upstill-Goddard and Wilkins, 1994),

But actually the experiment had been stopped after 52 hours due to a technical fault in the analysis of SF_6. Nonetheless, this was long enough to identify differential behaviour between the two tracers, ascribed to selective diffusion along the longer flow paths between the injection and abstraction wells.

Also in 1994, although unpublished, was a pilot study by an MSc student at the University of East Anglia (UEA) (Strongman, 1994), who used SF_6 alongside CFC 11 and CFC 113 in a karst conduit in northern England (White Scar Cave). The very low recovery of 0.0029% of SF_6 was not considered encouraging, but agreed with the work performed by Biggin (1991). Again, the karst conduit was vadose and therefore the potential for atmospheric partitioning was very high. An almost identical result was recorded by Robinson (1996), another UEA MSc student, who again used CFCs 11, 113 and SF_6 within a vadose karst conduit (Wookey Hole). The SF_6 recovery this time was 3.7%, those of CFCs 11 and 113 8.3% and 91% respectively. The control tracer dye, rhodamine WT, had 103% recovery.

The next published study was again from Wilson and Mackay (1996), and repeated both of the aims of the previous work, but further including measurements of the octanol-water partition co-efficient of SF_6 (see also Section 3.3.5). The refined tracer preparation method (still using diffusion through PTFE tubing) achieved a tracer concentration 60-80% of SF_6 solubility. Three column experiments with different media (glass beads, carbonate sand and high-organic-fraction carbon sand (2.5%)) were conducted, SF_6 showing negligible difference in behaviour to bromide in two of the experiments. In the

third (carbonate sand), however, subtle differences in breakthrough tailing are reported. These were not fully understood but posited to be a function of the relatively large intragranular porosity of this media as compared to the other two. The octanol-water partition experiment, combined with the result from the high organic carbon sand, demonstrated that SF_6 would not significantly partition to solid organic phases but would partition to liquid organic phases. The partition coefficient derived is stated as unsuitable for application to geologic materials. The authors also include the following strong justification for further development of SF_6 as a groundwater tracer:

"The advantages gained in the use of gases like SF_6 over the more conventional ionic compounds for non-reactive conservative tracing should in many cases outweigh the disadvantages. However, the relatively new field of gas tracer research has not yielded enough data to allow the assessment of their transport behaviour in all geologic settings. This poor understanding of the behaviour of gas tracers in saturated porous media with a wider range of geologic properties suggests that more study is necessary if gases like SF_6 are to be widely applied as injected non-reactive conservative tracers."

The challenge has not been widely taken up. One research group (Department of Oceanography, Florida State University) has produced four papers on the subject, and another (Geological Sciences, University of California,) has produced a single paper. As this work comprises all of the recent literature on the topic, all of these articles are reviewed in more detail below, beginning with the four papers (Florida State) that may be grouped together:

Dillon *et al.* (1999), describes two types of experiment performed in, respectively, coastal Miami (oolitic) and Key Largo (coralline) limestones. Experiment Type I was repeated a total of three times at two different locations (sites A and B). 70 L slugs of SF_6 sparged water were flushed down residential toilets into septic tanks, to see whether the tanks (in the unsaturated zone, c. 1 m below ground level) were influencing (drinking) water quality in the shallow fresh-water lens (5-8 m thick) perched atop a much larger saline water body. Targets (wells, 2 m deep) were 20 and 27 m from the septic tanks. Experiment Type II injected SF_6 into the Big Pine Key limestone (which has no freshwater lens) either by simply sparging the water in a small-diameter screened borehole, or by removing up to 100 L of water from the borehole, sparging it and then re-injecting. The targets were a monitoring well (3 m distant) and Florida Bay, 26 m distant.

In both cases the limestones are karstic, unconfined and subject to tidal oscillation, although the magnitude of this effect is not reported for the Type I experiments. The results of the Type I experiments are:

1. Significant contamination of samples taken immediately following injection at site A.
2. Increased background levels (240 times atmospheric equilibrium) at Site B (two blocks distant from Site A) prior to the third experiment (6 months after the first).
3. Increased background levels at Site A but no conclusive breakthrough.

The Type II experimental results also illustrate problems: three separate injections are performed, the hydraulic gradient changes direction (due to tides) several times during the experiment and, by the end of the experiments, there is confusion regarding which injection was responsible for which peak, and the PVC well casing had also become contaminated.

The next paper (Corbett *et al.,* 2000a) describes SF_6 use as a conservative tracer to identify the extent of nutrient uptake (phosphate and nitrate) in, and movement of, saline groundwaters of the Key Largo limestone, again in the Florida Keys. Radioactive ^{131}I (iodine) was also used as a conservative tracer in one of three experiments performed at the same site with four month intervals. The injection method was to bubble SF_6 through 200 L of water contained in an open drum, which was then siphoned into a waste-water disposal well (27 m deep, cased to 18 m), followed by 1000 L of waste water. The results were better than the previously reported work (Dillon *et al..,* 1999), with the SF_6 and ^{131}I tracers behaving similar to one another (with some apparent loss of SF_6). Groundwater velocities based on SF_6 transport varied by a factor of 20 (over 5 m) between experiments, which is explained by reference to changing tidal and climatic conditions.

Corbett *et al.* (2000b) conduct three tracer tests with SF_6, again to examine the transport of septic tank wastes, although on this occasion through a thin (7-10 m), coastal, unconfined, medium-fine sand aquifer overlying a silty-clay aquitard on St. George's Island, Florida. The experiments are performed by injecting 190 L tracer volumes (sparged with SF_6) directly into the drainfields associated with the septic tanks (and not into the tanks themselves). The first site drainfield was however raised c. 1 m above the surrounding ground, and therefore the tracer was injected directly into the unsaturated zone. No results were recorded from this experiment. In the other two experiments the tracer was injected either directly into or just above the saturated zone (it is not clear from the paper). Following injection the experiments ran for in excess of 250 days, during which time only very low transport velocities are recorded alongside small dilution factors (3-5) and peaks at various monitoring wells (c. 3 m deep) occurring at 55 – 290 days. This is a more encouraging result, as it seems to indicate that much of the injected tracer remained within the groundwater.

The fourth paper from the group (Harden *et al.*, (2003)), reports experiments designed to compare the tracers SF_6, fluorescein, rhodamine and a bacteriophage, although the field application is essentially the same as that of Corbett *et al.* (2000b), namely mounded drainfield sites in a shallow, sandy, unconfined, coastal aquifer. The injection methodology is the same, and again an earlier experiment seriously interferes with the results of a later experiment. Furthermore, the interpretation of the results comparing the behaviour of the tracers takes no account of the fact that the SF_6 was injected into the unsaturated zone and could easily have been affected by unsaturated zone migration and subject to an 'excess air' phenomenon following the heavy rainfall the authors note. It is therefore feasible that the findings of Harden *et al.*, (2003) are open to a significantly different interpretation than that given by the authors of the paper.

The fifth paper (Gamlin *et al.*, 2001) describes an experiment in which SF_6 was added to a 9 km stretch of infiltrating river (Santa Anna River, California) to examine subsequent groundwater movement. The experiment managed to trace groundwater over a period of 18 months following injection, finding average groundwater movement to be c. 2 km yr^{-1}, thereby demonstrating the long term applicability of the method. Again in this experiment significant losses from the surface water prevented any tracer mass balance being performed, although it was calculated that three million m^3 of water were successfully marked by tracer.

From these five papers (Dillon *et al.*, 1999; Corbett *et al.*, 2000a and b; Harden *et al.*, 2003; Gamlin *et al.*, 2001) a number of lessons may be drawn. The main ones are as follows:

- Care should be taken not to contaminate the field site.
- Bubbling SF_6 through an open container or well clearly results in a large gas release in the immediate vicinity of the sampling points.
- Injection of tracer solution into the unsaturated zone may lead to 100% tracer loss (Corbett *et al.*, 2000b).
- SF_6 tracer injection into either the unsaturated zone or a shallow, unconfined water table may lead to gas migration throughout the field area. The 'excess air' phenomenon following heavy rainfall may thus contaminate the entire field site.
- Multiple injections are unfeasible.

3.5 ENVIRONMENTAL IMPACTS AND INTERNATIONAL LEGISLATION.

CFCs are well publicised ozone-depleting and greenhouse gases (Table 3.5). The importance of the former led to the introduction of legislation (The Montreal Protocol) curbing production of the most common CFCs, which in turn resulted in the promotion of replacement gases for industrial/commercial applications (usually hydrofluorocarbons). These replacements are also controlled, but under the later Kyoto Protocol (1997), which has yet to be ratified by some leading industrial nations. The reason for the failure of some industrial nations to ratify the Kyoto Protocol is because of its call for major reductions in carbon dioxide emissions. Emissions of methane, nitrous oxide, hydrofluorocarbons, perfluorocarbons and sulphur hexafluoride are also to be significantly controlled (The Kyoto Protocol to the United Nations Framework Convention on Climate Change, 1997).

	pptv (atm) AD1750	pptv (atm) AD1998	Global Warming Potential (100yr horizon)	Atmospheric lifetime (years)
CO2	280	367	1	50-200
CFC 11	0	268	4600	45
CFC 12	0	533	10600	100
CFC 113	0	84	6000	85
CCl4	0	102	1800	35
SF6	0	4.2	22200	3200

Table 3.5 Atmospheric abundance, Global Warming Potentials and atmospheric lifetimes of CFCs 11, 12 and 113, CCl_4 and SF_6. All figures from Intergovernmental Panel on Climate Change (2001).

Elkins (1999) describes the Montreal Protocol as follows:

" In 1987, 27 nations signed a global environmental treaty, the Montreal Protocol to Reduce Substances that Deplete the Ozone Layer[9], that had a provision to reduce 1986 production levels of these compounds by 50% before the year 2000. This international agreement included restrictions on production of CFC-11, -12, -113, -114, -115, and the Halons (chemicals used as fire extinguishing agents). An amendment approved in London in 1990 was more forceful and called for the elimination of production by the year 2000. The chlorinated solvents, methyl chloroform (CH_3CCl_3), and carbon tetrachloride (CCl_4) were added to the London Amendment."

The Montreal Protocol is notable as one of the most successful pieces of international environmental legislation in history. The Kyoto protocol is representative of the more widespread subjugation of environmental law to the interests of economic growth. The effects of the legislation can be observed in Figure 3.1.

In terms of studies using SF_6 as an artificial tracer, its Global Warming Potential is usually ignored. Typically it is referred to as a suitable tracer due to its conservative properties and ease of detection at

[9] *Montreal Protocol on Substances that Deplete the Ozone Layer*, 15 pp, United Nations Environmental Programme (UNEP), New York, 1987.

very low concentrations (e.g. Upstill-Goddard and Wilkins, 1995; Wilson and Mackay, 1995; Dillon *et al.*, 1999; Corbett *et al.*, 2000 A & B; Hirtz *et al.*, 2001; Boyd and Law, 2001). It has also been claimed that release of SF_6 to the atmosphere 'will pose no adverse environmental impact' (Wilson and Mackay, 1993). One group of authors refer to it as 'an environmentally friendly gas tracer' (Huisman *et al.*, 2004 A), in obvious ignorance of its enormous and well publicised Global Warming Potential (IPCC, 2001), greater than that of any other gas known to man. Thus, with an atmospheric lifetime of 3200 years, releasing SF_6 is not something that can be undone on the timescale of human civilisation.

For fuller reviews on the ozone depleting nature and greenhouse warming potential of the CFCs, CCl_4 and SF_6, the reader is referred to the Intergovernmental Panel on Climate Change (IPCC) at http://www.grida.no/climate/ipcc_tar/wg1/index.htm.

3.6 SUMMARY OF CHAPTER 3

Chapter 3 has introduced the CFCs, CCl_4 and SF_6 as hydrologic tracers, in both their environmental and artificial capacities.

As environmental tracers, it has been outlined how these compounds came to be identified as potential water tracing and age dating tools, and how subsequently various technical and conceptual improvements have refined their application. The chemistry and atmospheric history of these compounds, approaches to interpreting results in terms of groundwater age, as well as factors responsible for changes in their concentrations within the ground, have been discussed.

In terms of their use as artificial water tracers, introduced specifically to track hydrological processes, this chapter has provided a comprehensive review. From this it may be seen how work presented in the literature has not met the requirements of fully developing a groundwater tracer suitable for quantitative use in public water supplies, a need identified in Chapter 1.

The chapter has also summarised the environmental legislation governing use of these tracers, and discussed them with reference to their significant global warming and ozone-depletion potential.

CHAPTER FOUR

METHODS AND EXPERIMENTS

It is one thing to show a man that he is in error, and another to put him in possession of truth.

John Locke (1690)
An essay concerning human understanding

4.1 INTRODUCTION

This chapter introduces the different types of experiments and measurements performed, and it describes the analytical methods with which measurements were made.

The descriptions begin with single-borehole experiments, detailing two types of experiment: borehole dilution gauging and vertical single-well tracer tests. The chapter continues by listing the tracer tests conducted between different points in the aquifer and the methodological protocols maintained. The tracer tests are divided into those employing conventional water-tracing substances (i.e. fluorescent dyes) and that employing sulphur hexafluoride. The injection system developed for the SF_6 tracer method is then described and its performance evaluated.

The remainder of the chapter is given to describing the analytical methods used for quantifying the fluorescent dyes and CFCs, CCl_4 and SF_6. These are detailed in terms of the exact instrumentation and components employed, the settings at which the instruments were programmed to run, and the degree of precision and uncertainty found in the results.

4.2 TYPES AND LOCATIONS OF EXPERIMENTS

4.2.1 BOREHOLE DILUTION TESTS

Several single borehole experiments were conducted on boreholes in Forge Valley and the Vale of Pickering. The majority were borehole dilution tests, but the method was adapted to include one vertical flow test in a borehole showing extremely swift tracer dilution. Experimental details are given in Section 4.3. Locations of all single borehole experiments are given, along with details of the tracers used, in Table 4.1 (see also Figure 2.16). The boreholes were distributed such that results would permit a comparison of flow conditions to be made between the immediate vicinity of the swallowholes, the edge of the unconfined zone, and in the confined zone. A location diagram of the experiments is shown together with the experimental results and data modelling in the next chapter.

Date	Borehole	Grid reference	Tracer	BHDT or Vertical flow	Duration (days)
28/07/2002	Seavegate Gill	SE 990 857	Photine CAQ	BHDT	1
29/07/2002	Brompton Dale Shallow	SE 943 823	Sodium Chloride	BHDT	2
29/07/2002	Brompton Dale Deep	SE 943 823	Sodium Chloride	BHDT	2
01/04/2003	Wykeham	SE 968 835	Sodium Chloride	BHDT	2
08/04/2003	Seavegate Gill	SE 990 857	Sodium Chloride	VF	2
11/04/2003	Derwent Ford	SE 992 844	Sodium Chloride	BHDT	2
12/04/2003	Swallowholes Borehole	SE 990 852	Sodium Chloride	BHDT	2
12/04/2003	Augmentation Borehole	SE 990 852	Sodium Chloride	BHDT	2
13/04/2003	Tetherings Plump	SE 976 827	Sodium Chloride	BHDT	2

Table 4.1. Details of tracers used in single borehole experiments

4.2.2 TRACER TESTS

Figure 2.16 also shows the different injection points for tracer tests, with Table 4.2 summarising the experiments. Fluorescent dye tracer tests were conducted between the following locations:

1) The Forge Valley Swallowholes and Irton (and the wider aquifer).
2) Seavegate Gill and McCains.
3) The Swallowholes Borehole and the wider aquifer (i.e. several boreholes).
4) Between the Brompton Vale observation boreholes and Brompton Springs.

There was often more than one experiment per location/target (Table 4.2) as the first tests always used the minimum amount of dye calculated as necessary to create a breakthrough curve (using equations provided by the Environment Agency (see Section 4.4.1.2 below and Environment Agency, 1998). These conservative estimates sometimes failed to produce a breakthrough curve.

The experiments may be divided into two types: 'Forced gradient' (i.e. toward or in the vicinity of an abstraction) or 'Natural gradient' (i.e. under the undisturbed conditions found in the aquifer). All but the Brompton Springs tracer tests fall into the former category. However, as the pumped condition is

the usual condition of the aquifer in the vicinity of the swallowholes (circa 2 km from Irton), the results may be considered representative of prevailing conditions. The various influences of pumping rate influence, groundwater levels and river losses to groundwater are discussed in Chapter 6.

All experiments were conducted after having submitted method statements to, and obtained the permissions of, the Environment Agency and Yorkshire Water Services Ltd..

Date	Target/s	Injection Borehole	Grid reference	Injection Depth (m)	Tracer	Amount (g)	Duration (days)	Passive detector (PD) Water Samples (WS)
21/05/2002	Irton	Forge Valley swallowholes	SE 990 852	NA	Fluorescein	2.86	1.5	WS
31/07/2004	Irton	Forge Valley swallowholes	SE 990 852	NA	Fluorescein	5	2	WS
01/07/2002	McCains & Irton	Seavegate Gill	SE 990 857	8.1	Photine CAQ	8.4	5	PD
Apr-03	McCains & Irton	Seavegate Gill	SE 990 857	9.1	Fluorescein	18.1	7	WS & PD
Apr-03	Local boreholes	Swallowholes Borehole	SE 990 852	23	Photine CAQ	54	7	PD
31/07/2002	Brompton Springs	Brompton Dale Shallow	SE 943 823	15.2	Photine CAQ	1.2	3	WS & PD
31/07/2002	Brompton Springs	Brompton Dale Deep	SE 943 823	46	Flavine	1.2	3	WS & PD
18/09/2002	Brompton Springs	Brompton Dale Shallow	SE 943 823	15.2	Photine CAQ	39.2	7	WS & PD
18/09/2002	Brompton Springs	Brompton Dale Deep	SE 943 823	46	Flavine	39.2	7	WS & PD
01/02/2003	Brompton Springs	Brompton Dale Shallow	SE 943 823	15.2	Photine CAQ	180	4	PD

Table 4.2 Tracer test details

4.3 SINGLE BOREHOLE EXPERIMENTS

4.3.1 BOREHOLE DILUTION TESTS.

Borehole dilution tests (BHDTs) measure the rate of dilution of an (ideally) uniform concentration of tracer in a borehole over time, which is related to the flux of water through the borehole. The borehole dilution tests were performed by lowering a weighted hose to the bottom of the borehole and filling the hose with a tracer[10]. Once the filled hose was in position, it was withdrawn (at a rate of approximately two metres per minute[11]) so that the tracer was slowly released from the bottom of the hose in (what was intended to be) an even distribution along the length of the borehole. The first BHDT employed a fluorescent dye, but for all subsequent experiments the tracer was a saturated sodium chloride solution[12], for which in-situ measurements could be made with the use of a borehole conductivity probe (a YSI 3000m Temperature-Level-Conductivity meter).

Once the hose had been completely withdrawn from the borehole the conductivity probe was introduced and measurements taken at given depths along the length of the borehole. These 'profiles' of the salinity distribution in the borehole were repeatedly measured over the following few hours, until the salinity in the borehole appeared to be unchanging or had returned to background levels (background measurements having been made prior to tracer injection).

The changing concentration of chloride (having a known relationship to conductivity and correcting for background) may then be plotted against the original concentration to show those sections of the borehole exhibiting the greatest dilution. The data may also be worked, with caveats, to give a specific discharge ($m^3m^{-2}d^{-1}$ or md^{-1}) for the aquifer in the vicinity of the borehole and, assuming a value for effective porosity, hydraulic conductivity. The data may also be combined with other tracer data to calculate porosity (if not assumed) and an average aperture width. The results from all borehole dilution tests are presented and discussed in full in Chapter 5.

---

[10] The internal volume of the hose beneath the water table was calculated based on the internal diameter of the hose, the depth of the borehole (or the length of the hose) and the depth of the water table.

[11] This was considered to be the optimum withdrawal rate. It represents a compromise between an uneven distribution of tracer if withdrawn too swiftly, and the temporal extension of the injection pulse, leading to uneven dilution, if withdrawn too slowly.

[12] Density effects are not corrected for during the analysis, although interpretation of results does take this factor into account. The ease with which measurements of conductivity could be taken, compared to the procedures necessary for using fluorescent dyes, outweighed any disadvantage accruing from density effects of using sodium chloride as a tracer. Disadvantages of using a fluorescent tracer included the greater difficulty in obtaining a sample from depth (using bailers), vertical mixing due to the passage of numerous bailers up and down the borehole, laboratory (fluorometer) analysis of samples as opposed to direct field measurement, preparatory and handling procedures for dyes, and obtaining permission to use dyes.

4.3.2 VERTICAL FLOW TESTS

Following an unsuccessful BHDT on the Seavegate Gill borehole using a fluorescent dye, it was decided to perform the same experiment using sodium chloride as the tracer. After failing to raise the salinity in the borehole to above background levels, even by taping together and filling three hoses, it was realised that the tracer was leaving the borehole faster than it was possible to get the conductivity probe in. This came as a surprise, but after a couple of preliminary tests it was noted that water was entering at the bottom of the borehole and moving upward very rapidly. Therefore it was decided that half-litre injection slugs, injected into the bottom of the borehole, could be measured as they moved upward, and that this would form the basis of an alternative form of dilution test.

In this adapted form of experiment, the bottom of the hose was stationed near the base of the borehole (above the influent fracture), and the probe stationed first at that point (to characterise the injection pulse) and then at successive positions higher in the borehole. This led to a series of breakthrough curves describing the evolution of a tracer pulse as it traversed the borehole from bottom to top. Results from this experiment are presented in Chapter 5.

4.4 FLUORESCENT DYE TESTS

4.4.1 FLUORESCENT DYES AND INJECTION PROTOCOLS

4.4.1.1 Dyes, preparation and injection

The fluorescent dyes used were Fluorescein Sodium (Acid Yellow 73), Photine CAQ (an optical brightener) and Nysolan Brilliant Flavine (Direct Yellow 96). These dyes possess different emission and absorption spectra to one another and are therefore distinguishable on this basis (Table 4.3). These properties permit the use of multiple dyes at the same time.

Dye	Absorption wavelength (nm)	Emission wavelength (nm)
Fluorescein	492	513
Photine CAQ	350	440
Flavine DY96	415	489

Table 4.3 Excitation and emission wavelengths of the fluorescent dyes used.

For the first of the forced gradient tests (Forge Valley swallowholes to Irton) the tracer was injected directly into a set of swallowholes draining the river Derwent through its eastern bank. For all dye tracer tests that were conducted from boreholes the tracer slug was injected through a hose positioned at the level of a hydraulically active fracture, as determined through previous borehole dilution testing. For all dye tracer tests the tracer injection is assumed to occur 'instantaneously', normally a valid assumption when comparing the time it takes to inject the tracer with the overall length of the experiment. Tracer injection was in any case rapid, injection always occurring over less than a five-minute period (with the exception of the SF_6 tracer experiment).

For all experiments, small volumes of tracer solution (usually a litre), containing the full mass of tracer, were prepared in the GTU laboratory and transported to site. Dye tracers were dissolved in London tap water which, being within a pH range of 7.5-9.0, was not expected to alter the fluorescence of the dyes used (Aldous *et al.*, 1987). Once the injection hose was stationed at the correct depth in the borehole, the prepared tracer solution was poured through a funnel into the hose and flushed through with at least 20 L of river or tap water.

During the tracer preparation and injection phases of experiments tracer handling procedures were observed to minimise the possibility of contaminating sampling equipment and personnel. These included, where possible, the use of different personnel for injection and sampling and the use of personal protective equipment (gloves and eye protection). Hoses and other equipment used for injection were bagged and labelled and, depending on the type of tracer used, disposed of.

4.4.1.2 Tracer injection mass calculations.

The mass input required to obtain a given peak output concentration at a given monitoring point has been described by the following equation (Equation 4.1, Environment Agency, 1998)

$$M = C_{PEAK}.A.\sqrt{4\pi r\alpha} \qquad (4.1)$$

Where

M = Mass injected (g)
C_{PEAK} = Peak Concentration required (g L^{-1})
A = Cross sectional area of injection pulse (m^2)
r = Distance between injection point and monitoring point (m)
α = Dispersivity (m)

The terms A and $\sqrt{\alpha}$ are unknown, although their product as derived from a previous tracer test may be taken as constant for the aquifer, and thus used to calculate the mass required. Equation 4.1 may be rearranged to give:

$$A\sqrt{\alpha} = M / C_{PEAK}.\sqrt{4\pi r} \qquad (4.2)$$

For example, ARUP (2000) give values from the 1999 tracer test between Forge Valley and Irton of M = 300g, C_{PEAK} = 0.000525 g L^{-1} (uncorrected for background) and r = 1500 m, which gives a value for $A\sqrt{\alpha}$ of 4161 m^3. Re-employing this value in Eq. 4.1, along with a desired C_{PEAK} of 5 ppb, or 0.000005 g L^1 (5µg L^{-1}), we can calculate that the required mass input value is 2.86 grams of Flourescein Sodium for an r of 1500m.

It should be noted that employment of this analysis rests on the assumption of radial flow to the well, which is not strictly met in the Irton system, although for the purposes of a rough estimate for tracer input the calculation is an acceptable first approximation, as the peak actually obtained by injecting 2.86 g was in fact 1.5 ppb. The margin of error in the (admittedly simple) equation is, firstly, on the conservative side (i.e. it overestimates the peak), and secondly, still quite a close estimate, especially considering the distance and the small amount of tracer involved.

Furthermore, where the target was not Irton, for example in the Seavegate Gill – McCains experiments, to maintain the conservative principle (i.e. to account for the potential impact on public water supply at Irton), it was always assumed that Irton was directly down-gradient of the injection point. The effect of this assumption was to reduce the amount of tracer injected, thus minimising the chances of actually obtaining a breakthrough at the desired target. As flowpaths in the aquifer north of Irton are not well

known, and as the entire point of the exercise was to help protect water supplies through the development of non-toxic tracers, this was considered an important principle to maintain.

4.4.2 SAMPLING

Depending on the objectives and logistics of the individual tests listed in Table 4.2, sampling campaigns extended from 1 day to 1 week, with samples being taken at intervals as close as 15 minutes. The sampling durations of various experiments are listed in Table 4.2. During this time samples were taken either by changing passive monitoring detectors stationed in the flow of water at the potential receptor, or by taking a water sample by hand or with the use of an (occasionally malfunctioning) automatic water sampler.

4.4.2.1 Passive detection

Photine CAQ and Flavine Direct Yellow 96 have the property of sorbing strongly to cotton. They may therefore be detected by allowing sample to flow through/over cotton-wool detectors. This permits dye to accumulate on the detector, and it is thus possible to obtain a positive result from several hours of accumulation where a water sample may not show a positive result due to analytical detection limits. As these cotton-wool detectors simply sit in the stream of flowing water, in either a borehole or at a spring, they are known as 'Passive' detectors. In those experiments where passive detectors were used, the relative fluorescence of the detectors was described using the following categorisation (Table 4.4):

Description of fluorescence	**Score**
Definite negative (dull, no fluorescence whatsoever)	**0**
Highly doubtful (one wispy patch of doubtful fluorescence)	**0.5**
Doubtfully positive (a few faint patches of fluorescence)	**1**
Faintly positive (definite wispy / cloudy patches of fluorescence)	**2**
Positive (detector not completely covered but has substantial patches (>30%))	**3**
Moderately positive (detector mostly or all covered by moderate fluorescence)	**4**
Strongly positive (intense fluorescence, largely uniform over entire detector, inside and out)	**5**

Table 4.4 Subjective points scale for tracer detectors (after Mottram, 2003)

During both emplacement and collection, care was taken not to contaminate the cotton-wool. This meant wearing rubber gloves when preparing the detectors, and avoiding contact with them during collection, achieved by only touching the nylon fishing line used to secure them in place. All detectors were kept in labelled plastic bags until they could be qualitatively analysed with the aid of an ultra-violet fluorescent lamp. As this is only a semi-quantitative method, water samples must be taken for a quantitative analysis.

4.4.2.2 Water samples

Of the dyes used, both Fluorescein sodium and Photine CAQ are photodegradable (United States Environmental Protection Agency (USEPA) 1988), so that water samples, when taken, were collected in 50 ml borosilicate brown glass bottles, kept in the dark and analysed as soon as was possible. Where possible all samples were refrigerated between being taken and being analysed. Analysis was performed on a Perkin-Elmer LS-55 Luminescence Spectrometer in the Groundwater Tracing Unit laboratory, Department of Earth Sciences, University College London.

4.4.3 MEASUREMENT OF FLUORESCENT DYES

4.4.3.1 Calibration

Calibration of the spectrometer (or fluorometer) was achieved by recording the signal strength associated with standards of known composition. Standards for each dye were made up in the laboratory between 1 ppb and 200 ppb by serially diluting initial flasks of dissolved tracer (again using London tap water). Initial flasks contained 1 gL^{-1} ± 0.01 g. After scanning a high-concentration standard so that the exact emission and absorption spectra of each dye could be recorded, several repeat measurements were made on each standard to ensure the use of representative values. New calibrations were performed for each experiment to compensate for any instrumental drift.

4.4.3.2 Detection limits of fluorescent dyes

The definition of detection limit for this study is the average blank signal plus three standard deviations of that signal. This definition is appropriate for minimizing the chances of either reporting an analyte that is absent, or failing to report an analyte that is present. The same definition was considered acceptable for Bateman's 1998 PhD thesis, 'CFCs in Groundwater', and was based upon the discussion in Miller and Miller (1993). This definition is also applied to the CFC measurements described in Section 4.6 and presented in Chapters 7 and 8.

For the fluorescent dyes the system blank signal was taken from repeat measurements of the fluorescence of distilled water at the wavelengths of interest. The detection limit assessed in this way was 0.005 μgL^{-1}, or approximately 5 ppt for both fluorescein and photine. As background levels of fluorescence (at the wavelengths of interest) in the aquifer are significantly higher than this value the detection limit is not of great practical significance.

4.4.3.3 Reproducibility of samples

Reproducibility is taken to be the average difference (in percent) between the values of repeat measurements on the same sample and the average value of all duplicated (triplicated etc.)

measurements. This is expressed as a percentage of the mean. The reproducibility of thirty repeated measurements of the same sample was 7.2 %.

4.5 SULPHUR HEXAFLUORIDE METHOD DEVELOPMENT

4.5.1 INTRODUCTORY REMARKS

This section will describe the system developed for injecting large volumes (500 L) of SF_6 saturated water into the groundwater flow system.

4.5.2 DESIGN AND OPERATION OF SF_6 INJECTION SYSTEM

Figure 4.1 illustrates the design of the injection system used to inject SF_6 tracer into the Forge Valley swallowholes and Plates 4.1 and 4.2 are photographs of the system in action.

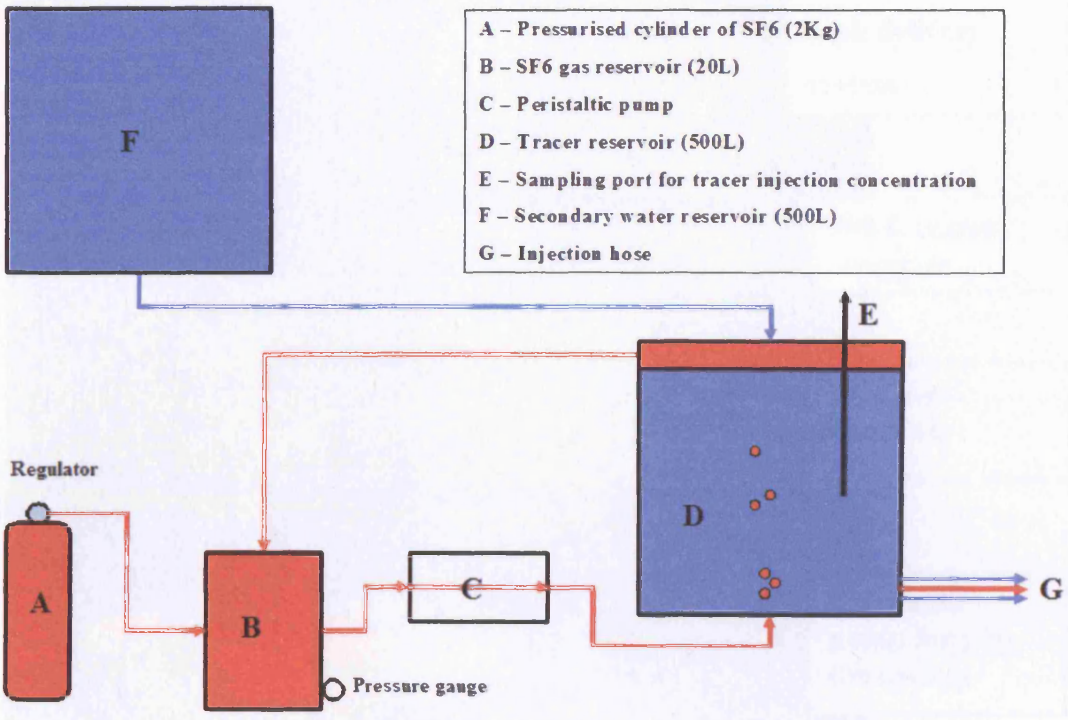

Figure 4.1 SF_6 tracer preparation and injection system.

From the figure it can be seen that the injection system comprises two 500 L reservoirs of water, an upper (F) and a lower (D), the latter being fitted with a gas circulation system (A – C). The circulation system consisted of a gas reservoir (B) supplied and pressurised at a constant pressure by means of a pressure-regulated 2 kg cylinder of pure SF_6 (A). Gas in the gas reservoir was circulated through the tracer reservoir by means of a peristaltic pump (C), which pumped SF_6 into the base of the tracer reservoir and collected what had not dissolved (i.e. most of it) from a headspace at the top of (D). The final concentration of SF_6 in the tracer solution was determined by extracting a sample through a sampling tap fitted at (E).

The secondary reservoir of water (F) was necessary to prevent the highly volatile SF_6 from degassing into increasing headspace in (D) as the tracer solution, once prepared through the sufficient circulation of gas, drained from (D). Without this reservoir, to permit the tracer to drain from (D) during injection, it would have been necessary to open (D) to the atmosphere. The connection between (F) and (D), controlled by a valve (not shown) was not opened until the point of tracer injection.

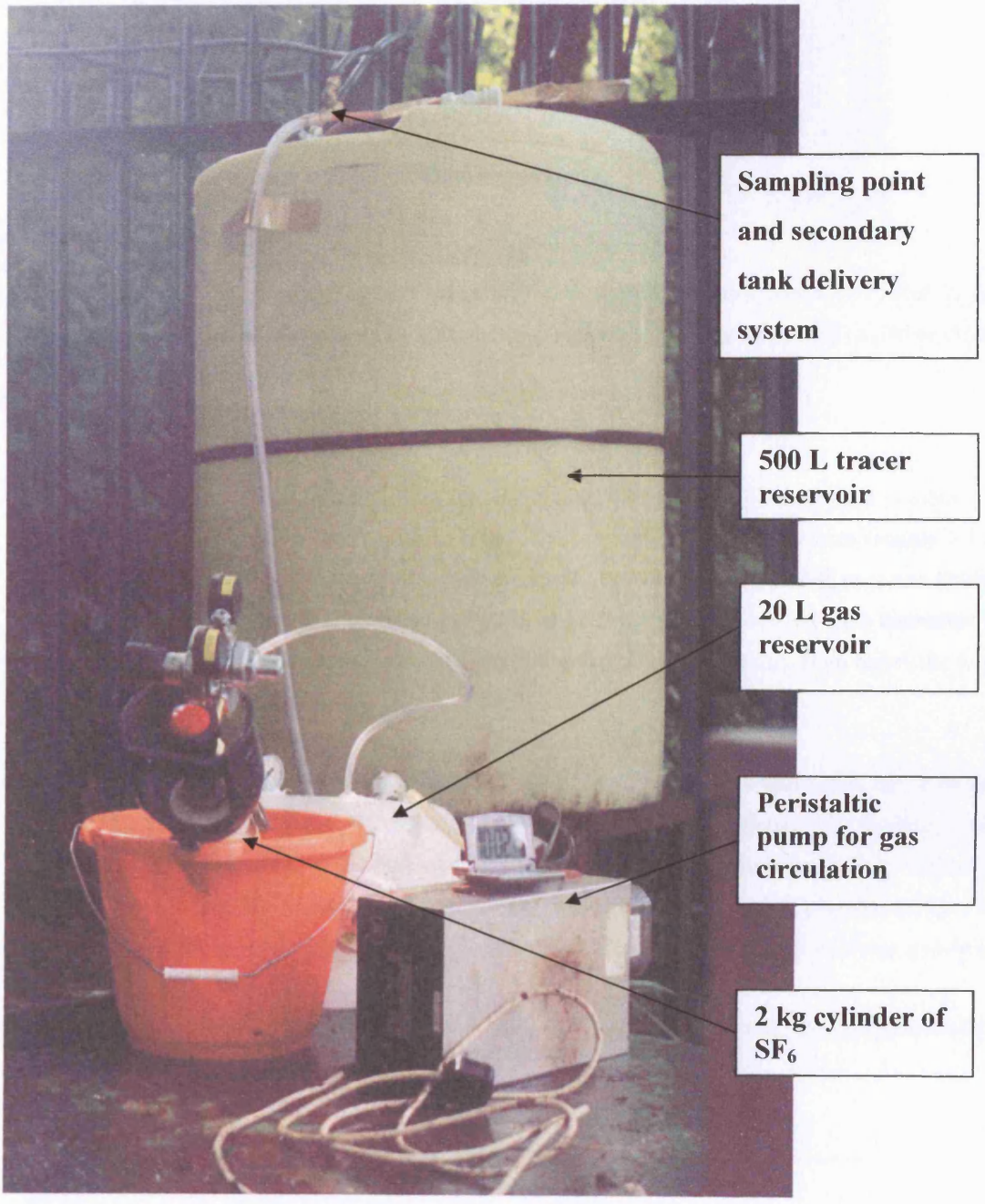

Plate 4.1 SF_6 gas tracer preparation system.

Plate 4.2 Detail of tracer sampling and secondary tank delivery system. Note A) Ground-glass syringe used for SF_6/CFC sampling; B) Placement of secondary tank in upper left of photograph.

4.5.3 MATERIALS AND CONSTRUCTION

The 500 L reservoirs were constructed from containers that previously held a flocculent employed in waste water treatment, supplied by Yorkshire Water Services Ltd. The reservoirs were roughly 1.3 m tall and 0.7 m in diameter and made of a heavy-duty plastic, to which it was possible to secure fittings for attachment to the gas circulation system and between reservoirs. The reservoirs were connected to one another with 1.25 cm diameter garden hose and household plumbing fittings. Both reservoirs were thoroughly cleaned before use.

The gas reservoir was made from a light but rigid plastic 20 L tank with a removable tap. This gas reservoir was attached to both the SF_6 cylinder and the tracer reservoir 'headspace' by flexible plastic tubing. It was further attached to the bottom of the tracer reservoir by a length of flexible, lab-grade peristaltic pump tubing, which was passed from the gas reservoir tap, through the peristaltic pump. The pump was able to pump easily against the pressure exerted by the 1.3 m of water in the tracer reservoir.

All joints were sealed either with silicone putty or, in the case of the gas cylinder, by the tightness of fit between the nozzle on the regulator and the tubing.

4.5.4 SYSTEM PERFORMANCE AND DESIGN FAULTS

During operation some flaws in the design were realised. The most severe of these were:

1. The system leaked gas.
2. The gas flow rate between the cylinder and the reservoir was only regulated by the outlet pressure on the gas cylinder, not by a flow metering valve.

Because of the first problem the gas circulation system was not able to retain gas under pressure. This leakage was exacerbated by the lack of a flow metering valve, which would have enabled greater control of the pressurisation of the system. However, as this had not been included in the design, the flow rate was dependent upon the leak rate, which was quite high. Furthermore, as gas was constantly escaping from the system, it was only possible to circulate gas until the cylinder was empty. A back-up cylinder had been purchased and this was also emptied in the maintenance of circulation.

Despite these problems SF_6 circulation was maintained for 1 hour 45 minutes prior to injection, leading to an injection concentration of approximately 20 mgL^{-1}, which is equivalent to about 50% of the solubility of the gas. It may thus be said that, in terms of achieving a high tracer concentration, the system performed quite successfully. In several other studies (see Chapter 3), satisfactory (if lower) concentrations have been achieved by bubbling SF_6 through water held in an open drum. In this study, due to design flaws, a total of 4 kg of gas were released, of which only about 10 g, or about 0.25%, were dissolved in the tracer solution. As one of the reasons for maintaining a 'closed' system was to prevent such emissions[13], the apparatus was unsuccessful.

The tracer injection itself, with the tracer reservoir being replenished from the upper reservoir, was a successful operation, although it was noted that the upper reservoir has to be able to replenish the lower at a higher (or at least equal) rate than the tracer is exiting the lower reservoir.

4.5.5 ADDITIONAL POINTS

i) Due to the steep banks in Forge Valley it was relatively simple to position the upper reservoir higher then the lower. In other circumstances it may be necessary to have some sort of platform upon which to place the upper reservoir.

ii) The water used in both of the reservoirs was taken from the River Derwent, and was therefore the same water as was flowing into the swallowholes.

iii) All sampling was conducted by the author whilst injection operations were undertaken by personnel from UCL and YWS Ltd. Thus SF_6 circulation and tracer injection was performed by different personnel than those conducting the sampling.

[13] As SF_6 has a Global Warming Potential 22,200 times that of CO_2 (IPCC, 2001), the emission of 4 kg of SF_6 is the equivalent of 88.8 tons of CO_2. If the system had operated as intended, the 10 g of SF_6 in the tracer solution, plus allowing 22.4 litres of circulation space (22.4 L = 1mole of gas at STP), would have led to the release of something like 156 g of SF_6, or about 500 kg of CO_2.

4.6 CFC, CCL_4 AND SF_6 INSTRUMENTATION, SAMPLING AND ANALYSIS.

4.6.1 INTRODUCTORY COMMENTS

The measurement of CFCs is typically performed using gas chromatography coupled with electron capture detection. However, this broad framework has been implemented in numerous ways, with variety particularly in choice of chromatographic column, sample preparation and sample taking/preservation procedures. Pioneering work in the development of routine methods includes that of Bullister and Weiss (1988), Busenberg and Plummer (1992) and Wallace *et al.* (1994) (see also Chapter 3). The method described below is essentially that of Bateman (1998) with modifications implemented by Atkinson (2002).

For SF_6 the method is essentially the same but with a different chromatographic column and different instrumental settings.

4.6.2 GAS CHROMATOGRAPHY WITH AN ELECTRON CAPTURE DETECTOR (GC/ECD)

CFCs, CCl_4 and SF_6 were all analysed on a Varian CP 3800 Gas Chromatograph (GC) with an Electron Capture Detector (ECD). The analytical array is depicted in Figure 4.2.

Gas chromatography is a method of separating a mixture of compounds in the gaseous phase. Basically this is performed by forcing the compounds along some form of tube (the GC column) to which the various compounds have different sorption affinities, thus leading to different travel times for different compounds along the length of the tube, and thereby separating them. A more theoretical consideration of the method is beyond the scope of this thesis, although detailed descriptions may be found in, amongst others, Willard *et al.*, (1988) and Poole (2003).

The Electron Capture Detector, specifically sensitive to halogenated compounds, was invented by James Lovelock (Lovelock and Lipsky, 1960). The detector is situated at the terminal end of the GC column and receives the inert carrier-gas passing through the column at all times during operation. As this gas (helium in the present study) enters the ECD chamber, it is ionised to plasma at high temperature (c. 300° C) together with a 'make-up' gas (nitrogen) used to ensure a sufficient gas supply to the detector (as column flow rates are typically lower than required by the detector). Plasmarisation is achieved by bombarding the nitrogen/helium mixture with a cloud of electrons emitted by the radioactive ^{63}Ni foil, of which one of two electrodes in the detector is coated. A voltage is applied across the ECD chamber and its maintenance is a function of the electron density of the plasma. As any halogenated compounds entering the chamber contain highly electronegative elements (chlorine and fluorine most relevant here) they capture electrons flowing across the ECD chamber, leading to a decrease in the current. The decrease occurs because the speed with which the free electrons move is vastly greater than the speed with which the more cumbersome ionised molecules of analyte move. What the detector actually measures is the increase in voltage necessary to maintain the current at a

specified level. Different detectors are capable of measuring this process in different ways, and more detailed explanations may be found in Lovelock and Lipsky (1960), Scott (1996) and Poole (2003).

4.6.3 THE CHROMATOGRAPHIC COLUMN

The chromatographic column for CFCs and CCl_4 was a capillary column (Durabond Megabore DB624 from JB Scientific) suitable for separating CFCs 11, 12, 113, CCl_4, chloroform ($CHCl_3$) and methyl chloroform (CH_3CCl_3). This was 60 m long with an interior diameter of 0.53 mm. This choice of column was based on that of Bateman (1998), who in turn based her selection on that of Haine (1992). An ideal column is one that clearly separates the analytes of interest without unreasonably extending the length of time required for a single analysis.

For the SF_6 tracer experiment it was necessary to change the column to a 5 angstrom Molecular Sieve (Mol5A from Supelco) (this choice was made by the author on the basis of commercial claims). The column was able to successfully resolve SF_6, CFC 12 and CFC 11, so that for every SF_6 sample taken, measurements of two different environmental tracers were also obtained. The reason that a different column was required for SF_6 analysis is that the DB624 column was unable to separate SF_6 and N_2O under the temperature and gas flow ranges possible on the CP3800 gas chromatograph. N_2O is a common component in Corallian groundwater.

4.6.4 SAMPLE PREPARATION

For all analyses the compounds of interest were prepared for injection onto the column using a purge-and-trap technique. This involved injecting the water sample into a glass tower through which bubbled a stream of helium, into which the analytes were preferentially partitioned. This gas was then passed through a Nafion dryer to remove water vapour, and then through a cold trap, to retain and focus the analytes.

The cold trap was maintained at -185°C by positioning just above the surface of some liquid nitrogen contained in an insulated receptacle. The temperature of the trap was maintained by a thermocouple with a sensor attached to the trap and a heating device immersed in the liquid nitrogen. If the temperature of the trap rose, the heating element would increase in temperature thus evaporating more liquid nitrogen, which in turn would cool the space above the liquid surface.

After stripping had continued for a sufficient time for all analytes to have been transferred from the sample to the cold trap (10 minutes was found to be sufficiently long), the temperature of the cold trap was raised by immersion in boiling water. The analytes, being transformed from the solid to the gaseous phase, were thus carried onto the GC column.

A detailed step-wise procedure for the operation of the sample preparation system is presented in Appendix 2.

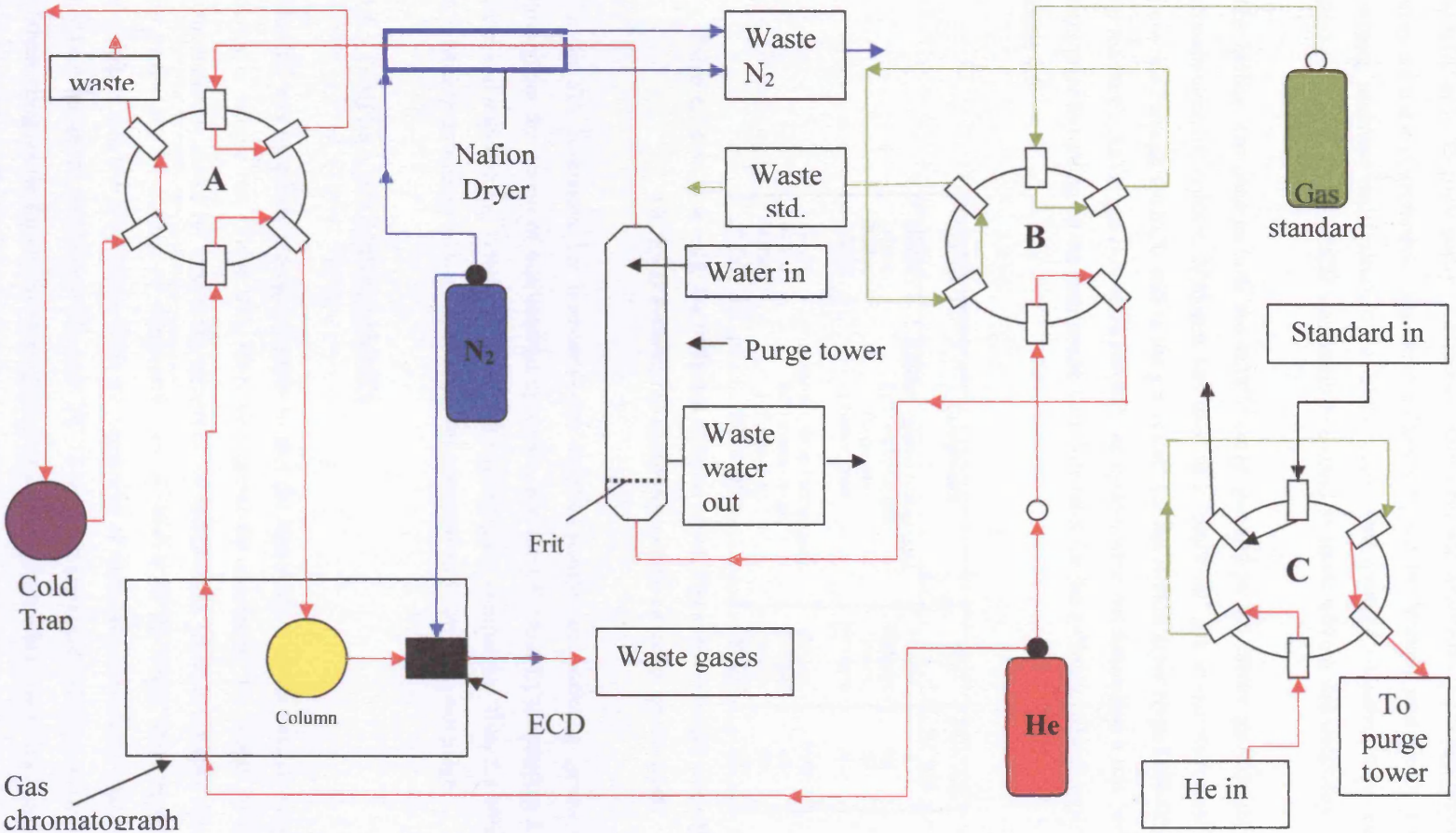

Figure 4.2 Gas chromatographic set-up. A) is the six-way *sample* valve shown in the trapping position; B) is the six-way *standard* valve shown in the ordinary position for purging water samples; and C) is the six-way *standard* valve shown in the position for injecting standards.

4.6.5 GASES AND FLOW-RATES

Two gases were used in the operation of the system, helium and nitrogen, both of which were supplied by BOC at ECD-grade purity. Additional refinement was achieved by passing these gases through an array of traps (Chrompack Gas-Clean Filters supplied by Varian) specifically for the removal of oxygen, moisture and hydrocarbons. These traps were changed whenever they indicated they were close to expiry. The GC-ECD was turned to a stand-by mode when it was necessary to change a trap.

The helium was used as both the sample purge gas and as the carrier gas for gas flow through the chromatographic column. Nitrogen was used as a 'make-up' gas to maintain a sufficiently high gas flow-rate through the ECD and as the gas stream for the Nafion dryer (type IMD-050-48S supplied by Perma Pure). As the gas flow-rates through the system were not automated it was necessary to set flow rates prior to turning on the instrument. Gas flow rates for the different column types used are given in Table 4.5

Column	Component	Gas	Flow rate mL/min
DB624	Capillary column (carrier gas)	Helium	5
DB624	ECD make-up gas	Nitrogen	50
DB624	Purge gas	Helium	60
DB624	Nafion dryer	Nitrogen	120
Mol5A	Molecular sieve (carrier gas)	Helium	0.66
Mol5A	ECD make-up gas	Nitrogen	45
Mol5A	Purge gas	Helium	60
Mol5A	Nafion dryer	Nitrogen	120

Table 4.5 Gas flow rates for different column types. Note that changes are only made to the GC/ECD system; the sampling system remains unchanged.

For the SF_6 experiment the instrument gas supplies (carrier and make-up gases) were not changed throughout the period of instrumental operation. For the CFC and CCl_4 sampling it was necessary to clean and maintain the system between different sampling campaigns. Thus the values given in Table 4.5, whilst representative, were not exactly the same for each sampling campaign.

4.6.6 TEMPERATURE PROGRAMMES

The GC was temperature-programmable so that the temperature of the column oven could be altered during a sample run (Table 4.6). This was useful for shortening the length of analyses. A lower temperature is useful for improving separation of compounds, whereas a higher temperature is useful for promoting the elution of compounds not of interest to the study. Both types of column were maintained at a low temperature from the beginning of each sample run until either CFC 12 and N_2O had been separated (DB624) or SF_6 and CFC 12 had been separated (Mol5A). Following the separation of these compounds, the slower eluting compounds could be made to move more rapidly by increasing the temperature. The higher temperatures served also to cleanse the column of a variety of halogenated compounds that were often present but neither identified nor quantified. This was necessary so that the column was clean for the start of the next sample run.

Column	Time mins	Rate Degrees C/min	Temperature Degrees C
DB624	0 - 6	0	60
	6.0 - 10.0	25	60 - 160
	10.0 - 14.0	0	160
Mol5A	0.0 - 5.0	0	35
	5.0-10.0	30	35-185
	10.0 - 25.0	0	185

Table 4.6 Temperature programmes for the GC oven for CFC and CCl4 analyses (with a DB624 column) and SF_6 and CFC 11 and CFC 12 analysis (Mol5A).

4.6.7 SAMPLE PREPARATION SYSTEM MATERIALS

The materials used for the sample preparation system were predominantly glass (the purge tower), stainless steel (all tubing and some nuts and ferrules), aluminium (6-way valves) and brass (nuts and ferrules). In addition a graphite ferrule was used to connect the sample preparation system to the capillary column and Teflon ferrules were used to connect stainless steel tubing to the purge tower. The Luer-Loks (used to connect the sample syringe to the purge tower) and syringe nozzles were made of plastic, and were thus the most likely sources of system contamination. They were replaced between sampling campaigns or when system blanks indicated a contaminated component. At least once contamination appeared to be due to a Teflon purge-tower ferrule.

The aluminium 6-way valves were supplied by Valco. The gas dryer was of the Nafion type, with an inner and an outer tube. The outer tube was made of stainless steel and the inner with a Nafion water-permeable membrane. The sample (purge) gas was passed through the inner tube whilst nitrogen was circulated in the opposite direction through the outer tube (see Figure 4.2). The drying is caused by rapid diffusion of water molecules through the membrane.

4.6.8 GAS STANDARDS

Two standards were used, one for the CFCs and CCl_4, and one for SF_6 (which also included CFC 12). The CFC standard was the same as that used by Bateman (1998) and was obtained by UCL from the University of East Anglia, who had originally obtained it from the National Oceanic and Atmospheric Administration (NOAA) of the USA. The cylinder I.D. is ALM-52760, it contains dried air collected at Niwot Ridge, Colorado, and was compared to primary NOAA standards between the 6^{th} and 9^{th} of May 1996 (Bateman, 1998). Its composition is given in Table 4.7

Species	Concentration ppt	Uncertainty ppt
CFC11	273.5	3
CFC12	544.7	5
CFC113	84.2	1.6
Methyl Chloroform	107.8	2
Carbon Tetrachloride	106.2	2
HFC-134a	3.7	0.08
Nitrous Oxide	313.4 ppb	3 ppb

Table 4.7 Composition of dried air in standard cylinder ALM-52760

The SF_6 standard contained 1 ppb of SF_6 and 1 ppb of CFC 12 in pure nitrogen. This standard was supplied by BOC gases with a stated compositional accuracy of 99.9%.

4.6.9 PEAK IDENTIFICATION

Peak identification is based upon elution time from the column. The elution time for any given compound will be the same for a given column under identical gas flow rate and temperature conditions. For the DB624 column the individual peaks were compared to the analyses of Bateman (1998), who in turn had compared her study to that of Haines (1992), who had used a mass-spectrometer as the detector and was thus able to quantify the relative masses of the molecules eluting at given times (and thereby identify the compounds of interest). Peak retention times varied between sampling campaigns due to minor variations in system set-up. However, these variations were small and the relative sizes of peaks (for gas standards) and order of elution all remained the same.

For the Mol5A column, peak identification was based on the superior detector response to SF_6 than to CFC 12. Identification was straightforward as these were the only two compounds in the standard. It was also possible to compare peak sizes to the Colorado air standard for confirmation. For CFC11 the comparison of detector response between standards run on both columns had to suffice as the method of identification. However, good agreement was observed and as nothing in the CFC standard exhibited a peak area greater than 50% of the CFC 11 peak area this was considered conclusive.

4.6.10 SYSTEM CALIBRATION

System calibration may be achieved by relating a known mass (or number of moles) of analyte to a detector response (measured by peak area). As the standard is of a known composition it is also possible to know the mass of analyte in a given volume of standard. Therefore the instrument may be calibrated over a range of concentrations by injecting the compounds of interest prepared from different volumes of standard. In this study loops of known volume ranging from 100 µL to 10 mL were used to construct calibration curves according to masses determined by use of the gas equation:

$$pV = nRT \qquad (4.3)$$

where

V is the volume of analyte in the standard (m^3)

R is the gas constant (8.3 $Jmol^{-1}K^{-1}$)

T is the temperature (K)

p is the atmospheric pressure (Nm^{-2})

n is the number of moles of analyte in the chosen volume

As an example, in a 100 µL sample loop there are 2.73×10^{-17} m^3 of CFC 11 according to the concentration multiplied by the volume ($273.5 \times 10^{-12} \times 1 \times 10^{-7}$ m^3). Arranging equation 4.3 yields (at STP):

$$n = \left(\frac{101325 Nm^{-2} * 2.73x10^{-17} m^3}{8.3 Jmol^{-1}K^{-1} * 298.1K} \right) = 1.12x10^{-15} moles$$

The instrument was calibrated at the beginning of each sampling campaign and system blanks and calibration samples were run interspersed with water samples to monitor for drift. As each sampling campaign tended to be only a few weeks in length little instrumental drift was observed. However, the sensitivity of the detector improved over the course of 2004 (see Section 4.6.15), which may be ascribed to sampling only relatively clean groundwaters and surface waters (i.e. no more landfill leachate samples), cleaning procedures and general improvements in maintenance and operation of the instrument. An example calibration chart (from the Seamer Carr landfill survey) is shown in Figure 4.3

At high concentrations the detector may not be able to measure peak areas as they exceed the scale of measurement. In this case the 'Range' of the instrument may be altered, which reduces instrument sensitivity tenfold and restores the otherwise too-large peaks back onto the scale. This obviously comes at the cost of losing resolution of the smallest peaks. Such a measure was necessary for high-concentration landfill samples and for some SF_6 samples.

A further problem pertaining at the high end of the less-sensitive range is that the ECD response becomes non-linear (i.e. for the very highest concentrations). No single curve could be made to fit the highest, or even the mid-range concentrations without distorting the lowest. As the lower and middle value concentrations were more frequent than the highest concentrations, yet as the highest concentration samples were some of the most important individual samples (e.g. at the peak of the SF_6 BTC, see Chapter 6), it was decided that it was better to fit the measured peak areas as closely as possible to the calibration curves. This necessitated fitting separate trend lines to different (overlapping) parts of the calibration curve. Where a measured peak fell on two trend lines, that chosen was the one with its centre closest to the data point.

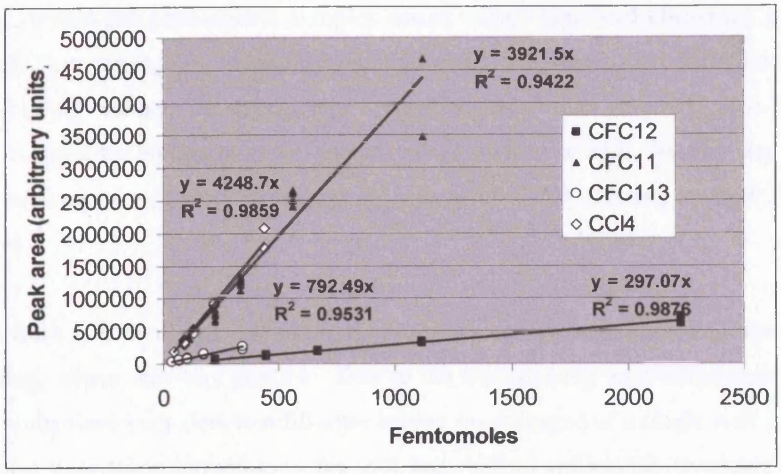

Figure 4.3 Example of calibration curves determined from repeat injections of known volumes of standard.

4.6.11 SAMPLING PROCEDURES

Sampling was by means of 100 mL, air-tight, ground-glass syringes. These syringes were necessary due to CFC abundance in the atmosphere, which can contaminate low-concentration or CFC-free samples. Conversely, they also prevent above-ambient concentration samples from de-gassing, which is more important for CFC contaminant studies and SF_6 tracer sampling.

Samples from pumping wells at Cayton Carr, Cayton Station Road and McCains were taken after sample taps had been freely run for 15 minutes, giving them sufficient time to purge the pipework between the sampling tap and the well. This was considered sufficient time after preliminary investigations of well-head parameter stability. The Irton sampling tap was continuously run so that purging was unnecessary. Samples were taken after flushing the syringes several times with water from the same source as the sample. Samples taken from unpumped boreholes were taken using dedicated plastic bailers. This is not an ideal method for obtaining samples for trace gas analyses, although the alternative to the bailers was the use of either dedicated 'Waterra' pumps, also plastic, or a submersible pump connected to a rubber hose, again not an ideal material. With these choices it was decided to use the plastic bailers as being the cheapest and simplest option. Bailers, when used, were rinsed with sample water several times prior to taking the final sample. Samples were taken from the bailers either by the use of a stainless steel tube inserted into the bailer, or directly from inside the bottom of the bailer as it was drained (prior to atmospheric contact). Sample retention time within bailers was usually less than a minute. Bailers were used in the contaminant study of Seamer Carr landfill, where they indicated that samples uncontaminated by leachate would not be seriously influenced by the use of the bailers, as several boreholes indicated concentrations well below atmospheric equilibrium. In the cases of contaminated waters it was found that the contamination signal far outweighed any use of plastic in the sampling equipment. Besides the Seamer Carr survey, such bailers were also used on the Augmentation, Swallowholes, Seavegate Gill and Tetherings Plump boreholes. The lowest concentrations recorded throughout the Corallian study were those from the Augmentation and Swallowholes boreholes (Chapter 7), again indicating that plastic bailers, if used

conscientiously, would not contaminate samples above values observed elsewhere in groundwaters sampled directly from springs or constantly pumped wells. Obviously as contamination due to this method of sampling cannot be completely excluded, ages derived from low-level CFCs in groundwaters sampled by bailers must be considered as minimum ages. Indeed, due to the ease of contamination of equipment, this point applies in general to all CFC dating anyhow (Busenberg and Plummer, 1999).

Samples taken from drift boreholes during the Seamer Carr survey were purged of three well volumes prior to sampling, where this was possible. Due to the occasionally low transmissivity of the drift deposits some wells were very slow to refill after having been purged of a single well volume. In these instances samples were taken immediately the well had refilled sufficiently to enable a sample to be taken.

Where samples were taken from pumping wells, springs or surface waters, samples were taken by submerging at least the tip and, if feasible, the entire syringe in the sample stream and withdrawing the plunger. For all samples, whether taken with a bailer or otherwise, syringes were thoroughly flushed with sample several times prior to taking the sample for analysis. Sampling continued until a bubble-free sample was obtained.

Samples, having been taken, were then placed in an insulated container (a 'coolbox') for transport to the laboratory. As sample preservation was considered to be a problem (personal communication A. Bateman, UEA) it was deemed necessary to analyse samples within 48 hours. This created severe logistical difficulties when the analytical equipment was based in London. However, after the laboratory had been transferred to the field area (at Seamer), sample analysis was, for almost all samples, conducted on the same day. No sample was analysed more than 48 hours after having been taken.

4.6.12 SUPPORTING MEASUREMENTS

Dissolved oxygen and temperature measurements of groundwater were taken at several locations throughout the Corallian using a Hanna dissolved oxygen and temperature meter. These results are presented in Chapter 7.

4.6.13 SAMPLING CAMPAIGNS

Preliminary CFC sampling campaigns were undertaken at the very beginning of the research period, during November 2001 and February 2002. At this time all CFC analyses were performed at the Groundwater Tracing Unit laboratory (GTU) at University College London. Together with the fact that the same analytical equipment was being used for numerous landfill samples at that time (Atkinson, 2002), the author's inexperience using the analytical equipment led to a poor quality of results. Thus the data obtained from these two sampling campaigns cannot be considered particularly reliable. In

general these results have not been used, although in certain instances these are the only available results for particular locations and have been drawn upon, with caveats, in the interpretation (see Chapter 7).

Little CFC work was conducted over the course of the next two years, as fieldwork focussed on established tracer techniques and time was spent becoming more familiar with the analytical equipment. By the end of January 2004, however, the GC-ECD and associated paraphernalia had been transported to a laboratory, in the centre of the field site, provided by Yorkshire Water Services Ltd. (at Seamer Waste Water Treatment Plant, Seamer). This proximity enabled a much greater turnover of samples, and the majority of 2004 was spent running the GC/ECD for CFC and SF_6 analysis. Additional sampling campaigns were therefore undertaken during February 2004 (CFCs), April 2004 (CFCs), June 2004 (CFCs) and August/September 2004 (SF_6 and CFCs). As it was necessary to frequently re-adjust system mechanics, the detector response, sensitivity and calibrations were variable for individual sampling campaigns. Some details are given in the following two sections.

4.6.14 DETECTION LIMITS

The detection limits given in Table 4.8 are based upon multiple analyses of 'blank' (i.e. non-sample) system measurements and taken as the blank signal plus three standard deviations of that signal. They are normalized to a 50 mL sample, which is the standard sample size used throughout this research.

Sampling campaign	CFC 12 pg/kg	CFC 11 pg/kg	CFC 113 pg/kg	CCl4 pg/kg	SF6 pg/kg
Feb-04	8.1	3.4	47.4	6	-
Apr-04	9.74	2.06	78.78	14.19	-
Jun-04	0.8	1.1	0.2	-	-
Aug-04	2.89	2.07	-	-	3.4
Nov-01	23.8	4.3	21.2	-	-
Feb-02	23.8	4.3	21.2	-	-
Atkinson (2002)	23.8	4.3	21.2	-	-
Bateman (1998)	0.3	1.9	2.5	0.5	-

Table 4.8 CFC, CCl_4 & SF_6 detection limits in $pgkg^{-1}$ for various sampling campaigns.

The values in grey for Nov. 2001 and Feb. 2002 are given as equal to those reported by Atkinson (2002) as the same equipment was being used at the same time in both studies, and a proper detection limit study was not made by the author at this time.

The Feb. 2004 sampling campaign was that conducted at Seamer Carr and extended up until the April 2004 study of some Corallian groundwaters. The high levels of CFCs resulting from leachate and leachate-contaminated groundwater samples contribute to the higher detection limits for these two campaigns. In particular a persistent CFC 113 signal was detected in many 'blank' (i.e. non-sample) system measurements. This is why the detection limit for CFC 113 is so elevated, and also why the detection limits of all CFCs for these two campaigns are higher than for the June and August sampling campaigns. By June 2004 the analytical equipment, and in particular the sample preparation system, had been thoroughly overhauled.

For the August 2004 campaign, the focus of which was the SF_6 tracer test, it was necessary to change the chromatographic capillary column (see Section 4.6.1.1). The method was thus optimised for SF_6. It was not possible to measure CFC 113 or CCl_4 with the new column. However, considering that the analyte of prime interest was SF_6, to achieve an additional measurement of both CFCs 11 and 12 with each tracer sample was an efficient use of the analytical equipment. For this sampling campaign the detection limits of CFCs 11 and 12 are good compared to the campaigns in early 2004, and at least approach those values achieved by Bateman (1998) and in the June 2004 campaign.

4.6.14.1 A note on SF_6 data quality.

A small but non-negligible signal from SF_6-contaminated equipment was consistently detected during the analysis of background water samples. On the basis of 16 measurements of the background SF_6 signal in Corallian groundwater, and two from a spring in the drift, the average signal was determined to be 0.83 pg kg^{-1} with a standard deviation of 0.48 pg kg^{-1}. This level of SF_6 could not be accounted for by equilibration with the atmosphere, as the maximum concentration resulting from this source was only 0.29 pg kg^{-1} in 2004.

This means either that the sampling or analytical methodology was not sufficiently rigorous to eliminate contamination, or that the Corallian is extensively contaminated with SF_6. The latter is much less likely than the former. In particular, there were only some 20 ground-glass syringes with which to take samples, such that syringes would have been used both during periods of high tracer concentration as well as low. The blank sample runs conducted regularly on the analytical system only check the analytical system post-sample injection. As these were consistently clean the analytical system can be eliminated as the source of contamination. It therefore seems that it was impossible to adequately remove all SF_6 from the sampling syringes during cleaning (which included high temperature baking, changing plastic nozzle components and repeated washing with analytical-grade cleaning agents). However, despite this problem, the supposed contamination contributes to an SF_6 signal of about three times the analytical system's detection limit (on the basis of repeat measurements of baseline height following non-sample analyses).

To account for the contaminant signal, a wide error margin has been adopted. This consists of the measured error signal (0.83 $pgkg^{-1}$) plus three standard deviations of the error signal (3 × 0.48 $pgkg^{-1}$), which gives 2.27 $pgkg^{-1}$. To make absolutely sure that any reported values are due to the presence of tracer rather than the background signal, an additional 50% of this value is added to give a minimum threshold concentration of 3.4 $pgkg^{-1}$.

4.6.15 REPRODUCIBILITY (PRECISION)

An analysis of precision for this study is based upon sample reproducibility, or the difference between two or more samples taken at the same location at the same time. It is stated as the average difference (in percent) between the values of each sample and the average value of all duplicated (triplicated etc.)

samples. By presenting error in terms of a percentage of signal size it is assumed that the majority of error is due to variability in system response when it analyses larger amounts of analyte. This is justifiable on the basis that the processes of loss of CFCs or SF_6 from a syringe depends upon the relative concentrations of those samples with respect to the atmosphere (i.e. diffusion along the syringe 'seal' is proportional to concentration differences); on the basis that larger concentrations may not be stripped so completely from a water sample as smaller concentrations over the same amount of time; that trapping may not be so effective; that detector response is non-linear at higher concentrations; that potential sorption to components in the sample preparation system will be proportional to concentration. These factors are considered to be more likely to introduce error on a sample-size basis than on a systematic basis, so that a percentage-error indication is considered more realistic than a uniform systematic error that is of the same magnitude regardless of sample size (although one presumably exists also). The results of the reproducibility studies are given in Table 4.9.

Sampling campaign	CFC 12 %	CFC 11 %	CFC 113 %	CCl4 %	SF6 %
Feb-04	29	25	25	11	-
Apr-04	24.8	15.1	9.3	24.4	-
Jun-04	31.6	26.5	19.6	-	-
Aug-04	31.4	25.8	-	-	22.9
Nov-01	29.01	13.9	59.1	11.8	-
Feb-02	18.9	43.9	31.4	36.3	-

Table 4.9 CFC and SF_6 sample reproducibility

In spite of the system maintenance measures referred to previously, the reproducibility remained poor for water samples. This is put down to the use of ground-glass syringes that are less-than-ideally gas-tight, as well as minor inter-sample variations in the conditions under which the sample preparation system was operated (as it was a manual operation system). Indeed, whilst the reproducibility of water samples was 22.9% for SF_6, the reproducibility of the gas standard was 0.46%. The poor reproducibility associated with samples but not with standards suggests errors consequent upon the use of ground-glass syringes and the injection of water samples into the purge tower. It should also be noted that the reproducibility statistics for this study were generally as good as those reported by Atkinson (2002). Reproducibility is reported in terms of error bars where appropriate.

4.7 CHAPTER SUMMARY

Chapter 4 has introduced the different types of tracer experiments performed as part of the research. These include single-borehole dilution experiments, a single-borehole vertical tracer test, qualitative dye tests using cotton-wool passive detectors, quantitative dye tests with different types of tracer dye and an experimental technique for employing dissolved-gas tracers. These experiments have been described in terms of protocols followed during the tests for injection and sampling. The chapter has also described the analysis of fluorescent dyes and discussed, in more detail, the analytical methods employed for the measurement of CFCs and SF_6 (a photograph of the field laboratory is shown in Plate 4.3) including a discussion and presentation of data uncertainty. The results obtained using the methods outlined in this chapter form the basis of the remainder of the thesis, beginning with a closer inspection of the borehole dilution tests.

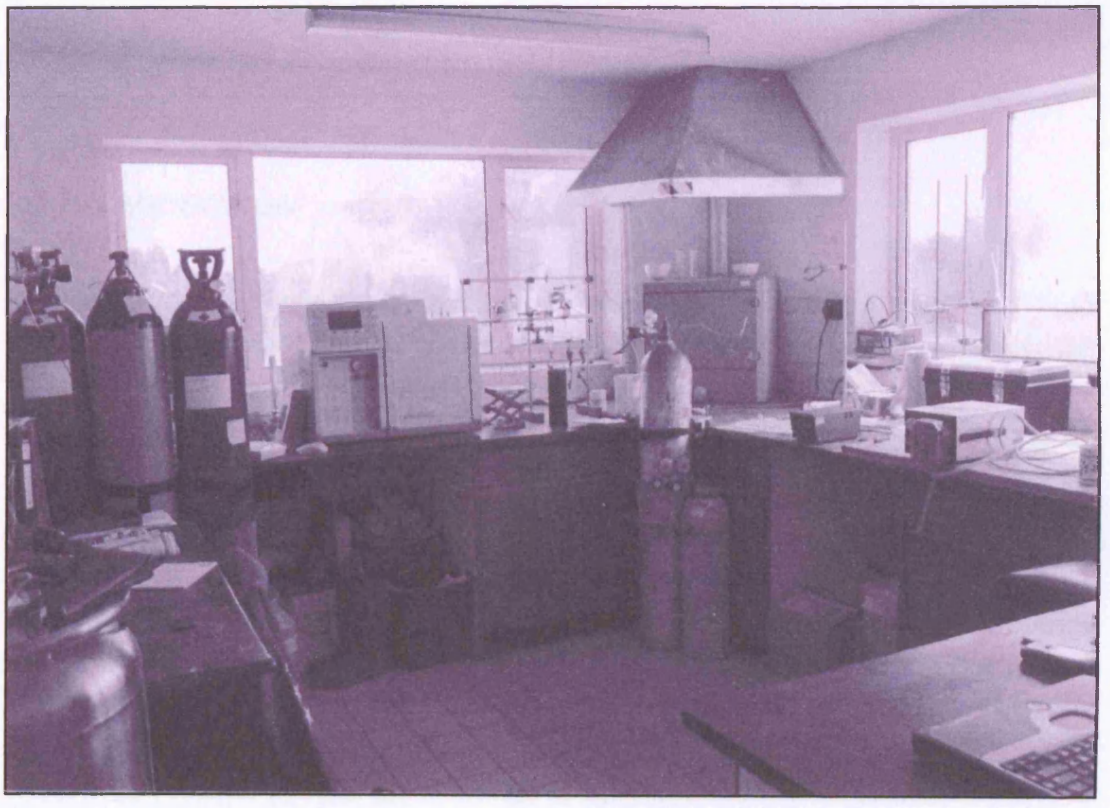

Plate 4.3 Field laboratory set up by the author at Seamer Waste Water Treatment Plant (see Figure 1.1 for location).

CHAPTER FIVE

RESULTS AND DISCUSSION I
GEOPHYSICAL LOGGING AND BOREHOLE DILUTION TESTS

"At 184 ft a strong inflow from a large cavity was observed..."

(Tate *et al*, 1970).

5.1 INTRODUCTION

This chapter presents the results and analyses (based on mathematical modelling) of borehole dilution tests (BHDTs) and a single borehole vertical flow test. As a precursor to an analysis of these results, the results from geophysical logging of several boreholes in the Irton and Forge Valley areas are presented. These greatly contribute to understanding flow conditions in the eastern Corallian, especially regarding the form of the borehole dilution tests. The geophysical results are presented first because later interpretation relies upon them.

Early work on borehole dilution tests (Halevy *et al.*, 1967; Drost *et al.*, 1968) focussed on the use of radioisotopes as tracers. Concern over the use of applied radioisotopes led to the employment of less contoversial tracers such as NaF (Grisak *et al.* 1977) and NaCl (Bellanger, 1984). Watson (2004) used fluorescein in the chalk of southern England for a series of dilution tests. For the research described herein sodium chloride was used due to the ease of measurement, and possible density affects have been highlighted where necessary. The interpretation of BHDTs typically assumes a homogeneous porous media over the interval tested and that horizontal flow is the only component contributing to dilution. However, as this assumption is unrealistic in the Corallian, the usual method of interpreting BHDT data (e.g. Halevy *et al.*, 1967; Drost *et al.*, 1968; Drost, 1983; Palmer, 1993; Environment Agency, 1998; Kumar and Nachiappan, 2000), which examines dilution rates at specific intervals in a borehole (and herein termed the 'standard' method), has been modified with a borehole-averaging procedure to account for vertical flows. Additionally, a curve-matching program has been used to reproduce the experimental results by calculating dilutions based on borehole characteristics and specific discharge inputs assigned by the user. The outputs from this model are compared to the results from the modified 'standard' method to facilitate greater insight into the behaviour of the aquifer and

to draw conclusions regarding the wider applicability of the analytical methods adopted. Following these analyses, the Seavegate Gill BHDT, in which the entire tracer mass disappeared so rapidly as to necessitate another form of experiment, is presented as a vertical single-well tracer test. The form of the result from this experiment is essentially that of a series of breakthrough curves describing the evolution of numerous tracer pulses along the borehole column. It thus forms a transitional form of experiment between the borehole dilution tests presented in this chapter and the tracer tests in the next.

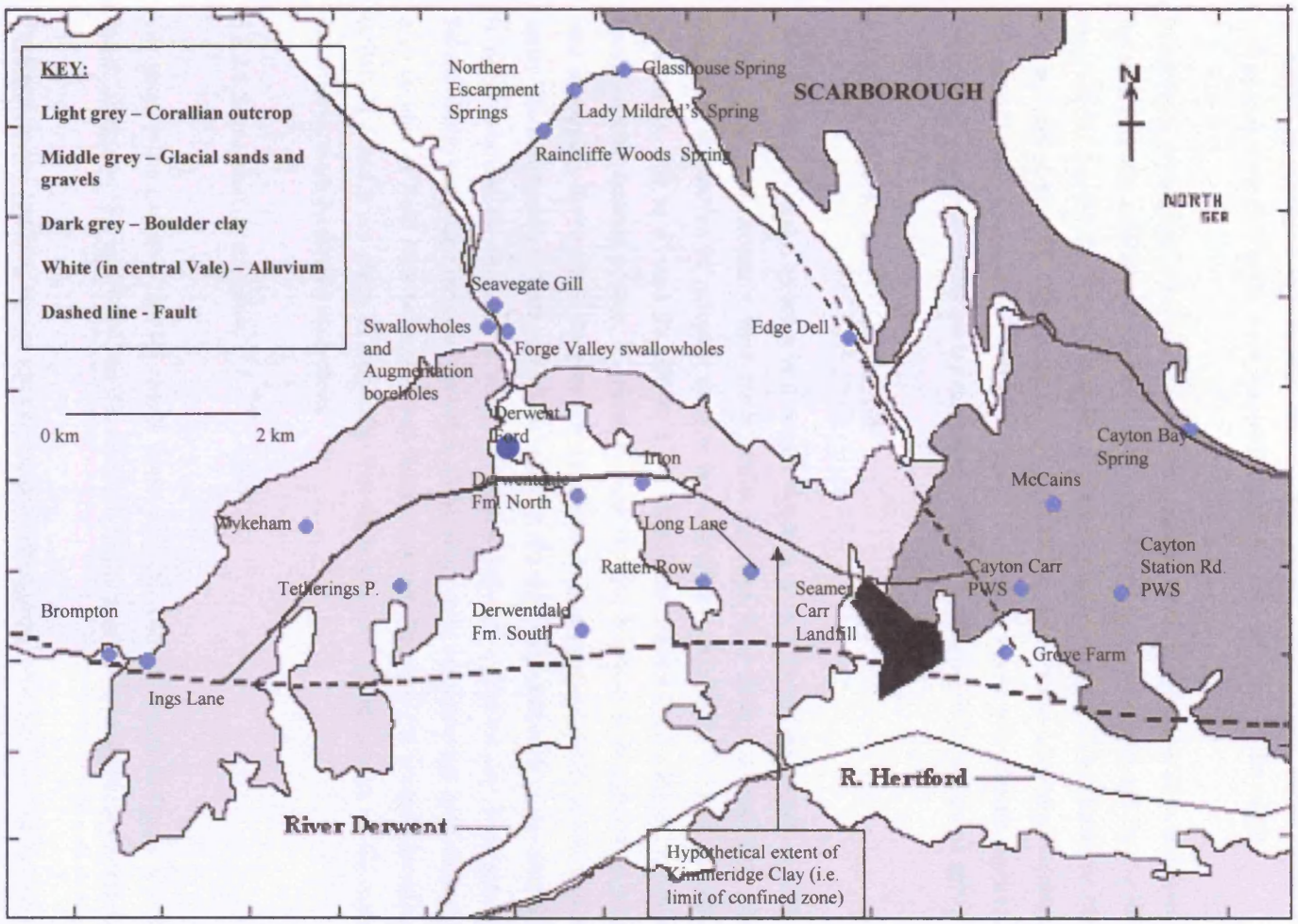

Figure 5.1 Geological schematic and experimental and sampling locations, eastern Vale of Pickering. Grid squares 1 km to a side.

5.2 GEOPHYSICAL LOGGING IN THE AYTON AREA.

5.2.1 INTRODUCTORY REMARKS

The geophysical logging of the Seavegate Gill, Augmentation and Swallowholes boreholes were all performed by European Geophysical Services Ltd. during August 2004. These results are presented here as part of the PhD as the work was performed under the direction of the author.

In addition, some geophysical material not undertaken as part of this research is summarised here. For the most part this material consists of logs for a number of wells drilled through the Corallian as part of the Osgodby Aquifer Storage and Recovery Scheme (also by European Geophysical Services Ltd.), but also includes parts of the 1981 geophysical survey of boreholes in the Ayton area (Beesley, 1981) and the 1969 logging of the Irton boreholes (Tate *et al.*, 1970). Please note that all depths referred to in Section 5.2 are metres below the borehole flange (mbfl). Actual borehole datums are given in the text.

5.2.2 INDIVIDUAL BOREHOLE LOGS

Where flow is recorded as being in a certain direction or of a certain magnitude, it must be borne in mind that all measurements were made whilst the Irton New Well was pumping. Although exact details are not known of pumping rates at the time of the geophysical surveys, pumping is usually between 14 000 m^3d^{-1} and 20 000 m^3d^{-1}, a significant amount. Accordingly, given a finite and interconnected fracture system, it cannot be said that any borehole is unaffected by pumping at the time of logging. However, as the pumping condition is the normal condition, and indeed the condition under which contaminant transport will occur (if it should), such distortion of the natural flow regime is not a problem for the current study. Note that logs are presented for Seavegate Gill and the Swallowholes and Augmentation boreholes, all of which were experimented upon during this study, to give an idea of fluid flow behaviour and fissure spacing. The logs for Irton Observation Boreholes (OBH) 2, 4 and 5 are given in Appendix 3 as these were not taken as part of this research and no experiments were performed upon them.

5.2.2.1 Seavegate Gill Borehole

The geophysical and flow logging results from Seavegate Gill are shown in Figure 5.2. The borehole datum (flange) is 38.1 maOD and the discussion in this section refers to depths below this datum.

Temperature and conductivity are virtually uniform throughout the borehole, with the vertical flow this implies being measured at between 2.3 and 4.2 cms^{-1} (upward) by the flowmeter. The CCTV and calliper logs show numerous fissures, several of which are associated with water flowing into or out of the borehole. In particular, major inflows and possible cross-flows occur at 32.2 m and 24 m, with smaller inflows/cross-flows at 22.6 m, 20.5 m and 18.6 m. Outflows occur at 11.1 m, 10.8 m and 9.7 m, with additional water being observed to flow upward behind the casing (from the CCTV log).

EUROPEAN GEOPHYSICAL SERVICES LTD
22 Hardwicke Industrial Estate, Hadnall, Shrewsbury Shropshire, SY4 4AS
Tel: 01939 210710 Fax: 01939 210532
Email: eurogeophys@compuserve.com Website: www.egs.lu

Figure 1 of 2 COMPOSITE GEOPHYSICAL LOG and CCTV OBSERVATIONS

CLIENT:	Yorkshire Water	DATE:	03.09.04
SITE:	East Ayton	PROJECT:	
WELL id:	Seavergate Gill BH	Logging Datum: Top of casing (flange)	ref: Seaver_A3.wcl

KEY Cal: Caliper mm, Gam: Natural Gamma api, T: Temperature °C, EC25: Electrical Conductivity µS/cm @25°C, DT&DC: Differential Logs, 0.4m NR: 0.4m Normal Resistivity Ohm.m, 1.6m NR: 1.6m Normal Resistivity Ohm.m, PR: Point Resistance Ohms, SP: Spontaneous Potential mV, LSD: Long Spaced Density g/cm³, HRD: High Resolution Density g/cm³, BRD: Bed Resolution Density g/cm³, Dnc: Density - compensated and borehole corrected g/cm³. Vp: P Wave Velocity m/s, Amp: P Wave Apitude %, TT: Transit Time (sonic) µs, FV: Fluid Velocity mm/s, CCL: Casing Collar Locator mV, pH: Acidity, ORP: Redox Potential mV, DO: Dissolved Oxygen % saturation, N, Nitrate as mg/l -N,
r: repeat run, u: up run, d: down run, p: pumped, s: static.

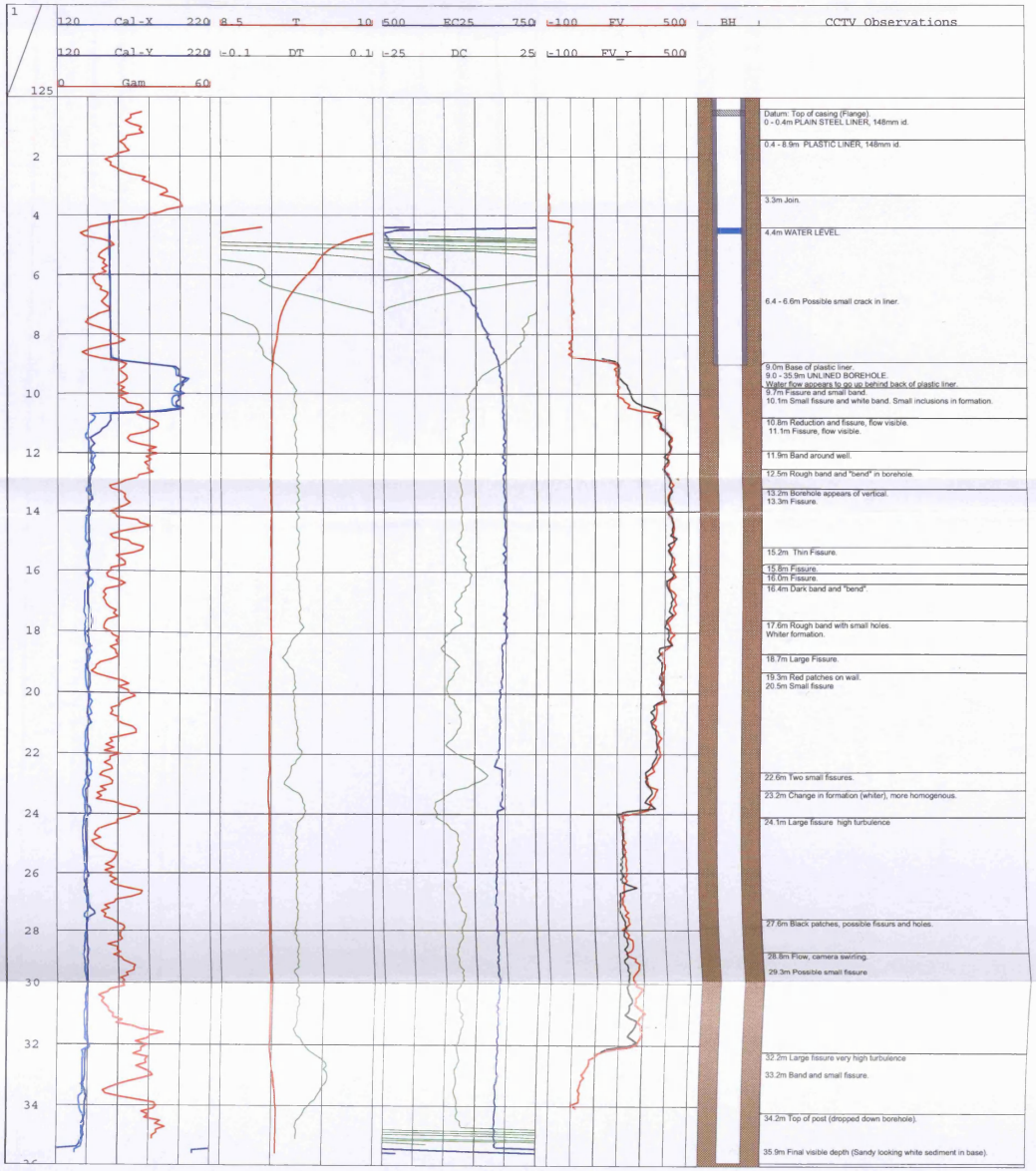

EUROPEAN GEOPHYSICAL SERVICES LTD
22 Hardwicke Industrial Estate, Hadnall, Shrewsbury Shropshire, SY4 4AS
Tel: 01939 210710 Fax: 01939 210532
Email: eurogeophys@compuserve.com Website: www.egs.lu

Figure: 53 COMPOSITE GEOPHYSICAL LOG and CCTV OBSERVATIONS

CLIENT:	Yorkshire Water	DATE:	02.09.04
SITE:	East Ayton	PROJECT:	
WELL id:	Swallowholes BH	Logging Datum: Top of casing (Flange)	ref: Swallow_A3.wcl

KEY Cal: Caliper mm, Gam: Natural Gamma api, T: Temperature °C, EC25: Electrical Conductivity µS/cm @25°C, DT&DC: Differential Logs, 0.4m NR: 0.4m Normal Resistivity Ohm.m, 1.6m NR: 1.6m Normal Resistivity Ohm.m, PR: Point Resistance Ohms, SP: Spontaneous Potential mV, LSD: Long Spaced Density g/cm³, HRD: High Resolution Density g/cm³, BRD: Bed Resolution Density g/cm³, Dnc: Density - compensated and borehole corrected g/cm³. Vp: P Wave Velocity m/s, Amp: P Wave Apitude %, TT: Transit Time (sonic) µs. FV: Fluid Velocity mm/s, CCL: Casing Collar Locator mV, pH: Acidity, ORP: Redox Potential mV, DO: Dissolved Oxygen % saturation, N, Nitrate as mg/l -N, r: repeat run, u: up run, d: down run, p: pumped, s: static.

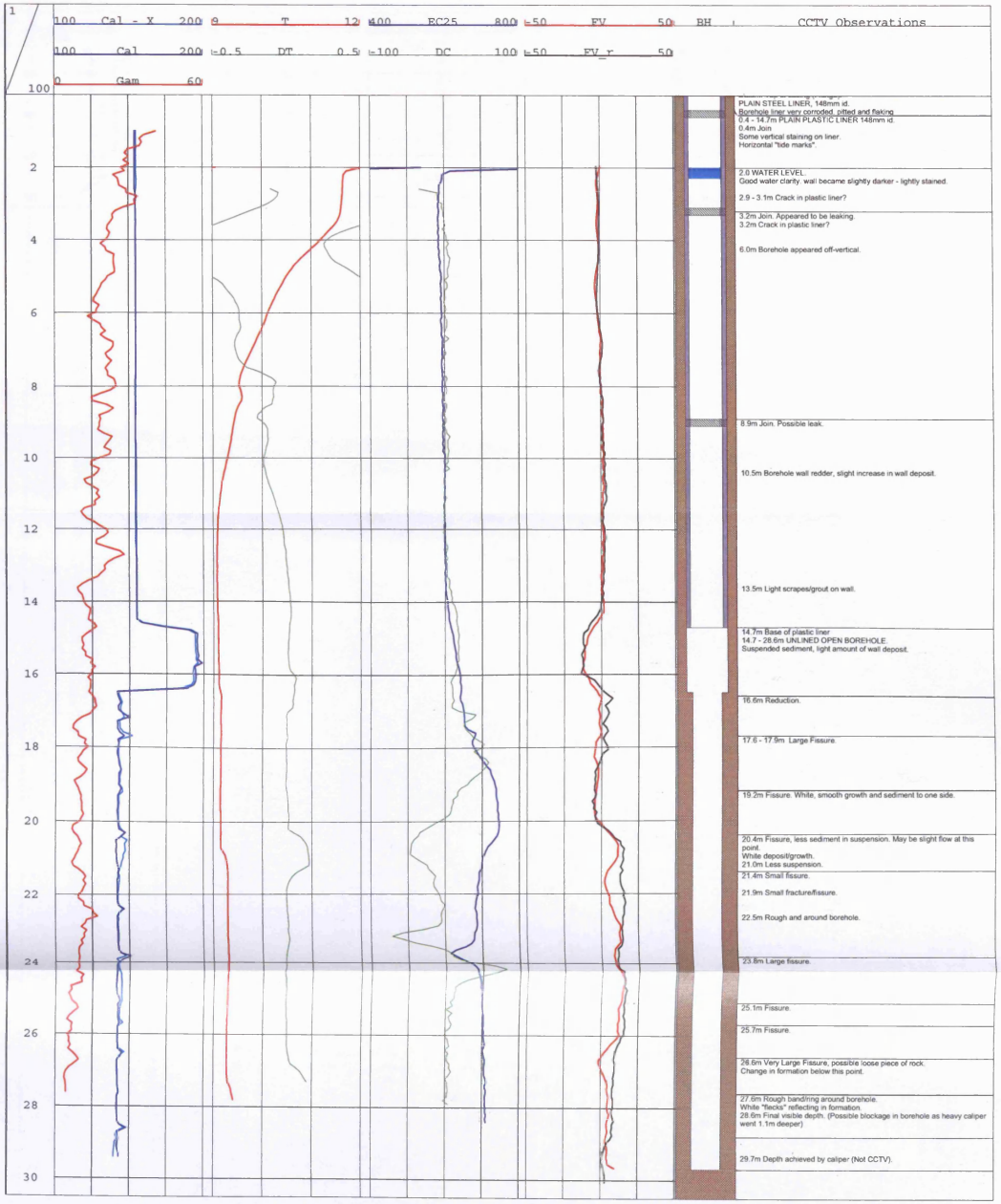

EUROPEAN GEOPHYSICAL SERVICES LTD
22 Hardwicke Industrial Estate, Hadnall, Shrewsbury
Shropshire, SY4 4AS
Tel: 01939 210710 Fax: 01939 210532
Email: eurogeophys@compuserve.com Website: www.egs.lu

Figure: 5.12 COMPOSITE GEOPHYSICAL LOG and CCTV OBSERVATIONS

CLIENT:	Yorkshire Water	DATE:	02.09.04
SITE:	East Ayton	PROJECT:	
WELL id:	Augmentation BH	Logging Datum: Top of casing (Flange)	ref: Augment_A3.wcl

KEY Cal: Caliper mm, Gam: Natural Gamma api, T: Temperature °C, EC25: Electrical Conductivity µS/cm @25°C, DT&DC: Differential Logs, 0.4m NR: 0.4m Normal Resistivity Ohm.m, 1.6m NR: 1.6m Normal Resistivity Ohm.m, PR: Point Resistance Ohms, SP: Spontaneous Potential mV, LSD: Long Spaced Density g/cm³, HRD: High Resolution Density g/cm³, BRD: Bed Resolution Density g/cm³, Dnc: Density - compensated and borehole corrected g/cm³, Vp: P Wave Velocity m/s, Amp: P Wave Apitude %, TT: Transit Time (sonic) µs, FV: Fluid Velocity mm/s, CCL: Casing Collar Locator mV, pH: Acidity, ORP: Redox Potential mV, DO: Dissolved Oxygen % saturation, N, Nitrate as mg/l -N,
r: repeat run, u: up run, d: down run, p: pumped, s: static.

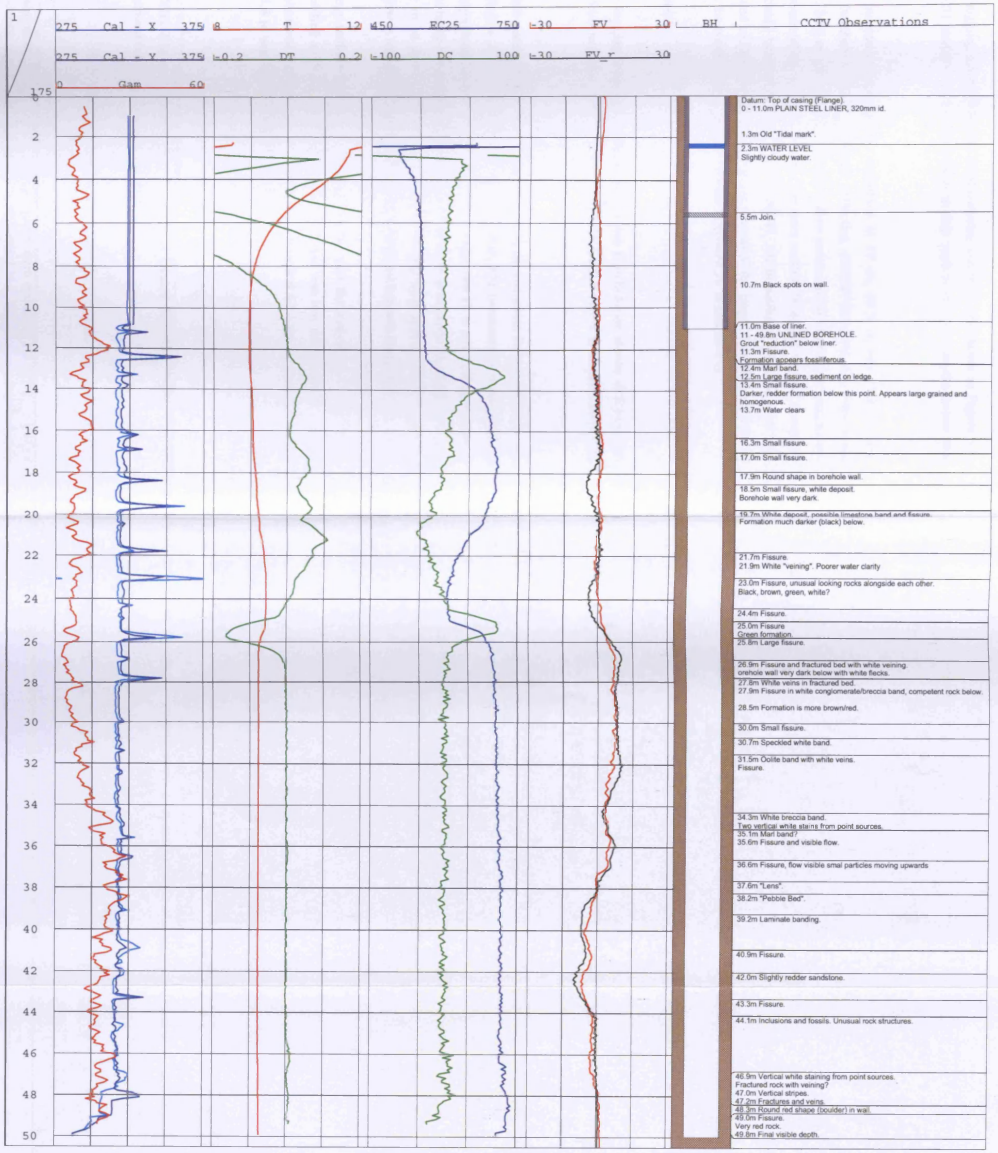

5.2.2.2 Swallowholes Borehole

The geophysical and flow logging results from the Swallowholes Borehole are shown in Figure 5.3. The borehole datum is 35.31 maOD and the discussion in this section refers to depths below this datum.

The conductivity profile indicates water quality variations at 17 m, 20.5 m and 23.8 m. The temperature profile of the borehole is almost constant, reflecting vertical flow, but also with minor positive variations at 17 m, 20.5 m and 26.5 m. The main inflow points derived from flow logging are at 20.5 and 26.5 m, with minor inflow at about 23.7 m. The main outflow is at 20.4 m with secondary outflow at 16 m and probably behind the casing (EGS, 2004). All in/outflows are associated with fissuring, with the CCTV and calliper logs clearly showing several of the larger fissures, and with the highest upward velocity in the borehole measured at 1.6 cms^{-1} between 26 m and 20.4 m.

5.2.2.3 Augmentation Borehole

The geophysical and flow logging results from the Augmentation Borehole are shown in Figure 5.4. The borehole datum is 35.00 maOD and the discussion in this section refers to depths below this datum.

The temperature log varies between the bottom of the casing at 11 m, and about 26 m, with variations of not more than 0.2° C. Below 26 m there is virtually no variation. The conductivity is also uniform below 26 m, but shows a significant decrease of about 50 μScm^{-1} between 18 m and 25.8 m, indicative of fresher water in the aquifer at this interval. The little flow that there is between 18 m and 25.8 m is shown by the flow meter to be downward, whereas above 18 m any flow appears to be across the borehole. Below 25.8 m flow is upward from about 38 m, but downward beneath that point.

The CCTV and calliper logs indicate that the aquifer is extremely well fissured down to about 28 m, with a major outflow identified at 25.8 m. Below 28 m the limestone was less well fissured, although major inflows were still observed in a fissured zone at 35.6 m, 38 m and 43.3 m. The upward vertical flow between 34 m and 25.8 m was measured at 0.75 cms^{-1}.

5.2.2.4 OBH[14] 2

The geophysical log of OBH 2 is given in Appendix 3. OBH 2 is located on-site at Irton WTW. All depths are metres below ground level, which is about 30 maOD.

[14] OBH stands for Observation Borehole. Several such boreholes were drilled as part of the Osgodby Aquifer Storage and Recovery scheme (Yorkshire Water Services Ltd.). Not all were geophysically logged through the Corallian before the borehole casing was emplaced.

The log was run between 35.1 m and 70 m. Conductivity is lower above 48 m than below 51 m, indicating fresher water, and both conductivity and temperature logs show significant variations between 48 m and 51 m. These points are associated with major influent fissures at 48.1 m and 50.7 m. Other large fissures were observed (with the CCTV) at 40.7 m and 60.7 m., many smaller fissures were also observed. The borehole was openly overflowing under artesian conditions at the time of logging, with the maximum rate of upward flow within the cased section attaining 150 cms^{-1}. Calculating from a borehole diameter of 15 cm, the flow was about 2300 m^3d^{-1}, or about 26 Ls^{-1}.

Freshwater shrimps were seen living in this borehole and a small eel was found at depth during drilling. These are clear indicators of the importance of sizeable fissures in transporting water from the river Derwent to the Irton site.

5.2.2.5 OBH 4

The geophysical log of OBH 4 is given in Appendix 3. OBH 4 is also located on-site at Irton WTW. All depths are metres below ground level, which is about 30 maOD.

OBH 4 was logged through the bottom of the Kimmeridge Clay, the full thickness of the Corallian and partially through the Oxford Clay. The temperature and conductivity logs were uniform above 65 m and between 65 m and 81 m. The freshest water, at about 420 μScm^{-1}, enters the borehole at 65 m and above, more conductive water (c. 440 μScm^{-1}) enters at 81 m, and between 81 m and the bottom of the aquifer at about 122 m the water is more conductive still, at about 470 μScm^{-1}. Below the Lower Calcareous Grit, the conductivity and temperature both increase gradually, indicating stationary water within the Oxford clay. The majority of flow entered the borehole through fissures between 52 m and 55 m, with minor contributions from fissures at 65 m, 80 m, and over the interval 80-105 m. All of this water flows upward to leave the borehole via a fissure at 32.5 m and through the bore under overflowing artesian conditions at a rate of about 4600 m^3d^{-1} , or 12 Ls^{-1}, with a velocity of about 23 cms^{-1}.

5.2.2.6 OBH 5

The geophysical log of OBH 5 is given in Appendix 3. OBH 5 is situated at Betton Farm, 1600 m north of Irton at TA08 002 856. All depths are metres below flange (mbfl), which is at about 67 maOD.

The Corallian is unconfined at Betton Farm, with a water level at 27 mbfl leaving some 20 m of unsaturated oolitic limestone above it. The temperature profile of the borehole is a fairly uniform 10.3° C above an inflow point at 61 m. Below this there is a steady increase, with a small reduction at 80 m, to about 10.6° C at the bottom of the Corallian (at 100 m). The conductivity was lowest over the interval 80 m to 95 m, below which it increased with depth. Above 80 m the conductivity varies little until about 65 m, above which point several orange-stained fissures seem to contribute the majority of

flow to the borehole (with a major fissure at 61 m). Several minor inflows are associated with fissures occurring between 80 m and 42.5 m. The low-conductivity interval, entirely within the Lower Calcareous Grit, may be associated with flow from the River Derwent, however, as this would have to flow both up-dip and up-gradient it seems unlikely. Fresher water at this depth may be associated with flow solely in the sandstone that has had little contact with the more soluble limestone beds, or may be due to rapid fracture flow to this depth (which is more likely). Above 90 m the water was flowing upward, with only one major outflow point identified with a fissure just beneath the bottom of the casing at 30.1 m

5.2.2.7 Irton Old Well

Irton Old Well was logged by Tate, Robertson and Gray in 1969 (Tate *et al.*, 1970). They used CCTV and measured the temperature and conductivity profiles (Figure 5.5), as well as measuring the flow regime in the well under different pumping conditions in the Old and New wells, with the aid of both a flow meter and a saline tracer. They also took measurements of tritium for the well and a number of other locations. In addition, ARUP (2000) conducted tracer testing with Photine and using cotton wool detectors stationed at the positions marked on the figure, and these results will be discussed in turn with other environmental and artificial tracer results. Briefly, from their logging work, Tate *et al.* (1970) identify two major influent fissures within the Old Well, one at 35 m and one at 56 metres below ground level, which is about 29 maOD. Under natural flow conditions, (i.e. with both pumps off) the water from the upper fissure flows upward, whilst that from the lower fissure splits, flowing upward and downward. With the New Well pumping and the Old Well off (i.e. the present-day pumping regime), all of the water entering the Old Well travelled downward to some unidentified fissure connecting the two boreholes beneath a blockage in the Old Well at about 75 m. Water velocity in the Old Well, under these conditions (New Well pumping at c. 14 000 m^3d^{-1}) is 1.5 cms^{-1}. These data will be discussed more fully in Chapter 6.

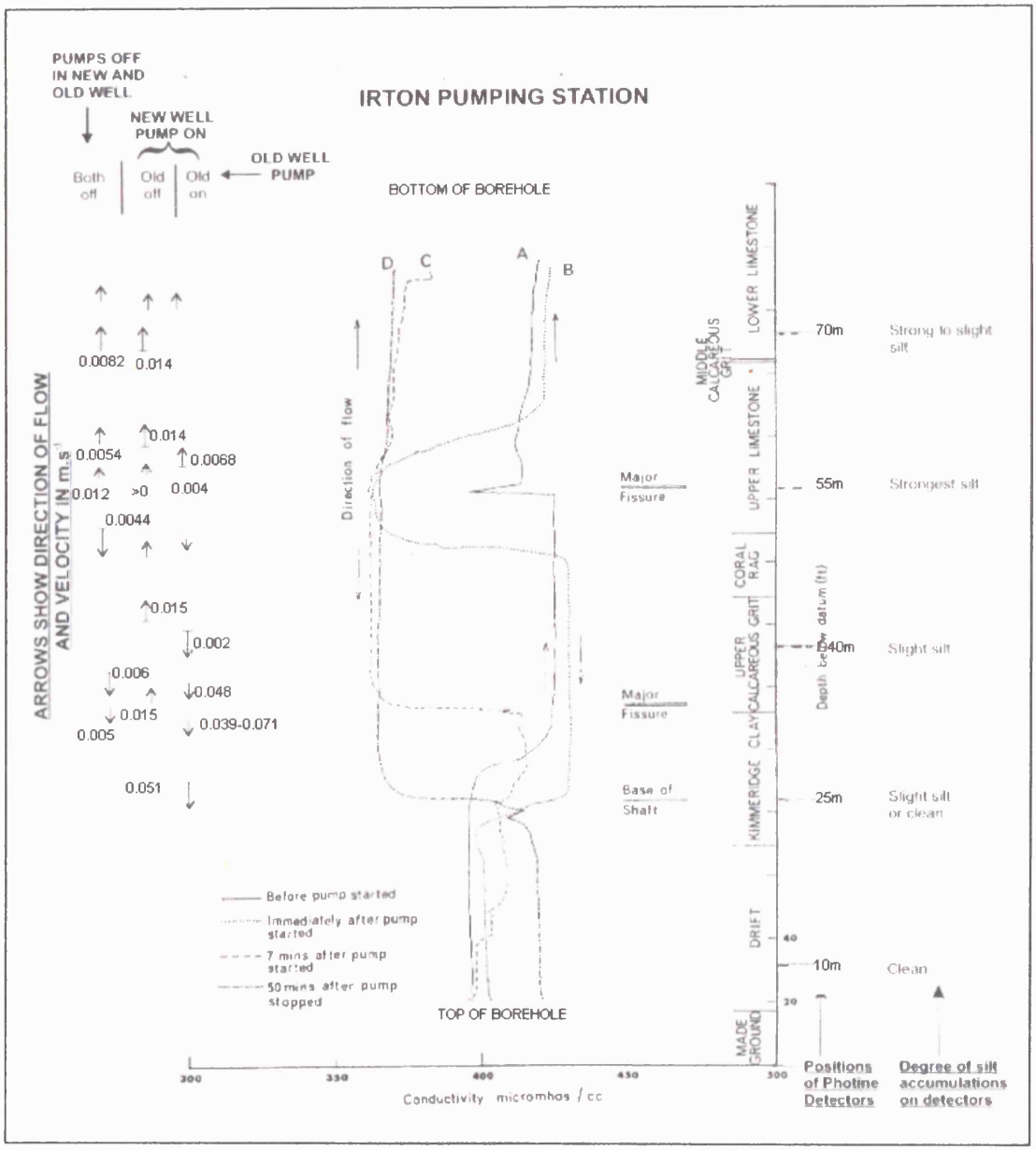

Figure 5.5 Geophysical and fluid log of Irton Old Well under different pumping regimes. Adapted from Tate *et al.* (1970).

5.2.3 FISSURE SPACING AND APERTURE

From the series of wells and boreholes logged through the Corallian, it has been possible to collate a body of information regarding the frequency and aperture size of fissures penetrating the Corallian.

On the calliper and CCTV logs, fissures have been qualitatively labelled 'very large fissure', 'large fissure', 'fissure' and 'small (or 'thin') fissure'[15]. By inspecting the CCTV footage of the three Forge Valley boreholes, it has been possible to tentatively assign a fracture aperture to each of these labels (see Table 5.1). It should be noted that the assigned apertures are only an approximation and that some exceptions have been made on closer examination of the geophysical logs. However, using the values from Table 5.1 as a rough guide, it is possible to detail spacing and frequency of different aperture sizes, and to derive a rough estimate of fracture porosity. These estimates are given in Table 5.2.

Fissure description	Assigned aperture
Very large fissure	5 cm
Large fissure	2 cm
Fissure	0.5 cm
Small/thin fissure	0.1 cm

Table 5.1 Apertures assigned to borehole log descriptions, based on an examination of CCTV footage of fissures.

Property	Oolitic Limestone	Calcareous Grit	Whole Corallian
Measured interval (m)	125.5	127.5	253
No. of boreholes	6	4	6
No. of fractures	80	43	123
Avg. fracture spacing (m)	1.57	2.97	2.06
Avg. fracture aperture (m)	0.0063	0.0071	0.0067
Spacing of fractures w. 5cm apertures (m)			136
Spacing of fractures w. 2cm apertures (m)			17
Spacing of fractures w. 0.5cm apertures (m)			4
Spacing of fractures w. 0.1cm apertures (m)			7
Fracture porosity	0.0037	0.0021	0.0029

Table 5.2 Fissure spacings and apertures for the Corallian Limestone as a whole and as subdivided into oolitic limestones and calcareous grits, derived from the geophysical logging of six boreholes in the Corallian.

From Table 5.2 it may be seen that two major differences exist between the two types of unit, the oolitic limestones and the calcareous grits. The first of these is that the average fissure spacing for the oolitic limestones is almost half that of the calcareous grits, at 1.57 m and 2.97 m respectively. It should be noted that most of the measured data for the calcareous grits is from the Lower Calcareous Grit, whereas the majority of measurements for the limestones are across both the Upper (Malton) and Lower (Hambleton) Oolites. There may thus be a bias in the data toward fissure spacing in the Lower

[15] All logs were performed by the same person.

Calcareous Grit, although this will not be important for those sites were the Upper Calcareous Grit is not present, such as at outcrop or in Forge Valley.

The second major difference is in the fracture porosity of the two units. Fracture porosity has been calculated by summing all fracture apertures and dividing this sum by the total interval over which the fractures occur, minus the summed fracture interval. This procedure results in an estimated fracture porosity of the limestone roughly twice that of the sandstone.

The values of porosity, aperture width and spacing are useful parameters for modelling the behaviour of groundwater, tracer and contaminant movement within the aquifer.

5.3 BOREHOLE DILUTION TEST RESULTS

5.3.1 RESULTS AND QUALITATIVE DISCUSSION OF MEASURED DILUTION (INCORPORATING GEOPHYSICAL LOGGING RESULTS).

5.3.1.1 Introductory remarks

The results of the borehole dilution tests are shown in Figures 5.6 to 5.12. They are presented together with qualitative discussions of the individual BHDT results. This aims to highlight those features of either greater or lesser significance that have a bearing upon the quantitative interpretation of the experimental results and which are drawn upon for both the modified standard method and the curve-matching method of interpreting BHDTs (Section 5.4). Because of the nature of the BHDT simulation (curve-matching) program used later in the chapter, the results (and later modelling) are presented in terms of depths below casing. The bottom of the casing in each borehole is therefore assigned to be at **zero** depth, and all results given as a function of this depth. So that the *actual* depths of these measurements/simulations are transparent, Table 5.3 gives all borehole elevation and casing details, as well as details of which part (formation or member) of the Corallian the borehole is open to. From this table it can be seen that the casing length may be used as an approximate guide to the depth below ground at which the zero depth is found for any given borehole. Exact elevations are also given.

Borehole name	Grid Ref.	BH Elevation (flange) maOD	Casing length m	Depth of BH maOD	Elevation of base of casing maOD	Formations penetrated
Augmentation	SE 990 852	35.00	11	50	24.00	LO & LCG
Swallowholes	SE 990 857	35.31	14.4	35	20.91	LO & LCG
Derwent Ford	SE 992 844	32.46	24	35.5	8.46	UCG or UO
Tetherings Plump	SE 976 827	29.86	30	80	-0.14	UCG, UO, LO, LCG
Wykeham Village Hall	SE 968 835	46.96	17.5	70	29.46	UCG, UO, LO, LCG
Brompton Dale Shallow	*SE 943 823*	*33.62*	*15*	*17.75*	*18.62*	*LO*
Brompton Dale Deep	SE 943 823	34.03	45	47	-10.97	LCG

Notes:
1) Casing length may be used as an approximate guide to the depth below ground level at which the BHDT results and modelling have their 'zero' points (i.e. the point at the top of the uncased section).
2) The elevation of the base of the casing, in maOD, corresponds to the actual 'zero' point used in the presentation of BHDT results and modelling.
3) LO - Lower Oolite, UO - Upper Oolite, LCG - Lower Calcareous Grit, UCG - Upper Calcareous Grit.

Table 5.3 The elevations of borehole flanges (datums) and the bases of borehole casings together with casing lengths, depths of boreholes and geological formations and members penetrated.

The results are given as plots of (C-Cb)/(C0-Cb) vs. depth, where C = concentration at any time, Cb = background concentration and C0 = starting concentration[16]. The results are presented in this way so as to permit comparison of the measured results with the output from the simulation models (Section 5.4). The 't' number on the graphs refers to borehole profiles taken beginning at that time (in minutes) following injection, e.g. t20 refers to the measurement profile commenced 20 minutes after the withdrawal of the injection hose. Unfortunately the length of time taken for a single profile may be significant in relation to dilution times, especially at early time. It is possible to correct this with an interpolation technique, although this has not been attempted here. It is also important to note that all

[16] As dilution may be initially rapid, the starting concentration is derived from the average concentration observed over the cased section of the borehole, into which tracer was also injected.

depths cited in the following discussions are depths below casing, as this too aids comparison between the experimental and modelling results.

It should be noted that the boreholes occasionally show elevated conductivity in the bottom metre or two. This is thought to be associated with the weight suspended from the bottom of the injection hose disturbing sediments settled at the base of the borehole.

5.3.1.2 The Augmentation Borehole

The Augmentation Borehole is an important borehole as it penetrates nearly the full thickness of the Corallian in the immediate vicinity of the Forge Valley swallowholes. From the geophysical logs it can be seen to exhibit a number of flowing fractures and variations in water chemistry, which are confirmed by the experimental results shown in Figure 5.6 below.

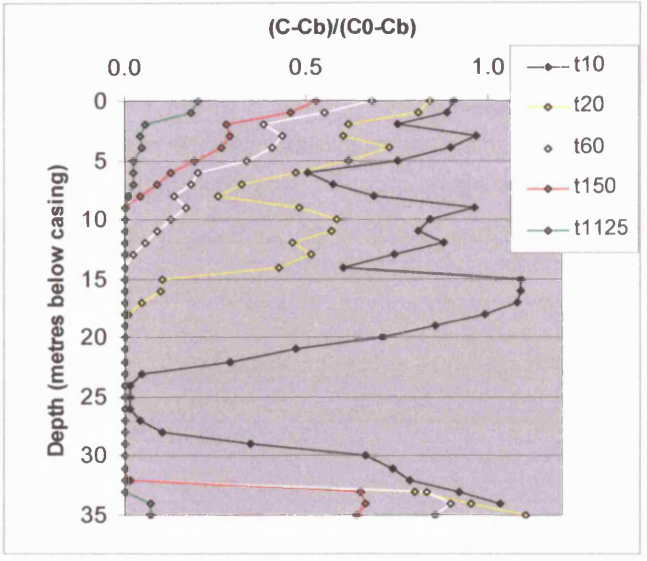

Figure 5.6 Augmentation Borehole dilution test. Casing length 11 m.

The most striking feature of the BHDT is the large deflection in conductivity centred around 25 m. This feature is associated with two strongly flowing fractures, one at 24.6 m and one at 25.6 m, and one lesser fracture at 32.3 m, all subsequently identified in the geophysical logging. The deflection may therefore be taken to be a product of very rapid initial dilution, as opposed to a fault in tracer injection (which would have to be a serious fault indeed to span an interval greater than 10 m). From the dilution test results, the water entering at around 25 m appears to diverge, creating both upward and downward moving fronts. This is confirmed by the geophysical logging.

From the geophysical log there is a decrease in the background conductivity between 9 m and 14 m, indicative of a river water contribution to the borehole. This is confirmed by the presence of tracer at this horizon within 24 hours of injection into the Forge Valley swallowholes (ARUP, 2000). Furthermore, from an examination of the geophysical logs, the flow in this part of the borehole is

downward. These important pieces of information enable the observed dilution between 9 and 14 m to be ascribed to an additional inflow of water, and not just the continued upward migration of water entering at the 25 m zone. The geophysical logs indicate that influent water from both the 25 m and the 9-14 m zones exits via a fracture at 14.8 m. Water also flows downward from 25.6 m to 32.3 m. Cross flow is occurring above 14.8 m as nothing else explains the active dilution (experimental) and zero vertical flow (logging) in this zone of the borehole. Below the 14.8 m point much of the flow seems to be vertical, although cross-flow cannot be eliminated.

It should also be noted that where the concentration appears to rise above C/C0 = 1 this is due to the fact that initial concentrations were not based upon what was measured in the borehole at that point (due to high initial dilutions) but to concentrations in the cased section of the borehole (as these were generally stable and considered representative of initial conditions).

5.3.1.3 The Swallowholes Borehole

Overall the Swallowholes borehole (Figure 5.7) shows an uneven distribution of tracer at t35, although it is even over the intervals 0 – 2 m and 3 – 11 m. This is suggestive of rapid dilution caused by vertical flow in the 3 – 11 m region. This hypothesis (as opposed to that of uneven tracer distribution) is supported by the lower background conductivity values below 6 m that correlate with the river-influenced zone in the Augmentation borehole, 18 m distant, and a possible flowing fracture at 9 m (confirmed by the geophysical logging).

However, in contrast to the Augmentation borehole, flow in the zone of rapid dilution is upward until a fracture at about 5.8 m (from the geophysical logging), and either horizontal or downward above this point.

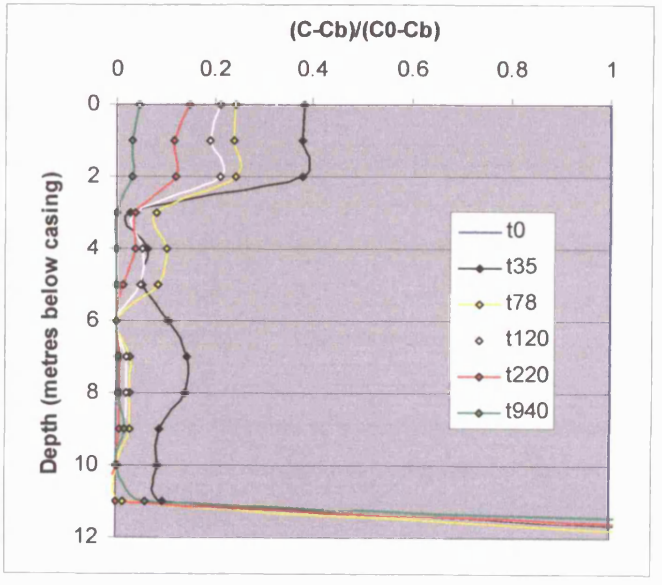

Figure 5.7 Swallowholes Borehole dilution test. Casing length 14.4 m.

The bottom of the borehole appears to be stagnant in terms of tracer dilution with elevated levels probably due to a combination of injection artefacts and disturbance of sediments.

5.3.1.4 The Derwent Ford Borehole

The borehole exhibits erratic dilution at earlier times (Figure 5.8), probably due to density effects associated with the sodium chloride present in the cased section of the borehole. This has largely resolved itself by 50 minutes, with steady dilution from then until 330 minutes, the last measurement.

A flowing fracture was recorded in this borehole at 2 m in the 1981 geophysical logging (Beesley, 1981). The early time measurements at this depth also indicate some enhanced dilution, although this is later masked, possibly by mixing associated with vertical flow, possibly by density-driven tracer movement from within the cased section. The borehole only approaches background concentration within 330 minutes at about the 6-7 m level. The t50 and t110 measurements indicate that this may also be a zone of preferential flow, although this is not noted in the report of Beesley (1981). Both the background temperature and conductivity of the borehole were constant, in 1981 (Ibid.) and in 2003 (this study), indicating vertical movement of groundwater.

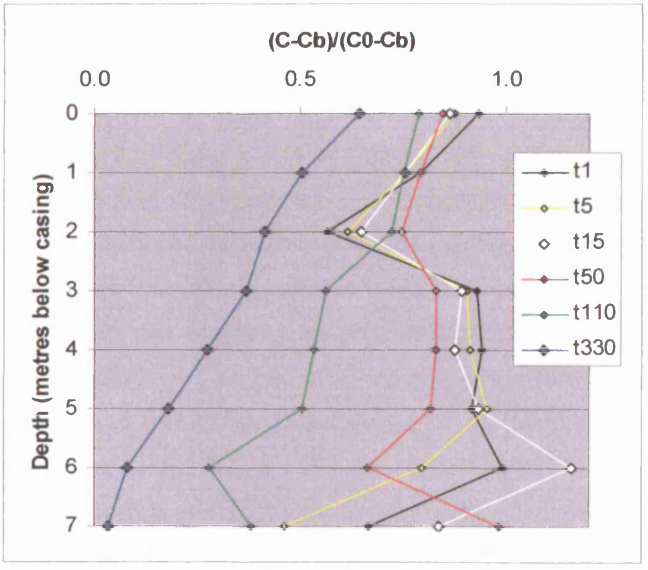

Figure 5.8 Derwent Ford Borehole dilution test. Casing length 24 m.

5.3.1.5 The Tetherings Plump Borehole

This borehole shows three contrasting horizons (Figure 5.9). The uppermost, from 0 to about 3 m, shows a steady but swift dilution, not quite returning to background within 445 minutes, the time of the final measurement. From 3 to 8 m, there appears to be very rapid initial dilution followed by a less rapid decline in conductivity, and below this there is a zone of obvious stagnation.

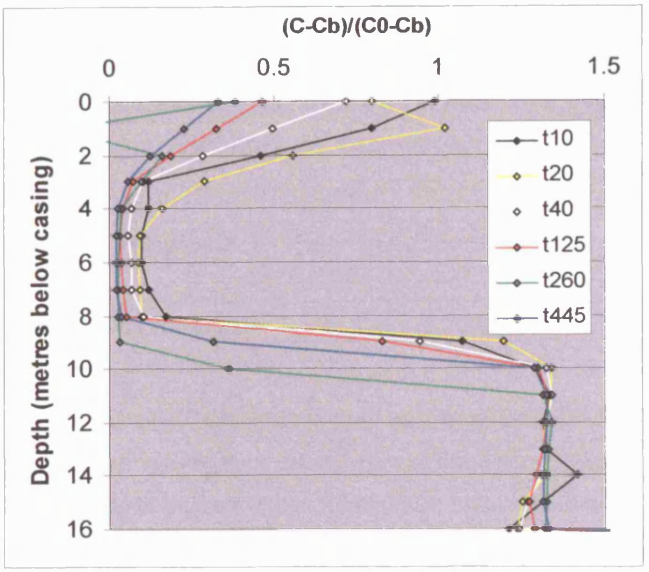

Figure 5.9 Tetherings Plump Borehole dilution test. Casing length 30 m.

The zone of 'rapid dilution' is of the most interest. It is not possible to tell whether uneven tracer distribution is responsible for the low concentration at t1. This may be the case, as should the same rate of dilution occur at times t>1 as between t0 and t1, it might be expected that the borehole returns to background (Cb) virtually immediately, which it does not. There are still measurable concentrations of chloride in this zone at all times subsequent to t1. However, in those parts of this and other boreholes where dilution is not so rapid, tracer distribution appears to be reasonably uniform (see below). In addressing this question, some further points may be noted. Firstly, in the zone from 0-3 m, dilution is more or less steady and the form of the recession is one whereby there is a smooth transition between the top of the 'rapid dilution' zone and the bottom of the casing. This may indicate that tracer is being diluted by upward flow from the zone of rapid dilution below. However, that the measurement at t20 is higher than that at t10 indicates that there may be some additional tracer entering this section of the borehole from the cased section above, as a result of density-driven flow. In fact, inspection of the measurements within the lower part of the cased section of the borehole (not shown) indicate a decreasing tracer concentration, so that density effects are in fact likely. The second point is that, at the top of the stagnant zone, tracer is removed considerably more slowly, with the first appreciable decrease at 40 m only occurring at 260 minutes. Moreover, at 9 m the concentrations fluctuate with time, with some later times showing greater concentrations than earlier times (i.e. t20>t10 and t445>t260). This suggests that some tracer from the zone of stagnation is being drawn upward into the zone of 'rapid dilution'. That the latter zone shows a swift decrease in concentration, followed by a maintenance of low concentrations, may be thus explained by the addition of tracer to this zone from either above or below at later times. It is therefore hypothesised that the 'rapid dilution' zone is just that: a 5 m horizon undergoing enhanced flow, and not a product of uneven tracer injection. In addition, the uniformity of concentration in this zone at later times is indicative of vertical flow, with that tracer entrained in the flow only exiting the borehole at a specific horizon. Assuming upward flow, this point is probably at about 3 m.

There is no geophysical information on the Tetherings Plump borehole except the somewhat insensitive temperature and electrical conductivity logs taken as background readings prior to the BHDTs. The conductivity log indicates a change from 0.48 mS cm^{-1} within the casing to 0.49 mS cm^{-1} at 3 m, and a second more significant change to 0.54 mS cm^{-1} at 4 m, which is the conductivity maintained throughout the remainder of the depth to which the probe could reach (17 m below casing). The temperature log shows a uniform 9.5° C throughout the uncased section.

5.3.1.6 The *Wykeham Village Hall Borehole*

The borehole at Wykeham (Figure 5.10) displays a more or less uniform distribution of conductivity at 1 minute after injection, with the exception of the uppermost few metres. Again this exception may be due to either preferential flow or to uneven tracer distribution. Following time t1 the tracer dilutes in a steady fashion at most depths, with the swiftest dilution occurring in the upper part of the borehole and getting slower toward the bottom. The broad movement of this 'front' of fresher water entering the borehole may be due to vertical movement stemming from inflow at the 1 – 2 m interval. This hypothesis is also supported by the uniformity of the background conductivity (measured as part of the BHDT; there is no geophysical log for this borehole). On the other hand, it may be due to different rates of horizontal flow throughout the upper part of the borehole, which cannot be discounted.

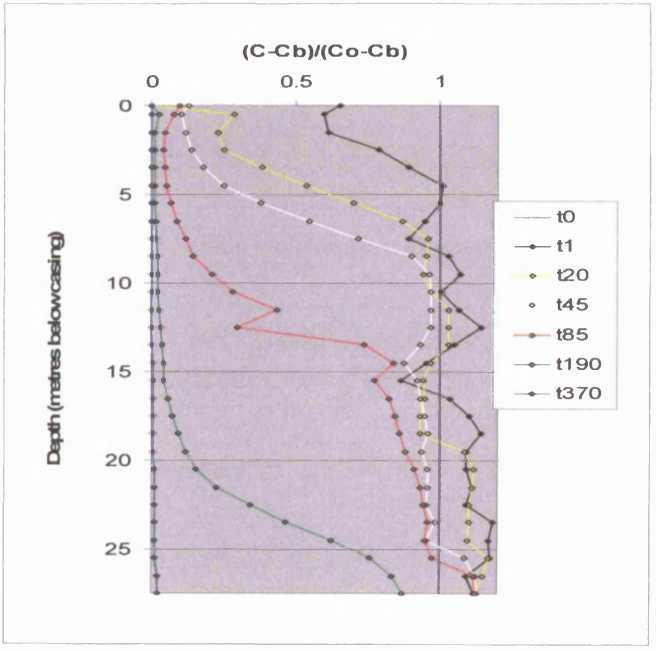

Figure 5.10 Wykeham Village Hall Borehole dilution test. Casing length 17.5 m.

Should vertical flow exist, it is notable that, in contrast to the majority of vertical flows identified during the experiments and logging, in the Wykeham borehole it appears to be downward. This may be explained by the location of the borehole, which is in the unconfined zone on the northern edge of the Vale of Pickering, where the groundwater is flowing down the dip of the aquifer. It is thus possible to identify this borehole as being in an area of recharge, in contrast with those in discharging areas where flow is strongly controlled by either pumping wells (in the confined Vale of Pickering east of

Brompton), the Ebberston-Filey fault (for example at Brompton) or a nearby river (or a combination of these), in which cases the vertical flow is predominantly upward.

5.3.1.7 The Brompton Dale Shallow Borehole[17]

This borehole shows unevenness in tracer distribution immediately after injection that may be attributable to either injection anomalies or immediate losses (Figure 5.11). However, the subsequent evenness between 0.4 and 2.0 m, together with the most enhanced potential dilution at 2.0 m (t1 onward), indicate the possibility of inflow at this point. The background conductivity is largely uniform, with a minor dip at the top of the profile that may be associated with the borehole casing.

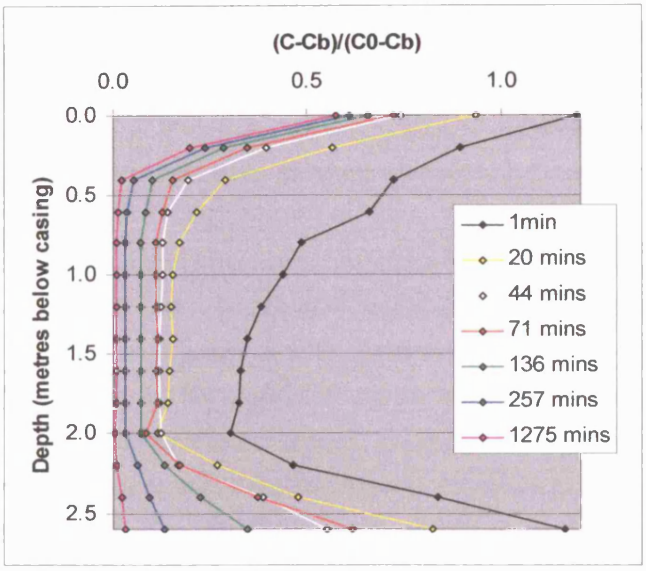

Figure 5.11 Brompton Dale Shallow Borehole dilution test. Casing length 15 m.

As the dilution is uneven, the background conductivity is uniform and the interval over which dilution is occurring is small (c. 3 m), the likelihood of vertical flow is high.

5.3.1.8 The Brompton Dale Deep Borehole

The Brompton Dale Deep Borehole (Figure 5.12) shows excellent uniformity in both tracer injection across the uncased interval and in subsequent dilution. The tracer injection profile, as represented by the t1 measurements, does not vary significantly from the average, except at 0.2 and 0.4 m, where it is above average, and at 0 m, where it is just below. Enhanced dilution at later times is evident across the interval 0 to 0.4 m and indicates that the elevated conductivity from 0.2 to 0.4 m is an artefact of injection, albeit a slight one.

[17] The BHDTs and tracer tests conducted at Brompton were all done in partnership with a fellow student, Patrick Mottram, who performed fieldwork with the aid of the author on the understanding that it would form a part of this thesis. The data, presented in his B.Sc. thesis (Mottram, 2003), has been reworked in the light of errors found to exist in the original interpretation.

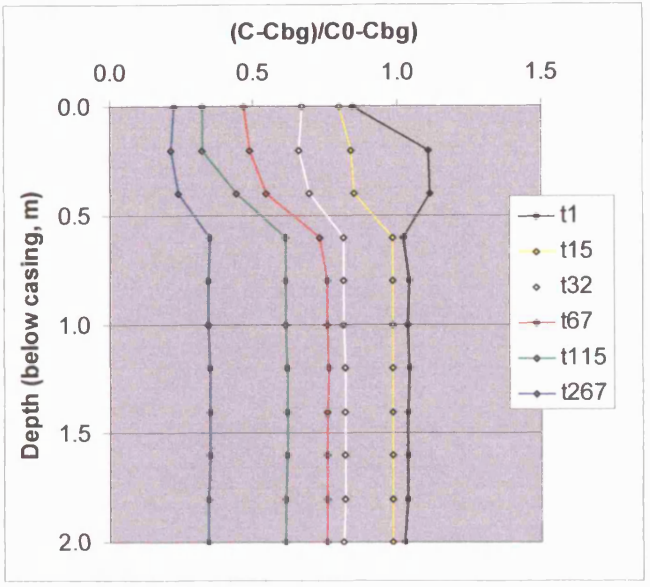

Figure 5.12 Brompton Dale Deep Borehole dilution test. Casing length 45 m.

The background concentration shows elevation in the same region as the enhanced dilution, which seems to indicate that there is some stratification within the aquifer at this point. Based upon geological maps of the area (Fox-Strangways, 1881; BGS 1998), it is likely that, at 48 m deep, the borehole is penetrating nearly the full thickness of the aquifer at this point in Brompton Dale, the upper parts of the Corallian having been removed by erosion. Given this information, and that the boreholes are only a couple of hundred metres from Brompton Springs, as well as measured differences in head, all indications are that there is an upward hydraulic gradient in the aquifer here. Therefore any vertical flow may be expected to be in an upward direction, although from the evidence of the BHDT the dilution may well result from purely horizontal flows.

5.3.1.9 General observations

Several general observations may be made about these graphs:

1. The boreholes generally return to their background concentrations within the space of a few hours.
2. In several of the boreholes, at specific horizons, the time taken to return to background levels is of the order of a few tens of minutes, or even a few minutes.
3. Differential dilution rates between depths are apparent for most experiments.
4. Much of the dilution appears to be due to vertical movement of tracer.
5. The data can be noisy and dilution at particular horizons does not always occur in a smooth order between measurements.

The first two of these observations demonstrate rapid groundwater flushing of the boreholes. The third observation clearly indicates preferential flow within the aquifer. The fourth (although requiring closer

scrutiny) confirms that vertical flow is an important (and possibly even completely dominant) component of flow, and this point is discussed more fully in Section 5.4.2.4. The final observation is one of heterogeneity of concentrations, the connotations of which will also be discussed below.

5.4 A MODIFICATION TO THE 'STANDARD' METHOD OF ANALYSING BOREHOLE DILUTION TEST DATA.

5.4.1 THE 'STANDARD' METHOD OF ANALYSIS

This section gives a stepwise description of the process followed to derive a specific discharge value for individual horizons within the boreholes. With some adjustment for tracer type, this is essentially an adaptation of the method given in the UK Environment Agency's guideline to tracer testing (Environment Agency, 1998), and which was first put forward by Halevy *et al.* (1967) and brought to a wider audience by Drost *et al.* (1968).

1. The data is plotted as conductivity versus time to give an idea of the overall form and quality of the dilution process.
2. Conductivity measurements are transformed to concentrations (C) according to the relationship:

$$y = 0.5786\,x - 0.2071 \qquad (5.1)$$

where y = chloride concentration (gL^{-1}) and x = conductivity ($mScm^{-1}$). This relationship was derived by calibrating the borehole conductivity probe response against several solutions of known concentration[18].

3. Post-injection concentration values are corrected for the measured background conductivity (Cb).
4. Ln (C-Cb) is determined and plotted against time for each individual depth at which measurements were taken.
5. A regression line (that should have a negative slope) is fitted to the data (using Microsoft Excel), and the slope of the line (termed 'A') is determined.
6. The specific discharge (flow per unit area of aquifer) for the particular horizon under consideration may then be established from the relationship

$$q = -\frac{\pi r A}{4} \qquad (5.2)$$

where q is specific discharge (LT^{-1}), A is the slope of the trend line (T^{-1}) and r = borehole radius (L). The derivation of Equation 5.2 is presented more fully in Appendix 4.

[18] It was noted that Mottram (2003) failed to perform this conversion, using simply conductivity values in the place of concentrations. This leads to erroneous results in the derivation of specific discharge values. Mottram's 2003 Brompton data has therefore been reworked.

The data reduction to the form of specific discharge in this way entails several assumptions, which must be highlighted for an examination of their validity.

5.4.2 PROBLEMS WITH IMPLEMENTING THE METHOD

5.4.2.1 Influence of the final measured data point

The logistics of sampling may mean that, in a rapidly flushed system, the borehole water returns to background long before the final measurement is taken, but well after the previous measurement. This often occurs where the last measurements were taken the day following injection, with no measurements having been taken during the night. The significance of this is that the slope of the Ln (C-Cb) dilution curve may be strongly dependent on the final measurement, if it is taken at a time much greater than the time taken to return to background. The problem is illustrated in the Figure 5.13.

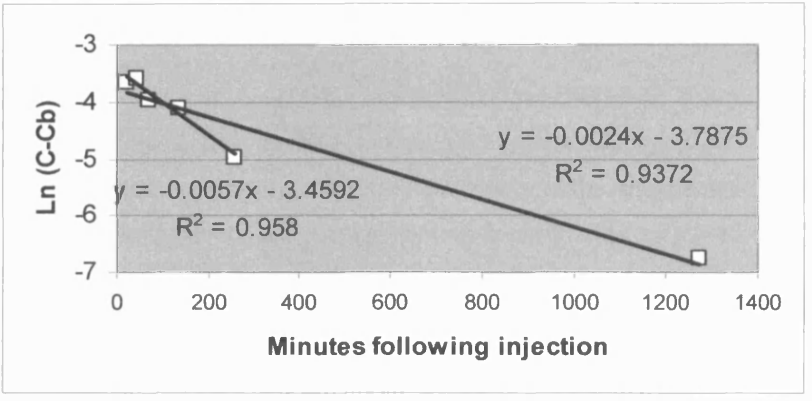

Figure 5.13 Brompton Dale Shallow Borehole, averaged Ln (C-Cb) against time.

From a comparison of the two regression lines on Figure 5.13 it can be seen that the difference in slope is approximately a factor of 2.5: -0.0024 including the final data point, and -0.0057 without it. Should the steeper recession be continued linearly (linearity being assumed in order to derive a slope), it would reach background at a time considerably earlier than is shown (and represented) by the final measurement.

5.4.2.2 Darcy's Law, turbulence and aquifer contribution to borehole flow

Darcy's law is assumed to be valid for a derivation of specific discharge from measured dilution. This is because the derivation of Equation 5.2 (see Appendix 4) contains a factor describing the relative width of aquifer contributing to flow within the borehole, due to distortion of the flow field created by the borehole. On the basis of Ogilvi's equation (cited in Halevy *et al.* (1967) and given in Appendix 4) this is calculated to be 2 for uncased boreholes (that is, the width of the aquifer contributing to flow in the borehole is twice the borehole diameter). However, Ogilvy's equation is designed primarily for porous (i.e. non-fissured) aquifers and relies upon a laminar flow assumption under the influence of a regional head gradient, whereas turbulent flow may be present in fissures in the Corallian, particularly

where they are large and hydraulic gradients steep. Other factors of potential importance include channelling and radial flow within a fissure toward or away from a point (if the head difference between two borehole-connected fissures is great enough to induce strong flow along the borehole, as observed in some cases). Such considerations militate against uniform aquifer contribution to borehole flow at any given depth. However, although unlikely to be correct, as no further information is available, the value of 2 has been used in the present work. Drost *et al.* (1968) cites a range for this value of 0.5 – 4.0 for sand and gravel aquifers. Should the factor be larger than 2 then q will be overestimated.

Turbulent flow within the borehole column itself will also lead to errors. The Augmentation borehole, from a calculation based on the logged flow speed in the borehole[19], at least approaches turbulence, if it is not actually fully turbulent. Although turbulent flow is probably not widespread it ought to be recognised that its effects will be to underestimate q.

5.4.2.3 Density driven tracer movements

Density effects are more likely to occur at the beginning of an experiment, due to higher tracer (salt) concentrations. However, as soon as the hose is removed from the borehole, and the column of water mixed by movement of the weight beneath the hose, the density of the salt-saturated solution decreases through dilution by borehole water. The average starting concentration measured for all experiments was about 1 g per litre, which means that the density of the water has been increased, on average, by 1/1000. This is only a small difference and unlikely to be responsible for much tracer movement, especially given the typically short duration of the experiments and the frequent rapidity of dilution.

Nevertheless, should the process occur it may have two opposing effects. If the tracer flows downward, it will both deplete an upper level and supplement a lower. This means that the upper level will exhibit faster dilution, with q being overestimated, whereas the lower level will exhibit a slower dilution, with q being underestimated. For a borehole-averaged derivation of q this effect ought to cancel itself out. For those boreholes exhibiting upward flow then it is expected that downward, density-driven flow is likely to be only a very minor factor.

For these reasons density-driven tracer movement is not considered to significantly affect the derivation of specific discharge values from the experiments. However, where it may be influencing the form of the dilution, this has been noted in the text.

[19] $Re = \rho vd/\mu$, where ρ = density (1000 kgm^{-3}), v = velocity (0.0075ms^{-1}), d = diameter (0.3m) and μ = viscosity (1.4 x 10^{-3} $kgm^{-1}s^{-1}$). Using these values, the Reynolds number in the Augmentation borehole is c.1600, which is approaching the turbulent threshold.

5.4.2.4 Vertical groundwater flow and errors in interpretation

Vertical flow within the borehole is the single most problematic obstacle to a derivation of specific discharge from the dilution data. Vertical flow will mean that the linearity of the Ln (C-Cb) versus time fit will be compromised, and thus the ability of a linear model to determine specific discharge at any given horizon. As the analysis assumes only horizontal flow, the total gradients (vertical and horizontal) represented by the derived specific discharge value will only have been assigned to horizontal flow, thereby overestimating q. An additional problem is that where there is a very rapid loss of tracer there may be only two data points from which to derive a slope, and in these cases the fit of the trend line will be misleadingly perfect.

N.B.: Vertical flow within the aquifer at any given locality may only be due to the presence of the borehole itself, connecting two otherwise poorly-connected fissures of differing hydraulic head. Any borehole may thus represent an artificially high locus of vertical permeability. However, as vertical fissures are known to exist in much of the aquifer where it is observed at outcrop, it is not unreasonable to suppose that flow along these features, where they connect separate horizontal fissures at different depths and with different hydraulic heads, may not at least be of a similar order of magnitude, given that the permeability and morphology of contributing/draining fissures is likely to be similar. In this case variations in volume of flow may be ascribed to differences in permeability of the horizontal fissures, control of this parameter being dependent upon external factors

5.4.2.5 Summary and implications of assumptions

The following list summarises the problems of reducing the data to specific discharge values as discussed above

- Influence of the final data point
- Contribution of aquifer width to flow in the borehole
- Turbulence in the borehole column
- Density-driven tracer movement
- Vertical groundwater flows
- Insufficient data due to rapid loss of tracer

In the case of vertical flow the basic assumption may be so severely compromised that it becomes meaningless to derive a specific discharge at a particular horizon. It is also impossible to separate the effects of individual factors at this time, as there is insufficient knowledge of the system to make more than a guess at the magnitude of some effects. Because of this combination of problems two different approaches have been taken to defining specific discharge values for the aquifer. These are a borehole averaging procedure (following section) and modelling the experimental results using a combination of explicitly stated vertical and horizontal flows (model description and output given in Section 5.5).

These approaches have different merits, but are complementary, as will be seen from the comparison of results given in Section 5.6.

5.4.3 BOREHOLE AVERAGING PROCEDURE.

5.4.3.1 Basis for the procedure

A borehole undergoing only vertical plug-flow without mixing or dispersion should exhibit a straight line plot of total tracer mass in the borehole versus time, that is, there is linear loss rate of tracer. This is because fresh water entering at (say) the base of the borehole gradually pushes tracer out of the top, so that there is a constant rate of decrease due to the constant rate of influent (and effluent) water. In contrast, a borehole undergoing horizontal flow with mixing and dilution should only display linearity on a plot of *log* mass versus time (Palmer, 1993; Environment Agency, 1998). This is because as fresh water enters the borehole it mixes with and dilutes the existing tracer-containing water so that, of the original amount of tracer, there will always be some remaining in the borehole, i.e. there will be an ever-decreasing presence of tracer.

One objection to this schema is that plug-flow will not occur without mixing or dilution in any case, vertical or otherwise, so that the difference between the two proposed regimes is artificial. This is true, but recognising that the length of a borehole is typically much greater than its diameter implies that mixing and dilution are much more efficient when operating during horizontal than vertical flow, given equal rates of groundwater flow. This begs the question: At what rate of groundwater flow is mixing equally operative over a length of (say) 25 m as it is over 0.25 m? Presumably this is some very small rate to enable mixing to occur completely over a length of 25 m before a significant amount of water has entered/left the borehole. At the high rates of vertical groundwater flow observed in the Corallian it is considered that a vertical plug-flow assumption is not invalidated by this objection.

Employing the above reasoning, plots of mass and log mass versus time were plotted for each borehole. The example of the Swallowholes borehole is shown in Figures 5.14 and 5.15, and the data derived from these plots are summarised in Table 5.3.

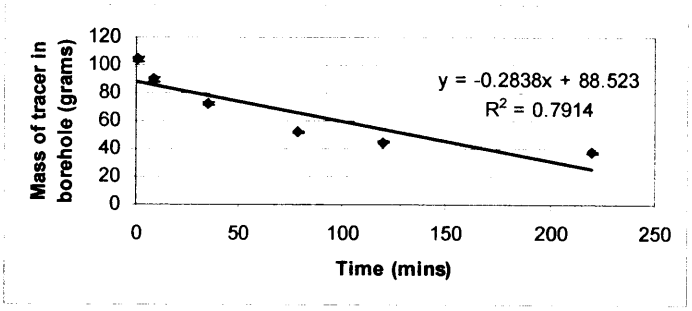

Figure 5.14 Mass of tracer in borehole column versus time. Data from the Swallowholes borehole.

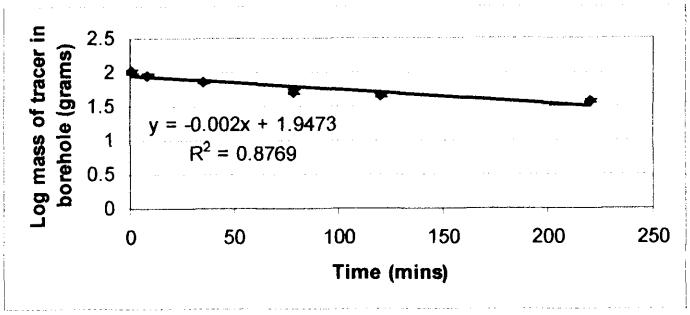

Figure 5.15 Log mass of tracer in borehole versus time. Data from the Swallowholes borehole.

Borehole	Mass versus time linear fit, r2 value	Log-Mass vs time linear fit, r2 value
Augmentation	0.60	0.81
Swallowholes	0.79	0.88
Derwent Ford	0.92	0.96
Tetherings Plump	0.92	0.93
Wykeham	0.97	1.00
Brompton Dale Shallow	0.55	0.68
Brompton Dale Deep	0.90	0.96
Vertical plug flow model	1.00	0.87
Horizontal flow model	0.93	1.00

Table 5.4 Comparison of linear fits (R^2 values) between mass versus time and log-mass versus time plots.

The table shows that the log-mass vs. time plots are more linear than the mass vs. time plots in every instance, although in several cases they are very similar. However, referring to the bottom two rows of the table, it can be shown theoretically[20] that a pure horizontal flow model will have an R^2 value of 0.93 when a linear trend line is fitted to a mass vs. time plot. Similarly, a pure vertical flow model with no dispersion will have an R^2 value of 0.87 when a linear trend line is fitted to a log-mass vs. time plot. This indicates that the similarity of the R^2 values for the boreholes should not be regarded as problematic in determining whether or not a particular borehole is validly described by a horizontal flow model. Furthermore, several of the boreholes exhibit an R^2 on the mass vs. time value very close to the 0.93 plot derived from a theoretical consideration (i.e. on a mass vs. time model, all boreholes (except Wykeham) fall closer to the horizontal than the vertical flow model). It is thus clear that the majority of boreholes experimented upon may be examined validly with an averaging procedure based upon an assumption of the dominance of horizontal flow processes.

Two boreholes, the Augmentation and the Brompton Dale Shallow boreholes exhibit considerably poorer fits to both the mass and log mass vs. time plots. Geophysical logging indicates that the flow regime in the Augmentation borehole is, in parts, at least approaching turbulence, if not fully turbulent. The velocities in the Brompton Dale Shallow borehole are not known, but it is possible that turbulence is responsible for the increased variance in the data from both of these boreholes. In this context it

[20] The subsequent values are derived by using the BHDT simulation model, explained in Section 5.5, to produce values of total mass in the borehole over a series of time intervals.

should also be noted that the Swallowholes borehole has an intermediate fit quality between the two boreholes discussed above and the remaining boreholes. The Swallowholes borehole is also shown to exhibit high vertical velocities, although not as high as those in the Augmentation borehole.

Overall, the data indicate that treatment of the problem with an averaging procedure is an acceptable way of understanding the data further provided that the mentioned caveats are borne in mind.

5.4.3.2 The procedure

The procedure is to straightforwardly average Ln (C-Cb) over the entire unscreened section of the borehole for each measurement time (t). Two examples are given below (Figures 5.16 and 5.17). The best-fit regression line is the thickest black line. As uncertainty in the determination of specific discharge will be due to uncertainty in determination of the slope of the regression (see Equation 5.3), the 95% confidence interval of the slope of the regression is shown as the red lines above and below the best-fit regression. Specific discharge is also calculated based on the maximum and minimum variation in slope at the 95% confidence interval and this analysis is presented with the derived values of specific discharge in Section 5.4.4.

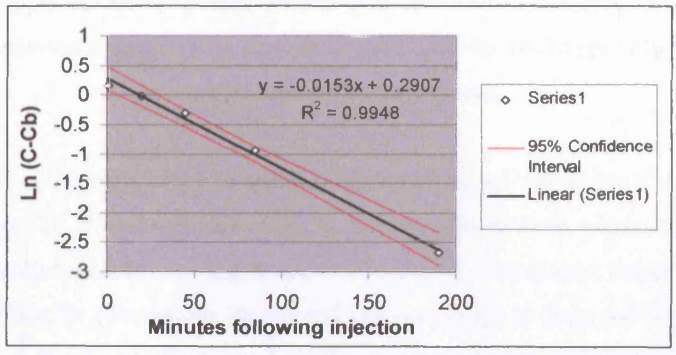

Figure 5.16 Ln (C-Cb) averaged over the unscreened section of the Wykeham Village Hall Borehole.

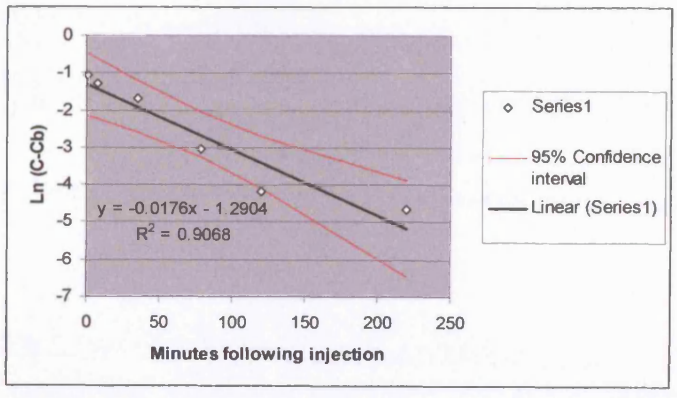

Fig. 5.17 Swallowholes Borehole averaged Ln (C-Cb). Final data point removed.

The slopes obtained from the plots are then processed in exactly the same way as described in Section 5.4.1, only that the q value derived represents a macroscopic value for the aquifer penetrated by the borehole at that point, rather than for the particular horizons at which measurements were taken.

5.4.4 MODEL RESULTS

5.4.4.1 Calculated Specific Discharge

The specific discharge values derived from the averaged Ln (C-Cb) versus t plots are presented in Table 5.4.

Borehole	Darcian flux m/d
Augmentation	5.14 ± 3.81
Swallowholes	1.14 ± 0.63
Wykeham	1.46 ± 0.23
Brompton Shallow	1.15 ± 0.46
Brompton Deep	0.42 ± 0.51
Tetherings Plump	0.41 ± 0.33
Derwent Ford	0.35 ± 0.18

Table 5.5 Macroscopic values of specific discharge derived from BHDTs. The uncertainty is the 95% confidence interval derived from calculating the specific discharge resulting from changes in the slope of the regression.

From the table there is clearly a range of specific discharge values within the Corallian. Qualitatively the highest values are all from boreholes either in the unconfined zone or associated with the Forge Valley Swallowholes (especially the Augmentation Borehole). The lowest values are from either the confined part of the aquifer (Tetherings Plump and Derwent Ford) or from the Lower Calcarous Grits (Brompton Dale Deep Borehole). These results will be discussed more fully in conjunction with results from the numerical simulations of the experiments, following their presentation in the next section.

5.5 NUMERICAL SIMULATIONS OF BOREHOLE DILUTION TEST DATA.

5.5.1 INTRODUCTION

Professor John Barker of UCL produced a BHDT simulation model to recreate the form of observed dilutions in a BHDT where vertical flow may be a significant component of total flow, and from which it may be thus invalid to derive groundwater fluxes using the 'standard' approach. The program produces a plot of C/C0 at a series of time steps. The user states the borehole dimensions and the number of intervals over which he/she wishes flow to occur and then varies the groundwater flow into and out of the borehole at particular intervals, inducing either or both vertical and horizontal flows, until the observed form of the experimental results is recreated. The model is written in Microsoft Visual Basic and executed in Excel as a spreadsheet model. The quality of the model fit to the data is made by eye. The model is essentially a forward-modelling programme, in that it attempts to determine observed dilutions by inputting flows, as opposed to determining flows by inputting the observed dilutions, although this, in effect, is the result.

The virtues of the model are that it enables a study of different inputs at different horizons and permits an examination of what result such inputs have on dilution of a tracer. For example, *in extremis*, the model permits an examination of what form a series of dilution curves would take should flow be either purely horizontal (Fig 5.18) or purely vertical (Fig 5.19). The model also enables a good approximation of actual flow volumes and velocities within boreholes, as may be seen from a comparison of finalised model inputs and measured velocities (Section 5.5.4 below). Furthermore, the model permits, through the capacity to state the depth at which flows are occurring, a more-or-less accurate representation of those horizons at which flow is actually entering or leaving the borehole modelled. This information may have been determined from geophysical logging or posited from an examination of the raw dilution data.

5.5.2 DESCRIPTION OF THE MODEL

5.5.2.1 Structure and formulation

The model structure and mathematical formulation is given in Appendix 5.

The user assigns borehole dimensions, the number of depth intervals into which the borehole will be split, the lengths of those intervals (intervals may be different to one another), flows in and out over intervals, starting concentrations over intervals, an exponent relating to the dispersion coefficient (see following section), the time step over which calculations should be performed, the maximum time for which the simulation should run and the time step for which outputs will be given.

5.5.2 2 Dispersion

Dispersion is given in the model as $D = \alpha v^x$, where D is the dispersion coefficient (L^2T^{-1}) , α is the generalised dispersivity (a distance, L, when x = 1), v is the vertical velocity in the borehole (LT^{-1}) and x is an exponent. The model assumes complete mixing within an interval over a single time step, so that dispersion is not an effective process for models undergoing only horizontal flow (Figure 5.18). The effects of varying the exponent in the dispersion term are illustrated in Figures 5.19 and 5.20.

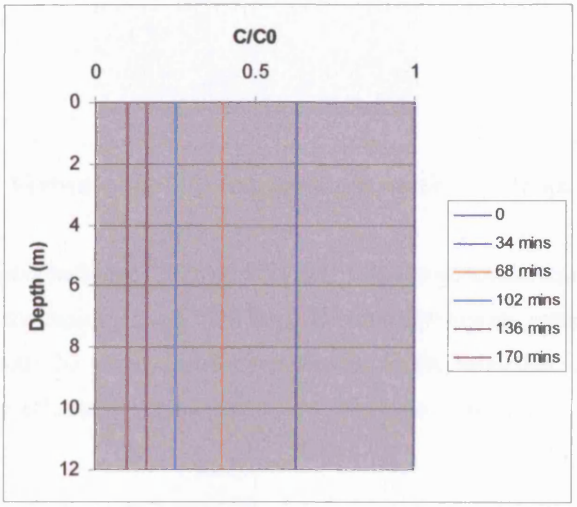

Figure 5.18 Dilution resulting from horizontal flow only.

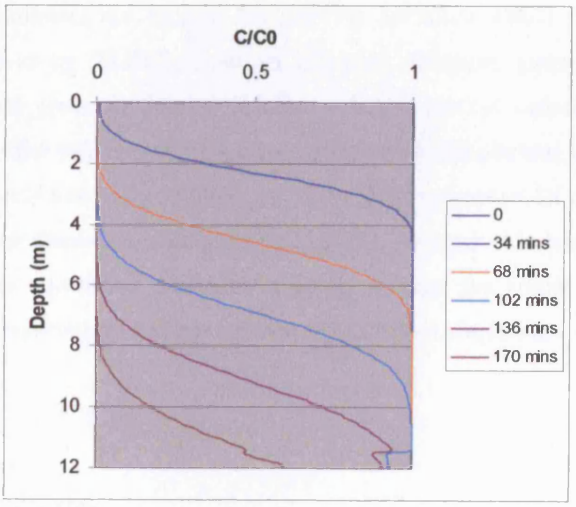

Figure 5.19 Vertical plug-flow (top to bottom) with x = 1 (low dispersion).

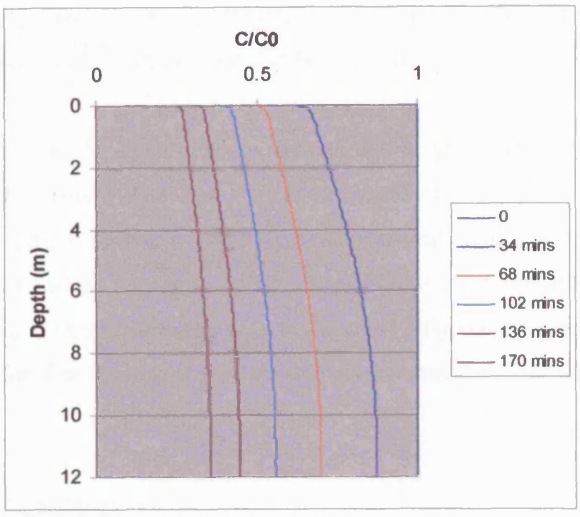

Figure 5.20 Vertical plug-flow (top to bottom) with x = 2 (high dispersion).

As may be seen from a comparison of Figures 5.19 and 5.20 the exponent in the dispersion term has a controlling influence on the rapidity at which a front of vertically moving water propagates through the borehole. This affects both the slope and the smoothness of the modelled curves and varies with a combination of borehole effects and the amount of volumetric flow within the borehole (see model results, below).

5.5.2.3 Model stability

Two dimensionless parameters are utilised for stability purposes within the model. These are a dispersion parameter, given by $2D.Dt/Dz^2$, and an advection parameter given by v.Dt/Dz (where D is the dispersion coefficient given in Section 5.5.2.2, v is the vertical velocity and Dt and Dz are, respectively, the model time step and depth interval over which calculations are performed). The first of these refers to the 'von Neumann' condition and is designed to prevent Dt being so large that solute can disperse over a greater distance than represented by a single interval in less than a single time step. The second, the 'Courant' condition, prevents Dt being so large that solute can be advected over a greater distance than represented by a single interval in less than a single time step.

5.5.2.4 Assumptions

The model assumes the following:

- Negligible molecular diffusion
- Darcy's law applies within the surrounding aquifer
- Negligible density-driven flow

The first assumption is justified on the basis that mechanical dispersion in boreholes in the Corallian is significantly higher than the free-water diffusion coefficients for a typical range of non-reactive

chemical species, given by Freeze and Cherry (1979) as 1.73 x 10^{-4} m^2d^{-1}. The latter two assumptions have been discussed in Section 5.4, which may also be regarded as relevant to the simulation model.

Two further points should also be noted. Firstly, that all depths given are depths below the bottom of the casing. Secondly, that fluxes into and out of the borehole are given as flows per metre of borehole[21], (i.e. volume/(time × borehole length)) and not per unit area of aquifer, as the model is only one-dimensional. Model q values for models with vertical flow are therefore only useful due to their power to cause vertical flow in the borehole, with the interval only useful as a proxy for the position of a fissure within the aquifer. For horizontal flow models they retain their customary meaning of specific discharge.

5.5.3 MODELLING PROCEDURE

Figures 5.6 to 5.12 (Section 5.3) show the measured dilution normalised to the starting concentration (C-Cb)/(C0-Cb) plotted against depth for each borehole. These are the experimental results that have been simulated with the BHDT model and should be referred to for a comparison with model outputs.

As the position of flowing fissures and the direction and velocity of vertical flows are clearly important to the form of the experimental results, those boreholes for which geophysical data exist were modelled first. In this way a conceptualisation of the behaviour of the aquifer was developed to aid model construction for those boreholes with fewer data.

For modelling the Augmentation and Swallowholes boreholes (for which good geophysical data exist), the major flows into and out of the boreholes are assigned to coincide with the major flowing fissures observed. The magnitudes of the major flows are determined by the velocities observed in the borehole (measured by impeller flow meter) and input into the models. The secondary flows observed in the logging are input at the correct depths but their magnitudes and directions are altered iteratively (by hand) in order to reproduce the experimental results. Following these steps, and after running the model, minor adjustments are made to improve the match (made by eye) between the model and the experimental results. These minor adjustments usually take the form of additional cross-flows to increase the rate of dilution at certain depths and small additions of vertical flow to alter the slopes of, and to smooth, the model dilution curves. Where necessary the models were run to examine both early-time and late-time behaviour (e.g. the Augmentation borehole). In general the approach was to employ only the minimum flow required to reproduce the overall form of the experimental results. Note that where a significant change in flow occurs over a short depth interval the modelled depth intervals are reduced for improved resolution at those points. This is not apparent in the output but can be seen in the tabulated model inputs given in Appendix 6.

[21] In the input tables in Appendix 6 the actual figures are given, only these need to be multiplied by the length of the interval to give the volume of flow entering the borehole.

From both the Augmentation and Swallowholes boreholes (and the Seavegate Gill borehole – see Section 5.2.2.1) it is clear that the controlling factor over the forms of the observed dilution is vertical flow. Because of this, where the BHDT results from the boreholes without geophysical logging data seem to indicate vertical flows (i.e. dilution centred on a certain depth and moving up or down the borehole) such vertical flows have been posited in the modelling. The presented models of those boreholes without geophysical information are the results of a trial-and-error process of changing inflows and outflows, both vertically and laterally. However, as model results are non-unique, where there is any ambiguity two models are presented, one based predominantly on vertical flows and one on horizontal. The differences in behaviour between these two types of model aid in the understanding of the models as well as the experimental data.

5.5.4 RESULTS FROM THE BHDT SIMULATION MODEL

The graphical model outputs are presented in this section. The tabulated inputs for all models are given in Appendix 6. Please note that, for a visual qualification of model performance, these results should be directly compared to Figures 5.6 to 5.12 (Section 5.3 above).

5.5.4.1 Augmentation borehole

The measured flow velocity was approximately 690 md^{-1} (upward) above two fractures at c. 25 m. Below those fractures the downward flow velocity was approximately 550 md^{-1}. Considering the cross-sectional area of the borehole, this is roughly equivalent to 50 and 40 m^3d^{-1} respectively, with flow exiting at 15 m (upward flow) and 33 m (downward flow). Between 7 and 14 m the model has a significant cross-flow, supported by the geophysical logging and the form of the dilution curves, and together these components represent the majority of flow in the borehole. They are, however, supplemented by some smaller additional vertical and cross flows exiting at the top and bottom of the boreholes. These give an improved reproduction of the dilution observed and are not without foundation (e.g. flow in Augmentation borehole is seen to be occurring behind the lining). The exponent in the dispersion term was set to 1 for this model (Figures 5.21 and 5.22) as that enabled an accurate simulation of the extremely rapid dilution observed at the start of the experiment, without adversely affecting the remainder of the model. The model input flows are given in Appendix 6.

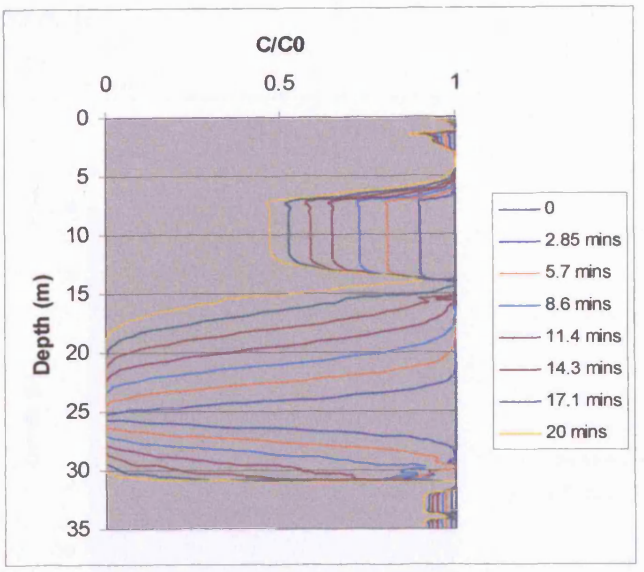

Figure 5.21 Early time model simulation of the Augmentation borehole dilution test results (compare to Figure 5.6). Casing length 11 m.

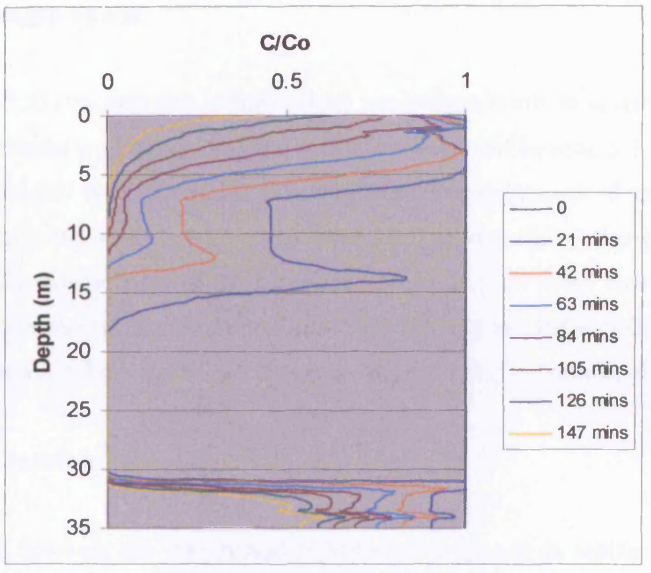

Figure 5.22 Later time model simulation of the Augmentation borehole dilution test results (compare to Figure 5.6). Casing length 11 m.

It was necessary to test the model over different time horizons as the later time horizons do not provide sufficient indication of the model response at early times, and vice-versa. It is possible to produce a model that reproduces the later time data faithfully, but does not do so for the early time (and vice-versa). The model is limited to a maximum amount of time outputs (i.e. lines on the graph), spaced at equal intervals, so that early time and late time cannot always be adequately shown on the graph together, as is the case with the Augmentation borehole, where it is clearly necessary to emulate the behaviour of the borehole both at very early time (in the first 20 minutes) and at late times (> 100 minutes).

5.5.4.2 Swallowholes borehole

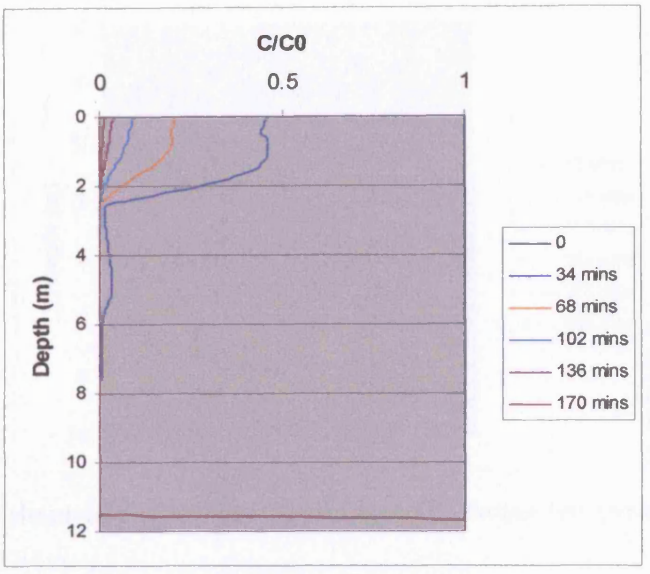

Figure 5.23 Model simulation of the Swallowholes borehole dilution test results (compare to Figure 5.7). Casing length 14.4 m.

In this model (Figure 5.23) the majority of flow (94%) was assigned only to horizons where a flowing fracture was observed in the geophysical logging (see Appendix 6 and Section 5.2.2.2). The volume of flow in the model is roughly the same as that calculated from a measurement of velocity and borehole diameter. The exponent in the dispersion term was set to 1.3 for this model as that gave an improved fit in the upper half of the borehole, to which a horizontal flow of 0.25 m^3d^{-1} was also assigned. The reproduction of the experimental results is satisfactory, especially given the corroborative nature of the influent and effluent zones in both model and borehole. Appendix 6 gives tabulated input values.

5.5.4.3 Derwent Ford borehole

For the Derwent Ford borehole the geophysical information is limited to noting vertical flow and a single flowing fracture at the top of the borehole, although judging from the BHDT there is obviously one at depth too. The model (Figure 5.24) is based upon vertical flow throughout the borehole, from bottom to top.

This simulation is a good reproduction of the experimental results and uses an exponent in the dispersion term of 1.5. This is necessary to reproduce the slope of the curves at both early and later times in the plot. However, inspection of the associated inputs (Appendix 6) shows that the total flow required to model the BHDT is only a low 0.45 m^3d^{-1} and which gives a maximum velocity in the borehole of 25 m d^{-1}.

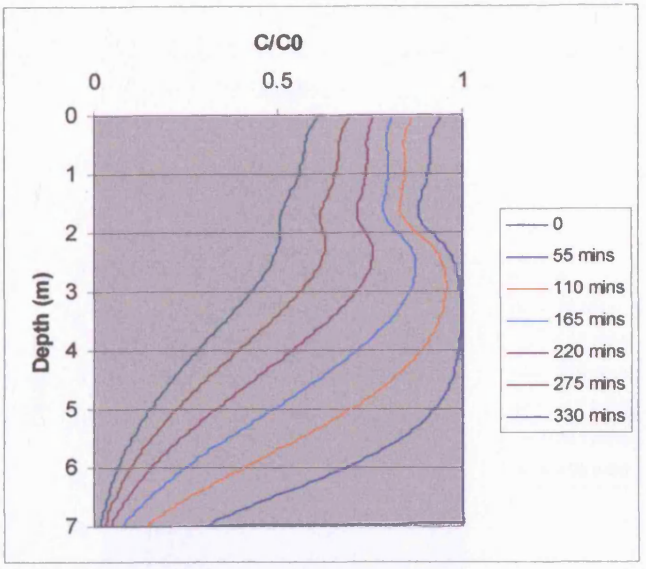

Figure 5.24 Model simulation of Derwent Ford borehole dilution test (compare to Figure 5.8). Casing length 24 m.

5.5.4.4 Tetherings Plump borehole

Based on an initial interpretation of the background measurements and experimental results, given in 5.2.3.4, this borehole has been modelled with purely vertical flow (Figure 5.25) with 5.6 m^3d^{-1} entering over the interval from 7.5-8 m. The majority of this flow exits at 3 m with minor components travelling downward (0.2 m^3d^{-1}) and continuing upward to the casing (1 m^3d^{-1}).

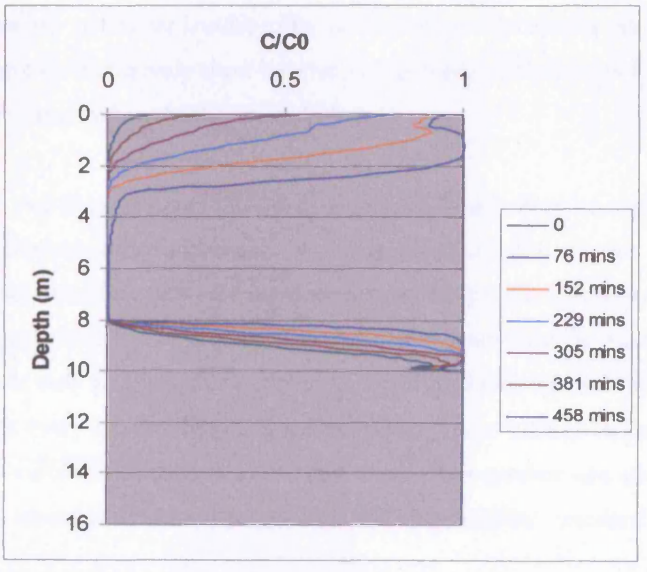

Figure 5.25 Model simulation of Tetherings Plump borehole dilution test: predominant vertical flow (compare to Figure 5.9). Casing length 30 m.

However, because of the lack of geophysical data and the possibility of non-unique model solutions, a second model based on the predominance of horizontal flow is also presented (Figure 5.26).

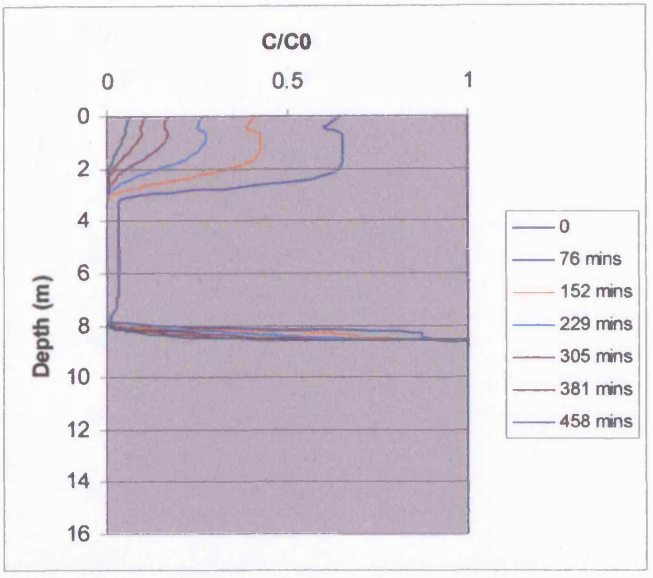

Figure 5.26 Model simulation of Tetherings Plump borehole dilution test: predominant horizontal flow (compare to Figure 5.9). Casing length 30 m.

This second model has a purely horizontal flow of 1 m^3d^{-1} per metre of borehole entering between 8.5 and 3 m, and 0.125 m^3d^{-1} per metre above that. On top of this a small component of vertical flow (0.2 m^3d^{-1}) has been included, from 8.5 m to the top, so that the model has smoother curves and so that the form of dilution in the upper part of the borehole is more accurately reproduced. The exponent in the dispersion term is set at 1.2 for both models, although this is of greater significance to the vertical flow model. This value for the exponent is based upon similar values obtained for the other boreholes modelled and not upon any particular benefit to the form of the model results (as the observed dilution is occurring so rapidly over a relatively short interval, the quantity of flow input to the model results in a straight dilution curve even when the dispersion is low.)

A comparison of the two figures demonstrates how similar results may be based on different flow mechanisms, which illustrates the importance of the geophysical data. In this instance the former model is preferred because of the similarity the experimental results show to other Corallian boreholes known to exhibit strong vertical flow, and the simplicity of reproducing the model results employing inflows and outflows at only four discrete horizons. In contrast the horizontal flow model requires an inflow and outflow at every depth interval in the borehole (i.e. a homogeneous aquifer) that is not supported by other evidence. Tabulated input values for both models are given in Appendix 6, although only the first model is used for a comparison with the modified 'standard' approach.

5.5.4.5 Wykeham Village Hall borehole

This model is exemplary in that the experimental data have been accurately reproduced employing flow at only two intervals (representing two fissures), one at the top and the other at the bottom of the borehole. In other words, the model is essentially a plug-flow model.

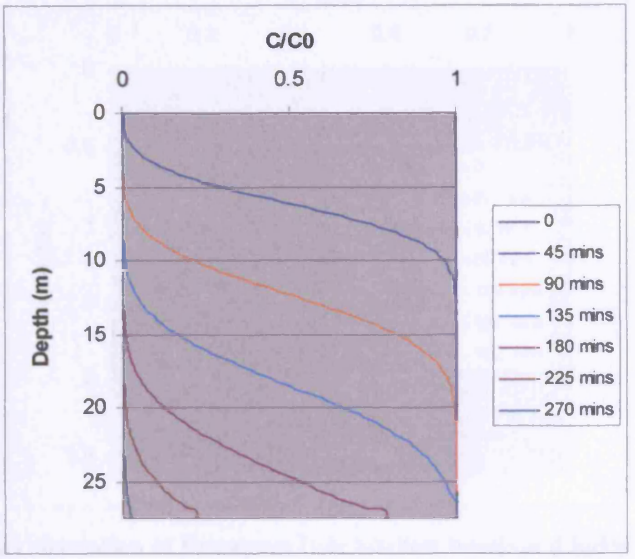

Figure 5.27 Wykeham vertical flow model (compare to Figure 5.10). Casing length 17.5 m.

The flow required by the model is 3.5 m^3d^{-1} using an exponent in the dispersion term of 1.2. The best exponent was determined iteratively using the slopes of the curves as a judge of the best fit. The magnitude of flow is mainly responsible for the average position of the individual curves. Input values are given in Appendix 6.

From the experimental data (Figure 5.10), if we postulate a single influx at the top of the borehole and moving downward, we can estimate the velocity with which it is moving. Assuming a start point of about 2 m, a freshwater front appears to reach 9.5 m within 45 mins, 14.5 m within 85 mins and 27 m within 190 mins. The average velocity calculated from these three estimates is 213 md^{-1}. This correlates closely with a model velocity of 198 md^{-1} based on the flow posited (3.5 m^3d^{-1}) and a borehole diameter of 150 mm.

The slightly enhanced dilution measured at the bottom of the borehole is not well reproduced. However, as this feature is only a minor component of the total dilution, extended attempts at including it in the model were not attempted.

5.5.4.6 Brompton Dale Shallow borehole

This borehole was modelled (Figure 5.28) using an exponent in the dispersion term of 1.4. A volumetric flow of 13.8 m^3d^{-1} is input over the interval 1.8 – 2 m, most of which exits over the interval 0.4 – 0.6 m (Appendix 6), minor components exiting at the top and bottom of the borehole. In this way it is very similar to the Tetherings Plump vertical flow model, only with a greater volumetric flow due to a larger bore size. For the same reasons as the Tetherings Plump borehole, and because the borehole is likely to be screened in the Malton Oolite, a vertical flow model is preferred.

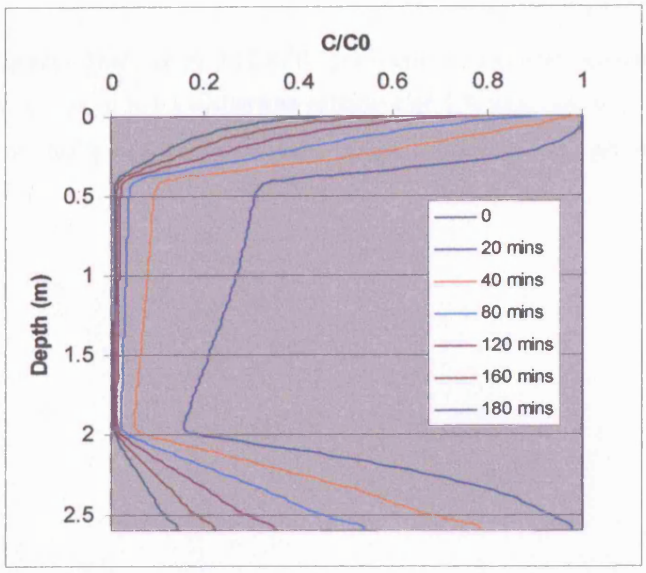

Figure 5.28 Model simulation of Brompton Dale Shallow borehole dilution test (compare to Figure 5.11). Casing length 15 m.

5.5.4.7 Brompton Dale Deep borehole

This borehole is unusual in that flow throughout the majority of the unscreened section appears to be uniform and horizontal, with a zone of higher flow nearer the top. To reproduce this slow and largely even dilution using a vertical flow model requires the exponent in the dispersion term to be set high, the best fit being given by an exponent of 2 or more. This does not compare favourably with the exponents necessary in the other models. It should be borne in mind that this borehole is screened entirely in the Lower Calcareous Grit, in which fissure density is lower than that in the limestones. For this, and because of the even form of the measured dilution, the preferred model for this borehole is one of predominantly horizontal flow (Figure 5.29).

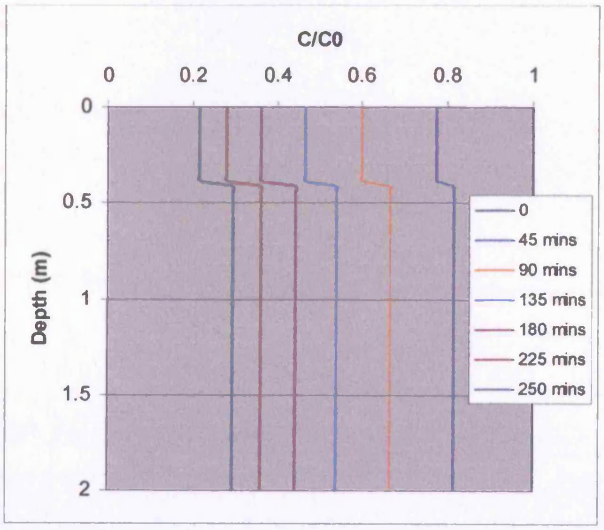

Figure 5.29 Model simulation of Brompton Dale Deep borehole (compare to Figure 5.12). Casing length 45 m.

The model has a horizontal flow rate of 0.12 m^3d^{-1} per metre of borehole between the bottom and 0.4 m and 0.15 m^3d^{-1} above that. It has a dispersive exponent of 1.3, although as it is a 100% horizontal flow model this does not make any difference to the output. Input values are given Appendix 6.

5.6 FURTHER DISCUSSION AND SUMMARY OF BOREHOLE DILUTION TEST RESULTS AND MODELLING.

5.6.1 FURTHER DISCUSSION

Overall the BHDT simulation model is useful for understanding the mechanisms and relative importance of the different components of flow, i.e. the vertical and horizontal components, and the different magnitudes of flow in different boreholes. The work with the models illustrates the importance of the geophysical information in determining the position of flowing fractures and the direction and velocity of flow within the borehole, as these data permit the models to be structured much more realistically, and therefore to be considered more reliable.

The 'standard' method (of Halevy *et al* (1967) and widely adopted by other workers) has been adapted to account for the significant vertical flows in the aquifer by using an averaging procedure justified by an analysis of the way in which total tracer masses were flushed from the boreholes. This averaging procedure resulted in a single value of specific discharge for each borehole, with the values given in Table 5.4.

Table 5.4 indicates that the boreholes may be divided into three groups: those with specific discharges less than 1 m d^{-1}, those with specific discharges between 1 and 2 m d^{-1}, and one with a specific discharge greater than 5 m d^{-1}. Broadly these three groups are, respectively, boreholes in the confined zone, those in the outcrop zone, and those adjacent to the Forge Valley Swallowholes. However, this simple schema does not quite capture the variation. Two points stand out, of which the first is that the Brompton Dale Deep borehole is almost certainly screened exclusively in the Lower Calcareous Grit, from which a direct comparison can be made with the Brompton Dale Shallow borehole, which is probably screened in the lower oolitic limestone. The Swallowholes borehole (which, too, is screened largely in the lower limestone) also groups with the outcrop boreholes, despite being close to both the Augmentation borehole and the Swallowholes themselves. This, together with the slow response (c. 8 days) of this borehole to tracer injection into the Swallowholes (ARUP, 1999), seems to indicate a diminished connection to the river in comparison with the Augmentation borehole. The depth of this borehole does not, however, reach the level of the strongest flowing fractures identified in the Augmentation borehole, which exhibits the highest specific discharge by a factor of c. 4.5.

In contrast to these boreholes screened at least partially in the oolitic limestones, the Derwent Ford and Fetherings Plump boreholes are both open to the Upper Calcareous Grit over the intervals upon which it was possible to experiment. The values derived are in close agreement with the Brompton Dale Deep borehole, again lending confidence to the analysis. Yet, whilst this interpretation appears to capture the variability in results that one may expect to find in the system, how do the 'standard' and simulation models compare?

Comparison of the two model types has been achieved by an examination of total volumetric flows. From the standard method this is simply q multiplied by the area of aquifer over which flow is contributing to the borehole, that is, the length of the uncased section by twice the width of the borehole (as discussed in Section 5.4.2.2). In the simulation model, flows are the sum of all those inputs necessary to reproduce the observed dilution, rather than being derived from it, so that the methods are, whilst comparative, essentially independent. The agreement in total volumetric flow between the two models is shown in Figure 5.30.

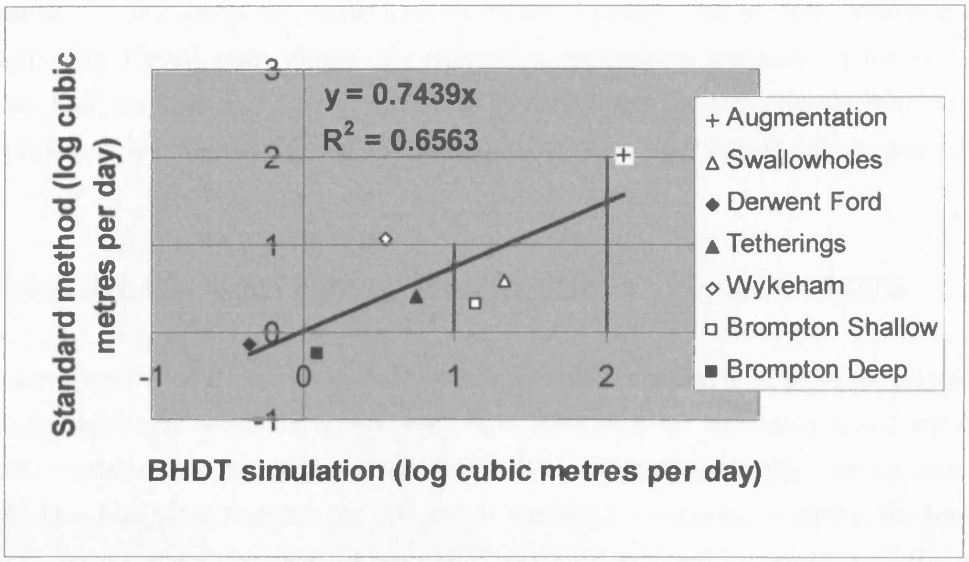

Figure 5.30 Comparison of total volumetric flows required by the Barker model and calculated from the 'standard' method. Note logarithmic axes to facilitate inclusion of the highest and lowest values.

The simulation models demonstrate how the experimental results may be reproduced largely through using vertical flows, but tempered by horizontal flows, and the geophysical data supports this approach. However, the previous examination of the log-mass and mass vs. time plots (Section 5.4.3.1) showed two things. The first is that the fitting difference between the plots describing the mechanisms of pure horizontal and pure vertical flow is relatively small. The second is that, whilst the boreholes may be undergoing significant vertical flow, mostly it is not of a pure plug- or piston-like nature. Thus, the correlation observed in Figure 5.30 may be explained with reference to vertical flow occurring on a length scale less than that of the borehole, with flows both up and down the borehole, with several influent and effluent horizons in each borehole and, in the Augmentation, Swallowholes and Brompton Dale Deep boreholes, significant horizontal flows across individual intervals (this is the only process apparently occurring in the last). Together these effects shift the form of tracer loss away from that which one would expect from a pure plug-flow model (i.e. with flow from one end of the borehole to the other) and toward that which one would expect from a horizontal flow model, with mixing and dilution. This illustrates that a borehole averaging procedure can produce a reasonably valid result even when vertical flow may be responsible for a considerable amount of dilution. However, one of the boreholes simulated using exclusively vertical flows is the one falling furthest from the trendline, the Wykeham borehole. As this falls to the left of the trendline it indicates either a deficit in the simulation

model or an over-steep slope in the 'standard' method. However, the fit of the regression to the averaged Ln (C-Cb) values for Wykeham is the best of any of the boreholes (see Figure 5.16), so that the former appears to be the more likely. (An additional argument obtains from the similarity in q derived from all outcrop boreholes.) It therefore seems that to model a BHDT using solely vertical flows, where in fact there is some component of cross-flow, can lead to an underestimate of volumetric flows through the aquifer.

The above discussion begets an additional point, and one that has wider implications than simply for the interpretation of experimental results from the eastern Corallian. That is, whilst modelling a series of BHDTs may provide some insight into regional or aquifer-wide processes, at the scale of the individual borehole there may be quite significant deviation from the regional behaviour. As can be seen from Figure 5.30, the data is quite scattered. There are potential pitfalls in relying upon individual results.

5.6.2 SUMMARY AND CONCLUSIONS FROM THE BOREHOLE DILUTION TESTS.

The data derived from the experiments has been successfully modelled in terms of the parameters of specific discharge and volumetric groundwater flow. With both the simulation model and adapted 'standard' methods of reducing the experimental data to hydrogeologically relevant parameters, decisions have been taken regarding the best way of applying the methods. An attempt has been made to identify the points at which these decisions have been necessary, and the criteria applied in making them.

The BHDTs are obviously useful for determining the most significant flow horizons within the Corallian limestone, although they are more useful when coupled with geophysical logging information, as for the Augmentation, Swallowholes and, to a lesser extent, Derwent Ford boreholes. The geophysics also enables more accurate and reliable modelling of the boreholes when using the simulation model. This reliability is reflected in a comparison of volumetric flows derived from both methods of analysis, although individual boreholes may not reflect any wider patterns in themselves. Nonetheless, by examining several boreholes it has been possible to observe the dominance of fissure flow as a mechanism for groundwater movement, and how significant, therefore, it will be in terms of contaminant transport. That fissure flow is an important mechanism in the hydrogeology of the Corallian was understood prior to this research. However, what the geophysical logging and borehole dilution tests show is not only what form and with what frequency such fissure flow occurs, but the extent of it throughout the aquifer. Vertical flow is a central feature in almost all of the boreholes upon which experiments were undertaken, and the experiments have also given insight into the magnitude and distribution of flow within different parts of the aquifer. This information is an important contribution to an improved conceptualisation of groundwater behaviour in the aquifer.

5.7 A SINGLE WELL VERTICAL TRACER TEST: SEAVEGATE GILL

5.7.1 INTRODUCTORY REMARKS

Following a number of attempts to raise the background conductivity of the Seavegate Gill borehole for the purposes of a BHDT, it was realised that tracer was being flushed from the borehole faster than could be measured. Some further preliminary tests indicated that groundwater was entering the borehole near its base and exiting near to the casing, so that the measurement of a series of tracer pulses injected at the same point and measured at different levels suggested itself. Similar experiments have been conducted by Drost (1983) and are also discussed in Kass (1998). The following are the results and analysis of this experiment[22].

5.7.2 RESULTS AND DISCUSSION

Figure 5.31 shows a series of breakthrough curves from measurements of the passage of successive injections of 1L slugs of sodium chloride-saturated tracer solution (injected at 35 m).

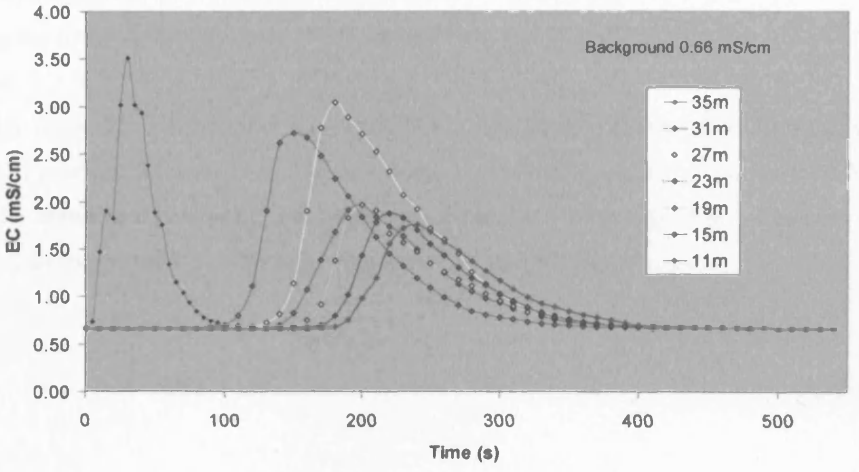

Figure 5.31 A series of breakthrough curves based upon injections at 35 mbfl and measurements at successive 4 m intervals above the injection.

The first curve at 35 m illustrates the shape of the input pulse, which on the time scale of the experiment cannot be taken as an instantaneous input. However, all times were recorded from the beginning of tracer injection so that peaks could be compared directly. Thus, from the peak arrival times (calculated by subtracting the time to the peak of the injection pulse from the time to peak of the breakthrough) it can be seen that the velocity of groundwater in the borehole is increasing with distance from the injection point at 35 mbfl. This is shown clearly in Figure 5.32. Note that each velocity is derived from the time taken to travel the whole distance from the injection to the sampling point.

[22] This experiment was undertaken before the offer of funding for the geophysical logging had been made. Had we had the flow meter data from the logs then we may not have performed the experiment.

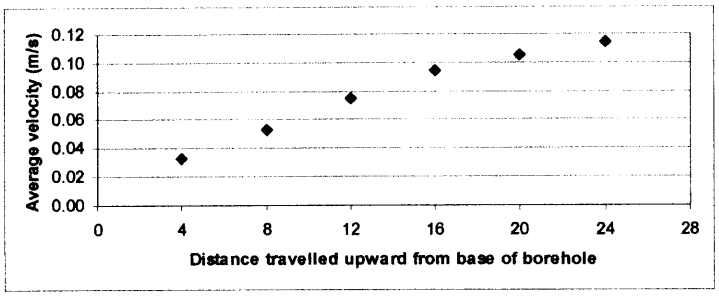

Figure 5.32 Increasing discharge with distance from the injection point at the base of Seavegate Gill borehole.

As the diameter of the borehole remains constant (barring fissures) over the interval in which all experiments were conducted, this implies an increase in volumetric flow as one progresses up the borehole. Furthermore, from Figure 5.31, there is a marked reduction in the area beneath the curves above 27 m. Examination of the geophysical log of this borehole (Figure 5.2 and Section 5.2.2.1) indicates major inflows and cross-flows associated with fissures at 32.2 and 24 mbfl, with additional inflows/cross-flows at 22.6, 20.5 and 18.6 mbfl and outflows at 11.1, 10.8 and 9.7 mbfl. On the basis that there is a significant increase in flow at 24 mbfl, it seems likely that a major inflow is responsible for diluting the tracer as it progresses along the borehole.

It is possible to examine this further by calculating mass recovery for each breakthrough curve, which is enabled by considering the volumetric flow based on the tracer velocity (distance travelled over time to peak), the borehole dimensions, and tracer concentrations (using Equation 5.1 to convert measured conductivity to concentration). The following integral was performed:

$$m = \int_0^\infty C(t)Q(z,t)dt \qquad (5.3)$$

where m = mass (M)

C(t) = concentration at time t (ML^{-3})

Q(z,t) = volumetric flow at depth z at time t (L^3T^{-1})

t = time (T)

The resulting table (Table 5.5) aids interpretation of the mechanism by which peak area is reduced.

Depth mbfl	Apparent mass recovery g
11	193
15	179
19	169
23	147
27	224
31	144

Table 5.6 Apparent tracer mass recovery at each sample depth.

The table shows that, whilst there is quite high variability in the amount of tracer recovered at each interval (average recovery ±1SD is 176 ± 30 g), there is no pattern of increased loss above a depth of 24 m. Rather, there is a trend toward increased recovery with distance travelled, although this is likely to be due to poor control over injection masses (which accounts also for the anomalously high value calculated for 27 m). It therefore seems probable that tracer is not being lost from the borehole because of cross flow at 24 m (or elsewhere) but is being significantly diluted prior to being flushed from the top section of the borehole. The maximum velocities in the borehole during the experiment[23], calculated on the basis of the vertical tracer testing, were 23,000 md^{-1}. The maximum velocities measured by the impeller flow meter were 39,000 md^{-1}. On the basis of the experimental results the calculated Reynolds numbers range from about 3000 at 31 m to over 10,000 by 11 m, fully turbulent along the length of the borehole.

5.7.3 SUMMARY

A tracer experiment was performed on Seavegate Gill borehole to examine the magnitude of vertical flows within the borehole. The results of the tracing indicate increasing velocity and increasing dilution of tracer as it travels upward along the borehole. These observations may be explained by addition of water from successive fissures contributing inflows at various points along the flow path of the tracer. The marked decrease in tracer concentration between 27 and 23 mbfl may be explained by these additional flows. The results of the tracer experiment were confirmed by subsequent geophysical logging. The work on this borehole contributes to an improved understanding of flow in the Corallian and is drawn upon in later chapters of the current work.

[23] Vertical tracing experiments conducted during April 2003, impeller flow-meter logging conducted during August 2004.

5.8 CHAPTER SUMMARY

Chapter 5 has presented the results of geophysical logging of a number of Corallian boreholes, experimental results from single borehole dilution tests, and the results of two different methods of interpretation. The first of these, the 'standard' method of interpreting BHDTs (Halevy et al., 1967, Environment Agency, 1998), was modified to account for processes contravening some of the usual assumptions made in deriving specific discharge values from BHDTs. The second type of analysis was a simulation model in which the flows were introduced at specific horizons in a borehole to recreate the observed experimental results. The latter modelling process was greatly facilitated by good geophysical logging and the two methods produced essentially independent results. Comparison of the model results, however, indicates that whilst they both largely agree in terms of the volumetric fluxes passing through the aquifer, individual comparisons used to extrapolate beyond a very local regime, are likely to lead to error. This can be minimised through experimentation on a wider range of boreholes. The borehole dilution tests are also supplemented with a single borehole vertical tracer test (or series of tests) from which additional information regarding flow in the aquifer can be derived. Results from all experiments are useful for further interpretation of tracer tests and CFC age data, as presented in the following chapters.

CHAPTER SIX

RESULTS AND DISCUSSION II
TRACER TESTS

"A distinction is often made between two fundamentally distinct senses of simplicity: syntactic simplicity (roughly, the number and complexity of hypotheses), and ontological simplicity (roughly, the number and complexity of things postulated). These two facets of simplicity are often referred to as elegance and parsimony respectively."

Alan Baker (2004)
Stanford Encyclopedia of Philosophy

6.1 INTRODUCTION

This chapter presents the results and modelling of tracer tests conducted as part of this research. It also includes a re-analysis of two tracer tests conducted prior to this work (Environment Agency, 1997; ARUP, 2000). The aim of the chapter is to determine a realistic conceptual model of the system and to provide a valid predictive model of flow and transport in the aquifer contributing to Irton and nearby public water supplies.

The chapter begins by introducing some statistical concepts useful for comparison of BTCs. The BTCs are then presented, as are passive (cotton-wool) detector results from several different tracer experiments. The statistical descriptions introduced are applied to the results for an examination of comparative features, together with more qualitative descriptions, all of which are presented together with the data.

Following presentation of the results is an appraisal of the various considerations that must be taken into account for any model of the system to be consistent with variability in the data. This involves conceptualisation of the aquifer and the flow field and relies upon experimental results as well as previously obtained hydrochemical, geophysical, pumping test and hydrological data.

Tracer transport processes are then considered, firstly with an overview of the primary processes that could be operative in the aquifer, and then by discriminating between the likelihood of these processes based upon information already held and with reference to the prior conceptualisation of the flow field. Once the most likely potential processes leading to the observed form of the data (e.g. breakthrough

curve tailing, peak dispersion, etc.) have been identified, elements of the system conceptualisation adopted to explain these differences are tested by comparison of the data to a number of mathematical models, each highlighting a different process. The main processes considered in this way are a geohydrological dipole, double porosity diffusion and hydrodynamic dispersion.

Once these processes have been examined and discussed the chapter proceeds with some further analysis aimed at determining basic relationships between tracer transport and pumping conditions within the aquifer.

6.2 TRACER TEST RESULTS AND PRELIMINARY ANALYSIS

6.2.1 INTRODUCTORY REMARKS

The tracer tests undertaken as part of this research may be divided into those conducted in Forge Valley using fluorescent dyes, that conducted with sulphur hexafluoride between the swallowholes and Irton and the wider aquifer, and those conducted in Brompton Dale toward Brompton Spring, also using fluorescent dyes. The results are presented in this sequence as the Forge Valley experiments fall together irrespective of tracer. Information regarding the analytical methods is given in Chapter 4 (methods).

Tracer breakthrough curves (BTCs) contain a variety of information either directly readable from the graphs themselves or obtainable through a combination of the measured concentration/time data and discharge data. Several basic parameters may be derived from statistical analysis of this data, *without reference to contaminant transport theory* (USEPA, 2002). These include such parameters as first arrival, peak concentration, the mean residence time of the tracer in the aquifer and the mass of tracer recovered. These parameters are discussed individually prior to presentation of the measured data so that they may form part of the initial appraisal of the results. The discussion of the parameters is based primarily on Gaspar (1987a and 1987b), USEPA (1998 and 2002) and personal communication with Prof. T.C. Atkinson, UCL.

All tracer injection and sampling locations are shown on Figure 5.1 (previous chapter). Tracer test data measured by the author are given in Appendix 7.

6.2.2 SOME BASIC STATISTICAL PROPERTIES OF BREAKTHROUGH CURVES

The following parameters may be determined from BTCs and sampling point discharge data.

- First arrival time
- Peak concentration
- Tracer mass recovered
- Mean residence time
- Mean tracer flow velocity

These parameters are defined as follows:

6.2.2.1 First arrival time

This is, straightforwardly, the time at which tracer is first measured above background concentrations at the sampling point. This depends upon the sensitivity of the analytical equipment and noise in the

background signal, so that wherever it is stated it is actually the first arrival above some definite concentration, rather than first arrival *per se.*

6.2.2.2 Peak concentration

For a unimodal BTC this is the maximum concentration that the tracer achieves at the point of sampling. A BTC may have multiple peaks, however, in which case each peak represents a local maximum of tracer concentration. Several of the BTCs discussed below have a dominant peak, which clearly represents maximum concentration, and one or more subsidiary peaks. In these cases only the highest concentrations are reported.

6.2.2.3 Mass recovery

The mass of tracer recovered may be calculated by numerically integrating the product of discharge and concentration over time (Equation 6.1):

$$m_t = \int_0^{t(end)} Qc.dt \qquad (6.1)$$

Where:

m_t is the mass of tracer recovered (M)

t is time (T)

t(end) is the time at which measurements ceased (T)

Q is discharge at the sampling point (L^3T^{-1})

c is concentration of tracer (ML^{-3})

This value is then compared to the mass of tracer injected (M_I) and given as a percentage. The mass recovery of a tracer indicates what proportion of a contaminant may be expected to be recovered at a discharge point, whether or not all discharge points have been monitored adequately, or whether other mechanisms of tracer losses (e.g. to matrix storage over the timescale of the experiment) may be operative within an aquifer.

6.2.2.4 Mean residence time

The mean residence time can be defined as the time before which 50% of the tracer is discharged. However, if the mass of tracer injected is given by M_I , and the mass of tracer recovered is given by m_t and as it is usually the case that $m_t < M_I$, then the mean residence time may be given with respect to either of these masses. These different mean residence times are labelled $t(m_t)$ or $t(M_I)$ respectively.

The mean residence time of tracer represented by the *measured BTC* is given by:

$$\int_0^{t(mt)} Qc.dt = \frac{m_t}{2} \qquad (6.2)$$

In contrast, the mean residence time of tracer with respect to the total mass injected is given by:

$$\int_0^{t(M_I)} Qc.dt = \frac{M_I}{2} \qquad (6.3)$$

Following from these two definitions, $t(m_t)$ will always be defined by the data, as it will always be less than t(end). On the other hand, $t(M_I)$ will only be defined by the data where m_t is greater than $\frac{M_I}{2}$.

As $m_t > M_I/2$ is not always the case in the experiments conducted as part of this research the mean residence time will be defined after equation 6.2 as opposed to equation 6.3 for all subsequent analyses. This permits a valid comparison for all tracer tests between the same injection/sampling points over the same time interval (e.g. 24 hours following tracer injection).

6.2.2.5 Mean tracer flow velocity

The mean tracer flow velocity is given by the distance travelled divided by the mean residence time. It is therefore dependent upon the definition of mean residence time. As this has been defined (Section 6.2.2.4) the mean tracer flow velocity is given by:

$$v_{MT} = \frac{x}{t(mt)} \qquad (6.4)$$

Where:

v_{MT} is mean tracer flow velocity (LT^{-1})

x is the straight-line distance between injection and sampling points (L)

t(mt) is mean residence time of the tracer (T)

Because some sinuosity in the flow path may be assumed it is likely that the mean tracer flow velocity is an underestimate of actual velocity (USEPA, 2002), although corrections have not been attempted in the following analysis.

6.2.3 FORGE VALLEY DYE TESTS

6.2.3.1 The Forge Valley swallowholes to Irton

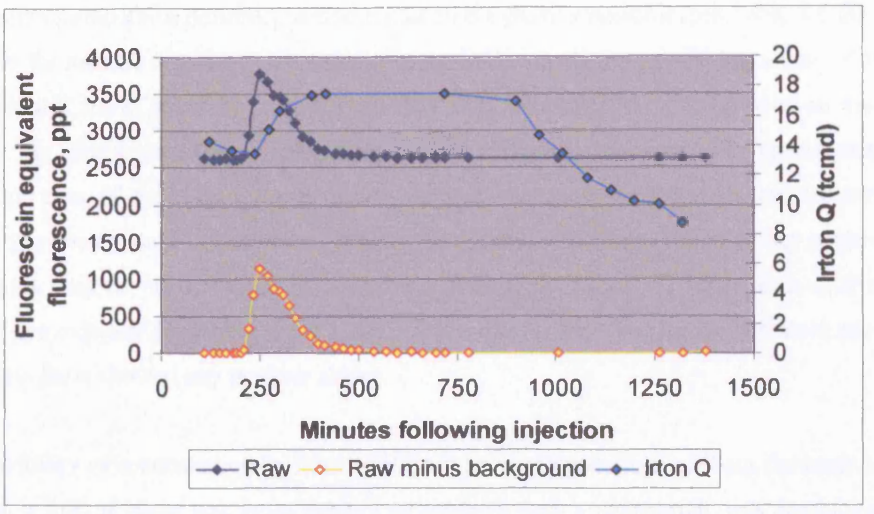

Figure 6.1 Fluorescein breakthrough curve at Irton, 21st May 2002.

Figure 6.1 shows the BTC for Fluorescein at Irton following injection of 2.86g at the Forge Valley swallowholes on the morning of the 21st of May 2002. First arrival was measured at 204 minutes, rising to a peak concentration of 1.15 ppb above background at 250 minutes. The mass recovery during the experiment was 49%, with the mean residence time calculated to be 324 minutes (5.4 hours). This indicates a mean tracer velocity of 8.65 km d^{-1}. Qualitatively, the breakthrough curve rises swiftly and smoothly but exhibits some tailing, and a secondary peak can be seen 'shouldering' onto the primary. This occurs shortly after an increase in pumping rate at Irton, although may be the result of more than one flowpath between injection and sampling points.

6.2.3.2 Seavegate Gill to McCains and Seavegate Gill to Irton

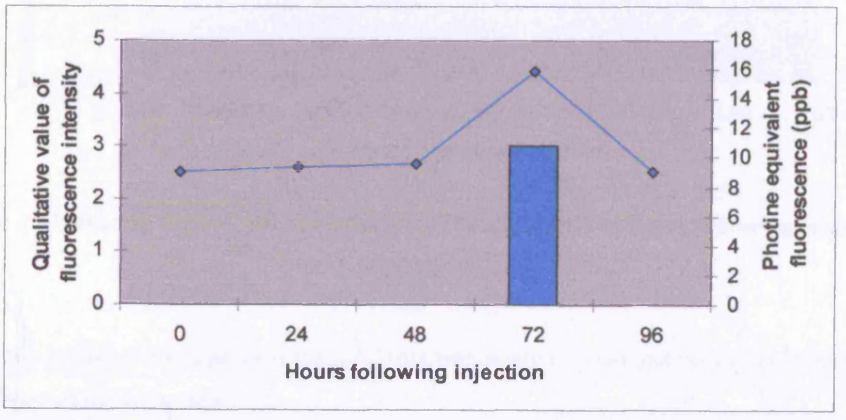

Figure 6.2 Photine breakthrough at McCains following injection on 9th July, 2002. Detectors changed and samples taken at hour shown.

Following injection of 32 g of Photine CAQ (8.6 g active ingredient) at a depth of 25 mbfl in the Seavegate Gill borehole, samples were taken, and passive cotton wool detectors changed, daily for 4 days at McCains and Irton PWS. The only positive sample occurred at McCains 3 days after injection (Figure 6.2), with a concentration about 6.3 ± 0.1 ppb above background (which was about 9 ppb). This was corroborated by a definite positive signal on the passive detector (see Table 4.4 for subjective points scale for passive detectors). The McCains borehole was being pumped at a rate of 100 m^3 d^{-1}, which is about 2.5% of its usual pumping rate due to maintenance work being done on machinery in the factory. By multiplying the pumping rate, the concentration (assumed to be representative of the concentration over 24 hours) and the sampling interval, a recovery of about 7% can be estimated. As neither the passive detector nor the water sample for the final day (day 4) showed any positive result it seems that the majority of the tracer reached the well between 48 and 72 hours, thus constraining the velocity of groundwater flow between 2.1 and 3.2 km d^{-1}. Neither the passive detectors nor the water samples from Irton showed any positive signal.

As the possibility of a connection to Irton could not be completely excluded on the basis of the first experiment, a further tracer test, in an attempt to establish such a connection, was conducted from the same borehole. On the 14th April 2003, 15 g of Fluorescein Sodium were injected at 9.1 mbfl, adjacent to the major effluent fracture that had by then been determined from the vertical-well tracer test and additional geophysical data (European Geophysical Services, 1981). The results from water samples, taken by automatic water sampler for 4 days, are given in Figure 6.3, which shows fluctuations in Fluorescein-equivalent fluorescence but nothing that could be ascribed to arrival of tracer dye.

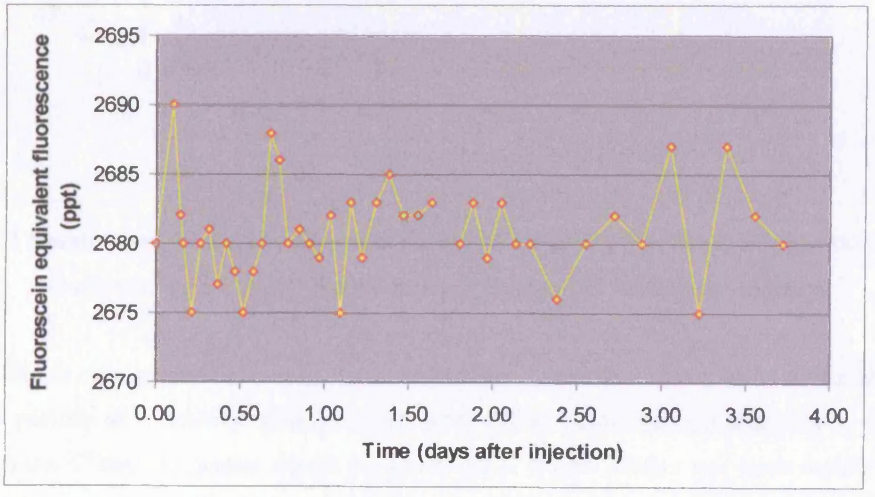

Figure 6.3 Measured fluorescence (Fluorescein wavelengths) at Irton following injection at Seavegate Gill.

This apparently negative result at Irton suggests that Seavegate Gill lies outside, or at least marginal to, the capture zone of the Irton well.

6.2.3.3 Swallowholes borehole to the Augmentation borehole and wider aquifer

Also on the 14th of April 2003, in conjunction with the Seavegate Gill – Irton test described in the previous section, 160 g of Photine CAQ (c. 35 g of active ingredient) were injected into the Swallowholes borehole at a depth of 23 mbfl (8.3 m below casing, in the centre of the zone of rapid dilution as determined from the BHDT). Passive cotton-wool detectors were installed in the Augmentation borehole at various depths and also in the Derwent Ford, Derwentdale Farm North, Wykeham, Seavegate Gill and Tetherings Plump boreholes, and in a stream of water from a sample tap at Irton (see Figure 5.1 for locations). Detectors were installed prior to the experiment (for background), and changed daily during the experiment. All background detectors were free from fluorescence except that from the Derwent Ford borehole, which may have been contaminated. No dye was detected at the Irton, Wykeham or Derwentdale Farm North boreholes, and the results from Derwent Ford are unreliable. The results are summarised in Figure 6.4 (refer to Table 4.4 for the subjective points scale used for passive cotton-wool tracer detectors).

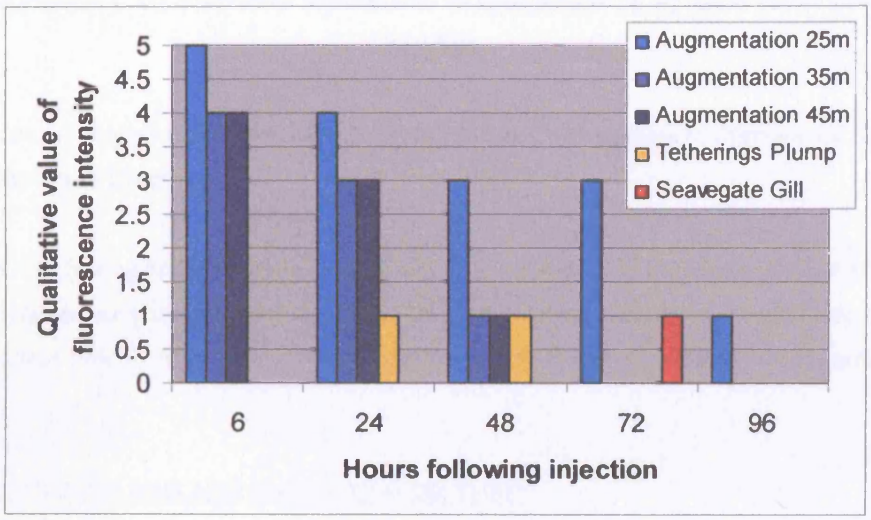

Figure 6.4 Results from passive cotton-wool detectors following Photine CAQ injection into the Swallowholes borehole. Detectors were changed at the hours indicated.

Figure 6.4 shows clear positive results in the Augmentation borehole within 6 hours of tracer injection. The tracer persists at a positive strength at 25 mbfl (14 m below casing) dropping to a doubtful presence on the 4th day. At greater depths the tracer signal is both weaker and more rapidly depleted, although still strong for the first 24 hours. The Tetherings Plump borehole shows 'doubtfully positive' results (see Table 4.4) within 24 hours of injection, indicating groundwater movement to the west, although the low-level loading of the detectors means that this result cannot be considered particularly reliable. The same applies to the Seavegate Gill borehole, which showed a doubtful positive result after 3 days. (However, this borehole also gave a weakly positive signal in the 1999 tracer test from the Forge Valley swallowholes (ARUP, 2000), which will be discussed in further detail below.)

An automatic water sampler was stationed at Irton in an attempt to quantify any dye arriving at the pumping station. The results of those measurements are given in Figure 6.5.

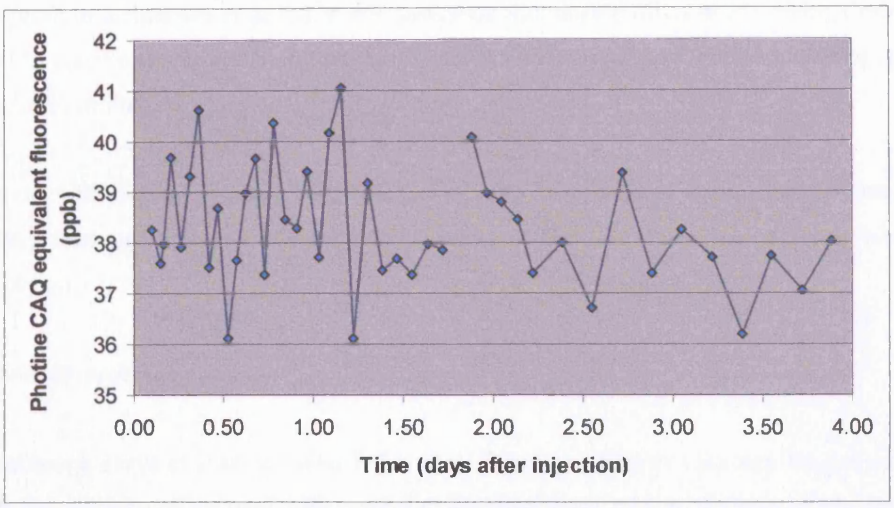

Figure 6.5 Photine CAQ equivalent fluorescence at Irton following injection at the Swallowholes borehole.

As for Figure 6.3, Figure 6.5 shows fluctuations in Photine CAQ-equivalent fluorescence, but nothing clearly indicative of tracer arrival.

Similarly to the Seavegate Gill experiment, the lack of tracer arrival at Irton indicates that groundwater flow is not immediately in this direction. As the Swallowholes borehole is on the west side of the river Derwent, direct flow to Irton may be prevented by the influent river water spreading radially in all directions.

6.2.4 THE SULPHUR HEXAFLUORIDE TRACER TEST[24]

6.2.4.1 Injection mass

The injection mass was calculated on the basis of a sample taken from the tracer preparation system (Chapter 4) and the volume of water in the tracer reservoir. A sample of 1 mL was diluted by a factor of 1×10^6 prior to injection into the sample purge tower. The dilution was undertaken in two stages, with the original sample (1 mL) being transferred to a one litre flask full of river water, from which a millilitre was taken, following mixing, and transferred to another litre flask full of river water. These transfers were performed using an Eppendorf precision pipette and represent a serial dilution of 2×1000 mL. The second dilution was made twice as the first time it was made there appeared to be an error in the dilution entailing a loss of SF_6. This led to two markedly different estimates of tracer injection concentration. However, as both 2nd series dilutions were made from the same 1st series flask,

[24] This experiment was combined with an injection of fluorescein. These results are also discussed under this heading.

it is considered that the second of these represents the more accurate value of tracer concentration. This is 19.88 mg kg^{-1}, which is about 50% of the saturation concentration at STP (Morrison & Johnstone, 1955). This concentration is also broadly in line with concentrations achieved with similar sparging tracer preparation techniques reported in the published literature (Dillon *et al.*, 1999; Corbett *et al.*, 2000a and b; Gamlin *et al.*, 2001; Harden *et al.*, 2003) and unpublished literature (Strongman, 1994; Robinson, 1996) literature.

The value of 19.88 mg kg^{-1} is considered to be the most reliable value of tracer injection concentration and implies a total mass injection of 9.94 g distributed over 500 L of water. Injection took place over a two hour period.

6.2.4.2 Breakthrough curve at Irton

The breakthrough curve at Irton is presented in three figures so that an idea may be gained of a) the magnitude and duration of the peak with respect to the tail (Figure 6.6), b) the form of the peak (Figure 6.7), and c) the distribution of mass recovery during the experiment (Figure 6.8).

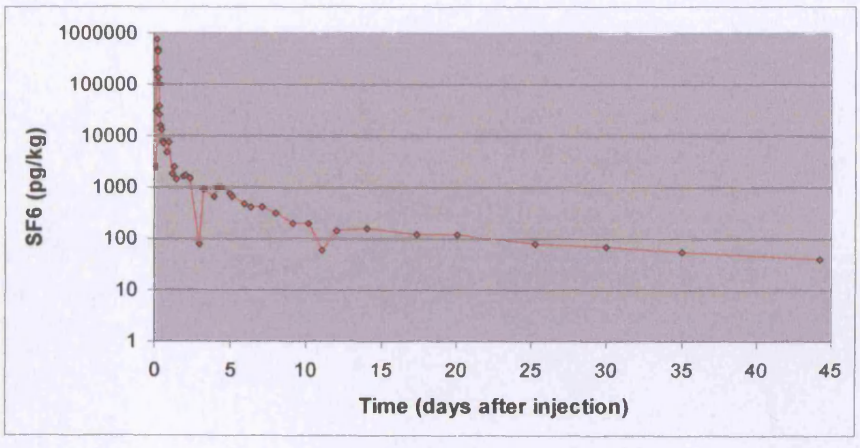

Figure 6.6 SF_6 breakthrough curve at Irton: semi-log plot over the duration of the experiment.

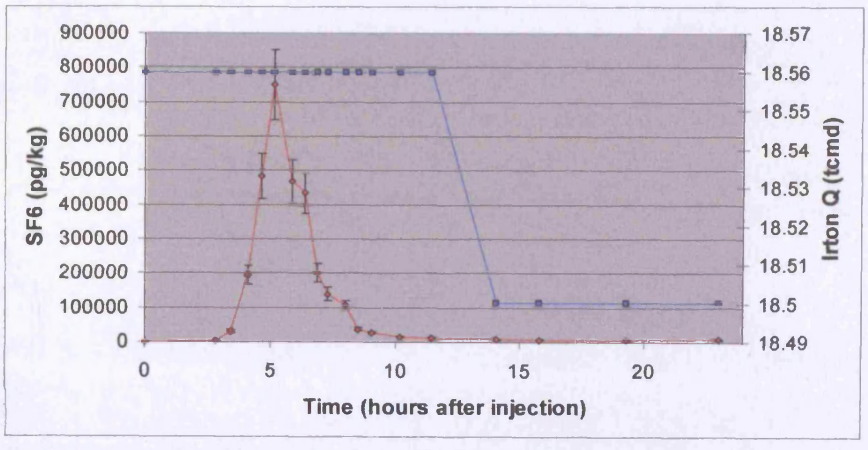

Figure 6.7 SF_6 breakthrough curve and pumping rate: 1st 24 hours.

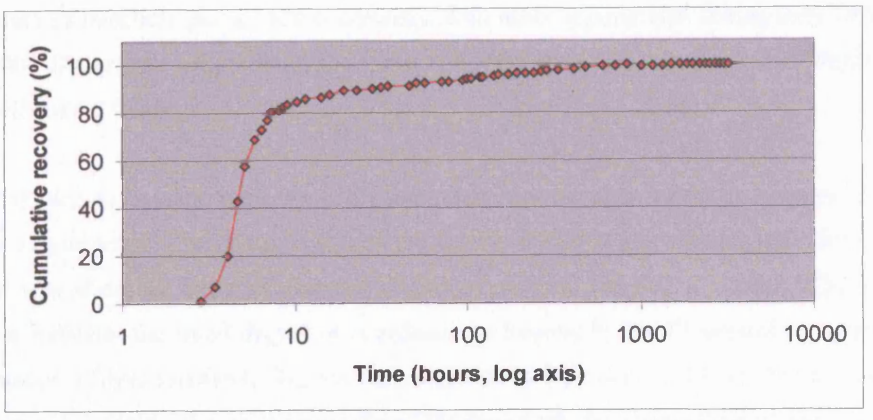

Figure 6.8 SF_6 cumulative recovery as a percentage of total recovery over the course of the experiment.

The first measured arrival at Irton was at 169 minutes after the commencement of injection, rising to a peak concentration of approximately 750 000 $pgkg^{-1}$ (≈750 ppt) at 307 minutes (Figure 6.6). Figure 6.6 also indicates that the concentration maintained in the tail of the breakthrough curve after 44 days is approximately 1.5 orders of magnitude above the detection limit (3.4 $pgkg^{-1}$). This represents a significant improvement over previous experiments in terms of the capacity of SF_6 to reveal the later-time characteristics of contaminant transport within the Forge Valley – Irton system. The mechanisms responsible for the form of this tail, and the attempts made to model it, form much of the remainder of this chapter.

Figure 6.7 shows that the peak rises smoothly, but declines less smoothly, showing two distinct 'bumps' within the first 10 hours. Although these are not as pronounced as the 'shouldering' peak found using fluorescein in Figure 6.1 they indicate the possibility of more than a single rapid pathway to the Irton well, especially given that pumping conditions were uniform for the duration of the main peak arrival. However, this is not supported by the fluorescein measurements (below) but will be addressed more fully in Section 6.7.

The mass of SF_6 recovered at Irton was 15.5% of the calculated injection mass, which is a poor recovery for the system, especially considering that fluorescein injected mid-way through the SF_6 injection gave a recovery of 76% (see below). The loss of tracer could be due to a number of factors. The first is that the calculated injection concentration is too high. Alternatively, the volatility of SF_6 could lead to significant losses upon injection, as injected water was observed to circulate around the 'sump' structure surrounding the active swallowholes prior to being drained into the ground. The injection into the swallowholes was also above the water table, so that should any phreatic surface exist within the fissures into which river water was draining there would be an opportunity for further degassing. Prior to the experiment it was not considered that losses via this mechanism represented a serious threat to the viability of the experiment, as the water table is typically only two or three metres below the bed of the river and transport is known to be rapid. However, this may have been a misconception of the system. Figure 6.8 shows the cumulative recovery of the total amount of SF_6 recovered. Of the total tracer recovered at Irton, c. 50% was recovered within 6 hours and c. 80%

within 8 hours of injection. For a valid comparison with other experiments lasting only 24 hours (e.g. the May 2001 fluorescein experiment), the mean residence time is 6.4 hours, which implies a mean tracer velocity of 6.3 kmd^{-1}.

Figure 6.9 shows the breakthrough curve obtained from the injection of 5g of Fluorescein mid-way through the SF_6 injection. The first arrival detected at Irton is also at 169 minutes (after injection of the dye, which was about 45 minutes after the commencement of the SF_6 injection). This equality in arrival times indicates the small degree of retardation undergone by the Fluorescein in comparison to SF_6. Attenuation of dyes relative to SF_6 has been demonstrated by Biggin (1991). The fact that it is not observed here is probably due to the rapidity of the transport, the channelling of the tracer and the periodicity of the sampling (which was approximately half-hourly at the beginning of the experiment – it is coincidental that samples were taken at exactly 169 minutes after commencement of both injections).

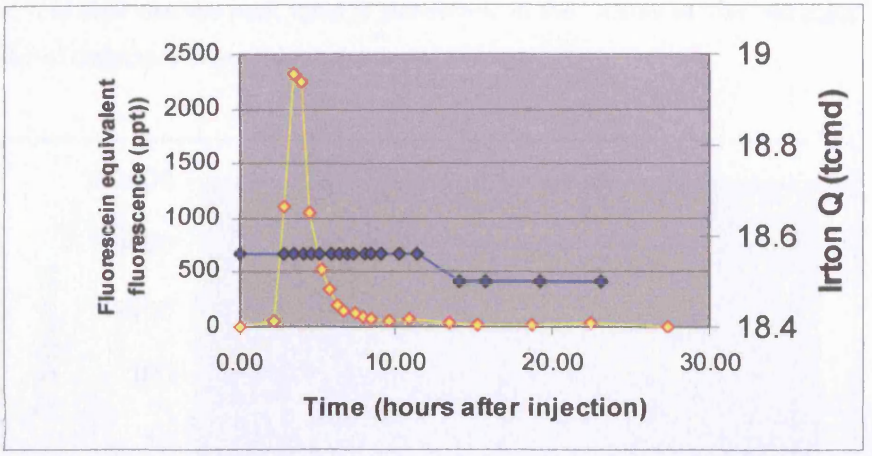

Figure 6.9 Fluorescein breakthrough (yellow) and discharge (blue) at Irton during the SF_6 tracer experiment.

Peak concentrations were reached more swiftly for the Fluorescein than the SF_6, as would be expected from a shorter injection period (c. 3 minutes compared with 2 hours for SF_6). Peak concentration was 2.38 ppb above background (0.262 ppb Fluorescein equivalent fluorescence[25]) and occurred at 204 minutes. The BTC did not quite return to background within 24 hours, due to both the higher mass injected and lower background fluorescence in this experiment than the previous Fluorescein experiment (Section 6.2.3.1). The mass recovery was 76%; the highest of any experiment conducted on the system and probably associated with an elevated pumping rate at Irton (this is discussed further in Section 6.9). There does not appear to be any indication of a secondary peak, with the discharge at Irton remaining a constant 18.56 tcmd for the duration of the main tracer peak.

[25] This background was an order of magnitude lower than previously measured background concentrations. The data has been checked for errors and this appears to be the correct value.

6.2.4.3 Breakthrough curve at Derwentdale Farm North borehole

The Derwentdale Farm North borehole is a non-pumped borehole that remained artesian (and therefore easy to sample) for the duration of the experiment. It is located 1500 m SSE of the swallowholes and 750 m WSW of Irton and provided an important second sampling location for the injected tracer. Again, results are shown on separate plots to highlight a) the magnitude of the peak in relation to the tail (Figure 6.10), and b) the form of the peak (Figure 6.11). No cumulative recovery curve is given as the discharge of water through the aquifer at this point is not known.

The first arrival at 137 minutes (which is a poorly-constrained upper limit) implies a groundwater velocity for the fastest flowpaths equivalent to that derived from both the SF_6 and fluorescein peaks arriving at Irton. However, the peak here is not recorded until 19 hours, indicating that the majority of tracer follows a slower flowpath. Judging from the position of measurement points on the BTC, the highest concentration measured is probably marginally lower than the true peak value (Fig. 6.11). Nonetheless, it is clear that the peak value is somewhere in the vicinity of 100 000 $pgkg^{-1}$, which is about an order of magnitude lower than that detected at Irton.

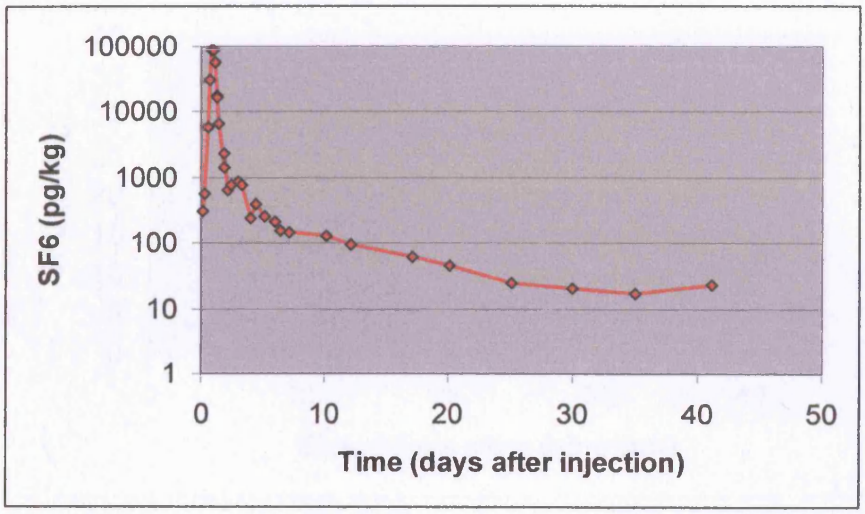

Figure 6.10 SF_6 breakthrough curve measured at Derwentdale Farm North: semi-log plot over the duration of the experiment.

The concentration in the tail of the breakthrough curve at the end of the experiment was about an order of magnitude higher than the detection limit. The mean residence time cannot be calculated as the well was artesian and only opened for the purposes of sampling, so that the discharge values for the aquifer at this point during the experiment are not known. However, on the basis of peak arrival, occurring at 19 hours following injection, a rough estimate of velocity may be made at 2 kmd^{-1}.

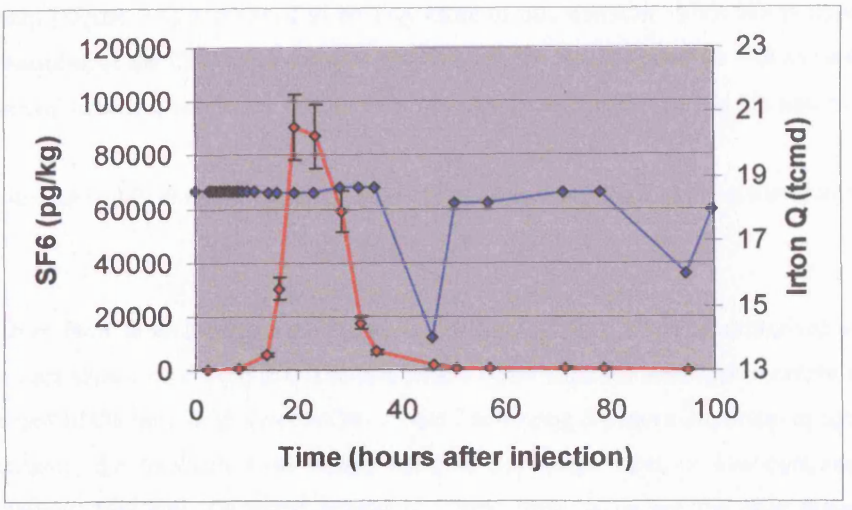

Figure 6.11 SF_6 breakthrough curve measured at Derwentdale Farm North: the first 4 days (also showing Irton Q).

6.2.4.4 Breakthrough curve at Derwentdale Farm South borehole

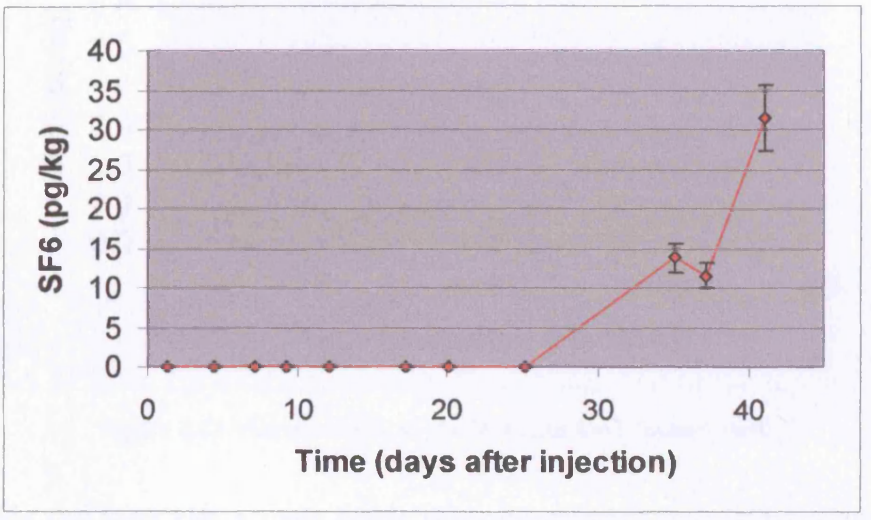

Figure 6.12 SF_6 breakthrough curve measured at Derwentdale Farm South borehole: semi-log plot over the duration of the experiment.

The first definite arrival at the Derwentdale Farm South borehole, (Figure 6.12), another borehole that was artesian throughout the experiment (although with considerably greater strength at this point further into the vale), occurred 35 days after injection. Unfortunately neither the peak concentration nor duration is known as the sampling was terminated at this location after 41 days, while the measured concentration was still apparently rising. Nonetheless this clearly positive result implies a groundwater velocity for the most rapid component of flow of c. 85 m d^{-1} (the borehole is 3 km from the injection point). The maximum concentration measured was 31.5 ± 8.5 $pgkg^{-1}$, which is about 4 orders of magnitude less than the peak recorded at Derwentdale Farm North borehole. The arrival of tracer at this location, which had not been monitored during previous tracer tests, indicates the rapid migration of young groundwater more or less directly to the Ebberston Filey fault, which from the

geological map (Figure 2.6) is inferred to be very close to this borehole. This fact is important for a fuller understanding of the CFC apparent ages presented in the next chapter, as well as confirming the overall pattern of extensive connected fissure flow throughout the eastern part of the aquifer.

6.2.4.5 Monitoring results from McCains, Cayton Carr House Lane PWS and Cayton Station Road PWS.

The results from these three locations are shown in Figures 6.13 to 6.15 and summarised in Table 6.1. The locations are shown on Figure 5.1. The two public water supplies are supplementary to Irton and only operate part of the time, with Cayton Carr House Lane being the more important of the two. Apart from maintenance, the McCains food factory operates its pumps more or less continuously (pers. comm. A. Sarney, McCains Technical Manager). These three wells are the only major Corallian groundwater abstractions to the east of Irton (Carey and Chadha, 1998).

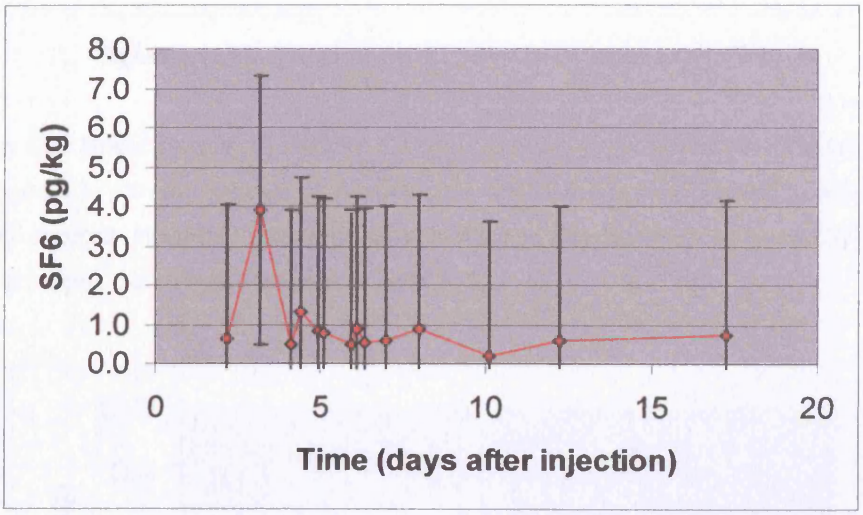

Figure 6.13 Measured SF_6 at the McCains food factory well.

The McCains data show only a single sample above the empirical limit of detectability for this experiment. However, this occurs at 3 days and 4 hours, which is broadly in line with the Photine CAQ test from Seavegate Gill conducted two years previously (positive at 2 days 22 hours) and the Photine CU test from the swallowholes in 1999 (ARUP, 2000; arrival between 2 and 5 days). The concentration of the peak (if it can be called that) at 3.9 $pgkg^{-1}$ was only marginally greater than the error. If we subtract the potential contaminant error this gives a peak concentration of 0.5 $pgkg^{-1}$. This extremely low positive result may be due to difficulties sampling the McCains well: the sampling tap emits an extremely strong flow of water that tends to entrain air upon exit. This made it difficult to obtain a bubble-free water sample, such that potential losses of SF_6 may have occurred at this stage (although the CFC 12 data, from the same samples, does not bear this theory out). Nevertheless, the low amount measured is still significant in that it represents a positive tracer identification and constrains travel times and flowpaths to this part of the aquifer. Assuming pumping at the maximum licensed rate (4.1 tcmd) and persistence of the peak at the measured level for 24 hours, tracer recovery

at this site may be estimated at 0.00007%. The mean tracer velocity calculated from the positive sample is 2 km d^{-1}.

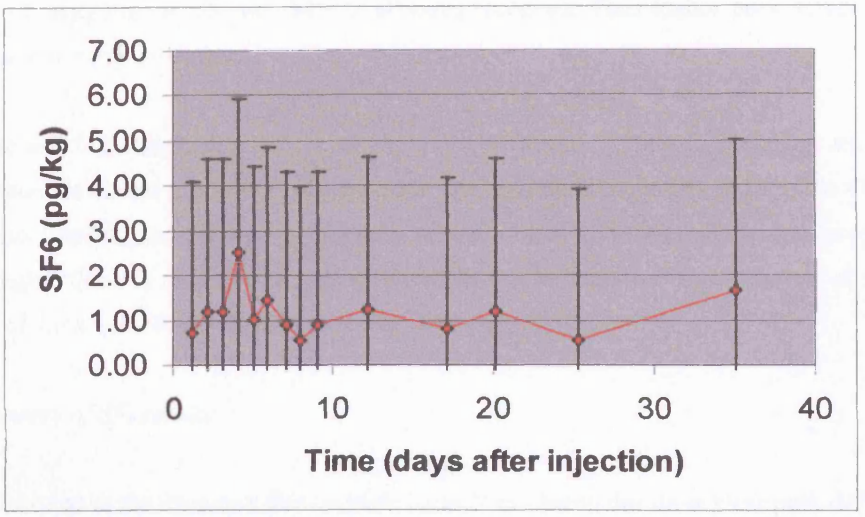

Figure 6.14 Measured SF_6 at Cayton Carr House Lane PWS.

The Cayton Carr House Lane PWS is about 6.25 km from the swallowholes (see Figure 5.1) but the results (Figure 6.14) do not provide conclusive evidence of tracer breakthrough given the limit of detectability adopted. However, sampling was continued at this location due to its importance as a public water supply, but no tracer arrival was identified.

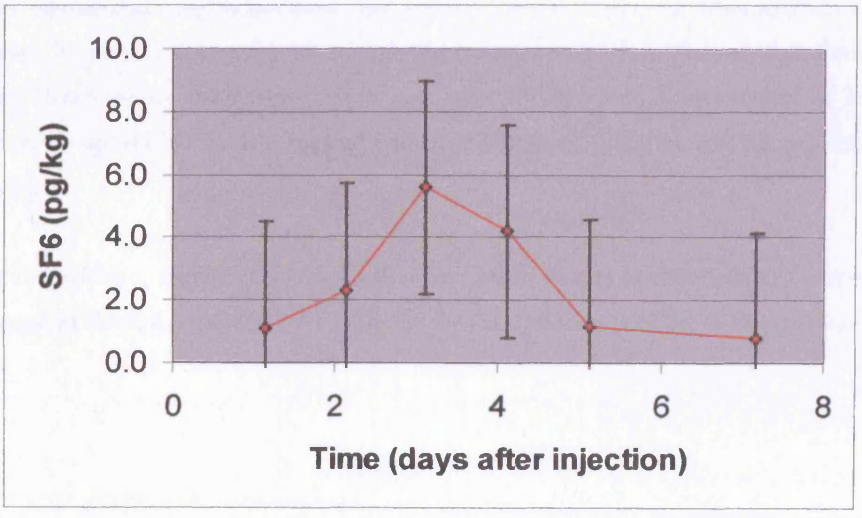

Figure 6.15 Measured SF_6 at Cayton Station Road PWS.

The Cayton Station Road PWS is to the east of both McCains and Cayton Carr House, in total about 7.25 km from the Forge Valley swallowholes. However, the BTC here (Figure 6.15) is better defined than those at McCains or Cayton Carr House. Figure 6.15 shows that SF_6 is well above the adopted detection limit at 3 days, falling to just above it at four days. If we subtract the potential contaminant signal, the peak concentration is 2.2 $pgkg^{-1}$, which is about four times that observed at McCains. The

fractionally earlier arrival at this borehole than McCains may be due to a superior connection between this borehole and the faster flowpaths in the aquifer, which may also explain the higher concentration. However, the small sizes of peaks detected at these three boreholes may be due simply to the periodicity of sampling, which was daily at all three locations. Thus higher peak values may have passed at some unsampled time.

The Photine and bacteriophage tracer results from 1999 (ARUP, 2000) do not show any arrival at Cayton Station Road, but positive results for both McCains (as mentioned) and Cayton Carr House, which is also noted to show increased turbidity at times when Irton also shows increased turbidity, reflecting higher flows in the Derwent. Altogether these results indicate the swift arrival of river water in this part of the aquifer following its capture by the swallowholes.

6.2.4.6 Summary of SF_6 results.

The data measured at the Irton and Derwentdale Farm North boreholes show clear peak definition and illustrate that BTC tailing can be followed for a period of weeks provided a tracer can be used which allows measurement at extremely large dilutions against extremely low background – which SF_6 does. However, on the basis of the best estimate of tracer injection mass, the tracer recovery appears to be much lower than for fluorescein.

Further afield, at the 6 – 7.5 km range, measured values indicate rapid transport (c. 2 kmd^{-1}), greater dilution and possible losses to storage. Despite the positive values being very low, it is encouraging that they are measured at roughly the same time and that they exhibit order-of-magnitude similarity in concentrations. The tracer detected at an intermediate distance of 3 km (Derwentdale Farm South) is also low but clearly above background levels and detectability. With a first arrival of 35 days this sampling location appears to lie in a zone of less-rapid transport (although still 85 md^{-1} on a straight-line flowpath).

The data presented here, together with qualitative and basic statistical descriptors of tracer transport, are summarised in Table 6.1 and form the basis for the theoretical modelling to be presented in Section 6.3 below.

Injection location	Monitoring location/s	Date	Distance (m)	Tracer	Mass (g)	Monitoring method	1st Arrival	Peak Arrival	Mean residence	Cpeak (measured)	Passive detector score (Max)	Recovery %	Vel. 1st arr. m/d	Vel. Cent. m/d
Forge Valley swallows	Irton PWS	21/05/2002	1950	Fluorescein	2.86	S (man)	204 mins	250 mins	5.4 hours	1.15 ppb	-	49.12	13 750	8650
Seavegate Gill BH	McCains	09/07/2002	6250	Photine CAQ	8.6	S (man) + PD	3 days	3 days	Unknown	6.94 ppb	3	8?	2100	-
Brompton Shallow BH	Brompton Springs	31/07/2002	250	Photine CAQ	1.2	S (man) + PD	6 - 24 hours	24 -48 hours	-	-	3.5	-	1000	-
Brompton Deep BH	Brompton Springs	31/07/2002	250	Flavine DY 96	1.2	S (man) + PD	No result		-	-	0	-	-	-
Brompton Shallow BH	Brompton Springs	18/09/2002	180 - 250	Photine CAQ	39.2	S (man) + PD	<48 hours	<48 hours	-	-	1 (post 48 hours)	40(Dbtful)	>125-	-
Brompton Deep BH	Brompton Springs	18/09/2002	180 - 250	Flavine DY 96	39.2	S (man) + PD	No result		-	-	0	-	-	-
Brompton Shallow BH	Brompton Springs	02/01/2003	180 - 250	Photine CAQ	180	PD	<24 hours		-	-	4	-	>180	-
Seavegate Gill BH	Irton PWS	14/04/2003	2125	Fluorescein	15	AWS	No result	No result	-	-	-	-	-	-
Swallowholes BH	Irton PWS	14/04/2003	1975	Photine CAQ	35	AWS	No result	No result	-	-	-	-	-	-
	Augmentation BH	14/04/2003	18			PD	6 hours	6 hours	-	-	5	-	>72	-
	Tetherings Plump	14/04/2003	2750			PD	24 hours	-	-	-	1	-	>2750	-
	Seavegate Gill	14/04/2003	400			PD	3 days	-	-	-	1	-	133	-
	Derwent Ford BH	14/04/2003	875			PD	No result	-	-	-	0	-	-	-
	Derwentdale Farm Nth BH	14/04/2003	1500			PD	No result	-	-	-	0	-	-	-
	Wykeham	14/04/2003	2625			PD	No result	-	-	-	0	-	-	-
Forge Valley swallows	Irton PWS	30/07/2004	1950	SF6	5.64	S (man)	169 mins	307 mins	6.4 hours	750 ± 180 ng/kg	-	15.6	16 600	7300
	Derwentdale Farm Nth BH		1500			S (man)	137 mins	19 hours	Unknown	90 ± 21.6 ng/kg	-	0.3	15 750	-
	Derwentdale Farm Sth BH		3000			S (man)	35 days	Unknown	Unknown	31.5 ± 7.6 pg/kg	-	-	86	-
	McCains		6250			S (man)	3.16 days	3.16 days	Unknown	3.9 ± 2.26 pg/kg	-	<0.001	2000	-
	Cayton Carr House Lane PWS		6250			S (man)	4.13 days	4.13	Unknown	2.53 ± 2.26 pg/kg	-	<0.001	1500	-
	Cayton Station Road PWS		7250			S (man)	2.15 days	3.12	Unknown	5.58 ± 2.26 pg/kg	-	<0.001	3400	-
Forge Valley swallows	Irton PWS	30/07/2004	1950	Fluorescein	5	S (man)	169 mins	204 mins	4.4 hours	2.33 ppb	-	76.37	16 600	10650

NB PD = Passive (cotton wool) detector, S (man) = Manual water sample, AWS = Automatic water sampler.

Table 6.1 Summary of tracer tests conducted by the author as part of this research.

6.2.5 BROMPTON DALE TO BROMPTON SPRINGS TRACER TESTS

6.2.5.1 Introductory remarks

These results were obtained by Patrick Mottram, an undergraduate student at UCL, as part of his B.Sc. dissertation (Mottram, 2003). Although most of the sampling and analysis was conducted by him, the experiments were designed and performed with the help of the author on the understanding that any results would form a part of this thesis. An introductory description of the springs is given in Chapter 2, and methods of tracer injection detailed in Chapter 4.

6.2.5.2 Brompton tracer test 1

1.2 g of Flavine, dissolved in tap water to make up 1 L of tracer solution, was injected into the Brompton Dale Deep borehole at a depth of 46 mbfl on the 31st July 2002. This was flushed through the injection hose with a further 20 L of tap water. This injection was immediately followed by an injection of the same amount of Photine CAQ at a depth of 15.2 m in the shallow borehole, and again flushed with 20 L of tap water. Passive cotton wool detectors were installed at 16 separate discharging locations along the limestone outcrop at the Mill Pond spring (Chapter 2), and changed 4 times within the 48 hours following injection (Figures 6.16 and 6.17). Water samples were taken for fluorimetric analysis.

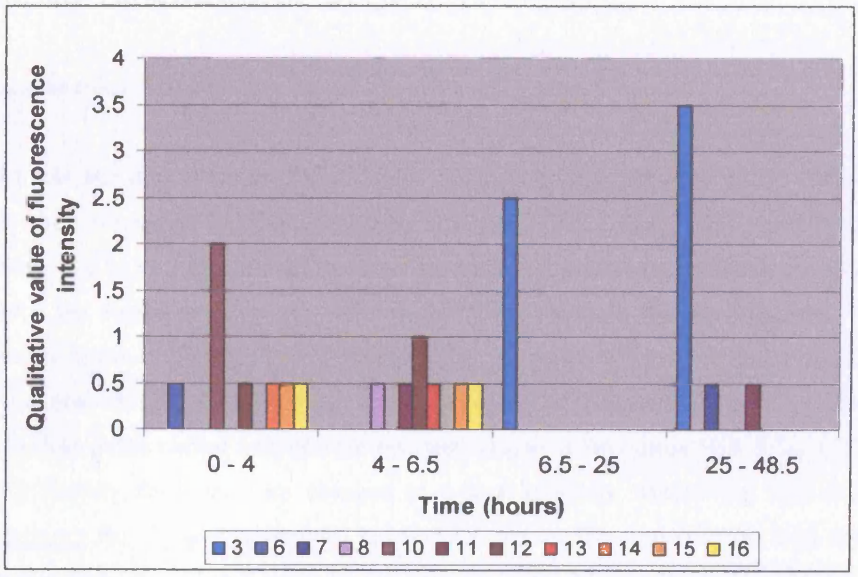

Figure 6.16 Passive detector results for Photine CAQ for Brompton tracer test 1.

The analysis of the water samples for Photine failed to record any elevation above background during the course of the tracer test. Of the 16 detectors one showed a faintly positive[26] result for Photine within the first 4 hours, which is thought to be a contaminated detector, and several detectors showed

[26] Refer to Table 4.4 for the scale of qualitative appraisal of passive detectors.

highly doubtful patches of fluorescence, which may also be a result of improper methodological procedures. However, one detector placed by a relatively strong discharge point at the western end of the spring showed a positive, rising to moderately positive, result between 6.5 and 25 hours. (The lower numbered detectors are to the west, the higher to the east).

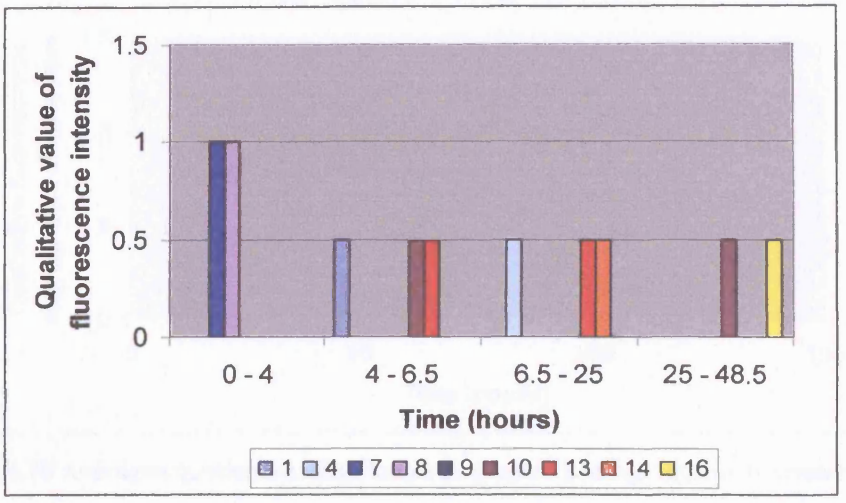

Figure 6.17 Passive detector results for Flavine from Brompton tracer test 1.

The Flavine passive detector results were largely inconclusive, with highly doubtful and doubtfully positive results from a number of detectors, and with no Flavine detected in the water samples taken. As the overall results were inconclusive the experiment was repeated.

6.2.5.3 Brompton tracer test 2

The second tracer test took place on the 18th Sept 2002, with larger amounts of the same dyes being injected into their respective boreholes (Photine shallow, Flavine deep). The amount injected was increased from 1.2 g to 39.2 g of active ingredient for each dye, and water samples were taken from the point at which the strongest observed positives had been taken in the previous test. The passive detection was reduced at Brompton Mill Pond (BMP), in order to focus on those discharge points considered the most likely to give a positive result, and extended to include a second set of springs that had begun to flow in the period between the two tests (those at Brompton Hall School (BHS)). (See Figure 2.19.) Passive detectors were changed at 6-hour intervals. Monitoring was also extended temporally to cover the six days subsequent to injection. During this time samples were taken every 1 hour for the first 36 hours, every 2 hours for the next 36, every 3 hours for the next 36 hours, every 4 hours for the next 24 hours and every 6 hours for the final 12 hours.

Unfortunately an error was made in the analysis of the passive detectors: the detectors for the first 48 hours were placed on white printer paper immediately prior to analysis and absorbed some blue fluorescent dye (optical brightener). Thus these detectors exhibit some additional fluorescence. The detectors subsequent to 48 hours do not share this problem, and the contamination was only with respect to Photine, not Flavine.

The results from the passive detectors were that no yellow fluorescence (Flavine) was observed on the detectors at all. Because of the contamination problem, an average of the qualitative value of fluorescence assigned to each detector is given for all detectors at the springs (Figure 6.18). The contaminated samples are shown as red dots, the uncontaminated as blue.

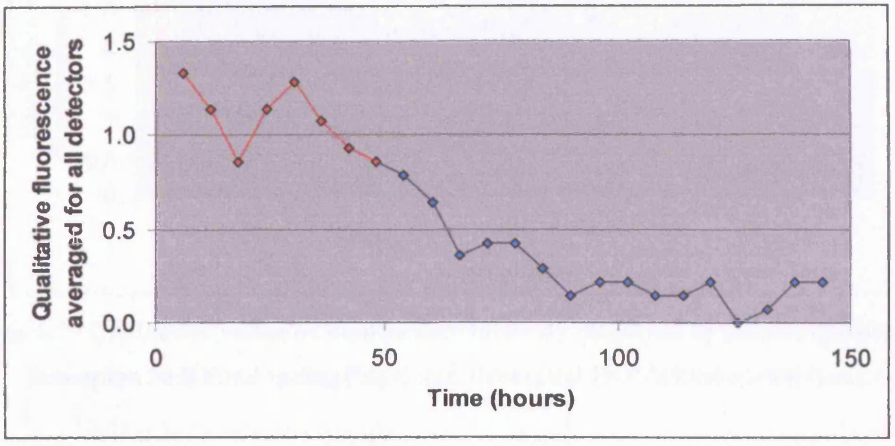

Figure 6.18 Averaged qualitative score for all Brompton Springs detectors, tracer test 2.

From Figure 6.18 it is clear that subsequent to 48 hours there is a steady decrease in the total amount of fluorescence observed across all of the detectors. This indicates that a positive tracer arrival occurred, and also that the magnitude of the contamination is small. This is because the peak values associated with the contaminated samples are not greatly higher than the first values of the uncontaminated detectors. It seems, therefore, that peak arrival occurs within 48 hours of injection. This pattern is supported by the water sample results. Again, no Flavine is detected but, although background levels for Photine are quite noisy, there is a definite increase in signal between 10 and 20 hours[27]. However, because of the non-definite nature of the results from this experiment, it was performed once again.

6.2.5.4 Brompton tracer test 3

For this tracer test Flavine was abandoned as time was short and no good positive result had been obtained from use of this dye. The mass of Photine CAQ was increased to 180 g (900 mL at 20% solution) of Photine CAQ and injected into the uncased section of the shallow borehole on the 2nd January 2003.

Over the following three days, Photine was detected at subjective scales of 2 or over during the peak tracer flow at all detector locations (see Figure 6.19). The strongest peaks were recorded at Brompton Hall School, which is the site closest to the injection borehole. The peaks at this site were recorded within 24 hours, whereas peaks at the BMP sites were distributed over the first and second 24 hour periods. It is clear that the peak of dye capture had passed by the third day, with detectors displaying reduced concentrations of dye by this time.

[27] Unfortunately this data is not available in detail for presentation in this thesis.

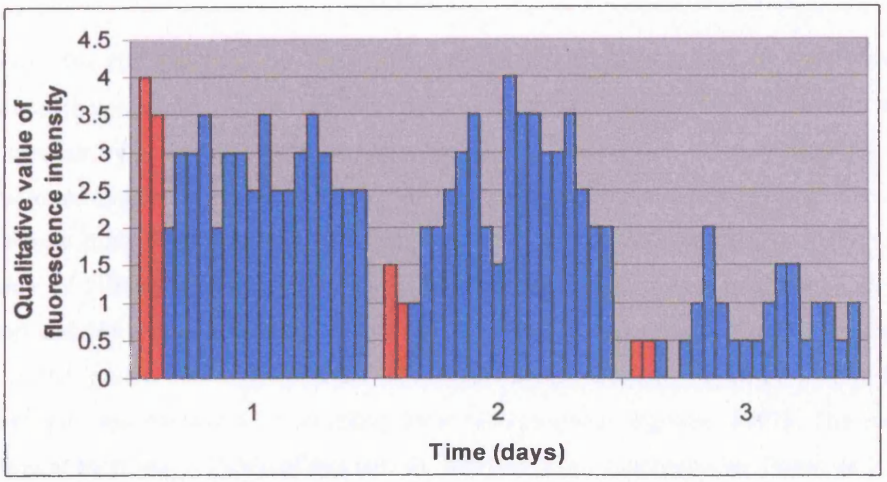

Figure 6.19 Qualitative values of fluorescence intensity displayed by passive detectors at Brompton Mill Pond spring (blue) and Brompton Hall School spring (red).

6.2.5.5 Summary of Brompton tracer tests.

The results from this series of experiments illustrate a clear connection between the shallow borehole and the springs. The swiftest arrival probably occurs within 12 hours, indicating a groundwater velocity of about 500 md^{-1}. Taking an average of all tests indicates that breakthrough occurs between 24 and 48 hours, implying an average groundwater velocity in the upper part of the aquifer (oolitic limestone) of about 125 md^{-1}. These velocities indicate that flow is occurring through fissures, which is confirmed by observation at Brompton Mill pond spring, where the water visibly exits along bedding plane fissures and vertical joints in the rock (see Plate 2.3).

6.2.6 TRACER TESTS CONDUCTED PRIOR TO THIS RESEARCH

6.2.6.1 1995 Bacteriophage test, Forge Valley to Irton preliminary tracer test.

The results from this experiment are given in the Corallian MODFLOW model files supplied by the Environment Agency (pers. comm. Environment Agency), on whose behalf the experiment was undertaken. The amount of bacteriophage injected is unknown, but hourly sampling showed that first arrival occurred between three and four hours, although concentrations were too high to be quantified. The peak remained above quantifiable limits (the maximum recorded value being 100 000 $pfumL^{-1}$) until twelve hours after injection, when they dropped by a factor of fifty and gradually tailed off to 120 $pfumL^{-1}$ at the end of the experiment, 23 hours following injection. These results are not presented graphically as subsequent tests are more informative.

6.2.6.2 1997 Bacteriophage test, Forge Valley to Irton and the Augmentation borehole

An estimated 1.0 x 10^{15} *Enterobacter cloacae* bacteriophage suspended in 10 L of water were injected into the swallowholes on the 13th of October, 1997 (Environment Agency, 1997). Samples were taken at hourly intervals by automatic water samplers stationed at Irton and at the Augmentation borehole. Irton was pumped at a constant 14.3 tcmd and the Augmentation borehole at 5.45 tcmd. The results are shown in Figure 6.20. First arrival at Irton was between 195 and 240 minutes, ascending to a peak concentration of 112000 pfu/mL by six hours. First arrival at the Augmentation borehole occurred between 495 and 540 minutes, although did not peak but maintained a variable concentration between 6500 and 10 000 pfumL^{-1} for the remainder of the test (which lasted a total of 23 hours). It was not thought that this was the result of sampling error (Environment Agency, 1997). The recovery of bacteriophage at Irton was c. 16.9% of that injected and that at the Augmentation Borehole 1.9%.

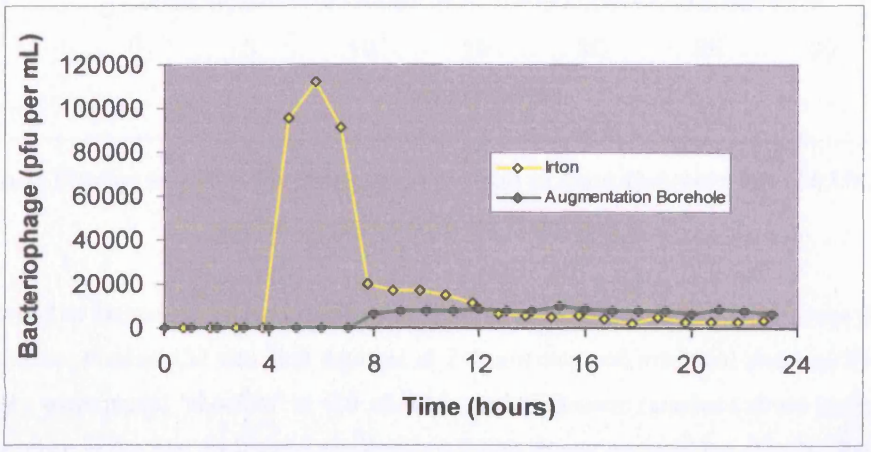

Figure 6.20 1997 UK Environment Agency bacteriophage tracer test between the swallowholes and the Irton and Augmentation boreholes.

6.2.6.3 1999 Photine CU and Bacteriophage test, Forge Valley to Irton and the wider aquifer.

The same wild strain of *Enterobacter cloacae* bacteriophage was chosen for this test, with 2.5 x 10^{15} phage suspended in 10 L of river water injected into the swallowholes on the 21st of October, 1999. This was performed in conjunction with the injection of 1.5 L of 20% concentration Photine CU diluted with a further 8.5 L of river water (ARUP, 2000).

Sampling was more intensive for this test, with a 15 minute interval at Irton for the first 24 hours, falling to daily and then several-daily intervals. Samples for bacteriophage were also taken at regular periods at Cayton Carr PWS, Cayton Station Road PWS, McCains, the Swallowholes borehole, the Augmentation borehole, West Ayton Quarry borehole, Derwent Ford borehole, Ratten Row borehole, Long Lane borehole and Cayton Bay springs. Passive cotton-wool detectors for Photine were installed in Irton Old Well and at Cayton Carr PWS, Cayton Station Road PWS, McCains, the Swallowholes borehole, the Augmentation borehole, West Ayton Quarry borehole, Derwent Ford borehole and in

Seavegate Gill borehole. BTCs measured at Irton, and scaled by peak height for comparison, are given in Figure 6.21.

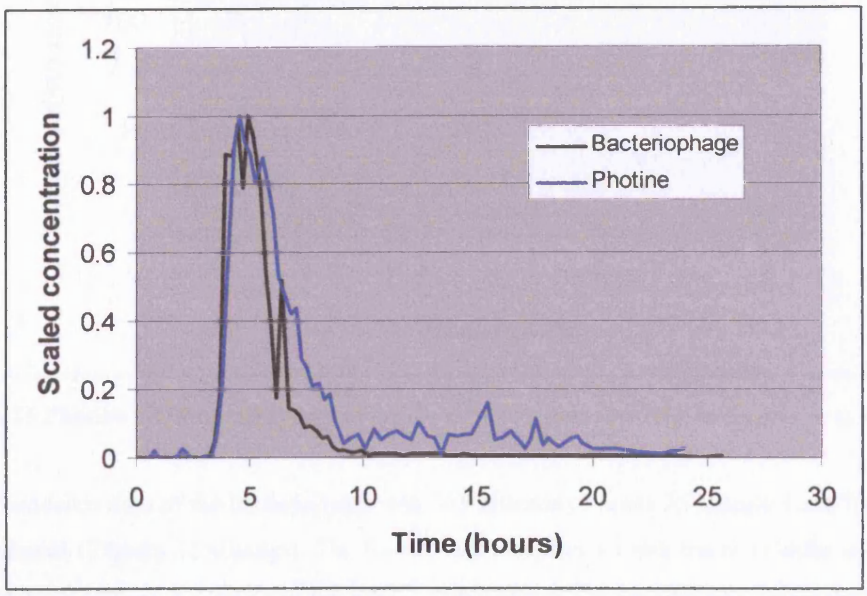

Figure 6.21 Photine and Bacteriophage breakthrough at Irton October 1999 (ARUP, 1999), scaled by peak height for comparison.

The first arrival of bacteriophage was detected at Irton at 190 minutes followed by peaks at 265, 295 and 385 minutes. Photine CU was first detected at 210 minutes and exhibited peaks at 270 and 330 minutes and a more muted 'shoulder' at 420 minutes. As both tracers remained above background for the samples taken in the first 24 hours these results are also shown on semi-log plots to illustrate BTC tailing (Figures 6.22 and 6.23). The tailing is more erratic in the Photine BTC as background fluorescence was relatively high compared to both peak and tail.

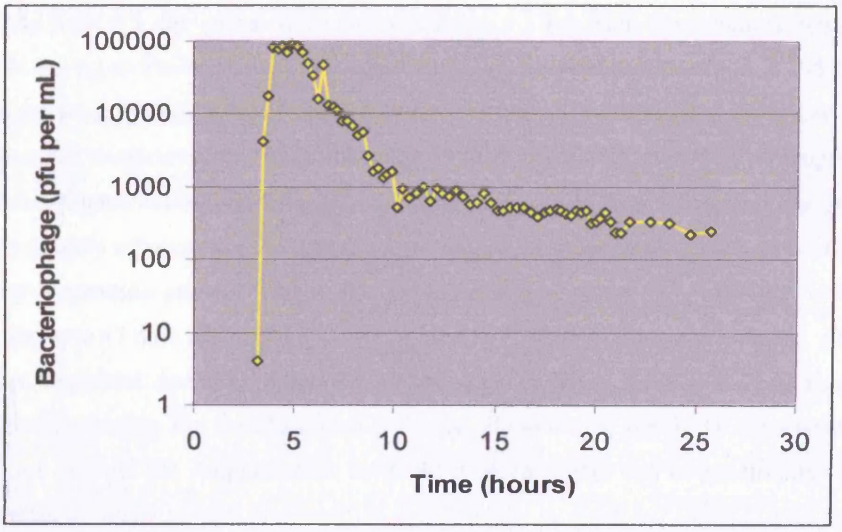

Figure 6.22 Bacteriophage breakthrough at Irton October 1999 (ARUP, 1999), semi log plot indicating tailing after 10 hours.

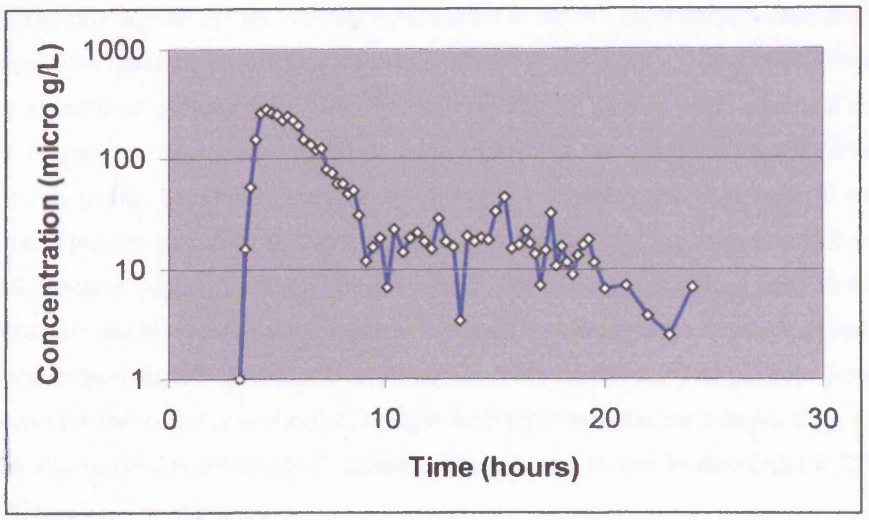

Figure 6.23 Photine CU breakthrough at Irton, semi-log plot showing tailing after c. 10 hours.

The mean residence time of the bacteriophage was 335 minutes (5 hours 35 minutes) and for Photine it was 453 minutes (7 hours 33 minutes). The former value implies a mean tracer velocity of 8.4 km d^{-1} whereas the latter implies a velocity of 6.2 km d^{-1}. Recovery of the Photine was 39.2% over 24 hours, but the bacteriophage recovery was only 5%. Bacteriophage are known to undergo sorption to silt and clay particles, so this may account for the losses, although the recovery from the 1997 test was nearly 17% when fewer bacteriophage were injected. Given that the pumping rate at Irton was approximately the same during both tests (c 14 tcmd), the discrepancy may lie in the difference in the volume of water entering the swallowholes. In 1997 this was approximately 0.014 $m^3 s^{-1}$, whereas in 1999 it was about 30 times greater, at c. 0.4 $m^3 s^{-1}$.[28] The visible turbidity of the Derwent is much greater during higher discharges.

In addition to Irton (east of the swallowholes) rapid tracer transport was observed to the south (at Derwent Ford, first arrival at 26 hours, peak at 4 days), to the west (at the Augmentation borehole, first arrival and peak < 1 day and at West Ayton Quarry, c 1 km from the swallowholes, first arrival and peak < 24 hours) and to the north (Seavegate Gill, passive detection positives at 2-5 days). These observations are strongly indicative of radial (but non-uniform) flow spreading the tracer plume in all directions from the swallowholes. Non-uniformity of flow is well-illustrated in a comparison of the results from the Augmentation borehole, with a response time less than a day, and the Swallowholes borehole immediately adjacent to it (c. 20 m) not showing a positive result until 8 days after injection, and then only a sporadic pattern. Tracer also persisted longer at the Swallowholes borehole, with positive results up to 47 days after injection, as opposed to 32 days in the Augmentation. ARUP (2000) consider these disparities due to poor connectivity between different fissures and less flushing of the system of fissures feeding the Swallowholes borehole. However, it should be remembered that the volumetric flow through the Augmentation borehole is much higher due to penetration of additional fissures at depth.

[28] The value of 0.014m^3s^{-1} is very low for the system – for all other tracer tests the value has been about 0.4m^3s^{-1}.

The results from this experiment are the only results prior to the SF_6 experiment to indicate the longer-term response of the aquifer to contaminant loading at the Forge Valley swallowholes. The monitoring of the 1999 experiment continued for 111 days at Irton and 49 days at other sites and consisted of replacement of photine detectors every week to ten days and sampling for bacteriophage. Passive Photine detectors (cotton wool) gave positive but gradually weakening results at Irton up until 42 days after injection. This was primarily from the pumped New Well (detectors placed at various levels in the Old Well indicated flowing fissures to be connected to the river and remained positive for 28 days). Detectors also gave positive results further east at McCains, indicating definite tracer arrival between 2 and 5 days and weaker signals up until 42 days after injection. At Cayton Carr positive detector results were recorded over the 7-15 day period (i.e. a single detector in position for 8 days). Both Cayton Carr and McCains also showed positive bacteriophage results between 10 and 15 days (ARUP, 2000).

6.2.7 SUMMARY OF SECTION 6.2

Section 6.2 has presented the main results from tracer test experiments conducted as part of this research. It has compared these with one another using some basic statistical concepts introduced for this purpose (see Table 6.1). The section has also reviewed in detail previous tracer experiments conducted from the same location as an aid to understanding the major experiment performed as part of this research, the SF_6 tracer test. In particular, results from the 1999 Photine and Bacteriophage tracer test reported by ARUP (2000) are central to developing a conceptual model of groundwater flow in the eastern Corallian and for strengthening the interpretation and appraisal of the SF_6 experiment (see next section).

6.3 INTRODUCTION TO MODELLING APPROACHES

6.3.1 INTRODUCTORY REMARKS

Section 6.3 introduces the modelling with respect to what the models are required to account for and the basis upon which decisions have been made regarding how best to implement them. The discussion begins with initial conceptualisation of the system and the requirements that modelling must meet in terms of specific observations in the field area. This leads to a basic network model describing some of the main observed elements. The benefits and limitations of this approach are then discussed and this is followed by a brief overview of processes likely to be operating on groundwater flow and tracer transport, in the eastern Corallian. Having presented the most likely processes to be affecting flow and transport the discussion then turns to the principles that have been followed when discriminating between processes for the purposes of modelling. In short, this section is an outline of the factors requiring consideration in the modelling and the logic behind the pursuit of certain models, and the order in which the subsequent analysis has been conducted.

Please note that all models used for the analysis of tracer breakthrough curves were written in Visual Basic and implemented in Microsoft Excel. All models were kindly supplied by Professor John Barker of UCL.

6.3.2 INITIAL SYSTEM CONCEPTUALISATION AND NECESSARY CONSIDERATIONS

6.3.2.1 Introductory remarks

This section identifies the prime considerations necessary for the production of a data-consistent model of the swallowholes-Irton-wider aquifer system. It draws upon previous work, in the forms of hydrochemical, abstraction and hydrological records, as well as tracer test data, and also the tracer test and geophysical data gathered during experiments made as part of this research. The central considerations identified are unified in terms of schematic diagrams. This section tightens the conceptualisation of the hydrogeology of the system prior to examining more theoretical models of system behaviour.

6.3.2.2 Contribution of river flow to pumped water at Irton.

A simple mixing model (Equation 6.5) based upon tritium, alkalinity and total hardness measurements for the River Derwent and the Irton Old and New Wells, under a variety of pumping conditions, may be used to determine the proportion of river water contributing to discharge from the Irton New Well. Results are given in Table 6.2.

$$ax + b(1-x) = c \qquad 6.5$$

Where a is the measured value of a river water component, b is the background aquifer value of that component, c is the value of the component measured at Irton, and x is the fraction of river water (consistent units).

Parameter	Date	River Derwent	Irton			Background (assumed)	Background Brompton	% River water
			New Well	Old Well 34m	Old Well 55m			
Tritium Units	22-23/4/1968	107	93	-	-	26	-	83
Tritium Units	22-23/4/1968	107	-	-	107	26	-	100
Tritium Units	22-23/4/1970	107	-	101	-	26	-	93
Alkalinity 1 (mg/L)	21/09/1981	84	106	-	-	-	215	83
Alkalinity 2 (mg/L)	16/10/1981	88	129	-	-	-	215	68
Alkalinity 3 (mg/L)	30/10/1981	90	95	-	-	-	215	96
Hardness 1 (mg/L)	21/09/1981	125	160	-	-	-	276	77
Hardness 2 (mg/L)	29/10/1981	131	186	-	-	-	276	62
Hardness 3 (mg/L)	30/10/1981	134	158	-	-	-	276	84

Notes:
1) Parameters numbered #1 were taken under normal pumping conditions at the start of the 1980 pumping test, i.e. 14 tcmd.
2) Parameters numbered #2 were the greatest values taken during the pumping test under maximum pumping conditions, c 26 tcmd.
3) Parameters numbered #3 are the values recorded at zero pumping after the water levels had recovered, i.e. Q = 0 tcmd
4) Brompton background values are averages from 1990 - 2002
5) The Tritium measurements were taken under steady pumping conditions of 13.7 tcmd

Table 6.2 Percentage contributions of river water to Irton abstraction for A) different fissures under the same pumping conditions and B) total abstraction under different pumping conditions, based on measurements of tritium (Tate *et al*, 1970), alkalinity and hardness (Barker and Courchee, 1981).

To use this model requires that a 'background' aquifer water be identified. For alkalinity and hardness values Brompton Spring has been chosen as a representative end-point of discharge from the aquifer. For tritium, background values in the aquifer are given as 26 TU by Tate *et al.* (1970), who took samples from a borehole at Seamer. Tritium in river water at 107 TU was also measured by Tate *et al.* (1970), some ten hours before sampling at Irton. The error associated with the tritium values is ± 10 %, whereas the error associated with the alkalinity and hardness data is unknown but probably small. The tritium samples were taken under conditions of steady, normal pumping (13.7 tcmd). Measured values for alkalinity and hardness were taken before, during and after the 1981 Irton pumping test (Barker and Courchee, 1982) and are presented to illustrate a potential range of values. It should be noted that, during the pumping test, the influx of water to the swallowholes was between 10 and 35% less than the discharge from the well, that is, the river had a low flow for the test. Based on average pumping rates and river losses (Aspinwall, 1994) the recharge to the aquifer from the swallowholes is usually about twice the discharge at Irton, so that the values derived from Barker and Courchee (1982) may not be representative of normal conditions. Generally speaking, however, the fundamental assumptions for the mixing model are that mixing occurs between a component of background aquifer water that is essentially well-mixed and constant over timescales of a few weeks; and that the other component is derived from rapid flow from the river. The results of the mixing model are given in Table 6.2 which,

in summary, shows that between 62% and 83% of the total water pumped at Irton was derived from the river at the times of sampling (exluding data from non-pumped, i.e. artesian, samples). This is one aspect of the system that needs to be accounted for in a data-consistent model. (Another is that the average pumping rate at Irton is, on average, 50% of river influx to the aquifer).

6.3.2.3 Flow in multiple fissures between the river and Irton.

Although an increase in pumping rate occurred during the May 2002 Fluorescein experiment (20 minute sampling interval, Figure 6.1), dual peaks are also notable on the 1999 Photine CU BTC, and even more so on the bacteriophage BTC (ARUP, 2000), both of which had a 15 minute sampling interval (Figure 6.21). The pumping rate was assumed to be steady during this test, but may have fluctuated. However, it is known that the average pumping rate during the 1999 test was different from that during the May 2002 test, so that dual-peaking may be inferred to be a function of multiple fissure pathways rather than pumping rate. The 1997 bacteriophage test (Environment Agency, 1997) had an hourly sampling interval so that temporal resolution may not have been sufficient to identify dual peaking. The sampling interval for the 2004 SF_6/Fluorescein test was about 30 minutes. The fluorescein BTC from this experiment (Figure 6.9) shows only a single peak, although this may be a function of very rapid injection (c. 3 minutes) and an elevated pumping rate, as well as the increased sampling interval. In contrast the SF_6, injected over a two-hour period, shows muted signs of multiple-peaking (Figure 6.7).

Further evidence supports the hypothesis of multiple flowing fissures operative between the swallowholes and Irton. This includes:

- Closed circuit television logging of Irton Old Well (Tate *et al.*, 1970)
- Vertical flow monitoring using a saline tracer and varying pumping rates, Irton Old Well (Tate *et al.*, 1970)
- Tritium analyses of different fissure waters within Irton Old Well (Tate *et al.*, 1970)
- Passive cotton-wool detector signals at different levels in Irton Old Well (ARUP, 2000)
- Indirect evidence from BHDT experiments.

The television logging, saline tracing and tritium work of Tate *et al.* (1970) on Irton Old Well, 45 m from the pumped New Well at which tracer breakthrough was measured, indicates two major flowing fissures, at 34 and 55 mbgl (the saline tracing, logging and lithological details are given on Figure 5.5). During the 1999 Photine tracer test ARUP (2000), passive cotton-wool detectors were placed at or near these fissures, with positive results of differing strengths. The cotton wool detectors also trapped silt, indicating turbulent flow between the river and the borehole. Tate *et al.* (1970) found that, under conditions of zero pumping at Irton (i.e. under natural gradient conditions), the inflow zone of greatest importance in the Old Well was the fissure in the oolitic limestones at 55 mbgl. However, when the New Well *was* pumping, it was the 34 mbgl fissure supplying the majority of water to the Old Well, with the lower fissure supplying only a small fraction (<10%) of the flow it supplied under natural

conditions. Moreover, with the New Well pumping, flow from both fissures travels *down* the Old Well (Tate *et al.*, 1970). These facts indicate that the New Well drains much of the flow in the fissure at 55 mbgl before it reaches the Old Well (which is marginally further to the east), but also that neither fissure is *directly* connected to the New well, because otherwise they wouldn't exhibit the influent tendencies observed while the New Well was pumped (i.e. a good connection would lead to flow exiting the Old Well via those fissures). The downward movement of water from both fissures is accounted for by Tate *et al.* (1970) with a hypothetical fissure connecting the Old and New wells at depth (the Old Well is partially blocked at c. 75 mbgl so that no geophysical measurements could be made beyond this point).

From the tritium and conductivity measurements (Tate *et al.*, 1970) and passive detectors (ARUP, 2000) it appears that the fissure at 55 mbgl transports solely river water, whereas that at 34 mbgl seems to deliver a component of background aquifer water (note that the river sinks in the Malton Oolite and the fissure at 55 mbgl is also in the Malton Oolite). The mixing model adopted suggests that water from the upper fissure contains 93% (±10%) of river water. In contrast, the water pumped from the Irton New Well contains 85% (±10%) river water (under the pumping conditions during sampling by Tate et al., 1970, which were 13.7 tcmd). On these grounds it appears that the Irton New Well derives additional water from a further fissure/fissure system fed by 'background' aquifer water.

In addition, although the measured tritium values for the fissures at 34 and 55 mbgl are within the range of uncertainty of each other (93% ± 10% and 100% ± 10% respectively), taking the figures at face value implies that the two fissures separate from one another *subsequent* to the swallowholes (and therefore subsequent to tracer injection) and that they do not rejoin thereafter until intersecting the Old Well. This must be the case[29] as otherwise it would not be possible for one fissure to retain its exact river water signature whilst the other does not. In other words, these fissure waters cannot both be diluted by background aquifer water prior to separating, as this would affect the composition of both and not just of one, as observed. Additionally, as the upper fissure is in the Upper Calcareous Grit, which is not present for 2/3 of the flowpath (Figure 2.6), for river water to get to this fissure it must be transported through vertical joints. Some of the main features of the above information can be summarised in the following diagram (Figure 6.24):

[29] On the strength of the data.

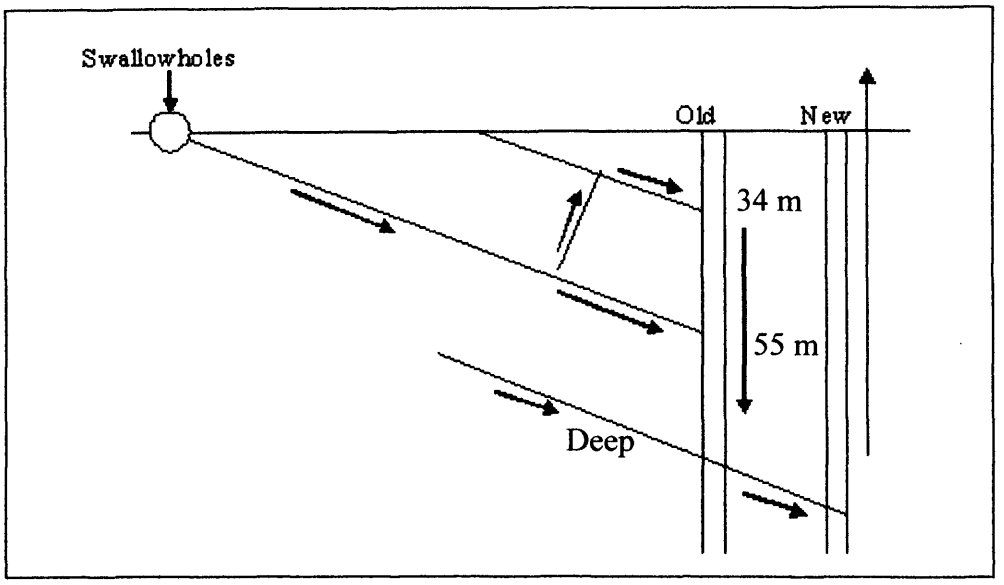

Figure 6.24 Schematic cross-section through the Irton wells showing intersection of bedding plane fissures and connection of bedding planes by joints (not to scale). Note that this schematic is only valid when the New Well is pumping.

The only problem with this representation (Figure 6.24) is that the New Well is in fact closer to the swallowholes than the Old Well (by about 45 m). On a two-dimensional diagram it is difficult to show that water travelling through the upper fissures *bypasses* the New Well before reaching the Old Well, from where it is then drawn downwards. This strongly indicates that, whilst laterally extensive bedding-plane fissures and lithological contrasts may be responsible for the majority of rapid flow (as observed in geophysical logging and borehole dilution tests – see Chapter 5), a degree of channelling within those bedding planes is highly likely. Additional evidence for this is given by Fox-Strangways (1892) in the quote given at the head of Chapter 2. So, whilst Figure 6.24 does not show fissures connecting the swallowholes directly with the New Well, the schematic is sufficient to show the relations between fissures at different levels in the two wells.

Following the above discussion, any model of the swallowholes – Irton – wider aquifer system consistent with the data must now account for the following:

- At least two rapid flowpaths, both capable of transmitting sediment, connecting the swallowholes with Irton.
- One rapid flowpath transporting solely river water.
- One rapid flowpath containing c. 6% of background aquifer water.
- Fissure channelling within particular horizons (namely at about 55 mbgl) is likely to account for a distribution of travel times.
- An additional fissure or fissures supply the Irton New Well with older, 'background' aquifer groundwater.

On top of these factors some additional considerations must be borne in mind:

- Under average conditions of river loss and abstraction, about 50% of the water entering the swallowholes is lost to the wider aquifer, with the other 50% being roughly equivalent to the volume that Irton pumps in 24 hours (from data given by Aspinwall and Co., 1994).
- A typical value of tracer loss is c. 50%.
- Some mechanism needs to account for BTC tailing.

A basic network model of the sort described by Atkinson *et al.* (1973) can be constructed on the basis of these considerations, and is shown in Figures 6.25:

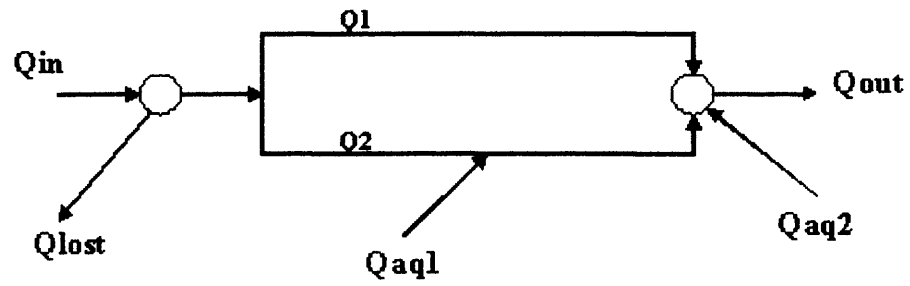

Figure 6.25 Basic network model of swallowholes – Irton – wider aquifer system.

In this model

- Qout = Q1 + Q2 + Qaq1 + Qaq2
- Qlost ≈ 0.5 Qin

The model represents most of what is likely to be happening on the basis of the assumptions and interpretations outlined in this and preceding sections. Q1 is a large, direct flowpath in the Malton Oolite; Q2 is a flowpath beginning in the Malton Oolite but traversing vertical jointing (upward) to join a flowing fissure in the UCG. Qaq1 represents the addition of background aquifer water to the Q2 flowpath. Qaq2 represents further background aquifer water contributing to the final composition of water pumped at the New Well. This may be derived from a fissure intersected only by the New Well, or from the deeper fissure noted in Figure 6.24, or from water entering an additional fissure between the swallowholes and Irton. Qlost represents water entering the swallowholes but not captured by Irton and is, on average, 50% of this leakage. Note that Qlost does not imply any particular mechanism, only a loss.

To make the network model at least semi-quantitative we can refer again to the model criteria (bulleted points) and average conditions. Here we see that Qlost = 50% of Qin, which is known. Qout is also known as it is the Irton PWS abstraction. The proportion of river water pumped under normal conditions is broadly constrained at c. 80% on the basis of three hydrochemical tracers (Table 6.2), so that Qaq1 + Qaq2 = 0.2 × Qout. The volume of river water present in Q1 and Q2 at any particular time may therefore be given by $V_{(Q1+Q2)}$ = Qout x (1 - 0.2) x dt, where dt is the mean residence time of the

tracers used on the system. The average mean residence time of the tracer tests presented in this chapter is 5.7 hours, so that if Qout = 14 000 m^3d^{-1} (a typical value) then the fissure system volume is calculated to be 2600 m^3.

6.3.2.4 Limitations of the network approach

The network model encompasses many of the bullet-points listed under 6.3.2.3. It may be visualised as a network of channelised and solutionally-enlarged fissures in which flow is turbulent, as it is capable of transporting silt-sized sediment. Moreover, as twigs and leaves are occasionally pumped at Irton at least one pathway is required to be on a centimetre scale. It is, therefore, a high-velocity network and as such is only relevant to flow and tracer recovery at Irton over the first 24 hours (or less) following injection.

However, there are some factors for which the simple approach adopted does not offer explanations. In particular it does not account for the degree of dispersion observed on BTCs over the first 24 hours, nor does it account for the extent or form of tailing following the passage of the main tracer peaks, and nor does it discriminate between tracer loss mechanisms when several such exist. To interpret the BTC as a whole requires consideration of a more elaborate set of processes than offered by the multiple-route network outlined above, although this does capture some important features. A consideration of these more elaborate processes, that is, a range of potentially operative processes, is offered in the next section.

6.3.3 PROCESSES POTENTIALLY AFFECTING GROUNDWATER TRACER TRANSPORT

6.3.3.1 Diffuse flow in a Darcian medium

The MODFLOW model (Aspinwall and Co., 1994) assumes laminar, Darcian flow throughout the part of the Corallian that it represents. It accounts for known rapid flow with corridors of high hydraulic conductivity (see Chapter 2) and is able to reproduce much of the variability in groundwater elevations and spring discharge observed, with caveats. It does not account for observed transport velocities. We may therefore consider the field situation to be one of a Darcian medium containing pipe-like structures (channelised fissures or solutionally enhanced conduits) as schematised in Figure 6.25. If this conceptualisation is most similar to the true case then we can expect any tracer breakthrough curve or pattern of breakthrough curves to reflect regional gradients or localised disturbances.

6.3.3.2 Hydrodynamic dispersion of tracers in a Darcian medium

Such dispersion is produced by meandering particles of water or tracer subject to velocity variations within pores and pore throats and the existence of multiple pathways (Domenico and Schwartz, 1998). These fluctuations in velocity, on the sub-continuum scale, lead to spreading of tracer particles (some moving faster than others). If the distribution of velocities is symmetrical about the average velocity,

then the longitudinal component of the dispersion will be Fickian[30] and which may be characterised by an average particle velocity and a dispersion coefficient describing the degree of spread of the tracer.

6.3.3.3 Hydrodynamic dispersion in pipe- or conduit-flow.

Due to shear forces in either laminar or turbulent flow, or to irregularities in conduit aperture, tracer will be subject to velocity variations as it moves along a pipe or conduit or fissure. If these are random they will also lead to a Fickian-type of dispersion. This is an advective process.

6.3.3.4 Sorption of tracer

If sorption is linear and rapid it will only act as a retarding mechanism, reducing apparent tracer velocity but not affecting a Fickian distribution of travel times (i.e. not leading to non-Fickian BTC tailing). However, the slowing-down of the tracer transport may allow other processes (such as diffusion into the rock matrix) to occur (which will be non-Fickian).

If sorption is non-linear or kinetically modified this can distort the slope of the BTC tail into a non-Fickian form, and lead to prolonged tailing. Irreversible sorption causes tracer loss.

6.3.3.5 Double porosity diffusion

Double porosity diffusion refers to transfer of mass between fissure and rock matrix via diffusion across the surface and into matrix blocks at times of high concentrations in fissures, and diffusion from the matrix back into the fissures once the concentration in the fissure has fallen below that in the matrix (e.g. following the passage of a tracer plume). It will produce non-Fickian tailing over a characteristic timescale determined by the apparent diffusion coefficient of the tracer, the porosity of the matrix and the fracture aperture (Barker *et al.*, 2000). As the timescale of the experiment may be less than that required for complete return of tracer to the mobile fissure water it can account for significant tracer losses. The characteristic timescale referred to is given by Atkinson and Barker (2001) as:

$$t_{cf} = \frac{(a/2\Phi)^2}{D_A} \qquad 6.6$$

Where

t_{cf} is the characteristic time for diffusion from fracture to matrix (T)

a is the fracture aperture (L)

Φ is the matrix porosity (Dimensionless)

D_A is the apparent diffusion coefficient (L^2T^{-1})

[30] The term 'Fickian' refers to proportionality between rate of transport of a quantity along a gradient and the gradient itself (Domenico and Schwartz, 1998).

6.3.4 DISCRIMINATION BETWEEN PROCESSES AFFECTING TRACER TRANSPORT IN THE EASTERN CORALLIAN

6.3.4.1 Summary of potential processes

The main aspects of the tracer BTCs that require accounting for are 50% tracer losses, BTC tailing and dispersion of the tracer within the first 24 hours.

50% tracer losses (on average) can be accounted for by a) Unequal strength in two poles of a dipole; b) Slowly reversible or irreversible sorption; and c) Double porosity diffusion.

Breakthrough curve tailing can be explained by a) The distribution of travel times between different flowpaths resulting from a dipole; b) Non-linear or kinetic sorption; and c) Double porosity diffusion.

Dispersion of the tracer within the first 24 hours can be explained by hydrodynamic dispersion along single or multiple pathways. Double porosity diffusion has insufficient time to operate given the centimetre size of the conduits expected[31].

6.3.4.2 Discrimination between processes

There is positive evidence for the existence of a dipole. The 1999 Photine tracer test provided strong evidence for radial flow centred upon the swallowholes. At Irton, flow is known to be moving toward the well from several directions, as proven by tracer movements in the Old Well and from the swallowholes. An extended pumping test on this well (Barker and Courchee, 1982) induced head changes in what was considered to be an oval cone of depression, with the long axes of the oval running east-west and extending up to 2 km from the well. The south-eastward regional gradient aspect that one may expect from a diffuse-flow (Darcian) medium with embedded conduit or pipe structures, is reflected in tracer arrivals at more distant locations, both south and east of Irton, in 1999 and in 2004. Because of the strong evidence in its favour, and because the dipole is potentially capable of explaining the features of significant tracer loss and extended BTC tailing observed during experimentation, it is the first theoretical model to be pursued for comparison with tailing.

A double porosity diffusion mechanism is equivalent to the dipole hypothesis in terms of explanatory power over tailing and tracer losses, but for which there is little additional evidence. Gresswell *et al.* (1998) examined diffusion of three different tracers (Fluorescein, Amino G Acid and Potassium Bromide) into blocks of Lincolnshire limestone (a rock similar to the Corallian, see Chapter 2). By modelling measured diffusion coefficients they found that the matrix would absorb only 5% of the tracer over the period of one day *if the concentration in the fissure was maintained.* As high concentrations are typically transitory during the experiments outlined in this chapter, it is unlikely that

[31] Briefly, if $a \approx 10^{-2}$ m, $\Phi \approx 0.1$ and $D_A = 10^{-10}$ m^2s^{-1}, then $tcf \approx 10^6$ s, or about 1 month.

double porosity diffusion into the matrix is responsible for the observed losses or tailing, although they could be contributory. On the other hand, diffusion may occur into immobile fracture waters, trapped within smaller, thinner, but frequent fissures. Double porosity diffusion is examined following comparison of a theoretical dipole with measured data.

Sorption as a mechanism for removal is not considered likely to have a major effect on SF_6, a particularly unreactive compound. The sorption studies that have been done with SF_6 are reviewed in Chapter 3. Volatile losses to the unsaturated zone may, however, be considerable, and this mechanism may be wholly or partially responsible for the low recovery of SF_6 (c. 15%). However, it cannot explain losses observed with dye or bacteriophage tracers. Bacteriophage are known to undergo sorption, which may account for both losses and tailing. This mechanism is therefore considered in comparison with the dipole and double porosity diffusion models.

Hydrodynamic dispersion will play a role regardless of the type of flow, whether it be through conduits, fissures or a porous medium. However, as it only accounts for spread of the tracer cloud and neither non-Fickian tailing or losses, it will be considered following the dipole and double porosity diffusion models.

6.4 CHARACTERISATION AND MODELLING OF A DIPOLE FLOW MODEL

6.4.1 INTRODUCTORY REMARKS

Dipole formulations have been presented by Da Costa and Bennett (1960), Hoopes and Haarleman (1965) and Grove *et al.* (1970). Such formulations typically describe a groundwater flow system in which injection and abstraction wells are situated in close proximity to one another. This is obviously analogous to the swallowholes - Irton flow system, although additional assumptions include a homogeneous, isotropic aquifer without a regional gradient, fully penetrating wells, recharge equal to abstraction and no dispersion along flowpaths. In this ideal case, pairs of flowpaths assume the form of circles of varying sizes intersecting both wells (Figure 6.26). The length of a flowpath depends upon its angle of exit from the recharging well, with the shortest flowpath lying along an angle of 180 degrees (i.e. a straight line connecting the wells) and the longest along an angle of 0 degrees (i.e. in the opposite direction to the abstraction well, although theoretically this flowpath is never recovered). The distribution of travel times is a function of the porosity of the medium, the distance between the wells, aquifer thickness and the pumping rate. If the effects of small-scale hydrodynamic dispersion are neglected, then it is the distribution of flowpath lengths that gives rise to the distribution of particle arrival times constituting a BTC. The purpose of Section 6.4 is to compare such a model with the BTC tailing observed in the SF_6 experiment. The mathematical formulation of the dipole model used for this comparison is given in the following section.

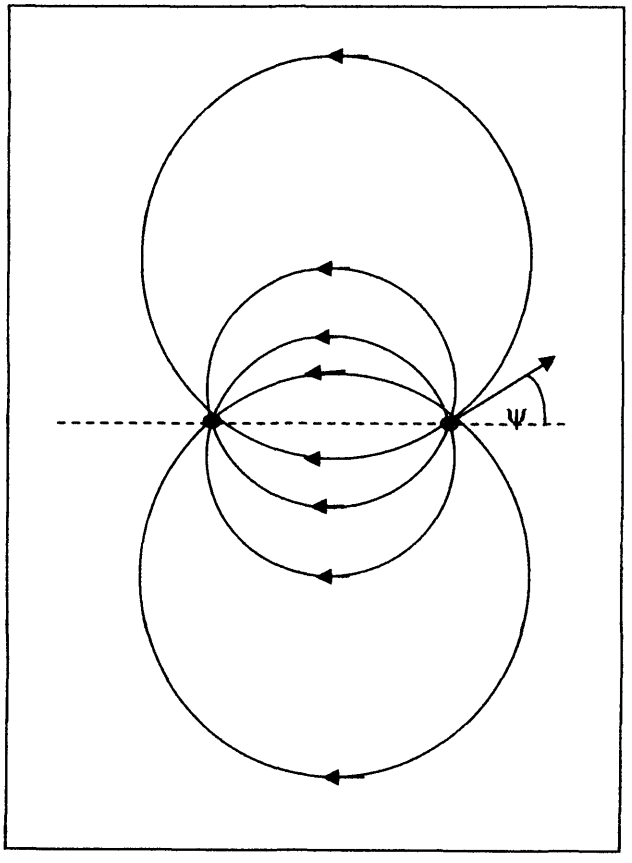

Figure 6.26 A dipole where ψ is the angle of departure from the recharging well in radians.

6.4.2 MATHEMATICAL FORMULATION OF A DIPOLE MODEL

The following mathematical model was constructed in Visual Basic for operation within Microsoft Excel.

Referring to Figure 6.26, the travel time for a particle leaving one well at angle ψ is given by

$$t_t(\psi) = t_b f(\psi) \qquad 6.7$$

where

$$f(\psi) = \frac{3(\tau^2+1)(\pi/2 + \tan^{-1}(1/\tau) + \tau)}{\tau^3} \qquad 6.8$$

and

$$\tau = \tan(\psi) \qquad 6.9$$

and

$$t_b = \frac{\pi\phi D^2 b}{3Q} \qquad 6.10$$

where

t_t travel time (T)
t_b is the breakthrough time (T)
D is distance between wells (L)
ϕ is porosity (Dimensionless)
b is aquifer thickness (L)
Q is the pumping rate for each well (L^3T^{-1})

As the angle increases from 0 to π the travel time decreases from infinity to t_b. Also, the amount of water exiting the recharge well in any direction over a given angular range is independent of the direction. The BTC consequent upon this configuration may then be given by the probability of arrival between t_t and $t_t + dt_t$., which is expressed as:

$$P(t_t) = \frac{1}{\pi \frac{df}{d\psi}} \qquad 6.11$$

From this information it may be calculated that, at late times (i.e. arrivals from flowpaths exiting the recharge well as ψ reduces from 180°), the slope of the breakthrough tailing approaches a steady -4/3 (Equation 6.12).

$$\lim_{\psi \to 0}\left[\frac{f(\psi)}{P(\psi)}\frac{dP/d\psi}{df/d\psi}\right] = \lim_{\psi \to 0}\left[-f(\psi)\frac{d^2 f/d\psi^2}{(df/d\psi)^2}\right] = -\frac{4}{3} \qquad 6.12$$

The recession of the BTC may then be formulated as $y = Ax^{-4/3}$ where A is a constant.

6.4.3 COMPARISON OF THE DIPOLE MODEL WITH THE SF_6 DATA

Figure 6.27 shows the data plotted as C/Cpeak vs. time together with the probability of arrival (P(tt)) vs. time as derived from the model.

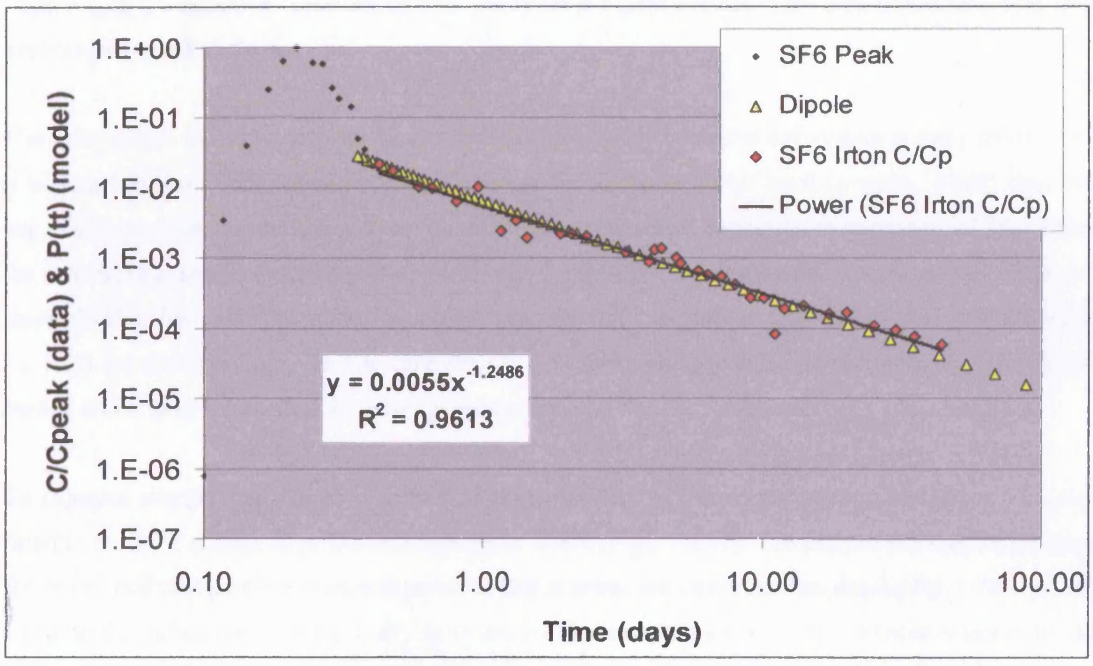

Figure 6.27 Comparison of dipole model with SF_6 BTC tailing at Irton.

From this comparison there is a strong similarity between the slope of the recession on the BTC tail and the theoretical tailing that would result from instantaneous injection of a tracer into an ideal dipole system. Using Excel it is possible to fit a 'Power' law to the data after t = 0.5 days, which gives $y = 0.0052x^{-1.25}$ which compares well with the theoretical slope stating that $y = Ax^{-4/3}$ as -4/3 = -1.333.

The model may be taken further with an examination of comparative recoveries (Figure 6.28). The idealised dipole system assumes 100% recovery so that for an effective comparison it is assumed that the total mass of tracer recovered in the experiment is 100%. This hypothetical recovery is shown by the red diamonds, whereas measured recovery is given by the blue triangles.

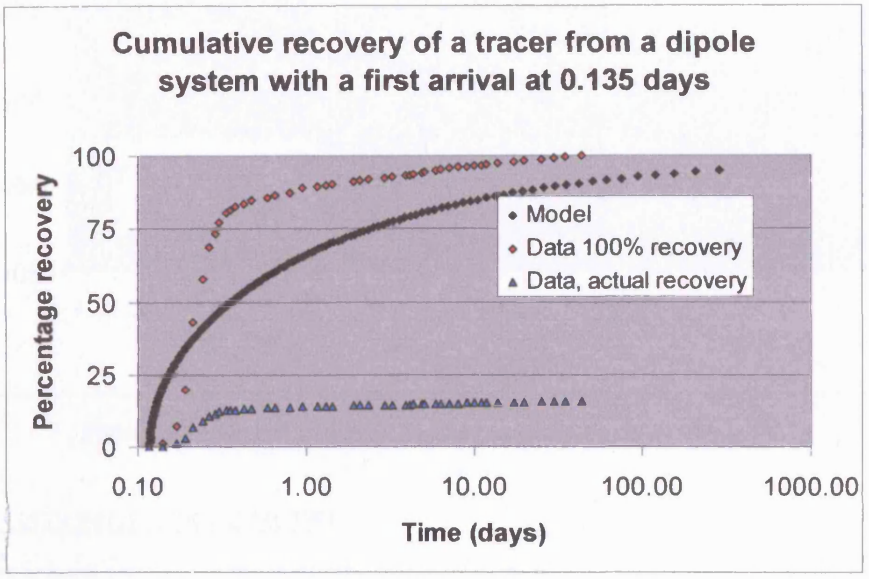

Figure 6.28 Cumulative recovery of a tracer from a dipole system with zero dispersion and first arrival (tb) at 0.135 days.

The comparison indicates that the dipole does not accurately represent the system at early times. This is unsurprising as neither does the dipole account for the presence of karst conduits, which lead to a very swift recovery of the majority of the total tracer recovered during the experiment. At later times the data and the model exhibits greater conformity, although the injected tracer accumulates in a more linear fashion than does the model. However, although this comparison is not as good as that shown by the P(tt) calculations, it is the late time data that is most important for comparison with the dipole model, and at later times there is some agreement.

To examine whether the dipole is truly a reliable characterisation of the system, the model was also fitted to the BTC measured at Derwentdale Farm North (Figure 6.29). The exactness of the fit between the model and the trendline is even superior to that at Irton, with the trendline displaying a 'Power' law closer to the theoretical -4/3, at -1.36. However, the Derwentdale Farm North borehole is not only 650 m west of Irton PWS and 1750 m SE of the swallowholes (i.e. in a significantly different location to the pumping well), but it is an unpumped borehole opened only for the purposes of sampling (it was artesian throughout the experiment). Its agreement with the dipole model, which should only describe tracer arrival at the pumped well, indicates that there are factors unaccounted for by the dipole but leading to similar breakthrough curve tailing. These factors are addressed in the following discussion.

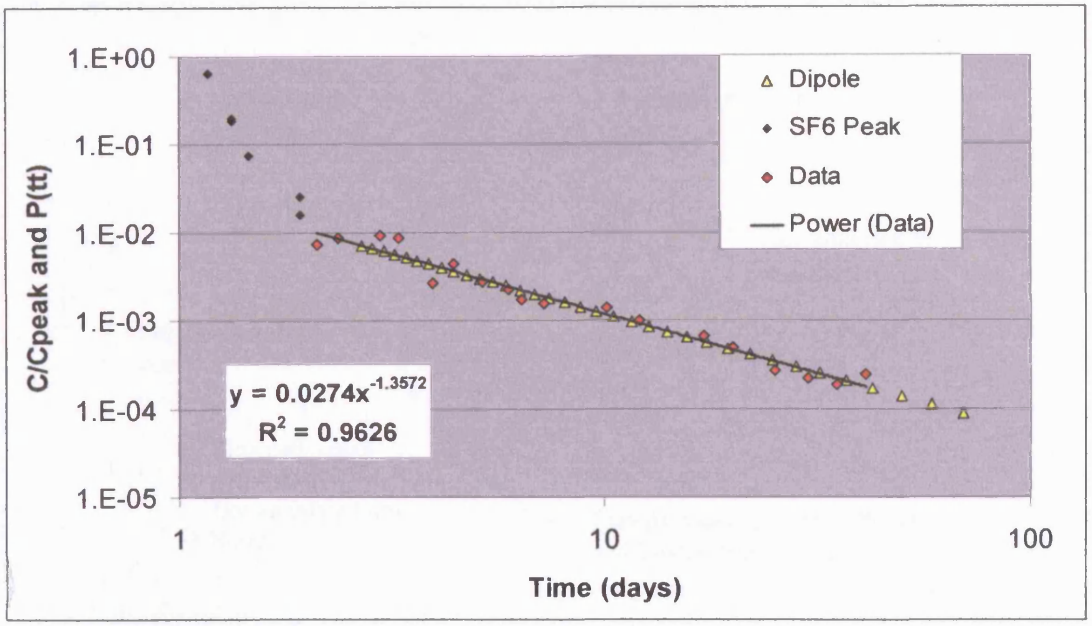

Figure 6.29 Dipole model fit to Derwentdale Farm North BTC.

6.4.4 DISCUSSION OF DIPOLE MODEL

In favour of the dipole conceptualisation of groundwater flow and transport between the swallowholes and Irton is the close match between the theoretical realisation of the dipole and the observed BTC data at Irton. On the other hand, the theory is for a symmetrical dipole in an homogenous flow field with zero regional hydraulic gradient and fully penetrating wells. The Irton borehole fully penetrates the aquifer, but the swallowholes are located at a particular horizon. Furthermore, the influx at the river Derwent is typically twice the abstraction: the average pumping rate at Irton over the period 1983 to 1993 was 17.3 tcmd, whereas the average loss to groundwater over same period was 0.4 m^3s^{-1} or 35 tcmd. The current abstraction record indicates similar abstraction rates, although at the time of the SF_6 injection flow gauging and abstraction records indicate that infiltration was 29.4 tcmd and abstraction was 18.6 tcmd, which is 63%, so that there was not equality between the dipole poles. Hydraulic conductivity is not uniform throughout the flow field either: the borehole dilution tests show higher Darcian fluxes close to the swallowholes and in the unconfined part of the aquifer, which is likely in part to be due to variations in permeability. It is probable that there is a higher permeability zone extending away from the swallowholes, due to chemically aggressive river waters dissolving the limestones and leading to increased fissure dimensions. Evidence for solutionally-enlarged fissures is found in several places, not least of which is the swallowholes themselves. Some constraint on the form of the dipole may also be expected from the position of the Ebberston-Filey fault and the unconfined part of the aquifer, which would serve to elongate and compress the dipole.

To some extent these departures from the simple dipole can be represented by a graphical flow-line model incorporating the known tracer connections, such as in Figure 6.30.

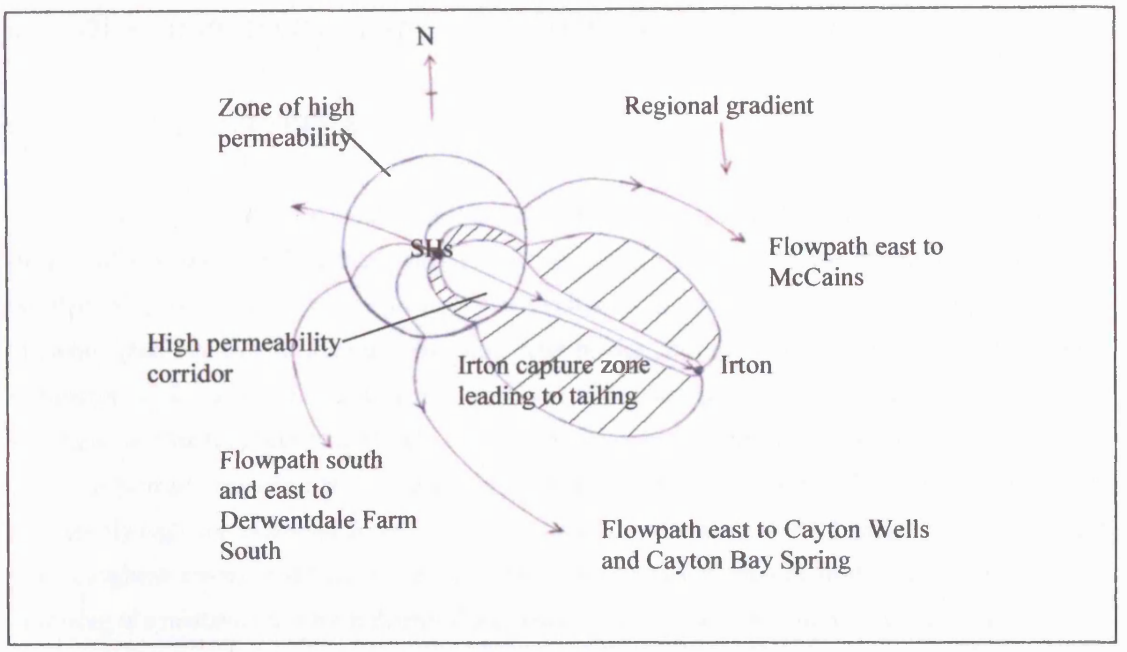

Figure 6.30 Conceptualisation of dipole flow field with local high permeability features and a regional gradient.

In this summary model, a high permeability corridor connecting the swallowholes with Irton and a higher permeability zone is centred on the swallowholes. With this conceptualisation the higher the hydraulic conductivity of the high-permeability corridor, the narrower it will be. The model also incorporates and indicates the role that refraction of flow lines may play when flow moves from an area of higher permeability to one of lower. The unequal dipole is represented by the 'hatched' area that will contribute to BTC tailing through longer storage time and thus the increased potential for double porosity diffusion. The high permeability corridor will control the form of the BTC over the first day.

In favour of *this* conceptualisation is that it can account for variable tracer recoveries at Irton by varying the relative strengths of the swallowholes source, the regional flow and the Irton sink. Tracer not recovered at Irton can either flow west or bypass the Irton capture zone and flow eastward, to be captured by one or other of the eastern wells or Cayton Bay spring. Thus, the recoveries at McCains, Cayton Carr, Cayton Station Road, Ratten Row and Long Lane, and the recovery at Derwentdale Farm *South* are all consistent with this model, as is BTC tailing.

However, whilst the above arguments combine to explain, in a qualitative way, tailing and tracer loss at Irton, they do not explain the tailing at Derwentdale Farm North, which has a slope of -1.36. Because of the position of this well on a single flow line, tailing *must* be due to either hydrodynamic dispersion and/or non-linear sorption and/or double porosity diffusion.

6.5 DOUBLE POROSITY DIFFUSION MODEL

6.5.1 INTRODUCTORY REMARKS

Double porosity diffusion has become increasingly recognised as a mechanism for the attenuation and storage of contaminants in groundwater since first being introduced to the literature by Coats and Smith (1964). The concept covers not only the division of an aquifer into matrix and fissure porosity, but more generally into flowing and stagnant water bodies (Brouyere *et al.*, 2000). The distinction is significant as, in an aquifer such as the Corallian that exhibits fracturing on several scales, major variations in lithology and karstic development, stagnant water bodies are not likely to be confined solely to primary porosity. Nonetheless, the principle is the same, being diffusion of solute from temporarily high concentration areas (flowing fissures/karst conduits) to low background concentration areas (stagnant water), and back again when the contaminant has been flushed from the fissure. The following is a mathematical formulation of the concept for comparison with observed BTC tailing.

6.5.2 MATHEMATICAL FORMULATION OF A DOUBLE POROSITY DIFFUSION MODEL

The concentration of a tracer (or other contaminant) at some distance (x) at any time (t) greater than the arrival time (ta) may be given by Equation 6.13. The equation is suitable for an instantaneous input and a single flowpath with matrix diffusion into an (effectively) infinite medium.

$$c_f = \frac{m}{v} c^I_{DP}(t, t_a, t_D) \qquad 6.13$$

Where:

m is mass of contaminant per unit cross-sectional area of fissure (ML^{-2})

v is velocity (LT^{-1})

C^I_{DP} (t, t_a, t_{cf}) is the concentration function (T^{-1}) given by:

$$c^I_{DP}(t, t_a, t_{cf}) = \frac{t_a}{\sqrt{4\pi t_{cf}(t-t_a)^3}} \exp\left[-\frac{t_a^2}{4t_{cf}(t-t_a)}\right] \quad t > t_a \qquad 6.14$$

Where:

t is time (T)

t_a is travel time (T)

t_{cf} is the characteristic diffusion time for a fracture (T) and is given by equation 6.6.

Parameters ta, m/v and t_{cf} may be fitted to the data to provide estimates of fracture aperture, given estimates of porosity and the apparent diffusion coefficient. This is achieved using the Solver routine in

Excel in the same way as used for the multi-component ADE modelling. Equation 6.14 has been put forward by Barker (1985), Maloszewski and Zuber (1985) and Atkinson *et al.* (2001).

The model is fitted to the data using the Solver tool in Microsoft Excel to minimise the sum of squares (residuals) between the model and the data. But, as the data has a large range of values, the model is biased toward the highest concentrations in the BTC, and will preferentially fit to the peak rather than the tail. By assigning weights (factors) to concentrations it was possible to achieve a crude parity between data points in the peak and the tail. For data points with concentrations between 0.01 and 0.1 ngL^{-1} the weight was 10000, for concentrations between 0.1 and 1 ngL^{-1} the weight was 1000, between 1 and 10 ngL^{-1} the weight was 100, between 10 and 100 ngL^{-1} the weight was 10, and for concentrations greater than 100 ngL^{-1} the weight was 1. Results presented are only the best-fit models.

6.5.3 RESULTS OF DOUBLE POROSITY MODELLING

At long times Equation 6.14 gives a power law response with a slope of –3/2, or -1.5. This is obviously closer to the Derwentdale Farm North data (at -1.36) than it is to the Irton data (-1.25). However, let us compare the model more closely with the data (Figure 6.31):

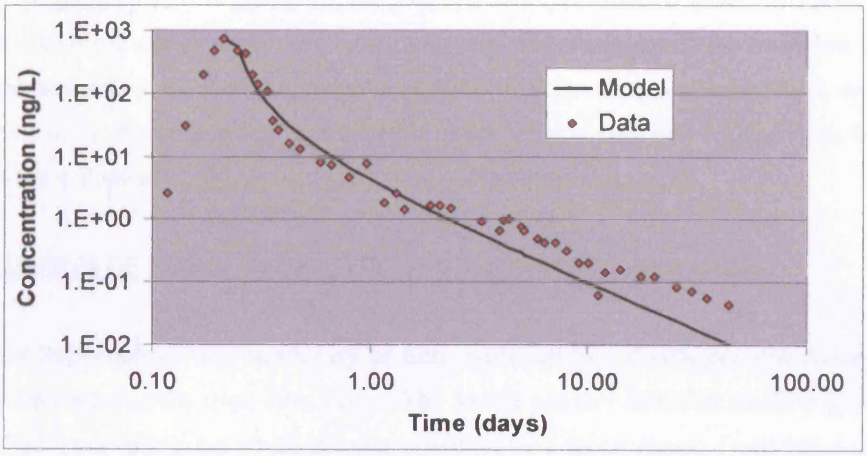

Figure 6.31 Dual-porosity model fitted to Irton SF_6 BTC.

The error in this model is measured by the root mean square error at 86 ppt, which is 11.5% of peak concentration. The model does not fit the rising limb of the BTC as it does not consider dispersion, and therefore the first arrival is essentially a sharp-fronted peak, but it does describe the peak and the immediately subsequent recession. It is obvious, however, that the tail of the measured BTC has a somewhat shallower slope than the model value; as noted above, after 0.5 days this is -1.25 for the data, as opposed to the model recession of -1.5, although the model only achieves this slope after about 3.5 days. This implies that retentive mechanisms additional to double porosity diffusion are operative within the aquifer. It may be that the inclusion of dispersion within this model would resolve the problem, although this has not been attempted. Also, the model only describes a single fissure, whilst it is certain that at least two are operative between the swallowholes and Irton. However, the effect of

incorporating additional flowpaths into this model is the presence of additional sharp peaks that are not observed in the data.

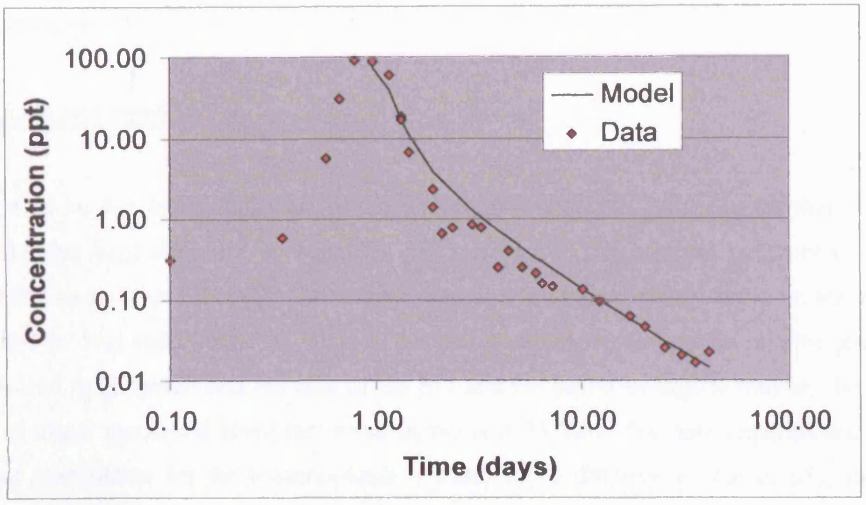

Figure 6.32 Dual-porosity model fit to Derwentdale Farm North SF_6 data.

For the Derwentdale Farm North borehole the model weighting was as follows: concentrations of 10-100 ppt are weighted by 1, 1-10 ppt by 10, etc. The best fit to the model (Figure 6.32) gives an RMSE of 19.3 ppt, which is 2.6% of peak value, much improved in comparison to the Irton data. The single fracture hypothesised by the model may be more realistic at Derwentdale Farm North and it can be seen that there is significantly greater agreement between the later data and the model. In fact the data *after* 7 days has a slope of -1.49, almost exactly that of the theoretical model.

6.5.4 DISCUSSION OF DOUBLE POROSITY DIFFUSION MODEL RESULTS

The tailing at Derwentdale Farm North may be fully explained by a double porosity diffusion model, due to the coincidence of the slope after 7 days. The double porosity diffusion model is also similar to the slope of the Irton tailing, but which is better explained by a dipole model. From this it appears that either the two tails (Irton and Derwentdale Farm North) observed have different causes, or both mechanisms (dipole flow and double porosity diffusion) are contributing. As both mechanisms produce what are similar slopes at large time (-4/3 for the simple dipole and -3/2 for double porosity) they cannot be easily distinguished on the basis of slope alone. However, the fraction of the tracer in the tail is less than 5% of the total tracer recovered at Irton, so that it is only this part of the tracer plume that is likely to be affected by double porosity effects, because along the main flowpaths apertures will be such that tcf is greater than 1 day. Outside of the enhanced permeability zone hypothesised in Figure 6.30, travel times are enlarged and fractures are potentially smaller (river waters beginning to approach equilibrium with the limestones with distance from the swallowholes, see Chapter 2), so that tcf will fall below observed tracer travel times (days) and double porosity diffusion becomes an effective tailing mechanism. This, together with the observation and modelling study performed by Gresswell *et al.* (1998) (discussed above) means that double porosity diffusion does not provide an explanation for much tracer loss, but can account for some of the observed tailing.

6.6 SORPTION AND VOLATILISATION

This section briefly discusses those losses that cannot be explained by reference to a dipole with poles of unequal strength.

6.6.1 VOLATILISATION OF SF_6

SF_6 losses may be due to volatilisation of the tracer upon injection. Evidence for this is offered, in particular, by the large disparity between the SF_6 recovery (15%) and the recovery of fluorescein injected at the same time (76%). In 1999 there was also a large disparity between the recovery of bacteriophage (c. 5%) and Photine (c. 40%) in the first 24 hours. However, the relative proportions of tracer recovered in the peaks and the tails of the SF_6 and the bacteriophage is roughly the same, with over 90% of tracer recovered being recovered in the first 24 hours for both experiments. Whilst the primary loss mechanism for the bacteriophage is likely to be different to that of SF_6, there is little difference in the behaviour of the remaining volatile and non-volatile tracers. This indicates that tracer losses in the case of SF_6 are likely to be due to volatilisation during injection and infiltration, because such losses would affect later components of the plume equally.

6.6.2 SORPTION OF BACTERIOPHAGE

Bottrell *et al.* (2000) measured typical pore throat sizes in the Oolites of the Lincolnshire limestone to be 0.3 μm with typical pore sizes 1 – 2 μm. An upper limit on pore throat size was placed at c. 1 μm. Bacteriophage, on the other hand, are typically between 0.1 and 0.3 μm and have a high molecular weight. It would seem, therefore, that the size of the pore throats may just be large enough to admit bacteriophage. However, the difference is not large and it is likely that bacteriophage could not enter pores without first coming into close contact with mineral surfaces, making sorption a more likely process. It should also be recalled that the river brings a lot of sediment into the aquifer, so that the potential surface area for sorption is much greater than just the surface of fissures. Due to the very rapid rate at which bacteriophage were lost following injection (in 1999), in comparison to Photine, it is not thought that diffusion into the matrix is a major factor, so that sorption is therefore the favoured explanation.

This mechanism, however, does not explain the observed dispersion in the BTC. In fact, close inspection of Figure 6.21 indicates that bacteriophage dispersion is considerably less than Photine dispersion, so that the bacteriophage is biased toward faster flow paths. Assuming that the two simultaneously injected tracers flow along the same fissures suggests that those bacteriophage approaching the walls of channels (where the presence of the slowest flowpaths lead to enhanced dispersion) become preferentially removed from the flow. The dispersion of tracers within the first 24 hours is not explained by either a dipole or a double porosity model, neither of which consider hydrodynamic dispersion at all.

6.7 HYDRODYNAMIC DISPERSION OF TRACER PLUMES BETWEEN THE SWALLOWHOLES AND IRTON DURING PASSAGE OF THE MAIN BTC PEAK.

6.7.1 INTRODUCTORY REMARKS

Following determination of likely causes of tracer loss and tailing, it remains to consider the form of the tracer breakthrough curves during the passage of peak concentrations at Irton. This examination returns to a network model of the system in which multiple pathways each contribute a component of the breakthrough curve. This therefore fits with the conceptualisation of the whole system as fissures/conduits embedded in a Darcian medium, and which has permitted explanation of BTC tailing and losses through a dipole realisation incorporating regional gradients and the potential for double porosity diffusion, sorption and volatilisation. The examination of the final component, hydrodynamic dispersion, utilises an advection-dispersion model capable of determining the contributions to a single (measured) BTC from multiple (hypothetical) BTCs arising from multiple pathways between the injection and recovery points in the aquifer.

6.7.2 DESCRIPTION OF THE MODEL

Equation 6.15 is a one-dimensional, non-radial, Fickian advection-dispersion equation describing the BTC with 4 variables: flowpath length, travel time to peak (equivalent to centre of mass in a Fickian system), the longitudinal dispersion coefficient and the initial mass per unit of system discharge (i.e. that through an individual conduit or fissure). It is written in Visual Basic for implementation in Microsoft Excel.

$$C_t = \frac{M_Q}{\sqrt{4\pi t_d t}} \exp\left[\frac{-(t-t_a)^2}{4t_d t}\right] \qquad 6.15$$

Where:

C_t = concentration at time t (ML^{-3})

M_Q = mass per unit discharge (MTL^{-3})

t = time (T)

t_a = x / v = Advective travel time (T)

x = Flowpath length (L)

v = Average tracer velocity (LT^{-1})

t_d = D / v^2 (T)

D = Longitudinal dispersion coefficient (L^2T^{-1})

The equation is fitted to the data using the Solver tool in Microsoft Excel, to minimise the sum of squares of the residuals between the data and the model, by changing the values of the parameters M_Q, x, t_a and t_d. However, it is necessary to give the model some idea of where to begin, as there is no guarantee that the minimum sum of squares it has found represents a 'global' rather than a 'local' minimum. Thus, by assigning values to the four variables close to what one may expect, for example 2000 m in the case of the length of the flowpath, one can approximate the results by eye before running the Solver tool. In this way one may at least approach the 'global' minimum. Convergence in the model occurs when successive iterations produce less than a change of 0.0001 in the sum of squares, which is sufficient accuracy when values are always greater than 1 (as they are).

In the model the *flowpath length* is set to 2000 m as an approximation of the distance between the swallowholes and Irton. This accounts for very little tortuosity which, for solution conduits, usually means an actual travel distance between 1.3 and 1.5 times the straight-line distance (USEPA, 2002), but as there is no information on this parameter a starting point 50 m greater than the straight-line distance has been used for convenience. The a*dvective travel time* is the time to peak and is easily fit by eye for a starting approximation. M_Q is the mass necessary to cause a peak of a certain magnitude under the discharge conditions specific to a single flowpath. Although there is only one correct value for injected mass, M_Q may have different values for each flowpath depending upon the completeness of tracer mixing in a volume of groundwater prior to that volume diverging along different paths. It is not unreasonable to assume a well-mixed volume prior to splitting, as not only does mixing appear to occur prior to entry into the ground (in the 'sump' structures built around the swallowholes), but also because the main split between the oolitic limestone and the UCG cannot occur until almost 2/3 of the distance to Irton (as discussed in Section 6.2). It is therefore reasonable to assume a single M_Q value. Multi-component models are therefore constrained to maintain equal M_Q for all flowpaths. The *longitudinal dispersion coefficient* is 'a measure of the rate at which a concentrated tracer mass spreads out along a flowpath' (Mull *et al.*, 1988) and can be defined as 'half the temporal rate of change in the variance of the tracer cloud' (Fisher, 1968). In the model it essentially controls the degree of spread of the component peaks, and in the first instance is fit by eye to the measured BTC. Vertical and horizontal dispersion also occur within the aquifer but they are less significant than dispersion along the length of the flowpath as they are likely to be limited by flow channel dimensions.

As discussed in relation to the double porosity model, the Solver routine attempts to minimise the sum of squares of residuals between the model curve and the data point, so that the model is biased toward the highest concentrations in the BTC. To counter this a weighting system was used, and which is given in the Table 6.3 (note the SF_6 weights are the same as those used for the double porosity diffusion model).

Data value >>	0.01 - 0.1	0.1 - 1.0	1.0 - 10	10 - 100	100 - 1000	1000 - 10000	10000 - 100000
BTC							
Bacteriophage 99	-	-	-	-	100	10	1
Photine 99	-	-	-	10	1	-	-
Fluorescein 2002	-	-	100	10	1	-	-
Fluorescein 2004	-	-	100	10	1	-	-
SF6 2004	10000	1000	100	10	1	-	-

Table 6.3 Weighting factors assigned to impart equality between high and low concentration data points.

This method is crude but at least addresses the problem positively. However, the associated problem of bias toward those parts of the curve containing more frequent data has not been addressed, but is considered to be less of a problem as there are usually more data points in the tail (with greater sampling intervals) than in the peak (with fewer points but shorter intervals).

6.7.3 RESULTS FROM MULTI-COMPONENT ADVECTION-DISPERSION MODELLING.

6.7.3.1 Model performance

The following graphs (Figures 6.33 to 6.35) are all based on modelling the May 2002 Fluorescein tracer test, chosen to exemplify the modelling output. The variables used to describe this model, together with output from 1 to 3 – component models for all modelled experiments, are given in Table 6.4.

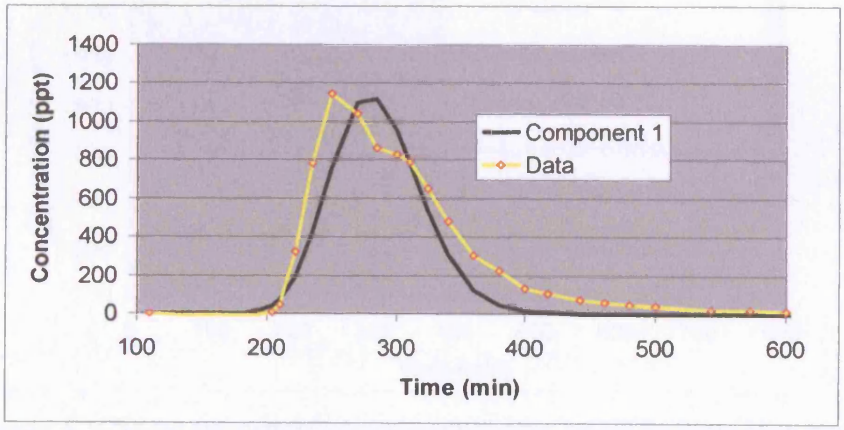

Figure 6.33 Single-component advection-dispersion model fitted to the May 2002 fluorescein BTC at Irton.

The fit of the model to the data for the single-component model (Figure 6.33) is given by the root mean square error (RMSE) at 147 ppt. As a comparative statistic between models this value is 12.8% of peak height. The model fails to capture the sharp front of the BTC, the arrival time of the peak, or the observed tailing.

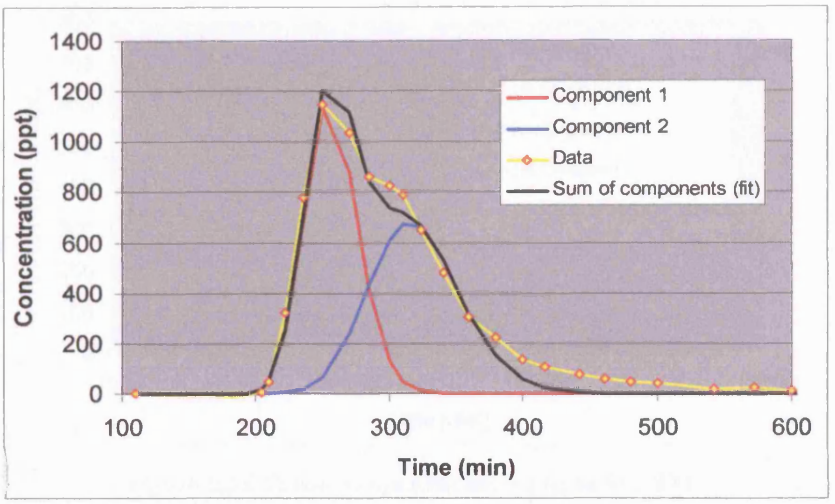

Figure 6.34 Two-component advection-dispersion model for Irton May 2002.

The two-component model (Figure 6.34) has an RMSE of 70 ppt or 6.1% of peak height. It manages to capture the peak quite well, and also reflects the secondary 'shouldering' peak, but does not capture the observed tailing. The addition of a third component (Figure 6.35) gives a model that also matches very well the front of the BTC but is even more satisfactory in reproducing the secondary peak, the recession of the BTC peak, and the tail of the curve up until it approaches background levels of fluorescence. The error in the three-component model is 24 ppt or 2.1% of peak height.

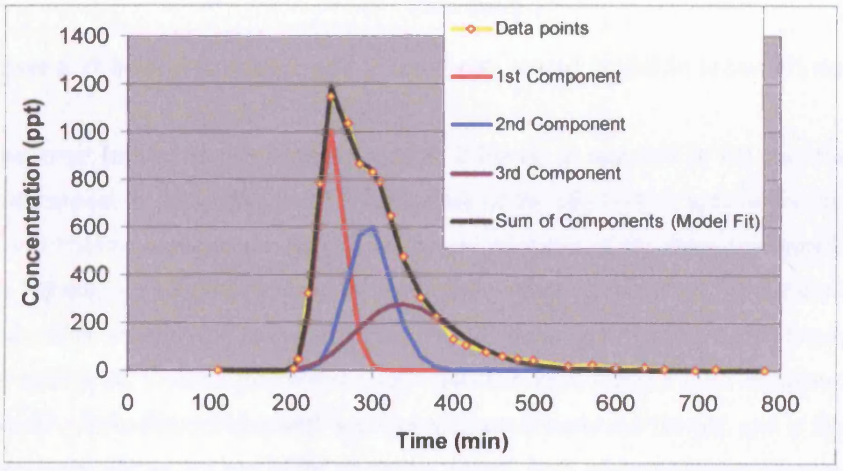

Figure 6.35 Three-component advection-dispersion model for Irton May 2002.

By way of comparison, Figure 6.36 also shows a three-component model, this time of the SF_6 BTC. In this case, however, the third component does not offer any significant improvement to the fit of the peak (RMSE = 59 ppt for the 2-component model and 51 ppt for the 3-component model), although it does address tailing. This is seen in Figure 6.37, which is the same model with a logarithmic y axis.

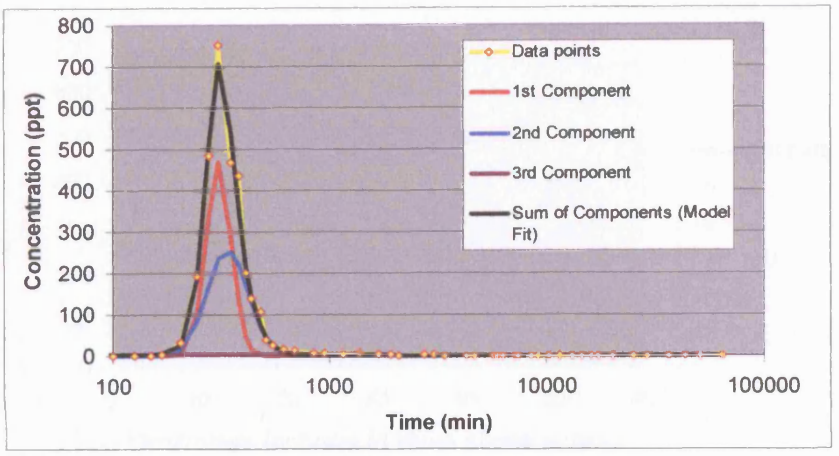

Figure 6.36 Three-component model fit to SF_6 BTC.

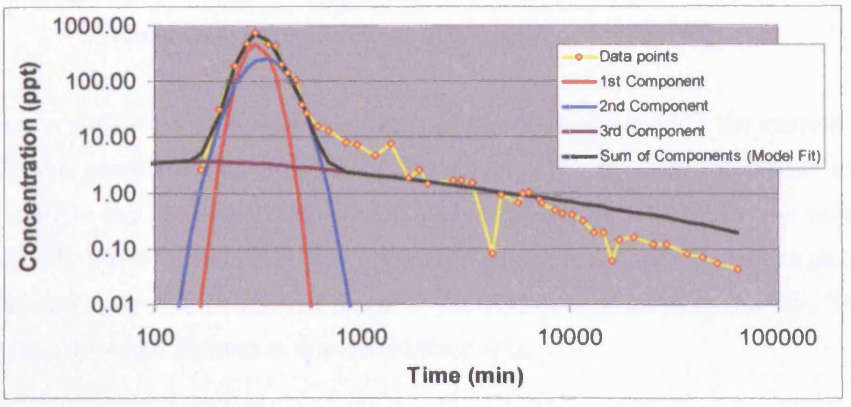

Figure 6.37 Semi-logarithmic plot of three-component model fit to the SF_6 data.

The SF_6 experiment had a tracer injection period of 2 hours, as opposed to the instantaneous input assumed by the model. It is possible that the main peak of the SF_6 BTC is more uniform than for the Fluorescein and Photine experiments for this reason, as injection of the dyes conformed much more closely to an instantaneous input. Evidence of multi-channelling on the SF_6 BTC is therefore likely to be 'smoothed out' in comparison to the dyes and bacteriophage (see Section 6.2). However, this is a matter of the main peak, whereas the central insight obtained from fitting a third component to the SF_6 data is that an advection-dispersion model does not adequately represent the tail, and in fact it does not *need* to represent the tail, as this part of the curve has already been addressed using other models.

6.7.3.2 Model sensitivity

One measure of the sensitivity of the model to individual parameters is shown in Figure 6.38. The sensitivity is shown as the RMSE as a function of ten-percentile increases in individual parameters, starting from the optimum solution as determined by the Solver tool. Each parameter is varied whilst the others are kept constant at their optimum values. The values are from a single-component model (Fluorescein 2002), but reflect the relative sensitivity of all models as they all formed of such individual components.

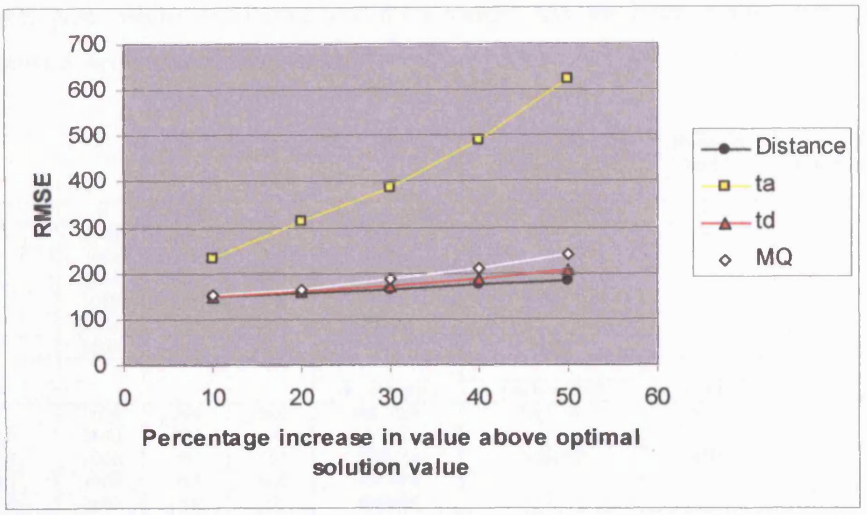

Figure 6.38 Sensitivity of a single-component ADE model to changes in individual parameters. (Data from the Fluorescein 2002 tracer test modelling).

The sensitivity to travel time is unsurprising given that this parameter controls the position of the peak and therefore the general overall position of the model BTC. In multi-component models such simulations indicate that the travel time of the first component is still by far the most dominant parameter, with the travel time of the second component being the next most important parameter. The parameters M_Q and t_d control the size and shape of the BTC as opposed to its position. There is very little sensitivity to flowpath distance as this is subsidiary to ta.

6.7.3.3 Model output

Table 6.4 gives the best-fit parameters for 1-, 2- and 3-component models for three dye tests, one bacteriophage test, and the SF_6 test. The left-hand column of the table refers to the experiment modelled, the number of components in the model, and which of those components the row refers to (for example, 'F2002 3.2' refers to the May 2002 Fluorescein experiment, the three-component model, and the second component). The 'Sum M_Q all components' column sums M_Q for all components of a single model for a comparison of total mass required for the whole model, which is generally the same between the 1-, 2- and 3-component models.

Excluding the SF_6 model, the table shows that, in three out of the remaining four experiments, a three-component model offers considerable improvement over a two-component model (see also Figures 6.34 and 6.35). For the 2004 Fluorescein experiment a third component does not significantly improve the fit, primarily because the peak is quite symmetrical without the 'shouldering' elements seen on other BTCs (Figure 6.9). It therefore appears, on the basis of three out of four models, that a three-pathway model provides a better description of hydrodynamic dispersion in the main peak than does a two-pathway model. However, common to the models are the relative shapes of the components, with the first component typically faster and less dispersed than the second or third components, suggesting

a more direct path, whilst the second and third components are more diffuse, being potentially transitory between the main peak and the tail.

BTC	x	ta	td	MQ	Sum MQ all components	Model fit RMSE	RMSE as a % of peak value
	m	mins	m	mg mins/m3	mg mins/m3	ppb	
Phot 1999 1	2000	320	45.7	45702	45702	46	16.1
Phot 1999 2.1	1998	280	17.3	23709			
Phot 1999 2.2	2014	380	30.8	23709	47418	19	6.7
Phot 1999 3.1	2000	265	8.6	15984			
Phot 1999 3.2	2000	329	10.6	15984			
Phot 1999 3.3	2000	411	25.8	15984	47952	9	3.2
				pfu mins/m3	pfu mins/m3	pfu	
Phage 1999 1	2078	294	26.4	10877800	10877800	9123	10.1
Phage 1999 2.1	2000	269	14	5980434			
Phage 1999 2.2	2000	337	32.5	5980434	11960868	6680	7.4
Phage 1999 3.1	2000	163	12.6	4041603			
Phage 1999 3.2	2000	219	10	4041603			
Phage 1999 3.3	2000	275	53.5	4041603	12124809	4163	4.6
				µg mins/m3	µg mins/m3	ppt	
F2002 1	1889	281	14.1	146311	146311	147	12.8
F2002 2.1	2000	255	6	58085			
F2002 2.2	2065	317	11.9	58085	116170	70	6.1
F2002 3.1	2000	250	4.5	41910			
F2002 3.2	2000	296	8.6	41910			
F2002 3.3	2000	342	32	41910	125730	24	2.1
				µg mins/m3	µg mins/m3	ppt	
F2004 1	1996	223	38	263142	263142	112	4.8
F2004 2.1	2000	217	24.1	151209			
F2004 2.2	2000	252	118	151209	302418	59	2.5
F2004 3.1	2000	193	15	97836			
F2004 3.2	2000	238	10.3	97836			
F2004 3.3	2000	292	109.4	97836	293508	51	2.2
				µg mins/m3	µg mins/m3	ppt	
SF6 1	2001	323	33.7	98091	98091	42	5.6
SF6 2.1	2000	313	17.7	49554			
SF6 2.2	2000	343	54.4	49554	99108	36	4.8
SF6 3.1	2000	311	17.9	48640			
SF6 3.2	2000	345	48	48640			
SF6 3.3	2602	3304	28430	48640	145920	30	4.0

Table 6.4 Fitted model parameters for the multi-component modelling of 5 BTCs measured at Irton following tracer injection into the swallowholes.

6.7.4 SUMMARY OF ADVECTION-DISPERSION MODELLING

A multi-component advection-dispersion model, employing the Solver tool in Microsoft Excel to minimize the sum of squares of residuals between model and data, has been used to account for the form of the main BTC peaks at Irton. It satisfies a number of observations regarding the hydrochemical composition of water entering the Irton Old Well (implying multiple routes), as well as multiple-peaking on BTCs, and is consistent with a wider conceptual model of flow in the eastern Corallian that includes a geohydrological dipole and double porosity diffusion.

6.8 FURTHER DISCUSSION

6.8.1 INTRODUCTORY COMMENTS

This section will present some further analysis of the data in terms of the general behaviour of the aquifer under a proxy contaminant load and relationships between the tracer behaviour and pumping conditions in the aquifer. This section also includes an appraisal of the SF_6 tracer method.

6.8.2 RELATIONSHIPS BETWEEN TRACER RECOVERY AND PUMPING RATE AT IRTON

Table 6.5 summarises the Irton pumping rates, 1st arrival times, peak arrival times and recoveries for six traces between the Forge Valley swallowholes and Irton.

Test	Tracer	Irton Q	1st Arrival	Peak arrival	Separation	24 hour recovery
		tcmd	hours	hours	hours	%
EA 1997	Phage	14.3	3.75	5.75	2	25.35%
ARUP 1999 a	Phage	14.3	3.2	5	1.8	4.8%
ARUP 1999 b	Photine	14.1	3.5	4.5	1	33.6%
Foley 2002	Fluorescein	17	3.4	4.2	0.8	49.12%
Foley 2004 a*	SF6	18.6	2.8	5.1	2.3	24.4%
Foley 2004 b	Fluorescein	18.6	2.8	3.5	0.7	76.37%

Table 6.5 First arrival times, peak arrival times, % recoveries and pumping rate for all quantitative tracer tests between the Forge Valley swallowholes and Irton PWS. The '*' indicates a two-hour (non-instantaneous) injection.

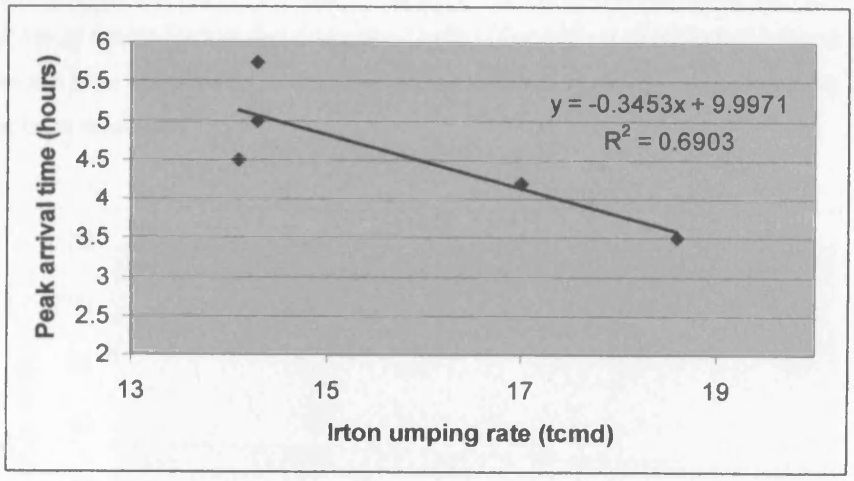

Figure 6.39 Peak tracer arrival at Irton as a function of pumping rate.

These statistics are also plotted against one another in Figures 6.39 and 6.40. In the first of these diagrams there is an apparent inverse correlation between peak arrival time and pumping rate. This diagram does not include the SF_6 data due to the 2-hour injection for this tracer. Similar relationships between tracer travel times and discharge of springs have been noted following repeat tests between

the same locations by Smart (1981), Stanton and Smart (1981), Mull and Smoot (1986) and USEPA (1998).

For Figure 6.40, a plot of tracer recovery against pumping rate, both the bacteriophage and SF_6 data have been omitted due to process-controlled losses not suffered by the dye tracers, leaving only the three dye tests. The data, however, indicates a trend for greater tracer recovery with increasing abstraction.

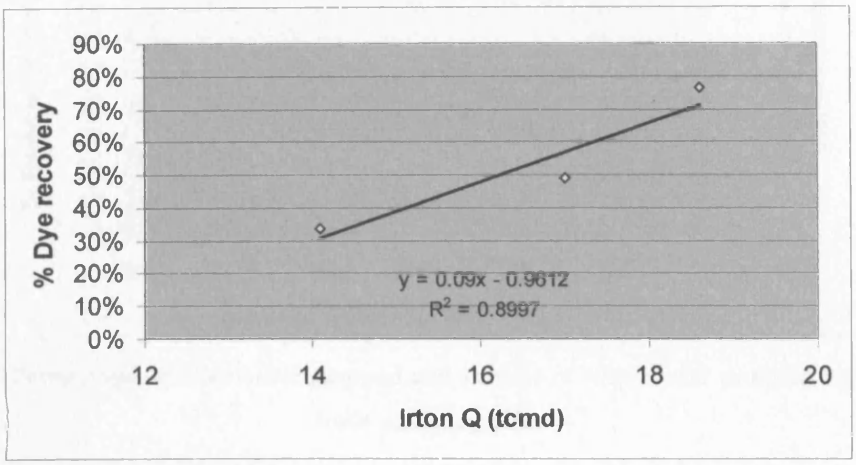

Figure 6.40 Percentage of tracer dye recovered as a function of Irton pumping rate.

In addition to the tracer recovery relationship with abstraction, the hydrochemical data given in Table 6.2 indicates differing contributions of river water under different pumping regimes (Figure 6.41). The data for a zero-pumping condition and for an average pumping condition (13.7 tcmd) are from Tate *et al.* (1970), and additional data for average and high pumping conditions taken during the 1981 Irton pumping test are given by Barker and Courchee (1982). The effects of differing influent conditions at the river have not been calculated, but the data indicates that at higher pumping rates the proportion of river water at Irton decreases.

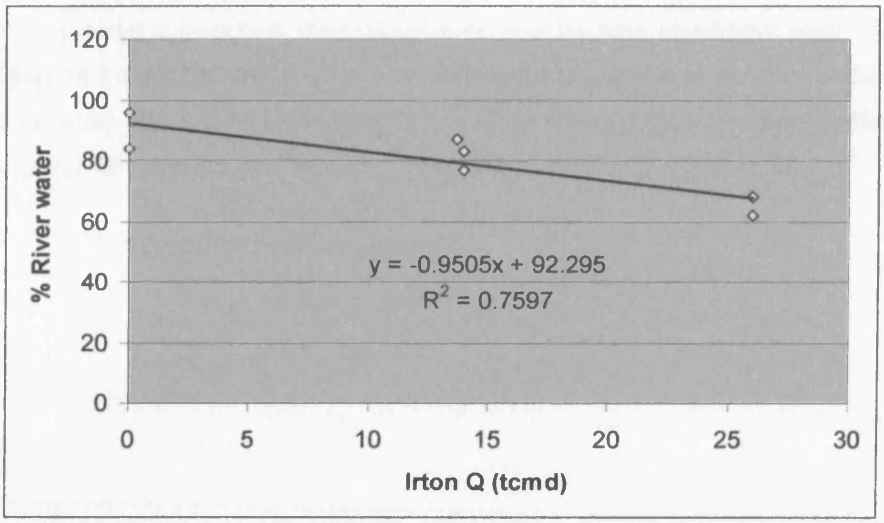

Figure 6.41 Percentage of river water pumped as a function of pumping rate.

However, that the proportion decreases does not mean that the absolute amount of river water pumped decreases. This is clarified by using the correlation determined on Figure 6.41 to determine the volumes of river water pumped in comparison to the total volume pumped at different pumping rates (Figure 6.42).

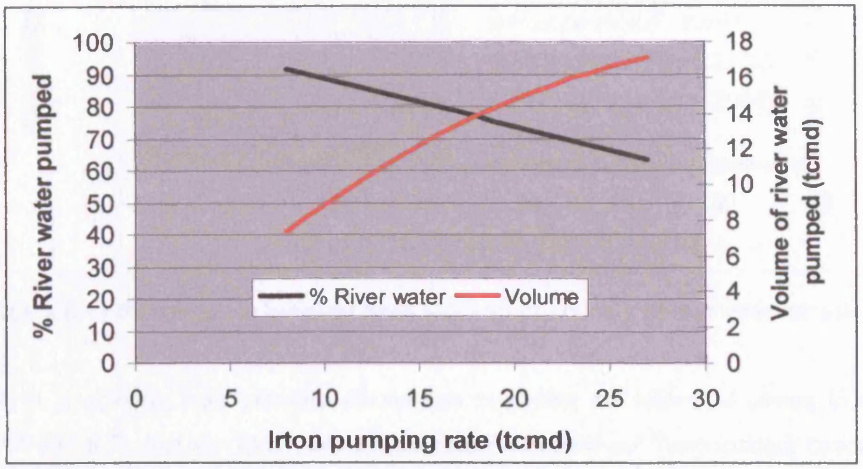

Figure 6.42 Percentage of river water pumped and volume of river water pumped as functions of Irton pumping rate.

The relationships determined in Figures 6.39 to 6.42 are clearly important in terms of aquifer management in the case of a pollution incident at Irton. The pollution monitors at Irton only measure the pumped, raw water. There is no such monitor upstream of the swallowholes. It is therefore probable that any contaminant observed will already be in the aquifer. The implication of the above tracer, hydrochemical and pumping relationships is that the best practice to resolve a serious groundwater pollution incident would be to maximise the pumping rate to clean out the aquifer before the contaminant has time to either spread or to undergo diffusion into the matrix or other (relatively) immobile groundwaters.

One further relationship is that between the concentration of the injected tracer and the maximum concentration measured at Irton New Well (Figure 6.43, note the semi-logarithmic plot). The data held is well constrained for the dyes and less well constrained for SF_6. It is also probably at the lowest end of the scale on which any real pollution incident would occur, but may be of some predictive use (or conversely, useful for calculating initial loads on the basis of measured concentrations).

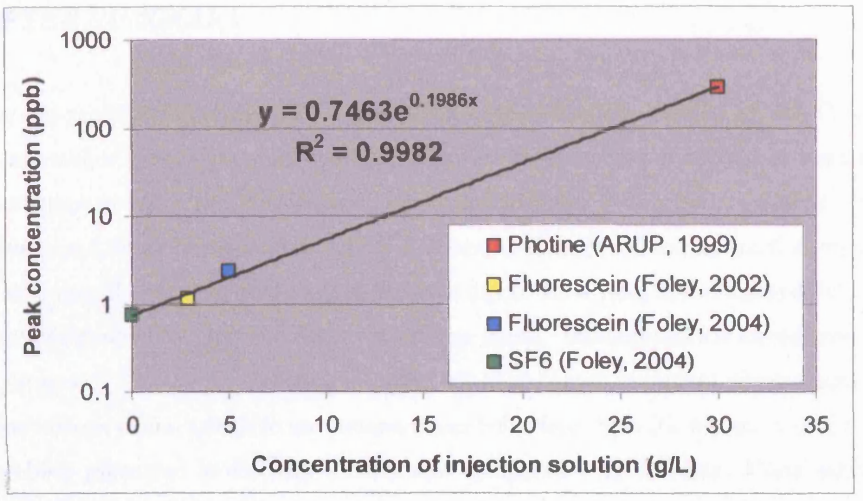

Figure 6.43 Relationship between peak size and injection solution concentration.

In addition, it is obvious from previous discussions regarding the nature of tailing in the aquifer (Sections 6.4 and 6.5), that the likely rate of decrease in a *dissolved* [32]contaminant concentration at Irton, at times greater than 1 day, will best be approximated by the slope of the recession of the SF_6 BTC at Irton *and* at Derwentdale Farm North. We might therefore expect a power-law recession of between -1.25 and -1.5, so that the persistence of contaminant above a certain concentration may be well constrained once information regarding concentrations has been taken after 1 day.

[32] A non-aqueous-phase liquid is likely to display different behaviour.

6.9 CHAPTER SUMMARY

This chapter has presented the results from several tracer tests conducted in the eastern Corallian, both by the present author and by previous workers. The results have been modelled in several different ways in an attempt to define those processes contributing to tracer losses, hydrodynamic dispersion of the tracer plume and breakthrough curve tailing. A conceptual model of channelled fissures or conduits embedded in a broadly Darcian medium exhibiting a dipole flow field superimposed onto a regional gradient, and constrained by high and low permeability zones, faulting and the unconfined part of the aquifer, is proposed. This conceptualisation unifies all of the most important observations made and permits a framework within which to understand tracer behaviour. Specific elements of the conceptual model have been presented in theoretical form and compared with the data. These elements are a simple dipole, double porosity diffusion and hydrodynamic dispersion along single flowpaths. Whilst none of these elements is able to individually capture all the variability within the system, together they offer deeper insight into the hydrogeology of contaminant transport in the eastern Corallian.

Additional analysis identifies key data for determining system response to contaminant loading under different pumping conditions. This analysis suggests potential management options in the event of future pollution incidents.

CHAPTER 7

RESULTS AND DISCUSSION III
CFCs AS HYDROLOGIC TRACERS IN THE EASTERN VALE OF PICKERING

"Every man, wherever he goes, is encompassed by a cloud of comforting convictions, which move with him like flies on a summer day."

Bertrand Russell (1928)
Sceptical Essays

7.1 INTRODUCTION

The results and interpretation of CFC and CCl_4 measurements made on ground waters from the eastern Corallian and associated drift deposits, and on the River Derwent, are presented here. These compounds were analysed as a part of this study due to their potential use as indicators of groundwater age and transport processes. They also share several characteristics with more toxic, halogenated organic compounds, such as various pesticides. This aspect of the study, whilst not emphasised below, was equally important due to familiarisation with the analytical equipment (GC-ECD) common to the analysis of a wide range of similar trace compounds in the environment. However, although individual chromatograms frequently indicated many types of halogenated compounds in groundwater, the majority of these were not identified and regarded merely as interference with the quantification of compounds of interest. Examples of such chromatograms are given.

More importantly, the CFC results are analysed by referring them to groundwater concentrations explicable with atmospheric CFC (and CCl_4) history on data 'cross-plots' and in terms of groundwater concentration ratios to modern rainfall. The chapter discusses the applicability of certain basic model types for deriving apparent ages and determining mixing between different groundwaters. Variability in the data is discussed with respect to the sample location and hydrogeology of the Corallian as well as of mechanisms of CFC removal and enrichment and additional methodological factors.

7.2 RESULTS

7.2.1 CFCs AND CCL_4

The CFC and CCl_4 results from all sampling campaigns are given in Table 7.1. Locations are shown on Figure 5.1, bar three exceptions. The first two are Ebberston and Cliff Farm springs, which occur within 100 m of each other where the Ebberston-Filey fault cuts the Corallian at Ebberston, some 4 km west of Brompton. The third exception is the Jenny Thrush spring, which is approximately 1 km west of the area shown on Figure 5.1, but on the northern escarpment.

Location	Grid Reference	Sample date	CFC12 pg/kg	CFC11 pg/kg	CFC113 pg/kg	CCl4 pg/kg
Cayton Bay Spring	TA 08 067 845	1.11.01	3248.49	1094.83		821.68
		1.11.01		2821.69		1108.73
		1.2.02	2809.54	1027.75		564.87
		1.2.02	2410.49	922.20		379.79
Brompton Spring	SE 98 944 822	1.11.01	605.59	901.59		790.23
		1.11.01	763.59	1083.44		742.99
		1.11.01				
		1.11.01		1217.91		713.95
		1.11.01		1240.84		1056.87
		29.3.04	1996.88	313.07	81.90	222.43
		29.3.04		466.57	84.24	106.65
		29.3.04		462.83	81.04	104.18
		1.2.02		10826.73	108.61	1376.78
		1.2.02		1658.55	264.14	293.74
		4.8.04	134.63	278.26		
		8.8.04	302.21	390.75		
		11.8.04	134.31	327.95		
		16.8.04	157.02	349.03		
		19.8.04	143.77	147.40		
Edge Dell Spring	TA 08 027 859	31.3.04		534.60	58.59	396.00
		31.3.04	333.58	609.91	82.28	395.83
Jenny Thrush Spring	SE 98 923 875	1.4.04	461.39	1028.18	130.60	366.68
Raincliffe Woods Springs	TA 08 002 886	3.4.04	110.08	588.30	24.39	192.80
		3.4.04	75.43	596.21	29.86	195.29
Glasshouse Springs	SE 98 997 884	3.4.04	1071.70	1005.96	244.53	225.96
		3.4.04	618.54	671.15	157.71	148.76
Lady Mildred's Spring	SE 98 992 879	3.4.04	458.51	591.78	63.08	203.46
		3.4.04	364.36	493.83	32.03	177.17
Cliff Farm Spring (Ebberston)	SE 98 900 832	4.4.04	238.38	746.63	65.76	899.03
		4.4.04	338.99	726.29	52.75	886.44
Ebb. Petrifying Spring	SE 98 899 834	4.4.04	32.63	721.49	51.04	311.48
Ings Lane Spring	SE 98 951 817	27.8.04	417.09	660.13		
		27.8.04	201.81	311.05		
Sawdon Beck Spring	SE 98 937 860	1.11.01		748.04		
		1.11.01		1020.05		967.21
		1.11.01		898.20		861.29

Table 7.1 Sample locations and results for all Corallian groundwater CFC and CCl_4 samples.

Location	Grid reference	Sample date	CFC12 pg/kg	CFC11 pg/kg	CFC113 pg/kg	CCl4 pg/kg
Irton PWS	TA 08 005 841	1.11.01		883.89		1111.74
		1.11.01		1127.45	<detection	936.76
		1.11.01	2140.86	2053.96	<detection	1504.51
		1.2.02		1102.83	15.90	1465.10
		1.2.02	197.91	3640.20	51.20	819.53
		3.8.04	238.00	360.28		
		3.8.04	252.46	355.06		
		3.8.04	277.00	373.67		
		4.8.04	230.37	402.72		
		4.8.04	337.61	542.28		
		5.8.04	219.34	354.31		
		5.8.04	374.89	463.77		
		6.8.04	284.81	476.89		
		7.8.04	226.65	330.94		
		9.8.04	199.84	348.24		
		10.8.04	212.82	403.35		
		11.8.04	266.77	406.46		
		13.8.04	242.70	366.11		
		16.8.04	253.76	389.96		
		19.8.04	357.96	469.01		
		25.8.04	429.91	851.01		
		29.8.04	308.51	513.11		
		3.9.04	420.11	580.66		
Cayton Carr House Lane PWS	TA 08 047 827	1.11.01	399.05	824.66		704.71
		1.11.01	271.79	828.97		640.75
		1.2.02		286.17	13.70	192.44
		1.2.02		222.17	12.28	108.66
		4.8.04	250.27	296.11		
		5.8.04	305.24	244.97		
		6.8.04	250.21	156.95		
		7.8.04	92.33	130.00		
		8.8.04	182.33	261.50		
		9.8.04	151.05	171.31		
		11.8.04	247.30	256.66		
		16.8.04	207.57	179.37		
		19.8.04	253.94	204.36		
		24.8.05	228.50			
		3.9.04	278.08	207.54		
Cayton Station Road PWS	TA 08 058 828	1.11.01		460.33	<detection	545.06
		1.11.01		570.80	<detection	541.72
		4.8.04	132.36	123.62		
		6.8.04	84.56	22.44		
McCains (borehole)	TA 08 051 836	1.11.01		968.67		1028.17
		1.11.01	1216.57	1093.29		959.92
		1.2.02	1495.90	9570.36	67.49	548.27
		1.2.02	553.28	657.57		108.26
		2.8.04	1600.78	383.98		

Table 7.1 Continued.

Location	Grid reference	Sample date	CFC12 pg/kg	CFC11 pg/kg	CFC113 pg/kg	CCl4 pg/kg
Ratten Row (borehole)	TA 08 011 830	1.2.02		692.96		143.46
		1.2.02		857.89	7.76	92.87
		1.11.01	488.03	1013.90	<detection	877.75
		1.11.01	2851.06	913.28	<detection	590.83
		4.8.04	222.25	126.69		
		6.8.04	232.12	122.00		
Long Lane (borehole)	TA 08 022 833	1.11.01	526.32	1084.37		714.75
		1.11.01		1167.14	<detection	882.57
		1.2.02		7662.26	206.35	554.83
Tetherings Plump BH	SE 98 976 827	4.8.04	193.40	128.43		
		5.8.04	138.57	97.90		
		6.8.04	184.54	195.67		
		8.8.04	312.69	303.14		
		10.8.04	18.66	46.73		
		19.8.04	289.63	180.14		
		25.8.04	195.31	194.47		
		3.9.04	261.51			
		9.9.04				
Seavegate Gill BH	SE 98 989 856	5.9.04	74.03			
		5.9.04	163.82			
		5.9.04	198.99	234.01		
Augmentation BH	SE 98 990 852	9.6.04		8.95	16.64	
		9.6.04	26.11	12.87	37.18	
		9.6.04	28.55	13.06	13.63	
		9.6.04		18.60	12.83	
		9.6.04		57.53	10.20	
		9.6.04		63.30	14.08	
		9.6.04		108.99	15.05	
		9.6.04		47.24	9.85	
Swallowholes BH	SE 98 990 852	8.6.04		12.92	8.93	
		8.6.04		9.62	11.62	
		8.6.04		35.38	12.84	
		8.6.04		40.53	12.81	
		8.6.04		62.97	7.59	
		8.6.04		292.51	5.82	
Derwentdale Farm North BH	SE 98 997 838	1.4.04	521.07	126.74	86.19	1.24
		1.4.04	574.17	903.21	67.93	95.97
		3.8.04	270.15	338.74		
		4.8.04	392.39	322.18		
		5.8.04	321.41	407.27		
		7.8.04	483.87	409.16		
		9.8.04	327.03	423.79		
		11.8.04	364.39	510.06		
		13.8.04	270.83	391.49		
		16.8.04	424.94	493.37		
		19.8.04	428.55	545.59		
		25.8.04	369.43	577.95		

Table 7.1 Continued

The associated precision and accuracy of these figures are given in Chapter 4 and are plotted as error bars on interpretative graphs in this chapter. For many sites it has been impossible to present a full suite of results (i.e. all CFCs in a sample). This is particularly so for the August 2004 sampling, which measured only CFCs 11 and 12 (together with SF_6). In other instances the CFC 12 measurement has been completely or partially masked by co-elution of a large nitrous oxide (N_2O) peak, an indicator of de-nitrification processes occurring in the aquifer. Additionally the CFC 113 peak is muted compared to both CFCs 11 and 12 as the electron capture detector is less sensitive to this species. This, together with the contaminant signal discussed in Chapter 4 mean that often it is impossible to determine CFC 113.

7.2.2 RESULTS FROM THE RIVER DERWENT

Northing	Date of sample	CFC 11 pg/kg	CFC 12 pg/kg	CFC 113 pg/kg
81250	31/05/2004	1479.39	707.50	227.80
81500	31/05/2004	607.34	360.22	88.56
81750	31/05/2004	946.58	656.72	166.63
82000	31/05/2004	590.66	363.16	130.23
82250	31/05/2004	586.40	260.57	119.08
82500	01/06/2004	1320.58	113.48	221.62
82750	01/06/2004	529.00	283.04	110.24
83000	01/06/2004	904.98	565.75	155.38
83250	04/06/2004	578.32	28.46	67.69
83500	04/06/2004	541.34	175.05	106.84
83750	04/06/2004	557.50	397.64	139.68
84000	04/06/2004	613.00	369.71	131.99
84300	04/06/2004	659.81	406.22	161.59
84600	04/06/2004	563.31	347.04	118.42
85250	04/06/2004	455.20	172.07	89.65
85250	04/06/2004	446.27	234.80	125.43

Table 7.2 CFC results from the River Derwent.

These results are depicted graphically and discussed in Section 7.4.

7.2.3 CONTAMINATION OF ANALYTICAL EQUIPMENT

Several of the samples reported indicate severe contamination of a site at one time, but not at another. This is particularly so of the sampling campaigns of November 2001 and February 2002, as discussed in Chapter 4. Where possible, samples from these campaigns have been removed from further analyses, although in some cases they are the only available measurements.

7.2.4 RESULTS OF SUPPORTING MEASUREMENTS

Dissolved oxygen (DO) and temperature measurements were taken in support of the CFC measurements. CFCs are redox-sensitive chemical species, degrading under anaerobic conditions. Recharge temperature is important as the equilibrium concentrations of CFCs in water in contact with the subterranean atmosphere are temperature dependent, and it is assumed that this is reflected in the bulk temperature of the groundwater.

7.2.4.1 Dissolved Oxygen

Preliminary measurements of DO indicated widespread oxidising conditions. Subsequently only a few representative locations were measured to confirm this. The results are given in Table 7.3 (locations on Figure 7.1).

	% Sat	mg/L
Irton	72.7	8.7
Cayton Carr	23.2	2.8
Cayton Bay	75.7	9.1
Derwentdale Farm North BH	81.8	9.8
Derwentdale Farm South BH	10.6	1.3
Brompton Spring	66.2	7.9
Augmentation BH	65.0	7.8

Table 7.3 Dissolved oxygen measurements from representative locations in the Corallian.

The table confirms the initial observations. However, two boreholes, both of which are southerly and approaching the Ebberston-Filey fault (Cayton Carr and Derwentdale Farm South), show lower DO values. This implies a greater residence time and the potential for CFC reduction. Furthermore, although all waters sampled showed oxidising conditions, examination of borehole core from observation boreholes drilled as part of the Osgodby ASR scheme at Irton indicated that the centres of oolitic matrix blocks could display reducing conditions. This was inferred from the grey colour of the blocks that weathered to a creamy colour upon exposure to the atmosphere, as well as deposits of ferric oxide associated with, in particular, the smaller 'hair-line' fractures traversing the blocks. It may be expected, therefore, that should CFC-rich water enter the matrix then the CFCs would be likely to be subject to degradation. These observations also suggest that 'hair-line' fractures play a role in groundwater flow in the aquifer.

In addition, Cayton Bay spring has an anomalously high DO value for one of the terminal discharge points in the aquifer. It is possible that, as water from this location is collected from several locations within the cliff-face before being transferred to a central well, it has the chance to become oxidised prior to sampling. This obviously has implications for CFC dating of Cayton Bay waters.

7.2.4.2 Temperature

The temperature measurements of borehole waters made as part of the geophysical survey (Chapter 5) indicate the assumption of equilibration between unsaturated zone air and infiltrating water at 10° C to be realistic (see also Chapter 4). The data is shown on the borehole logs given in Chapter 5 and in Appendix 3.

7.3 CFC & CCL_4 DISTRIBUTIONS IN THE CORALLIAN

This section provides an initial overview of CFC and CCl_4 distribution in the Corallian by presenting maps of the distribution of best estimate concentrations (on the basis of repeat samples) in the Corallian. Such maps are presented for each of the CFCs and for CCl_4 throughout the main field area, extending from Brompton in the west to Cayton Bay in the east. They are shown in Figure 7.1 to 7.4.

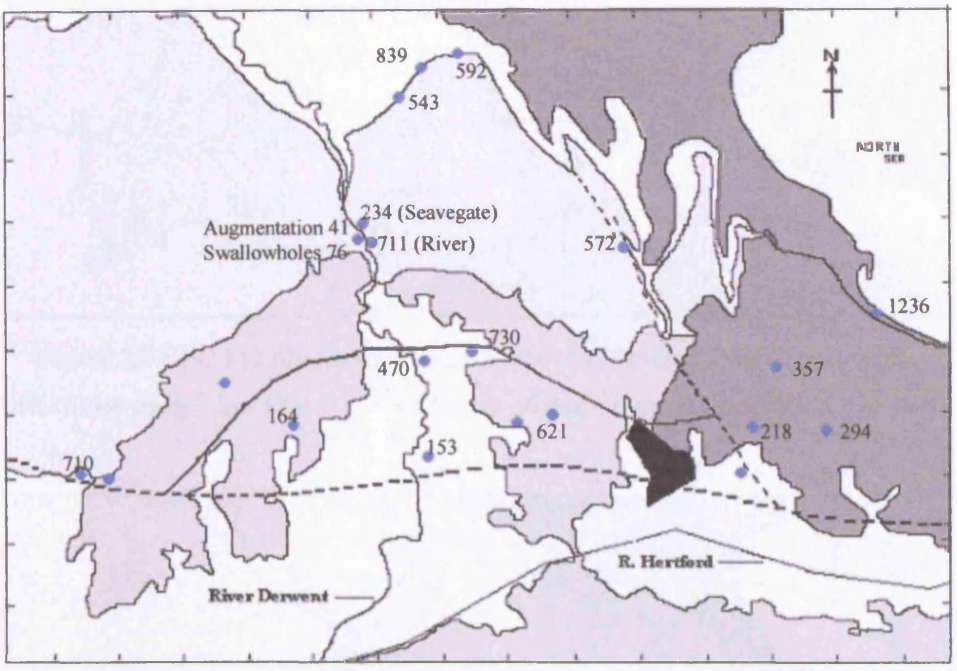

Figure 7.1 CFC 11 distribution in groundwater, eastern Vale of Pickering.
All values pgkg^{-1}. See Figure 5.1 for key to geology. Grid squares 1 km to a side.

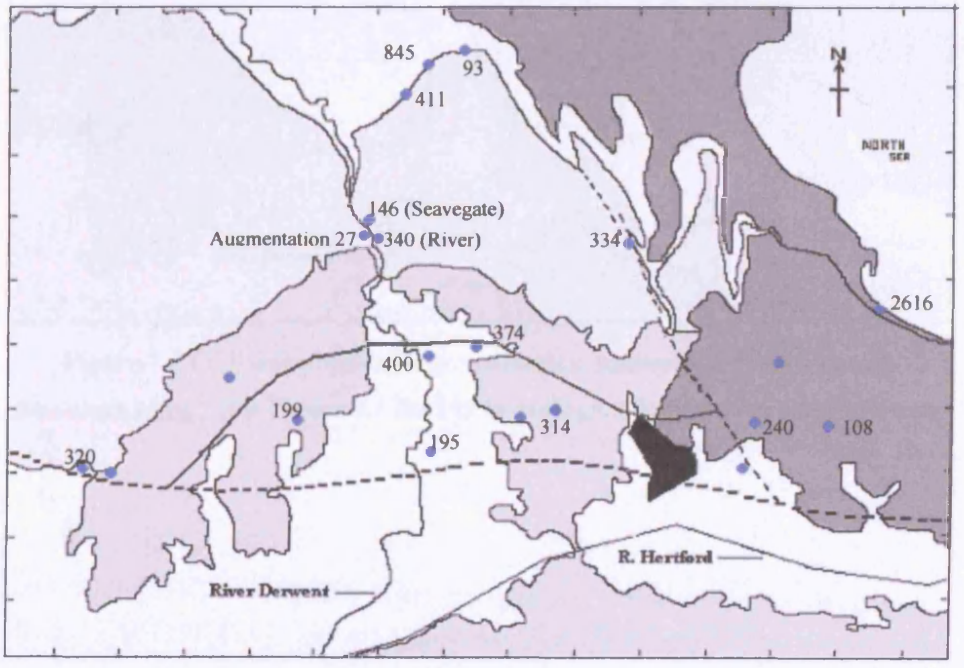

Figure 7.2 CFC 12 distribution in groundwater, eastern Vale of Pickering.
All values pgkg^{-1}. See Figure 5.1 for key to geology. Grid squares 1 km to a side.

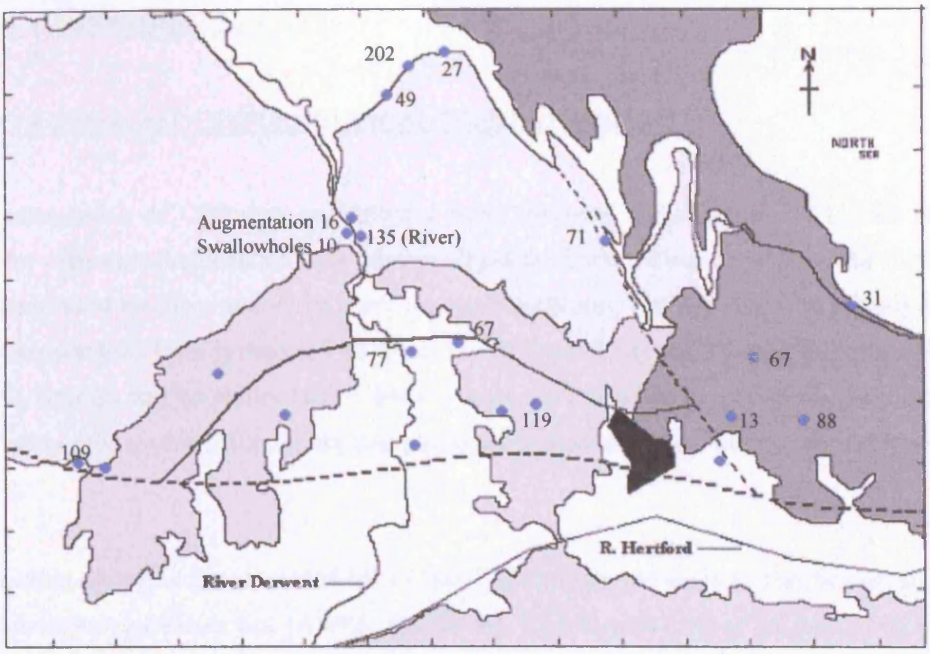

Figure 7.3 CFC 113 distribution in groundwater, eastern Vale of Pickering.
All values pgkg^{-1}. See Figure 5.1 for key to geology. Grid squares 1 km to a side.

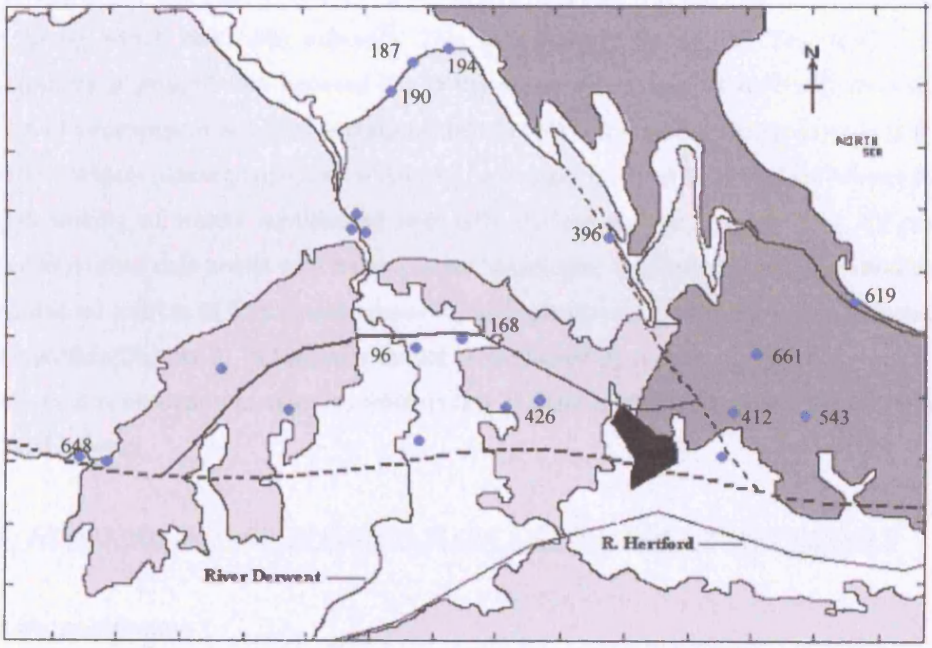

Figure 7.4 CCl_4 distribution in groundwater, eastern Vale of Pickering.
All values pgkg^{-1}. See Figure 5.1 for key to geology. Grid squares 1 km to a side.

7.4 DATA INTERPRETATION

7.4.1 DATA CROSS-PLOTS OR HISTORICAL TREND DIAGRAMS

For the presentation of CFC data on historical trend diagrams (Figures 7.6 – 7.11) the replicated samples for each sampling location have been averaged to obtain a clearer picture of the relationships between individual locations and to see if any grouping is evident. The data has been initially separated into samples obtained from springs (all of which except Cayton Bay spring issue from the unconfined part of the aquifer) and boreholes (all of which except the Forge Valley boreholes are drilled in the confined part of the aquifer). The former data points are plotted as circles, whereas the latter are plotted as squares.

CFC data cross-plots plot the concentrations of two CFCs against one another. The data are also plotted with an air-water equilibrium line (AWEL, the curved, black line in each of the plots) that represents the historic ratio between the two CFCs as dissolved in recharging groundwater at a temperature of 10° C. Excluding additional processes, a sample plotting along this line would represent the CFC ratio of an unmixed groundwater sample recharged at a particular time. In other words, as the ratio of two CFCs is unique to any one year, a sample displaying that ratio may be expected to have fallen as rain in the year during which that ratio existed[33]. This is a piston-flow model. The AWEL is further supplemented by a straight line between the composition of modern rainfall and the origin. This represents a two-component or binary mixing model of modern (recently-recharged) and old (pre-CFC) groundwaters. Waters plotting anywhere within the 'envelope' of the AWEL and the mixing line ought to represent mixing of waters equilibrated with only the atmosphere at some time. Of course, the situation of individual data points with respect to the 'envelopes' is affected by various other processes, such as additional sources of CFC (contamination), biologically-mediated degradation, sorption and so on, as discussed in Chapter 3. Where data cannot be explained by reference to the historically possible concentrations it is necessary to examine whether any of these additional processes are responsible for the measured values.

7.4.2 THE APPROPRIATENESS OF PISTON-FLOW AND BINARY MIXING MODELS

7.4.2.1 Model justification

The piston-flow assumption of CFC transport in groundwater has been widely employed in the literature. Recent examples include Rademacher *et al.* (2002) and Katz (2004). The effects of dispersion are discussed by, amongst other, Busenberg and Plummer (1992) and Plummer *et al*, (1993). Generally speaking, as the CFC input function increases linearly with time, dispersive effects only become significant for waters older than 20 years (Cook & Solomon, 1997). The simplifying piston-flow approach adopts a non-dispersing and non-mixing flow regime and implies that individual packets

[33] In fact, as CFC concentrations have declined over the last decade some non-uniqueness in ratios has arisen for water recharged during this time.

of water retain their identity as they travel between points of recharge and discharge. Studies employing the principle include some conducted in karstic or fractured rocks (Katz *et al.* 1995; Rademacher *et al.*, 2002). Other studies adopting the piston-flow principle include Burton *et al.* (2002) and Bateman (1998).

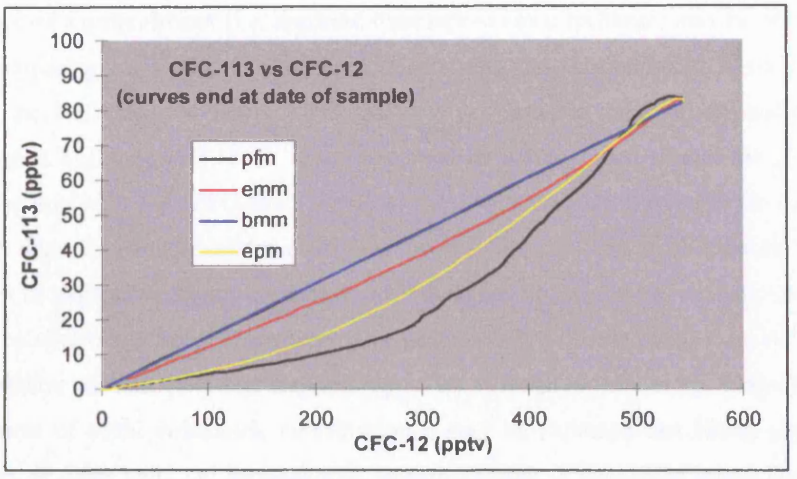

Figure 7.5 Exponential (EMM) and Exponential-Piston (EPM) mixing models falling within the envelope created by Piston Flow (PFM) and Binary (BMM) mixing models (after Bohlke, 2004).

Other commonly used, simple models with which to interpret CFC data are exponential mixing models and exponential-piston models (a hybrid) (e.g. Busenberg and Plummer, 2004). However, as Figure 7.5 shows, any dateable result from these models will fall within the boundaries of the PFM-BMM envelope, so that they are essentially limiting cases (Bohlke, 2004). Because of this, and because of a large degree of scatter in the data, the PFM-BMM envelope is used as the primary reference for understanding variability in the data.

In the present study there is strong evidence from geophysical logging and both tracer and borehole-dilution testing to indicate that some type of mixing model is appropriate for examining recharge ages. The borehole dilution tests consistently show that water within any given borehole is derived from multiple fissures, often with considerable separation between them (Chapter 5). Tracer tests show major disparities between observed groundwater velocities (Chapter 6) and apparent groundwater ages derived from CFCs (below) and tritium (Chapter 6) on the basis of a piston-flow assumption. A binary mixing model is the simplest mixing model that may be assumed. This simplicity is warranted by:

- Uncertainty in the data.
- Uncertainty regarding the contribution of matrix to fracture flow.
- Applicability of the model to single CFCs.
- Comparability of results from additional hydrochemical tracers (e.g. tritium and alkalinity; see Chapter 6 for this application).

The end-members of the mixing model in the data cross-plots (envelope diagrams) are a modern and a CFC-free water. However, for individual sampling locations it may be more appropriate to select

alternative end-members, and in these cases equation 6.5 will be used. Such cases are presented as part of the discussion of the results (Section 7.4.4).

7.4.2.2 Apparent age

The apparent age of a groundwater (i.e. apparent time lapsed since recharge) may be obtained either on the basis of comparing individual CFC concentrations with the reconstructed historical equilibrium values, or on the basis of comparing CFC ratios with historical equilibrium ratios. The former procedure (single-CFC age) will result in an apparent increase in age should the packet of CFC-containing water mix with old (CFC-free) water, as the resultant dilution reduces the concentration of CFC measured. This is not the case for dating on the basis of CFC ratios, as dilution with CFC-free water ought not to change the ratio, but simply to reduce the concentration of each CFC by an equal factor. Should mixing occur between two or more waters with different ratios then the resulting ratio will be an alteration of both (all) that depends upon the respective volumetric contributions of each water. In mixtures of equal volumetric contribution it may be expected that biases occur toward the youngest waters as these have the greatest CFC concentrations. It should be noted that, as ratios are dependent upon more than one CFC, the opportunity for interference from contamination and non-conservative removal is greater than that for single-CFC age dates. This does in fact create significant problems as may be seen in the drift away from the envelope diagrams presented in the next section. It should also be stressed that groundwater 'age' determined in these ways is more of a conceptual handle on the data than a reflection of actual age, hence the term 'apparent'. CFC ratio ages are discussed further in Section 7.5.1 following graphical presentation and discussion of the results below.

7.4.3 DATA CROSS-PLOTS

The data cross plots are shown in Figure 7.6 to 7.11

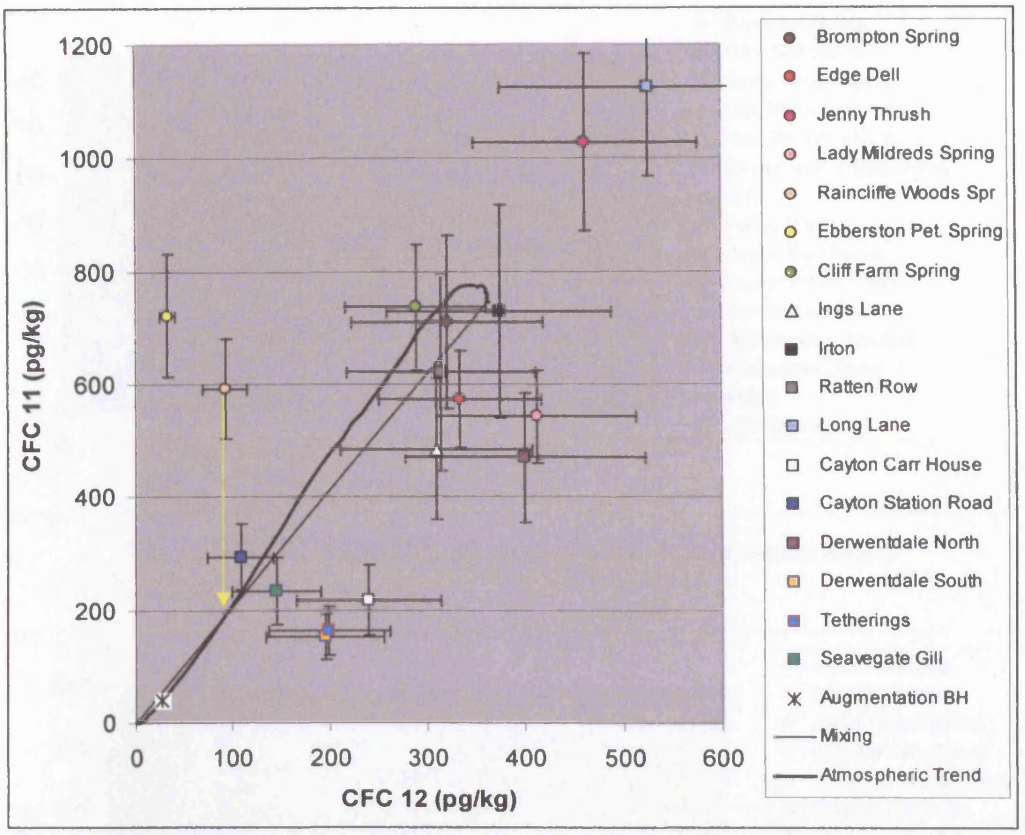

Figure 7.6 CFC 11 vs. CFC 12 data cross-plot, averaged concentrations.

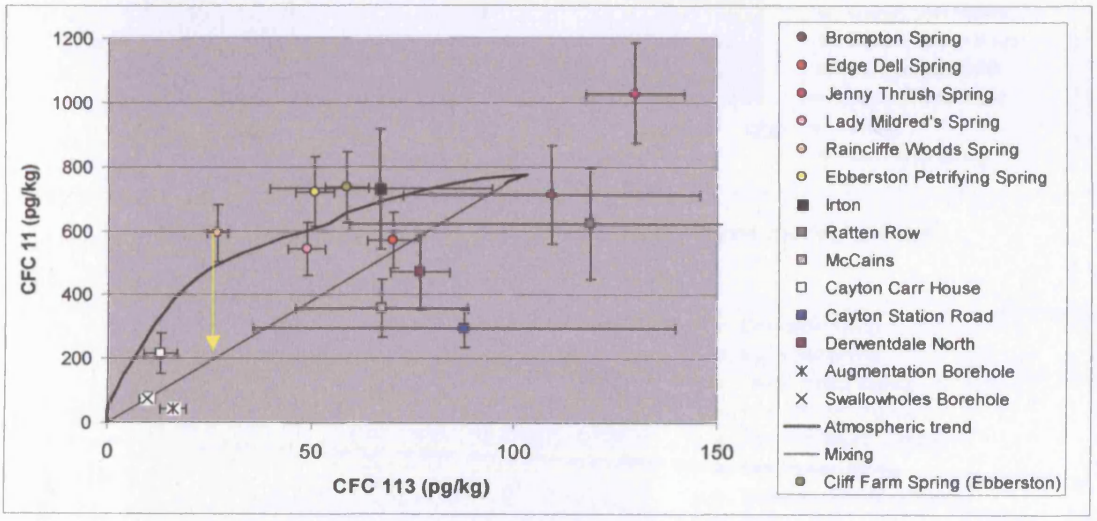

Figure 7.7 CFC 11 vs. CFC 113 data cross-plot, averaged concentrations.

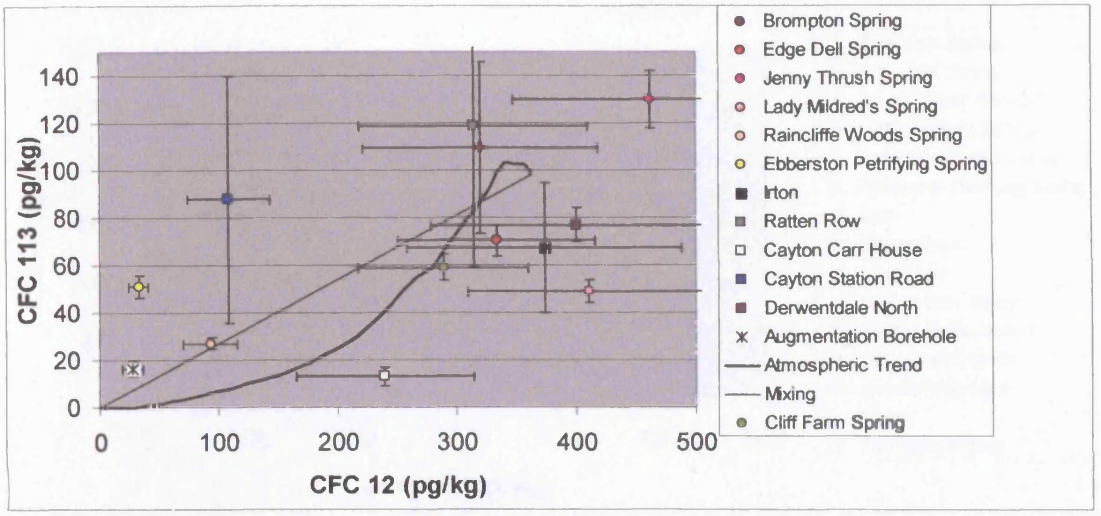

Figure 7.8 CFC 113 vs. CFC 12 cross-plot, averaged concentrations.

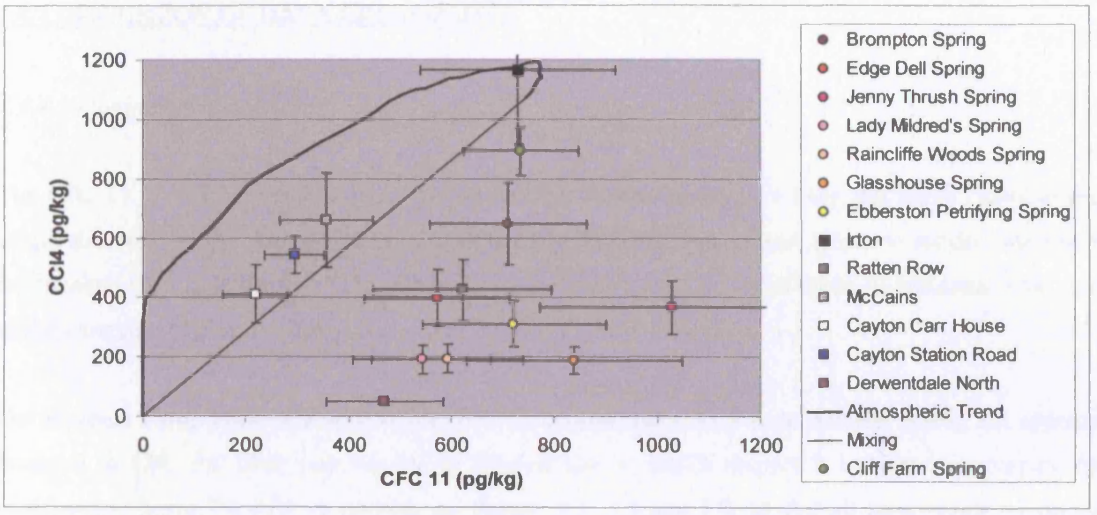

Figure 7.9 CCl_4 vs. CFC 11 data cross-plot, averaged concentrations.

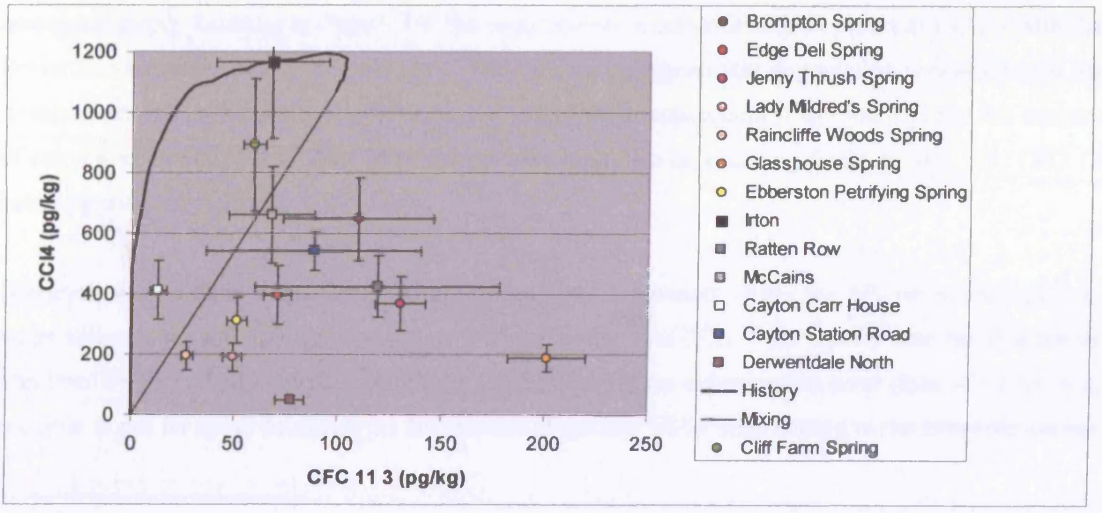

Figure 7.10 CCl_4 vs. CFC 11 3 data cross-plot, averaged concentrations.

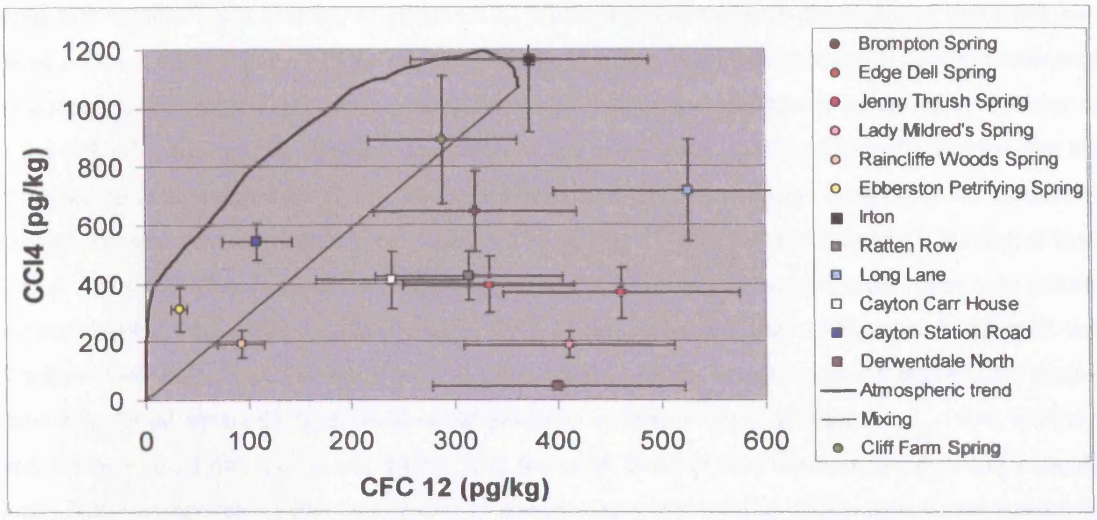

Figure 7.11 CCl_4 vs. CFC 12 data cross-plot, averaged concentrations.

7.4.4 DISCUSSION OF DATA CROSS-PLOTS

7.4.4.1 Discussion

The CFC 11 vs. CFC 12 plot (Figure 7.6) shows that several borehole waters plot much closer to the origin than any of the spring waters, although other borehole waters plot closer to modern air-water equilibrium (AWE, at the tip of the curve). Unsurprisingly, Irton is one of these, as is Ratten Row, one of the closer boreholes to Irton.

Derwentdale Farm North borehole has a CFC 12 concentration similar to modern AWE, but appears depleted in CFC 11. This may be due to degradation, in which respect it is better to compare its position on Figure 7.6 with its position on Figures 7.7, 7.8 and 7.9, so that all compounds measured may be taken into consideration together. Figure 7.7 shows the same sample in a similar position relative to the envelope: slight depletion in CFC 113 with respect to CFC 12 (but which has a large associated error). Looking at Figure 7.9, the same sample location is *very* depleted in CCl_4 – with the lowest concentration of any groundwater[34]. This strongly suggests that degradation is operative on the waters produced at this well, despite the known river water component (from tracing) and the amount of oxygen measured (Table 7.3). This process may well also be affecting CFCs 11 and 113, CFC 12 being the most recalcitrant.

However, it is curious that with a *definite* present-day component (from the SF_6 tracer testing), this water still exhibits a CCl_4 concentration so low. Assuming that CCl_4 in the aquifer does not degrade in less than 24 hours under aerobic conditions, and assuming no experimental error (loss of CCl_4), it is possible to put an upper boundary on the amount of modern water contributing to the borehole, on the

[34] The data gives two measurements (replicates) of CCl_4 from the April 2004 sampling campaign, which are both low (<100 $pgkg^{-1}$). There are also two measurements of each of the CFCs at this time, plus a further 12 measurements of CFCs 11 and 12 during August 2004.

basis that modern water contributes *all* the CCl_4. Whilst the older water in the aquifer at this point may be of different ages, if it is all CCl_4 free, then, for the purposes of a mixing model, it may be considered as a single component of a binary mixture. The result of such a calculation is a modern component of 4.5 ± 6.3 %[35]. Adding two standard deviations to the mean gives a 99% confidence interval that the contribution is not more than 17.1%. The concentration of CFC in a mixture containing this amount of present-day water would therefore be $C_{Present} \times 17.1\%$. For CFC 12 this is 61.5 $pgkg^{-1}$, leaving at least 340 ± 102 $pgkg^{-1}$ unaccounted for (uncertainty stated on the basis of sample error). The only natural waters possible of contributing this level of CFC 12 are recharged after 1982, whereas Happell and Wallace (1998) record a CCl_4 half-life of 14 ± 4 years in oxidising groundwater. Oceanographic studies have also found strong CCl_4 removal under oxidising conditions (e.g. Wallace *et al.*, 1994; Bullister and Wisegarver, 1998; Lee *et al.*, 1999). It is therefore feasible that water sampled at Derwentdale Farm North comprises a small component of present-day water mixing with waters young enough to retain the majority of their CFC signature (with small losses) but old enough to have lost all of their CCl_4. This remaining water would comprise over 80% of the water pumped. CFC degradation losses are explored further below.

Returning to Figure 7.6 it is possible to see a general pattern of CFC 11 depletion common to most borehole and some spring waters. The lowest concentrations of both CFCs are in boreholes either more distant from the swallowholes or to the south or west of the swallowholes, away from the main flowpaths emanating from Forge Valley. The exception to this pattern is the Augmentation borehole, which represents an average value of samples taken at several depths within the borehole. The Swallowholes borehole does not plot on Figure 7.6 as the CFC 12 peak was masked by N_2O. However, on Figure 7.7 (CFC 11 vs. CFC 113) the Swallowholes borehole plots very closely to the Augmentation borehole, as one may expect from their geographical proximity. As these two boreholes also have a proven river water component, a binary mixing model may again provide an estimate of the upper limit of this contribution to the water sampled. On this basis the component of river water for the Augmentation borehole is 10.6 ± 8.5 %[36] and for the Swallowholes borehole is 10.1 ± 10.0 %. This leaves the remaining water free of CFCs (in contrast to Derwentdale North). As the geophysical logging and borehole dilution tests tell us that much of the water in these boreholes issues from fissures in the Lower Calcareous Grit, apparently this water takes several decades to travel from outcrop to the Corallian beneath the Forge Valley swallowholes.

In contrast to the borehole waters, spring waters are fairly evenly distributed both above and below the envelope (Figure 7.6). Brompton springs, fault-dammed at the southern boundary of the Tabular Hills and fed by a shallow, underdrained dale, issues from the well-fissured Malton oolite and exhibits a composition close to that of AWE. Brompton spring also plots in a similar place on both Figures 7.7 and 7.8. Figures 7.9 to 7.10 show relative depletion in CCl_4 for this water. From dye tracer tests (Chapter 6) there is a known rapid-flow component. As hydraulic head in the dale is elevated above the

[35] Mean of % contribution determined from 2 measurements of CCl_4 ± 1sd

[36] This is the percentage contribution calculated from individual measurements averaged for all CFCs in all samples (i.e. the mean %) ± 1σ.

level of the spring it should drive some deeper circulation below the spring, and indeed an upward gradient is observed between the deep and shallow boreholes in Brompton Dale. Brompton spring is conceptually amenable to a binary mixing analysis assuming the deeper water to be CFC free, not an unreasonable supposition given the values recorded in the Lower Calcareous Grit in Forge Valley. On this basis high CFC 11 and 12 concentrations indicate a large component of modern water (> 90 %), although sufficiently old to have lost approximately half atmospherically equilibrated CCl_4. As the same argument applicable to Derwentdale Farm North is applicable here, i.e. that all of the CCl_4 present is derived from modern recharge, then a binary mixing model between a present-day water (i.e. no CCl_4 losses) and water old enough to have lost all of its CCl_4 but young enough to retain its CFC signature, gives approximately a 50/50 mix. It should be noted that sample signature may be expected to vary with discharge at Brompton, and that the data point plotted represents a conglomerate of samples taken over a 2.5 year period. Either way, these groundwater compositions indicate system drainage to be at least partially conduit-controlled rather than diffuse-dominated.

Two springs plot to the left of the graph: Ebberston Petrifying Spring and Raincliffe Woods spring. As CFC 12 is considerably less susceptible to degradation than CFC 11 (see Chapter 3), the two springs may well reflect older waters (mid-20th Century) contaminated by CFC 11. However, referring to the data, we see that there is only a single measurement for Ebberston Petrifying Spring, whereas for Raincliffe Woods spring there are two samples of excellent agreement across all CFCs and CCl_4. Concentrating, therefore, on the Raincliffe Woods data, we may project the data points backwards (see yellow arrows on Figures 7.6 and 7.7) to hypothetical starting points controlled independently by the CFC 12 and CFC 113 data respectively – and look for agreement. In this case we can see that there *is* agreement, with both CFC 12 and CFC 113 predicting an original CFC 11 concentration of c. 200 $pgkg^{-1}$. This is also reflected by the position on which the Raincliffe Woods sample plots on Figure 7.8. Using CFCs 12 and 113 in a BMM between modern and old waters indicates a modern composition of 26.5 ± 4.8 % (2 measurements of 2 CFCs = 4 measurements). Overall it seems likely that this spring is contaminated with CFC 11, similar to another nearby northern escarpment spring, Glasshouses, which is contaminated with all three CFCs but depleted in CCl_4 (see Figures 7.1 – 7.4). Jenny Thrush spring is also contaminated with CFC 11 (and 12) but as it is located some way to the west it cannot be considered related to the same source of CFC 11 contamination. Other clearly contaminated samples include those from the Long Lane borehole and Cayton Bay Spring (not plotted on Figure 7.5).

Cliff Farm spring, some 100 m away from the Ebberston Petrifying Spring but on the opposite (eastern) side of the bottom of a small dale, shows a composition close to modern AWE on all of the diagrams, although it too appears to have minor CFC 11 enrichment in comparison to the other CFCs and CCl_4. In fact, CCl_4 values for this spring (derived from two, closely-agreeing samples) are the closest to AWE of any groundwater other than that at Irton. It therefore seems likely that this is either a relatively young water (although it is issuing from the LCG) or that it has time to approach equilibrium with the atmosphere between leaving the ground and being sampled. In hindsight this possibility seems likely, as the spring was weak and difficult to sample directly from any fissures.

A further spring draining the outcrop, Edge Dell, is definitely situated along a major fault (see Figure 2.6). This probably explains why this water has a CFC composition close to modern AWE, although with apparent minor losses of CFCs 11 and 113. Following the fault to the south-east leads to the public water supply boreholes at Cayton Carr House Lane (CCH) and Cayton Station Road (CSR). These plot similarly to one another toward the bottom third of the AWEL in Figure 7.6 and also plot low in Figures 7.9 and 7.11. However, whilst CSR appears to be elevated in CFC 113, which pushes it away from the envelope in Figures 7.8, 7.9 and 7.10, this is on the basis of a single CFC 113 measurement from the first sampling campaign (Nov. 2001) and cannot be given any great weight. CCH, on the other hand, has at least two (closely agreeing) CFC 113 samples (albeit from the same campaign), four CCl_4 samples, and multiple (>10) samples for CFCs 11 and 12. It therefore looks not only as if both CFCs 11 and 113 are also depleted in the south-eastern part of the aquifer, but that this is part of a general trend indicating increased residence. Taking the CFC 12 concentration at face value, the apparent age of this water is 23 ± 2 years (mean ± 1 s.d., n = 12). A BMM indicates 66% modern water, although simple mixing of an old and a new water cannot explain relative enrichment in CFC 12. It is thus more likely that there is a combination of waters of different ages at this borehole, ranging from present-day (as proven by tracing) to water old enough to have undergone CFC 11 and 113 losses, and to CFC-free water.

Figures 7.9 – 7.11 indicate that degradation of carbon tetrachloride throughout the aquifer is more significant than contamination, as no sites plot above the present-day air-water equilibrium (Irton exhibiting the closest match).

7.4.4.2 Additional remarks

Section 7.4.4 has interpreted the variability in the CFC data in terms of operative factors such as degradation and contamination. However, it has done this within a broader conceptual scheme of the Corallian built up from previous findings of both the author and other workers. The differences between individual groundwaters are, therefore, also noted as being due to the type of sampling point (spring or borehole), location in the Corallian, lithology, fissuring, hydraulic gradients etc.

It should also be noted that the above discussion is not exhaustive, but hopefully gives a sufficient explanation of general properties by way of examining particular data points or groups of data points. It is obviously involved and one could wish for better quality data, as undoubtedly this would tighten the interpretation. Nonetheless, whilst many data indicate CFC contamination of the aquifer, three CFCs are better than one, so that often one of the three remains unaffected by any particular process, or at least there appears to be some agreements between data classified by independent principles. (CCl_4 is occasionally useful.) In particular, observed losses of the compounds of interest mirror the order of reactivity noted throughout the literature: CCl_4 > CFC 11 > CFC 113 > CFC 12. This is of particular interest in an aquifer considered to be oxidising and indicates that the influence of the matrix upon contaminant transport within fissures is significant over a timescale of several years.

Apparent ages of water may be derived from the data once care has been taken to filter it for non-conservative processes. However, it appears that mixing of different age waters is so prevalent that to state any date with precision is inadmissible on the basis of the CFC data. Thus, in several instances, it seems more plausible to present mixing models on the rough and ready assumptions of modern and CFC-free waters and on this basis the values in Table 7.4 are given.

	CFC 11			CFC 12			CFC 113			Average
	%	SD	n	%	SD	n	%	SD	n	
Irton PWS	103	117	18	59.6	16.7	20	68.7	62.4	3	77.1
Cayton Carr House Lane PWS	29.3	7	12	66.2	20.5	13	13.3	1	2	36.3
Cayton Station Road PWS	39.5	35.3	4	30	9.3	2	89.8	-	1	53.1
McCains Chipe Fictory	47.9	42.5	14	-	-	-	68.9	-	1	58.4
Ratten Row	83.4	53.5	6	86.8	41.6	3	-	-	-	85.1
Swallowholes BH	10.2	14.5	6	-	-	-	10.1	3	6	10.1
Augmentation BH	5.5	4.7	8	7.5	0.5	2	16.5	9	8	9.9
Tetherings Plump BH	22	11.1	7	55.1	25.9	8	-	-	-	38.5
Derwentdale Farm North BH	63.1	23.6	14	111	24.6	14	78.6	13.2	2	84.3
Derwentdale Farm South BH	20.6	23.3	9	53.9	24.7	9	-	-	-	37.2
Seavegate Gill BH	31.4	-	1	40.2	17.8	3	-	-	-	35.8
Cayton Bay Spring	-	-	-	-	-	-	32	21.1	2	32
Brompton Spring	95.4	65.5	12	88.4	71.8	7	-	-	-	91.1

Table 7.4 The percentage of modern waters contributing to Corallian groundwater on the basis of CFC concentrations in rainfall (and river water) and groundwater.

However, it is clear that the lower concentrations observed demand minimal modern waters, so that the paradox between large apparent age and observed fissure flow rates does require solving. Again a solution may lie in the matrix.

7.4.5 ADDITIONAL EVIDENCE FOR CFC DEGRADATION

In this study CFC 11 degradation is only qualitatively recognised by the presence of an additional peak closely associated with CFC 11 elution from the gas chromatograph, and which is assumed to be the first degradation product of CFC 11; HCFC 21. Such peaks are noted by Bateman (1998) who conducted her analysis using the same chromatographic column as used for the majority of this study[37]. They are observed in particular on chromatograms from the Augmentation and Swallowholes boreholes, but at other locations too, such as at Brompton. Such locations also tend to show the high nitrous oxide levels associated with nitrate reduction and which mask the CFC 12 peak on the chromatogram. This process is not necessarily associated with CFC 11 degradation, as may be observed from Figure 7.12, which depicts two chromatograms taken from springs on the northern escarpment. The first large peak (from the left) is N_2O. The small peak immediately adjacent to it is CFC 12, from which it can be seen how a large N_2O presence could obliterate a small CFC 12 signal. The next sizeable peak after CFC 12 is that of CFC 11. Note that in both chromatograms this is clearly a sharp, single peak. The first degradation product of CFC 11 (HCFC 21) would appear either very close to, or partially merged with, this peak, if it were to be found at all. CFC 113 appears as a very small peak (more of a bump) shortly afterwards.

[37] It is only possible to observe them on analyses of samples taken prior to the SF_6 experiment. The only boreholes where this is important are the Derwentdale South and Tetherings Plump boreholes, as all other sample locations were sampled prior to the GC column change.

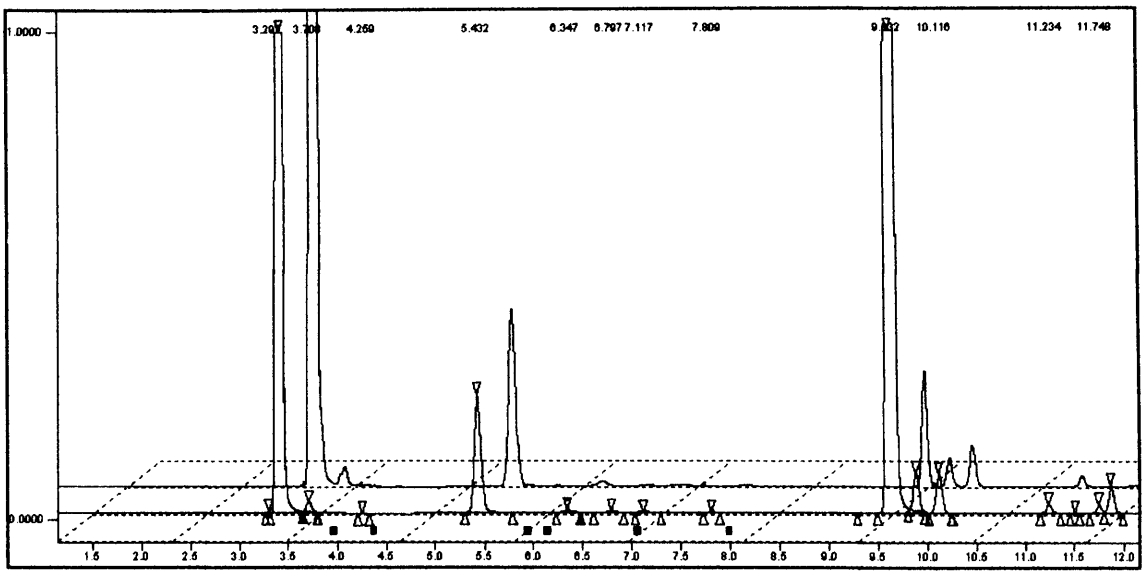

Figure 7.12 Two example chromatograms showing Glasshouses Spring (front) and Lady Mildred Spring (rear). See text.

The next large peak (Figure 7.12) is one of three. These are, respectively, $CHCl_3$ (tri-chloromethane, the first degradation product of CCl_4), CH_3CCl_3 (tri-chloroethane) and CCl_4 (carbon tetrachloride). In an atmospherically equilibrated sample, $CHCl_3$, the first peak, should be the smallest of the three (and CCl_4 the largest). It is thus clear that there is significant $CHCl_3$ enrichment in the north-eastern part of the aquifer. The CCl_4 depletion observed both here and elsewhere is thus likely to be due, in part, to biologically mediated transformation to $CHCl_3$. However, from the size of the $CHCl_3$ peak on the Glasshouses Spring chromatogram, it is unlikely to be due solely to CCl_4 degradation. Thus it seems possible that there is a source of trichloromethane somewhere on the outcrop of the aquifer (this spring is also contaminated with CFCs 11, 12 and 113). However, the point remains that nitrate and CCl_4 reduction may occur in the Corallian whilst CFC 11 remains untransformed. Figure 7.13, on the other hand, clearly shows additional peaks abutting CFC 11. Note also that ECD sensitivity is reduced for compounds with fewer halogens, so that equal peak areas do not indicate equal amounts of analyte, although in several instances the sizes of adjoining CFC 12 – HCFC 21 peaks were more or less equal.

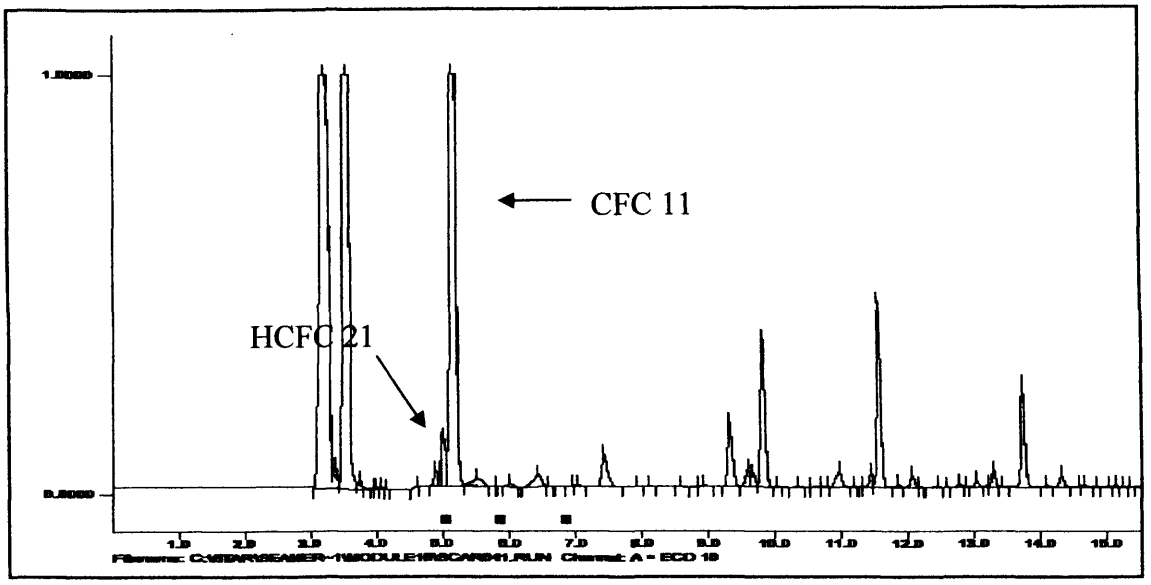

Figure 7.13 Chromatogram qualitatively indicating presence of the CFC 11 degradation product HCFC 21 (this chromatogram in fact from Seamer Carr).

7.4.6 MECHANISMS OF CFC ENRICHMENT

Some groundwaters sampled are so elevated in CFC that nothing but a point source contaminant can explain the concentrations observed. Such is the case for Glasshouses Spring (CFCs 11, 12 and 113 and trichloromethane) and Cayton Bay Spring (CFCs 11 and 12 and trichloromethane) (see Figures 7.1 – 7.4). As the land above the aquifer is considerably more developed toward the coast, residentially, industrially and militarily, it is not surprising that Cayton Bay, as a major natural discharge point for the aquifer, should experience greater levels of trace organic compounds.

Sources of contamination of Corallian groundwater are likely to be varied. The outcrop zones are typically agricultural, although there is a Royal Air Force radio station on Irton Moor, as well as numerous residential settlements. Plummer *et al.* (2000) refer to CFC 11 concentrations in groundwater elevated to 8 times atmospheric equilibrium, probably as a result of impurities in pesticides. Key *et al.* (1997) also report fluorinated pesticides as containing traces of CFCs. Similar agriculturally-related instances of CFC contamination include those reported by Spurlock *et al.* (2000) and Delin *et al.* (2000). Additional sources of contamination are very likely to be due to waste disposal on the outcrop. As the Corallian is a local building stone, there are very many small, disused, local quarries dotted across the Tabular Hills, and these are supplemented by small, natural gullies (e.g. at the head of Sawdon Beck and along Seavegate Gill). Inspection of these sites reveals dumping of agricultural and domestic wastes, including vehicles and other machinery, over many decades (although they mostly appear overgrown at present).

One of the most important sources of contamination in the aquifer is the River Derwent, which drains a large agricultural catchment prior to entering Forge Valley. ARUP (2000) report 15 pollution incidents on the upper reaches of the Derwent between 1982 and 1987. This factor probably accounts for the somewhat erratic concentrations of CFCs within the confined zone of the aquifer, although the

mechanism cannot be expected to affect the unconfined (spring) waters, as the majority of these are above the level of the swallowholes.

7.4.7 RIVER DERWENT CFC PROFILE

7.4.7.1 Atmospheric Equilibrium Ratios

Atmospheric Equilibrium Ratios (AERs) are the concentration of a CFC in a sample divided by the CFC concentration one would expect from atmospherically equilibrated water, subject to assumptions outlined in Chapter 3. An AER greater than 1 indicates a sample that has been enriched in some way, most likely through some local source of the CFC. An AER less than 1 indicates a sample with a CFC concentration explicable by reference to the atmosphere. Therefore CFC AERs are a good way of comparing waters with respect to modern equilibrium and also to compare different levels of contamination. Figure 7.14 exemplifies this in terms of a longitudinal CFC profile of the River Derwent between northings NGR TA 08 486000 and 481000 m.

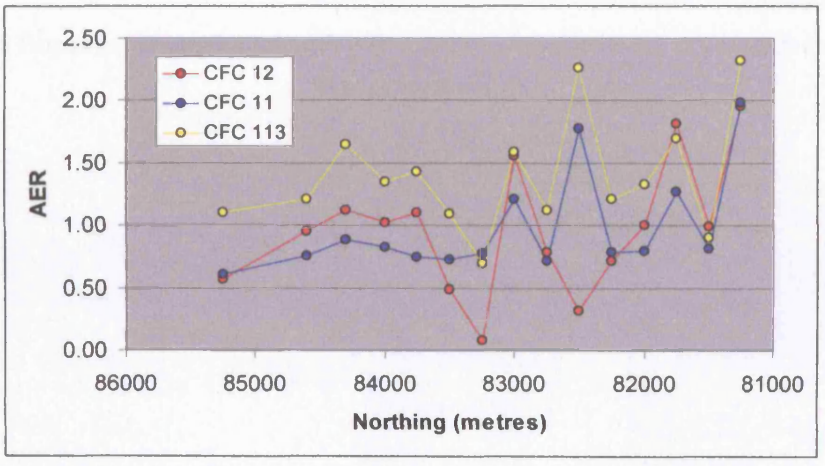

Figure 7.14 River Derwent CFC profile moving south from the Forge Valley swallowholes.

From the graph, there is a slight but persistent increasing trend among all three CFCs over the course of the sampling interval (c. 7.25 km of river). Variability in the data is roughly mirrored between CFCs indicating either a systematic error or a real phenomenon. Samples were taken over the course of five warm and largely rain-free days in mid-June, 2004, so that trends due to climatic factors may be disregarded. System performance was not noticeably erratic at this time either, with several well-replicated measurements from the Augmentation and Swallowholes borehole taken shortly afterwards (see Table 7.1). In particular, CFC 113 is above equilibrium along most of the entire interval measured, and rising in the south. CFC 12 is more-or-less at equilibrium over the northern part of the reach, with negative fluctuations possibly due to the influence of land drains discharging to the river as it moves into the Vale of Pickering (as at northing 83400). CFC 11 moves toward equilibrium with the atmosphere. The River Derwent above the swallowholes in Forge Valley is fed partly by springs issuing from the northern escarpment of the Corallian and Osgodby aquifers, so that under-equilibrated

water probably indicates a groundwater component. In places domestic and agricultural refuse was observed to be caught amongst branches, reeds etc. in the river.

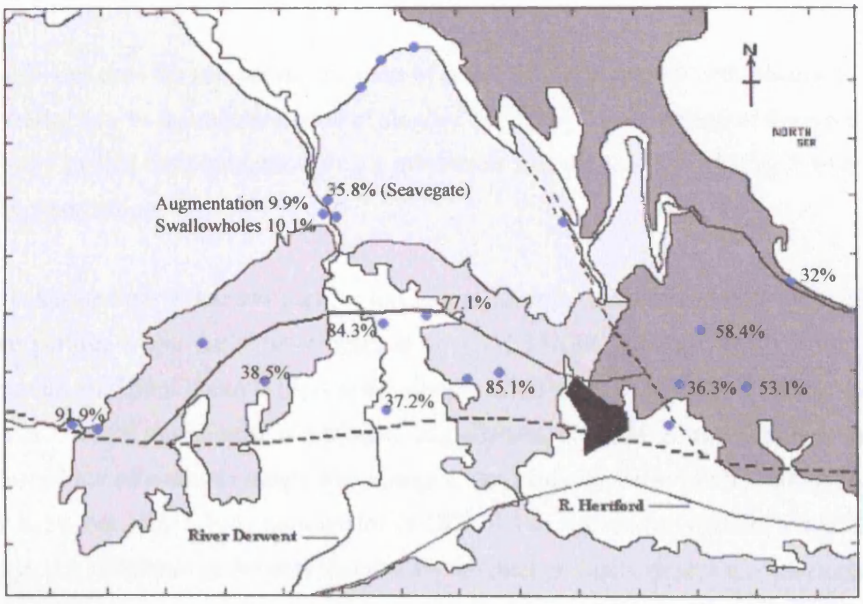

Figure 7.15 Percentage contributions of river water/modern recharge to groundwater, eastern Vale of Pickering.

7.5 FURTHER DISCUSSION

7.5.1 CFC RATIO AGES

CFC ratio ages are taken by comparing the ratio of two CFCs in a sample with historical equilibrium ratios, in a similar way to the determination of single-CFC ages. The advantage of the ratio approach is that dilution of a sample with old (zero-CFC) groundwater will not lead to a change in ratio, but only a reduction in concentration.

Most ratios calculated are either too high or too low to be matched with a historically existing ratio. The data that permits a plot for most samples is the CFC 11/CFC 12 data, as the maximum ratio is about 2.4 and the minimum about 0.17, a small amount of CFC 11 depletion still produces a dateable ratio. In contrast, where enrichment is a product of pollution, the ratio is more strongly affected, and thereby is moved out of dateable range. For example, the historical ratio of CFC11/CFC113 does not fall below 7.6, so that only a little enrichment in CFC 113 is required to depress the ratio out of the dateable range. An additional problem is that dually-enriched or dually-depleted combinations of CFCs give specious ratios.

Due to processes operating to enrich and deplete one or more CFCs in a sample, most ratio ages are considered unreliable and are not presented.

7.5.2 MIXING REVISITED

In Table 7.4 the percentages reported for each CFC were the averages as determined from the number of measurements cited. Data was subsequently excluded from the table on the basis of being higher than 100% of the atmospheric equilibrium value plus one standard deviation. In effect this excludes most contaminated samples but retains those seemingly enriched by only a small factor (and, of course, any depleted). The final column is the average of the remaining averages, and is plotted on Figure 7.15, from which some sensible patterns emerge.

Figure 7.15 agrees with previous findings from the aquifer, in that a corridor of higher permeability (represented by the Irton, Derwentdale Farm North and Ratten Row boreholes) is reflected by greater percentages of modern water, whereas more peripheral boreholes, or those not in the general direction of the main drainage, such as at Seavegate Gill, Derwentdale Farm South and Tetherings Plump, exhibit clearly lower percentages of modern water. The McCains and Cayton Station Road boreholes show similar, but reduced, modern components, whereas Cayton Carr House appears to be in something of a backwater. The dissolved oxygen data from Cayton Carr also support this interpretation, although the operatives at Irton pumping station note that this borehole undergoes turbidity fluctuations in line with major fluctuations at Irton as derived from the Derwent.

7.6 CHAPTER SUMMARY

Chapter 7 has presented CFC and CCl_4 data from Corallian groundwaters and the River Derwent. The distribution of these compounds have been mapped and their concentrations interpreted with reference to historical air-water equilibrium values on data cross-plots that also encompassed simple assumptions regarding the groundwater flow system. Much of the data is noisy and affected in places by, especially, degradation of CCl_4 and CFC 11 (and minor degradation of CFC 113) and contamination with CFCs 11, 12 and 113. Additional evidence for CFC degradation is discussed. Apparent ages of groundwaters are not considered to be as meaningful as mixing proportions between old and young waters, the distribution of which show distinct patterns explicable with reference to the basic conceptualisation of the system presented in Chapter 6. The patterns of CFC distribution in the aquifer offer insight into residence times and processes within the aquifer. Of particular interest is the widespread loss of CFC 11 in groundwater in a predominantly oxidizing aquifer. This result has implications for the removal of at least one major ozone-depleting gas of high global-warming potential, as many such aquifer CFC sinks may not have been identified due to their superficially oxidizing character. Groundwater contamination, on the other hand, is much more variable, indicating the presence of point-source contaminants and possibly contaminant pulses moving along the Derwent from time to time. A further study of CFC contamination in the Vale of Pickering is given in the next chapter.

CHAPTER 8

RESULTS AND DISCUSSION IV
SEAMER CARR LANDFILL, A CFC SURVEY

Or:

What we might call, by way of eminence, the dismal science.

Thomas Carlyle, 1850

8.1 INTRODUCTION

Seamer Carr landfill represents the largest potential source of CFCs in the field area. Through working with the Environment Agency (York Office), on other aspects of this research, it became clear that there was a lack of understanding of how significantly Seamer Carr landfill was impacting groundwater and surface water in the Vale of Pickering. As a further landfill CFC study was the logical progression of the work done by Bateman (1998) and Atkinson (2002), and as this would also clarify the relationship between the landfill and the Corallian aquifer, it was decided that a CFC survey of Seamer Carr would form a component of the research.

The survey comprised the measurement of CFCs 11, 12 and 113, and CCl_4, in water samples from 28 locations (groundwaters and surface waters) as well as measurements of landfill leachate and landfill gas. Temperature and conductivity measurements of adjacent and nearby surface waters are also presented. The chapter begins with a brief note on previous work conducted on the site. It continues with a more detailed report of site topography and hydrology, which in turn leads to a discussion of hydrogeological conceptualisation based upon a critical review of the existing conceptualisation and primary data. The chapter continues with the presentation of results in the form of CFC and CCl_4 profiles of two drainage dikes and the River Hertford and envelope diagrams of CFC and CCl_4 concentrations in groundwater. The chapter reworks material directly from reports written by the author and submitted to consultants responsible for coordinating a larger environmental impact assessment of Seamer Carr at the time (CarlBro, 2004).

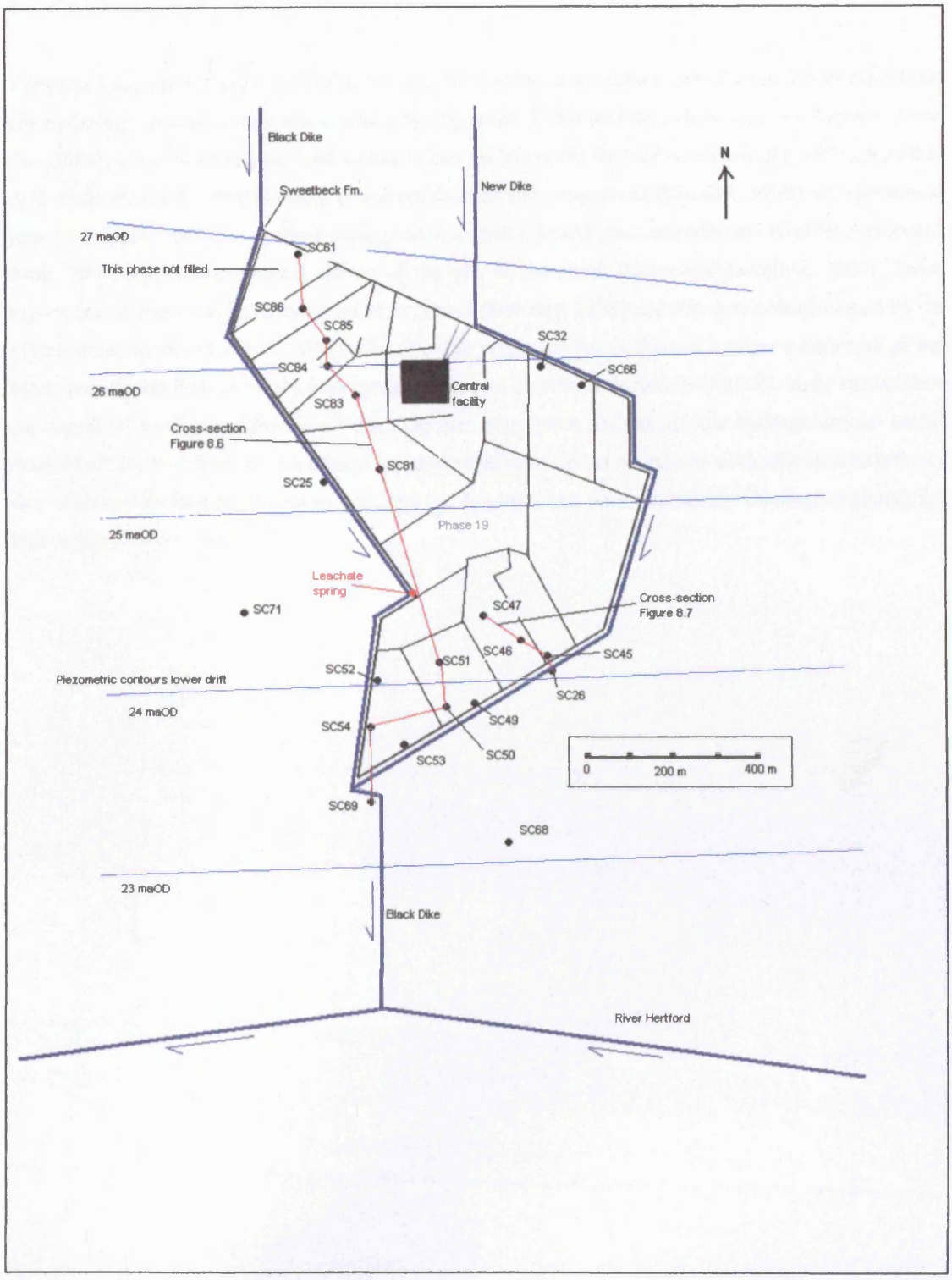

Figure 8.1 Seamer Carr landfill site layout indicating main drainage ditches and the River Hertford; boreholes used for either sampling, water level measurements or to construct cross-sections; positions of cross-sections; approximate piezometric contours in the lower drift; the central site facility (including leachate sump and methane-fuelled electricity generator) and separation of landfill into phases (Phase 19 labelled).

8.2 PREVIOUS WORK

Yorwaste Ltd., the company managing the site, has produced or commissioned a number of reports on site hydrology, hydrogeology and leachate management. These include a desk study by Aspinwall and Co. (1996), a review of geology and hydrogeology by Yorwaste themselves (Yorwaste, 1995), a further desk study (SECOR, 1998) leading to a more detailed risk assessment (SECOR, 1999), an operational plan (Yorwaste, 2000), a leachate management assessment and recommendations (Golder Associates 2000, 2001) and a hydrological survey of the carr to the south (Hann and Lovelace, 2000). These reports are further supplemented by an M.Sc. thesis (Delaney, 2000) and a review commissioned by the environment agency (Carlbro, 2004). The research presented herein formed a major component of the latter, namely the formation of a conceptual site model and the undertaking of a CFC study to elucidate the degree of leachate migration off-site. The site description and conceptual hydrogeological model detailed below are based upon a critical re-interpretation of the above reports with reference to primary data sources provided by Yorwaste Ltd. and the Environment Agency, namely lithological (borehole) logs and piezometric data.

8.3 SITE DESCRIPTION

8.3.1 SITE DESCRIPTION AND LOCATION

Seamer Carr landfill is located approximately 8 km south of Scarborough (see Figure 7.1). The waste disposal facility comprises 19 phases of landfill, a leachate storage lagoon, a municipal waste and recycling centre, and a small area dedicated to wildlife habitat. The site area is approximately 59 hectares in total and has received predominantly domestic and light-commercial wastes (Delaney, 2000). There are approximately 90 boreholes on site, drilled progressively as the site was developed. Figure 8.1 illustrates the site layout, the boreholes used for deriving cross-sections, as well as CFC sampling locations. The surrounding land use is summarised by SECOR (1999) as follows:

North: Eastfield Industrial Estate (0.8km). Residential estates of Crossgates and Eastfield, 1km north.
North-east: Scarborough – Filey railway along perimeter
East: Agricultural land.
South-east: Agricultural land.
South: Agricultural land. River Hertford 0.5km from site perimeter.
South-west: Agricultural land.
West: Agricultural land. A64 (T) Seamer by-pass approximately 1km.
North-west: Yorkshire Wildlife Trust Nature Reserve situated within old disused sand and gravel workings (Burton Riggs) that now forms several ponds.

8.3.2 TOPOGRAPHY AND HYDROLOGY

8.3.2.1 Topography

The topography beneath and immediately around the landfill (actually a landraise) descends from somewhat hummocky (morainic) terrain, at approximately 30 maOD in its northern part, onto flatter, drained carr lands (c. 25 maOD, former lake bed) in its southern part. Prior to tipping, some gravels were either removed or levelled on site, so that a fairly even pre-tip surface gradient appears to have been the result (see also Figure 8.6, Section 8.3.3).

8.3.2.2 Hydrology

The eastern end of the Vale of Pickering is drained by the River Hertford, which is fed by an extensive and well-developed network of drains and dikes. This extensive network is intended to make the low-lying carr lands in the centre of the Vale suitable for agricultural purposes. The River Hertford (due to considerable engineering now essentially a very large ditch) is a tributary to the River Derwent, joining its course some 6 km downstream (west) of Seamer Carr landfill. Flow in the River Hertford is estimated to be c. 50 Ls^{-1} (Aspinwall, 1996). However, the nearest surface watercourses to the landfill site are the New Dike and Black Dike drainage channels that bound the western, north-eastern, eastern and

southern extent of the Seamer Carr facility (Figure 8.1). The New Dike enters the site from the industrial estate to the north, it then flows south-east through a culvert along the (north-eastern) boundary with the railway line before re-emerging as an open ditch to run along the eastern and southern boundaries of the site. The Black Dike flows south along the western site boundary. The Black Dike converges with the New Dike and another drainage ditch (fed from the west) at the southern tip of the landfill, and then flows southwards across Star Carr to the River Hertford.

Results of preliminary measurements of temperature and conductivity of the Black and New Dikes, made as part of this research, are shown in Figures 8.2 to 8.5. They show measurements taken on 04/02/2004, a dry, cold day (approaching zero degrees), when ambient air and runoff temperatures were low. The conductivity trend in the Black Dike (Figure 8.2) is strongly augmented by the influence of a leachate 'spring' that was issuing from Phase 19 adjacent to the dike. At the time of measurement this 'spring' was flowing weakly over the edge of the bund containing Phase 19 and into a small depression, from which it was only a very short distance from the dike (< 5 m). This is most probably responsible for the step in conductivity between 500 and 650 m (Figure 8.2). Groundwater seepage from land abutting the wastes (i.e. within the area enclosed by the two dikes) is visible at the southern end of the Black Dike. Agricultural land to the west of the landfill also contributes flow to the Black Dike through regularly spaced (c. 25 m) field drains, approximately 1.5 m below the soil surface. This is likely to account for some of the increase in temperature, if not conductivity also (Figure 8.3). Along the New Dike there is also a steady increase in temperature (Figure 8.5), although fewer field drains were in evidence east of the landfill in early 2004. However, the conductivity profile (Figure 8.4) shows only a weak upward trend following the influx of another drainage ditch flowing from the east. This ditch is responsible for the strong dip in the profile at c. 1000 m. Altogether the temperature profiles indicate greater groundwater influence on dike flow toward the south, whilst conductivity changes are strong in the dike obviously affected by leachate but less apparent in the other. Flow gauging has not been performed on these watercourses, although Aspinwall (1996) estimates 10 and 5 Ls^{-1} respectively.

The effective rainfall for grassy ground (i.e. surplus depth of precipitation after allowing for an estimate of actual evapotranspiration) is given by Aspinwall (1994) as 265 $mmyr^{-1}$, and adjusted (Aspinwall, 1996) to 360 $mmyr^{-1}$ for "bare ground or waste covered by soil", that is, taking into account the nature of the partially covered ground surface. On site some ponding occurs over the top of the landfill, particularly on the restored phases in the south (Phases 16, 14, 12 and 5), with surface runoff captured by the Black and New Dikes.

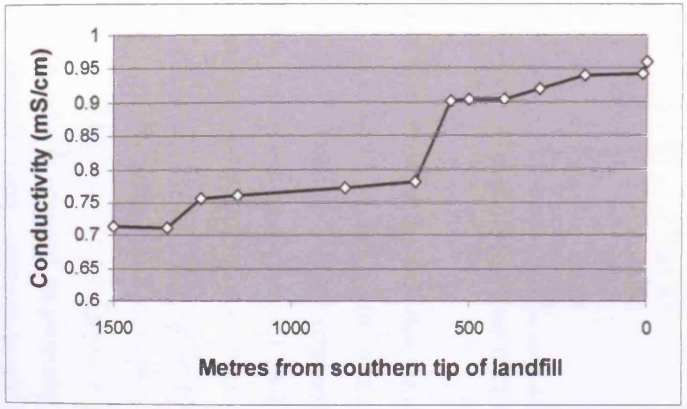

Figure 8.2 Conductivity profile of the Black Dike (north to south).

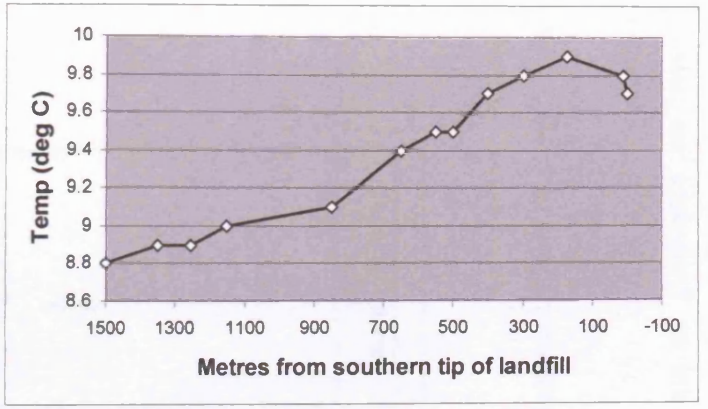

Figure 8.3 Temperature profile of the Black Dike (north to south).

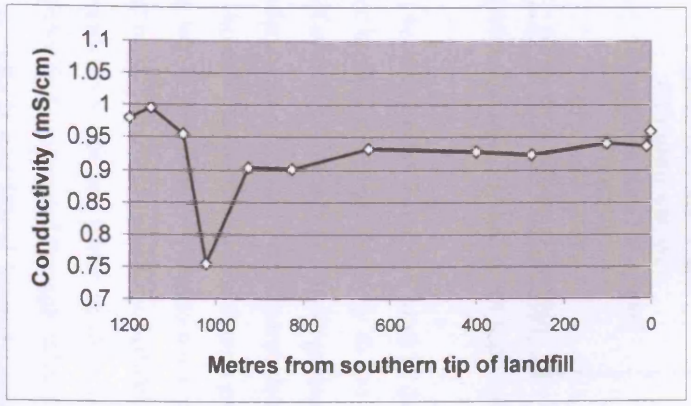

Figure 8.4 Conductivity profile of the New Dike (north to south).

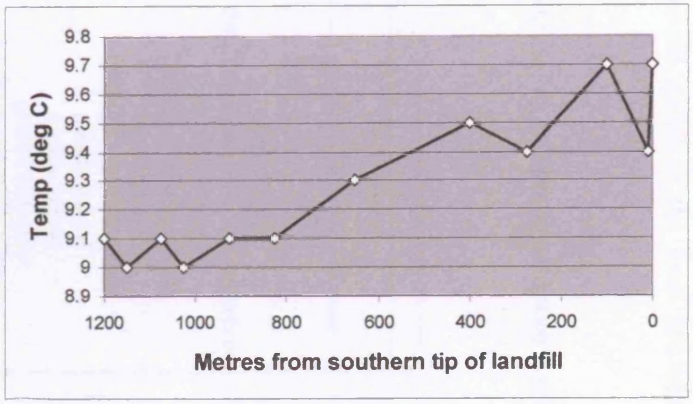

Figure 8.5 Temperature profile of the New Dike (north to south).

8.3.3 HYDROGEOLOGICAL CONCEPTUALISATION

Using lithological information derived from a nearly-complete set of borehole logs, plus monitoring of piezometric heads during 1997 and 1998 (SECOR, 1998; Delaney, 2000; Golders, 2000; pers. comm. Yorwaste; see Appendix 7 for this data), a conceptual model of the local hydrogeology was constructed.

Table 8.1 shows an example borehole log, in fact the first log to have been drilled on-site in 1977 (SC1).

BH1 drilled 1977		
Depth of change mbgl	**Thickness m**	**Description**
0	0	
1.92	1.92	Black peat
2.87	0.95	Silty sand with clay and organics
3.19	0.32	firmish silty clay
3.32	0.13	sandy clay with gravel
6.75	3.43	sandy gravel
7.25	0.5	sandy clay with gravel
15.09	7.84	sandy gravel
17.89	2.8	sandy gravel
21	3.11	gravel with clay
21.2	0.2	sandy clay with gravel
21.47	0.27	Silty sand with clay
23.63	2.16	silty sand w. clay and gravel
27.72	4.09	silty sand
28.61	0.89	silty sand w. clay
36.11	7.5	sandy clay with sand partings

Table 8.1 Borehole log from SC1 illustrating frequent variations in sediment type with depth.

From this log it can be seen that the drift is extremely heterogeneous. However, most of the boreholes were not drilled to this depth (many of the shallower boreholes penetrating only to the base of the wastes), although several are screened in the lower half of the drift, that is at a depth greater than 10 m (these are noted on Figure 8.1 and subsequently referred to as 'lower' drift boreholes; boreholes screened above this depth are termed 'upper' drift boreholes). The comparison of these logs shows that individual units may or may not be present beneath the whole site. However, due to most of the deeper boreholes exhibiting the sort of heterogeneity observed in SC1, there appears little justification for the conceptual division of the Quaternary deposits into separate upper and lower aquifers units, with a variably present aquitard, as proposed by Aspinwall (1996) and propagated through subsequent reports (e.g. SECOR 1998, 1999; Delaney, 2000). Given the vertical and lateral heterogeneity it is both conceptually easier and more defensible to consider the drift as a single heterogeneous mass, and this approach is adopted here.

Only one borehole (SC66) penetrates the top of the Corallian, doing so at 43 m below ground level having passed through some 11 m of Kimmeridge Clay. This point (Figure 8.1) is clearly north of the Ebberston-Filey fault, which is inferred (from the BGS *Solid and Drift, 1:50 000* geological map) to

pass beneath the southern part of the site. The measured heads from SC66 are given in Table 8.2, with a comparison of piezometric head from the nearest borehole screened in the lower part of the drift (SC32, c. 150m distant). This table clearly illustrates an average head difference of greater than 2.5m over the course of a year.

Date	SC66 Corallian maOD	SC32 lower drift maOD
Jul-97	27.7	25.7
Sep-97	27.88	25.64
Oct-97	27.89	25.62
Nov-97	27.87	25.68
Dec-97	28.16	25.66
Feb-98	28.45	25.63
Mar-98	28.86	25.62
May-98	28.95	25.7
Jun-98	28.97	25.61
Avg.	28.30	25.65
Difference (m)		2.65

Table 8.2 Piezometric levels at the top of the Corallian (SC66) and in the lower part of the drift (SC32) between July 1997 and June 1998. See Appendix 7 for complete data set.

The Corallian is artesian throughout large parts of the eastern Vale of Pickering (to over three metres above ground level at Irton), although at SC66 the Corallian water level does not rise above the ground surface (at 30.17 maOD). The observed upward gradient between the Corallian and the lower drift is continued in a more muted form through the drift, where vertical head differences of several centimetres are observed in a number of dual-level observation boreholes screened at different depths in the drift (Table 8.3).

Borehole	Upper maOD	Lower maOD	Difference m
SC26	24.01	24.14	0.13
SC68	23.8	23.99	0.19
SC69	23.46	24.01	0.55
SC70	24.49	24.4	-0.09
SC71	24.93	25.1	0.17
SC72	25.21	25.39	0.18
SC73	25.97	26.14	0.17

Table 8.3 Average monthly piezometric heads in dual-level piezometer installations at Seamer Carr over the period January 1997 to June 1998. Note that a positive difference implies an upward gradient (and vice-versa). Data reworked from that given in full in Appendix 7. Piezometer locations are shown on Figure 8.1.

As at least part of the landfill site is north of the Ebberston-Filey fault, and as the Kimmeridge Clay is thin north of the fault (as shown in SC66), it is likely that it does not completely confine the Corallian,

or that the fault acts as a conduit for flow itself. It is probable, therefore, that the upward gradient observed in the drift deposits is due to the greater upward gradient observed between the Corallian and the drift.

On the basis of data compiled from SECOR (1998), Delaney (2000), Golders (2000) and additional data supplied by Yorwaste Ltd. (personal communication) (all data given in Appendix 7), analysis of piezometric heads across the landfill site indicates a north to south hydraulic gradient of about 0.003. This is comparable to values given by Aspinwall and Co. (1996), who cite between 0.003 and 0.008 and by SECOR (1999), who also cite 0.003. These values indicate a drop in hydraulic head of approximately 4 m between the northern and southern ends of the landfill, which is considerably greater than the vertical head differences observed at individual points.

To analyse the position of piezometric heads with respect to the base of the wastes, and to construct a piezometric map of the site, piezometric data from boreholes screened in the lower part of the drift, where the hydraulic heads are highest, have been used to plot Figures 8.6 and 8.7 (along cross sections shown in Figure 8.1) and to plot the potentiometric surface shown in Figure 8.1.

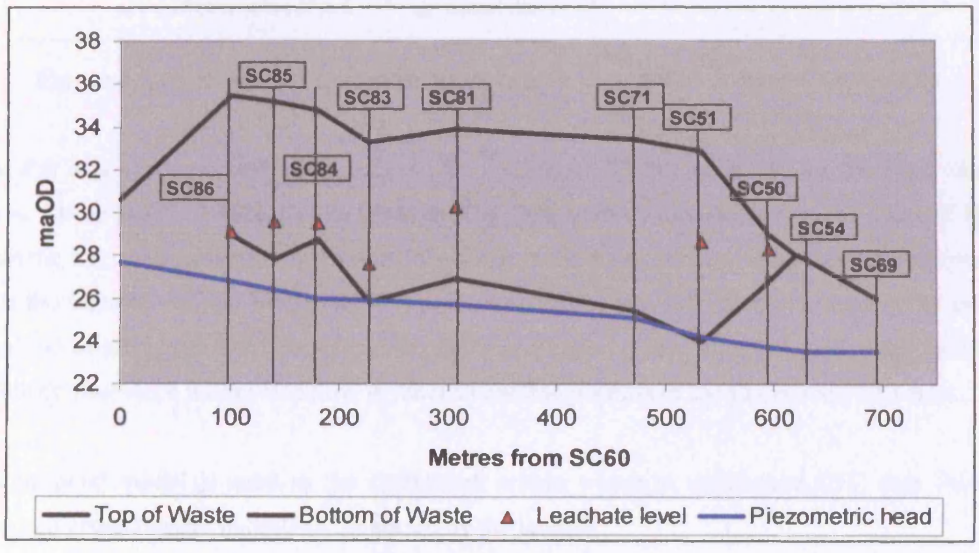

Figure 8.6 Cross section through Seamer Carr landfill, north to south (left to right). See text for further details.

Figure 8.6, a schematic north-south cross-section across the landfill site, shows that the hydraulic head in the lower part of the drift overlaps the base of the wastes as one moves southward. This is because the slope of the potentiometric surface is shallower than the slope of the ground surface, so that eventually the latter intersects the former. It is certainly possible that this results in groundwater discharge to the wastes, as the temperature (and possibly conductivity) profiles of the Black and New Dikes indicate the increasing prevalence of groundwater discharge to the surface toward the southern part of the landfill. Additionally, within individual phases (refer to Figure 8.1 for phase locations),

different levels of leachate can be observed (red triangles indicating measured leachate levels). These data points have not been joined together because they are in separate, bunded phases (apart from wells SC51 and SC50). A similar construction (Figure 8.7) can be made for Phase 12 (and part of Phase 5). The leachate level in Phase 12, as in several of the (unlabelled) phases in Figure 8.6, is obviously perched above the base of the wastes and is considerably higher than can be accounted for by groundwater heads within the drift.

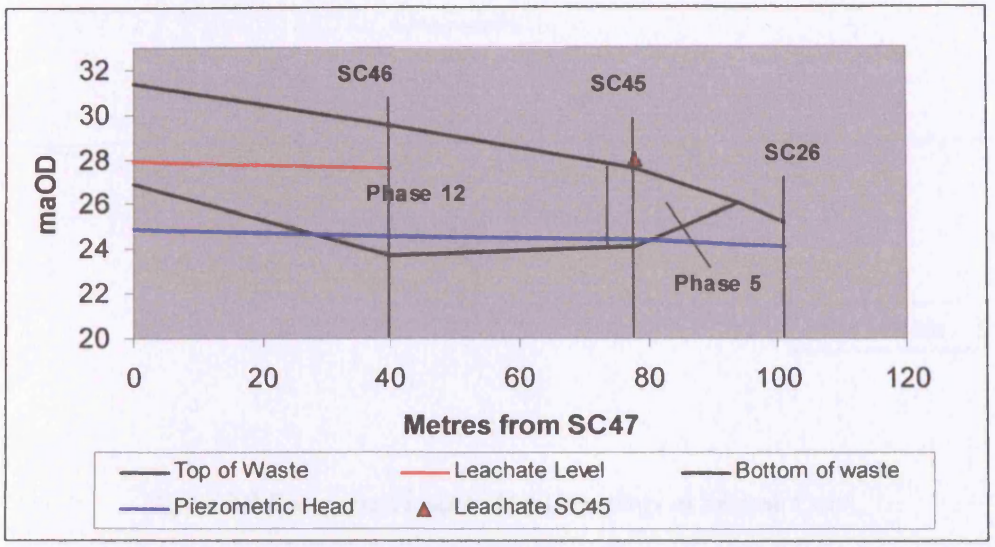

Figure 8.7 Cross section drawn through Phases 12 and 5 of Seamer Carr landfill.

Figure 8.8 is a simple conceptualisation of site hydrogeology that accounts for the main observed features. These are the hydraulic gradients driving flow both southward across the site and upward beneath the site; the position of the piezometric heads in the lower drift in relation to the position of the base of the wastes; leachate heads within the waste above the possible hydraulic head in the drift; the intersection of the piezometric heads and the drainage network in the southern part of the landfill; the probable driving force for upward flow in the drift and the position of the Ebberston Filey fault.

The conceptual model is used as the framework within which to understand CFC data from both surface and groundwaters potentially impacted by the landfill.

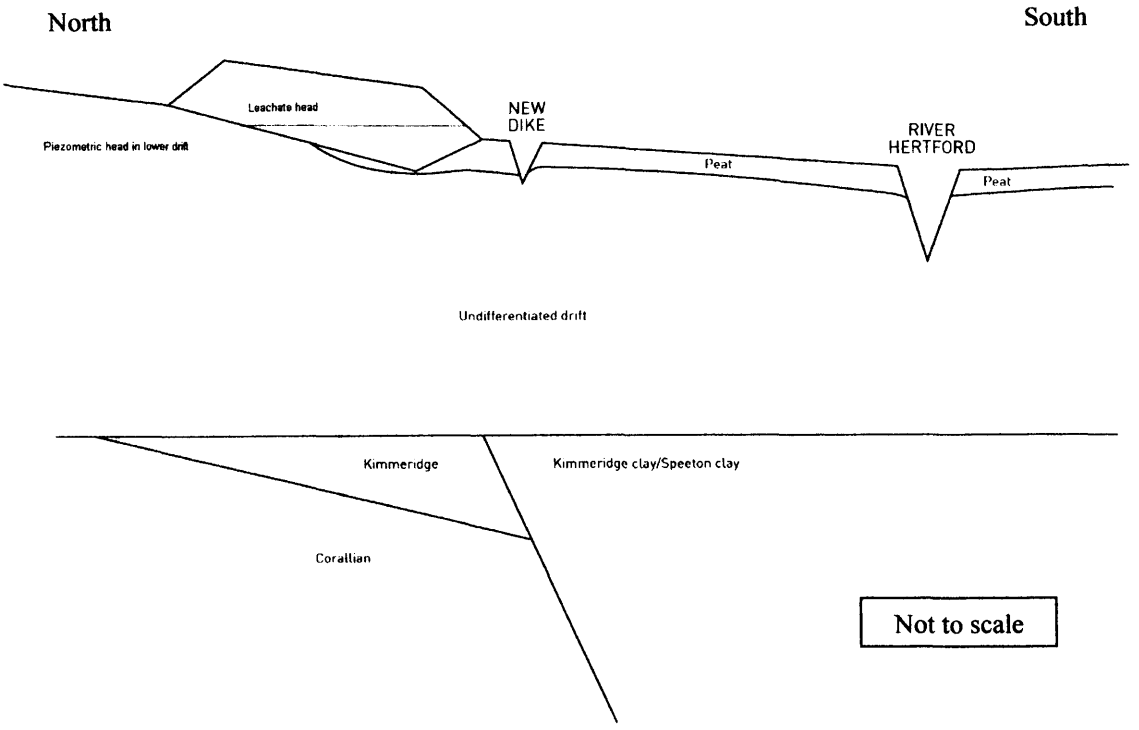

Figure 8.8 Conceptual model of hydrogeology at Seamer Carr.

8.4 SAMPLING SITES FOR THE CFC SURVEY

Sampling sites were chosen on the basis of earlier site inspections with the aim of investigating the relationship between the River Hertford and possible contamination spreading from the landfill. Watercourses adjacent to the landfill were obvious potential receptors for leachate contamination, and so CFC profiles of the New Dike, the Black Dike, and the River Hertford were made. Groundwater from the drift aquifer beneath and adjacent to the site was sampled from locations chosen on the basis of previous hydraulic head and water quality data.

Sampling procedures, analytical method, detection limits and measurement errors are presented in Chapter 4. The majority of samples were analysed on the day of collection and all samples were analysed within 24 hours of collection.

8.5 RESULTS AND DISCUSSION

8.5.1 DATA

All CFC and CCl_4 results are given in Table 8.4

Location	Grid reference	Sample Date	CFC12 pg/kg	CFC11 pg/kg	CFC113 pg/kg	CCl4 pg/kg
River Hertford	TA08 082 804	24/02/2004	*393.67*	*560.48*	*488.85*	*1291.85*
River Hertford	TA08 056 806	24/02/2004	369.36	611.03	5265.03	1264.25
River Hertford	TA08 056 806	24/02/2004	117.50	495.98	5337.29	1309.82
River Hertford	TA 08 390 811	24/02/2004	53.36	622.41	4053.61	1312.56
River Hertford	TA 08 390 811	24/02/2004	406.67	860.38	4453.42	1367.44
River Hertford	TA 08 440 810	24/02/2004	56.99	732.27	5131.01	1323.69
River Hertford	TA 08 440 810	24/02/2004	6.70	972.14	5055.28	1233.20
River Hertford	TA 08 360 812	24/02/2004	168.47	700.51	4276.84	1311.35
River Hertford	TA 08 360 812	24/02/2004	123.03	452.59	4173.22	1311.67
River Hertford	TA 08 320 812	24/02/2004	246.76	649.26	3467.26	1327.00
River Hertford	TA 08 320 813	24/02/2004	202.48	723.18	3352.39	1361.74
River Hertford	TA 08 290 811	24/02/2004	7695.12	1792.79	2171.94	1154.67
River Hertford	TA 08 290 811	24/02/2004	21556.07	2511.63	2138.25	1272.92
River Hertford	TA 08 260 810	24/02/2004	19667.13	1260.57	2333.17	1185.17
River Hertford	TA 08 260 810	24/02/2004	16884.38	1156.90	2026.54	1126.94
River Hertford	TA 08 220 809	24/02/2004	16167.34	1190.55	1736.93	950.24
River Hertford	TA 08 220 809	24/02/2004	15257.11	1166.06	1926.19	1014.24
Black Dike	TA 08 029 829	25/02/2004	865.28	796.63	119.15	994.63
Black Dike	TA 08 029 829	25/02/2004	866.40	945.31	241.18	1143.02
Black Dike	TA 08 032 820	25/02/2004	37274.49	8097.11	132.45	893.64
Black Dike	TA 08 032 820	25/02/2004	91404.86	7722.03	150.51	892.94
Black Dike	TA 08 031 815	25/02/2004	47202.28	5157.49	202.46	1055.75
Black Dike	TA 08 031 815	25/02/2004	47290.49	3895.96	119.99	965.05
Black Dike A64	TA 08 028 833	25/02/2004	306.79	1007.95	<detection limit	1456.80
Black Dike A64	TA 08 028 833	25/02/2004	123.71	764.84	130.05	1493.17
New Dyke	TA 08 031 815	25/02/2004	368.18	590.13	268.27	1418.63
New Dyke	TA 08 031 815	25/02/2004	978.75	708.00	205.79	1391.54
New Dyke	TA 08 036 819	25/02/2004	338.92	1310.55	266.57	1602.33
New Dyke	TA 08 036 819	25/02/2004	922.63	626.22	138.17	1357.57
New Dyke	TA 08 037 823	25/02/2004	466.89	3908.95	851.72	1704.06
New Dyke	TA 08 037 823	25/02/2004	426.49	4992.55	982.68	1973.10
New Dyke	TA 08 034 831	25/02/2004	*639.68*	*758.38*	*137.68*	*910.33*
Grove Fm	TA 08 044 821	26/02/2004	<detection limit	146.02	17.75	9.98
Grove Fm	TA 08 044 821	26/02/2004	<detection limit	6.20	22.07	13.93
OBH SC25 deep	See map Seamer Carr	06/04/2004	154.82	146.95	29.20	49.98
OBH SC61	See map Seamer Carr	06/04/2004	92.78	210.56	37.16	106.58
OBH SC61	See map Seamer Carr	06/04/2004	264.52	1060.91	60.07	120.61
OBH SC68	See map Seamer Carr	06/04/2004	229.10	338.72	97.66	127.35
OBH SC68	See map Seamer Carr	06/04/2004	7.39	62.76	<detection limit	117.76
OBH SC71	See map Seamer Carr	06/04/2004	80.25	88.10	26.22	81.99
OBH SC71	See map Seamer Carr	06/04/2004	86.18	119.07	32.83	92.68
OBH SC53	See map Seamer Carr	06/04/2004	3301.44	304.91	35.70	306.48
OBH SC53	See map Seamer Carr	06/04/2004	4619.44	145.75	17.20	154.24
OBH SC49	See map Seamer Carr	06/04/2004	486.69	150.32	18.19	116.73
OBH SC49	See map Seamer Carr	06/04/2004	253.35	157.59	18.85	163.31
OBH SC 54	See map Seamer Carr	06/04/2004	846.68	433.89	41.04	160.52
OBH SC54	See map Seamer Carr	06/04/2004	659.26	175.85	13.87	82.09
OBH SC52	See map Seamer Carr	06/04/2004	123.17	56.29	<detection limit	37.03
OBH SC52	See map Seamer Carr	06/04/2004	129.66	107.65	26.04	80.88
OBH SC26 Deep	See map Seamer Carr	06/04/2004	*171.77*	*219.57*	*63.20*	*127.25*
OBH SC26 Shallow	See map Seamer Carr	06/04/2004	367.15	85.66	21.24	52.30
OBH SC26 Shallow	See map Seamer Carr	06/04/2004	434.24	200.84	18.58	120.19
Leachate sample	See map Seamer Carr	06/04/2004	293104.48	3896.82	<detection limit	57.88
Landfill Gas	See map Seamer Carr	06/04/2004	2449037.60	336749.18	28658.63	621.28
Landfill Gas	See map Seamer Carr	06/04/2004	2346314.92	311512.36	12479.01	626.98

Table 8.4 CFC and CCl_4 results from Seamer Carr landfill site.

8.5.2 THE BLACK AND NEW DIKES

As the Black and New Dikes run broadly from north to south, Atmospheric Equilibrium Ratios (AERs, see previous chapter for the definition) have been plotted as metres north of the latitudinal line at NGR TA08 480000. For example, Figure 8.9 shows AERs for the Black Dike sampled at Northing 483200, 482850, 482000 and 481600 (i.e. north to south). Similarly, River Hertford CFC AERs are plotted as metres east of the longitudinal line at Easting, NGR TA08 500000. These watercourses do not run due north-south or east-west, but this approximation is sufficient to elucidate the impact of the landfill on them and permits their easy location on an Ordnance Survey map.

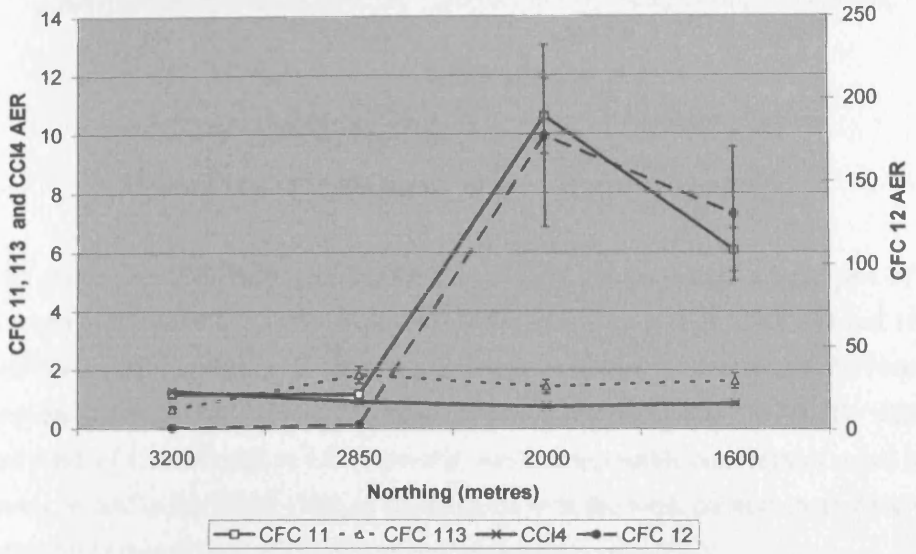

Figure 8.9 CFC AER profile of the Black Dike. Note dual axes.

Figure 8.9 shows the AER for CFCs 11, 12 and 113, plus CCl_4, along a profile of the Black Dike, from north to south (left to right). There are only four sample locations. The first is c. 1 km north of the landfill. This location represents water that has drained the housing and industrial estates to the north, but is upgradient of, and not expected to be impacted by, the landfill and is thus a background sample. The second point is at the very northern tip of the landfill site (at Sweetbeck Farm). The third is adjacent to the leachate 'spring' referred to in Section 8.3, and the fourth is just before the Black Dike meets the New Dike, i.e. at the southern extremity of the landfill.

It is obvious from Figure 8.9 that the landfill is significantly affecting the AER of CFCs 11 and 12 in the Black Dike, CFC 12 being some 180 times the concentration that may be expected from atmospheric equilibrium. CFC 113 and CCl_4 do not exhibit any significant change due to the presence of the landfill, with AERs of up to 1.75 accountable for by other industrial/domestic sites in the area. The CFC 113 content of landfill leachate is very low in any case (see Table 8.4). In comparison with the conductivity profile of the Black Dike, where there is an increase in conductivity at this same point, the sensitivity of the CFC method can be seen. The conductivity profile increases from about 0.8 $mScm^{-1}$ to 0.9 $mScm^{-1}$, an increase of about 12.5 %. In contrast, the CFC 12 profile increases from an AER of about 1 to an AER of 180, a factor of 180. This is 1440 times more sensitive than the conductivity, a standard and widely-applied indicator of landfill contamination (e.g. Fetter, 1998).

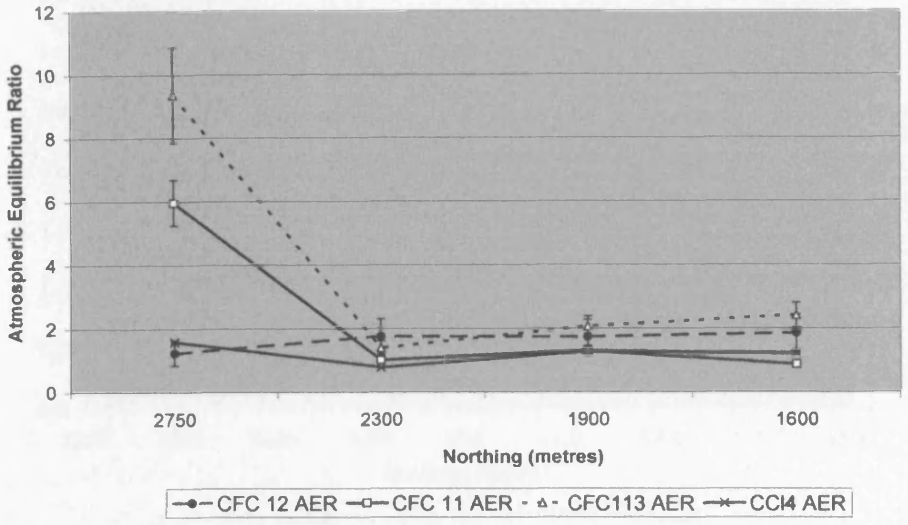

Figure 8.10 CFC AER profile of New Dike (north to south).

Figure 8.10 shows the CFC AER profile of the New Dike, which drains a large part of Eastfield industrial estate to the north and shows high background concentrations of CFCs 113 and 11 before it has reached the landfill site. These elevated AERs have reduced to c. 1-2 by the time the New Dike has flowed past the entire landfill. The only steady increase observed is that of CFC 12, rising from a background AER of 1.23, through to 1.86. However, whilst this possible contaminant signal is nowhere near as strong as that in the Black Dike, in combination with the weak positive trend observed in the conductivity profile dike (Figure 8.4) it should not be dismissed completely.

8.5.3 THE RIVER HERTFORD

Figure 8.11 shows the CFC AER profile along the River Hertford from west (on the left) to east. The river flows from the right to the left, with most of the samples upstream of the confluence of the Hertford with the Black Dike (which is at 3100 m). Along this upper stretch CFC 12 exhibits AERs less than 1 until it jumps to about 40 times atmospheric equilibrium (AE) at the first point (at 2900 m) past the confluence. CFC 11 behaves similarly, reaching nearly 3 times AE at the same point. That the concentrations of both CFCs 11 and 12 are consistently just below AE until this point indicates that groundwater and runoff feeding the Hertford in its eastern reaches is not contaminated by CFCs (either from the landfill or any other source).

The same, however, cannot be said for CFC 113, which shows strongly elevated AERs (c. 50) from what appears to be a point source somewhere downstream of NGR TA08 082 804 (i.e. downstream of point 8200 on the diagram) CFC 113 shows a steadily declining trend (to AER < 30) in the Hertford after the supposed point-source, which continues past the confluence of the Hertford and the Black Dike, in line with the undetectable levels of CFC 113 in landfill leachate.

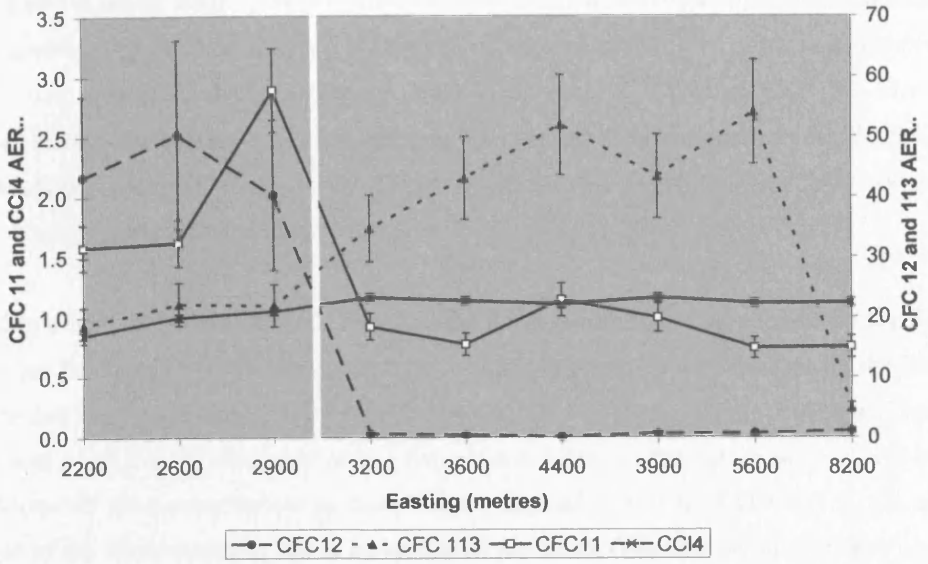

Figure 8.11 River Hertford CFC AER profile. White line marks position of confluence.

CCl_4 exhibits a fairly uniform AER of 1, indicating equilibrium with the atmosphere and an absence of further sources.

8.5.4 LEACHATE CONTRIBUTION TO DIKE AND RIVER FLOW

Equation 6.5 is used to calculate mixing proportions between leachate and surface waters. The calculation is performed individually for both CFCs 11 and 12, as these are present in significant concentrations in leachate and landfill gas, but not in background samples. CFC 113 and CCl_4 are excluded as they either have high and variable background values (CFC 113) or there is little difference between the leachate and the background signal (CCl_4). The results are given in Table 8.5

Watercourse	CFC 12	CFC 11
	%	%
Black Dike (Gas-Eq.)	4	1
Black Dike (Leachate)	22	-
Hertford (dike contribution)	30	40
Hertford (leachate contribution)	1.2	0.4
Hertford (leachate contribution)	6.6	-

Table 8.5 Calculated percentage contributions of leachate to flow in the Black Dike and the River Hertford based on CFC 11 and CFC 12 measurements.

Results of this simple model indicate that the minimum leachate contribution to flow in the Black Dike is between 1% and 4%, and the maximum contribution is 22%. Two figures are given for these calculations (the first two rows). The first is based upon the contribution that would be expected from a leachate that was in equilibrium with the landfill gas. As this is higher than the measured leachate value the volumetric contribution is smaller (top row). The second row gives volumetric contributions on the basis of actual measured leachate concentrations. As these samples were obtained from the leachate collection sump in the main compound (Figure 8.1), which is open to the atmosphere and collects

leachate from the whole landfill, these values are lower than the water-gas equilibrium concentrations, so that a greater proportion of leachate is required to account for the concentrations observed in the dike. The two columns reflect calculations made with either CFC 12 or CFC 11. The CFC 11 calculation for the Black Dike is not presented as the concentration measured in the Black Dike was higher than that measured in the leachate, indicating that the sump leachate does not accurately represent leachate escaping from Phase 19.

To calculate mixing between the Black Dike and the River Hertford, the value used for the Hertford is obviously the background Hertford concentration of CFCs 11 and 12, whereas that for the Black Dike is from the sampling point closest to the river (c. 500 m). Any de-gassing along the stretch between this measurement point and the river will reduce the concentration, so that the value used will lead to an underestimate of dike contribution to river flow. The third row in Table 8.5 is the calculated percentage of the River Hertford that is derived from the Black Dike downstream of their confluence. Consequently, using the range of possible values of leachate contribution to Black Dike flow, it can be calculated that the contribution of leachate to total flow in the river is between 0.4% (based on CFC 11 in equilibrium with landfill gas, a low estimate) or 6.6%, based on the CFC value actually measured in leachate (a high estimate).

As the measured leachate concentrations are likely to be lower than the concentrations in leachate in Phase 19, the highest estimates are probably overestimates.

There are a number of mechanisms by which landfill gas can be out of equilibrium with the leachate. Firstly, the temperature used for calculating the gas-water equilibrium temperature may be too low, although this is unlikely to explain the large difference observed. Other factors include the swift removal of landfill gases to the methane-burning plant in the central compound (as CFC 12 is highly volatile it will be released in the gas phase; if this occurs above the 'leachate' table in the wastes then its removal may be too rapid for equilibrium to occur) and differential behaviour of CFCs with respect to organic matter buried in the wastes.

8.5.5 CFC DATA CROSS PLOTS FOR SEAMER CARR GROUNDWATER

Please note, in the following series of graphs, that where the legend refers to a sample as either 'upper' or 'lower' it refers only to that sample's position within the drift and not to whether the borehole in question is a dual-level installation. Figure 8.12 plots CFC 12 against CFC 11 for all groundwater samples taken at Seamer Carr.

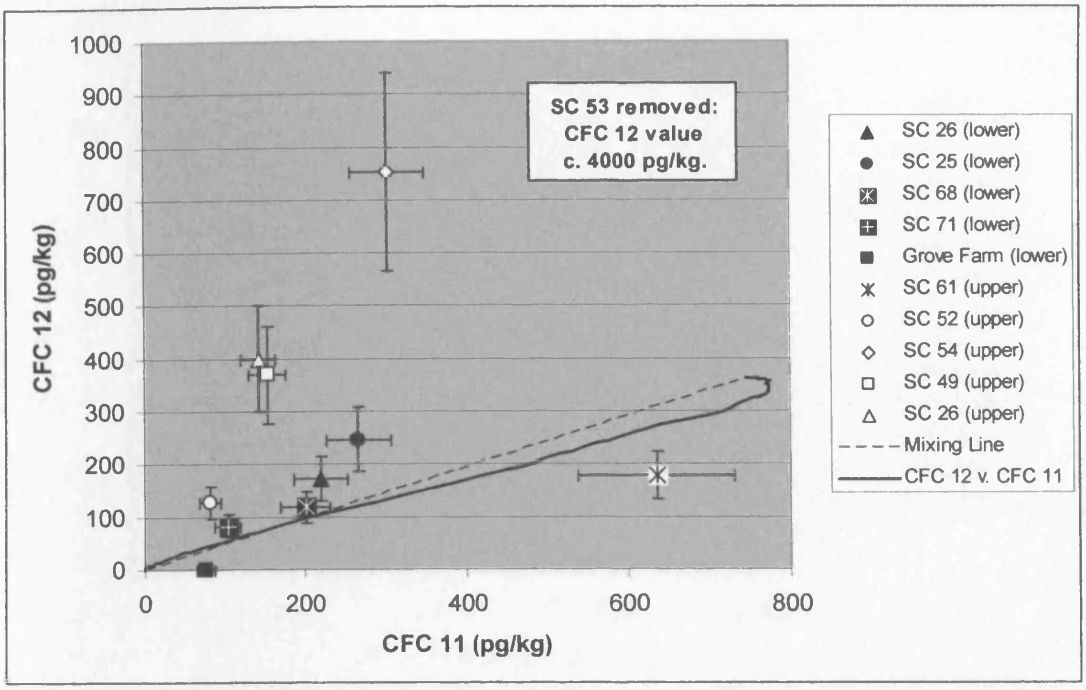

Figure 8.12 Historical trend diagram of CFC 12 plotted as a function of CFC 11 for Seamer Carr groundwaters.

There is a degree of grouping in the data, with data points falling closest to the historical trend and mixing lines (i.e. the envelope) being predominantly groundwaters sampled from the lower drift. Apart from SC61, the only groundwater sampled north (upgradient) of the landfill and likely to be the most recently-recharged, and SC52, which groups with the lower drift groundwaters, groundwaters from the upper drift plot well above the envelope. These are SC26 (upper), SC53, SC54 and SC 49 and are highly likely to have been influenced by landfill-derived contamination.

Looking at the lower drift samples, SC25 and SC26 exhibit slightly enhanced CFC 12 with respect to CFC 11. This enrichment is small, however, so that it is more probably due to anaerobic losses of CFC 11 than CFC 12 contamination. This notion is supported by considering where these two samples might have plotted prior to CFC 11 losses. Assuming that the initial concentrations result solely from atmospheric equilibrium, and that CFC 12 has undergone no degradation or other loss (it being the least degradable or sorption-prone CFC, see Chapter 3), the initial position on the historical trend line, as suggested by the CFC 12 concentration, would be approximately 600 $pgkg^{-1}$ CFC 11 for SC25 and just above 400 $pgkg^{-1}$ CFC 11 for SC26. Making a similar adjustment on Figure 8.13 (CFC 113 vs. CFC 11) also puts these two data points close to the historical trend line at approximately 600 $pgkg^{-1}$ i.e. in roughly the same place with respect to both CFC 12 and CFC 113 (although a little too high for SC26). The same argument also applies to SC52, which would plot on an original position of c. 300 $pgkg^{-1}$ on both figures. The argument further suggests little or no CFC 113 losses in the lower drift.

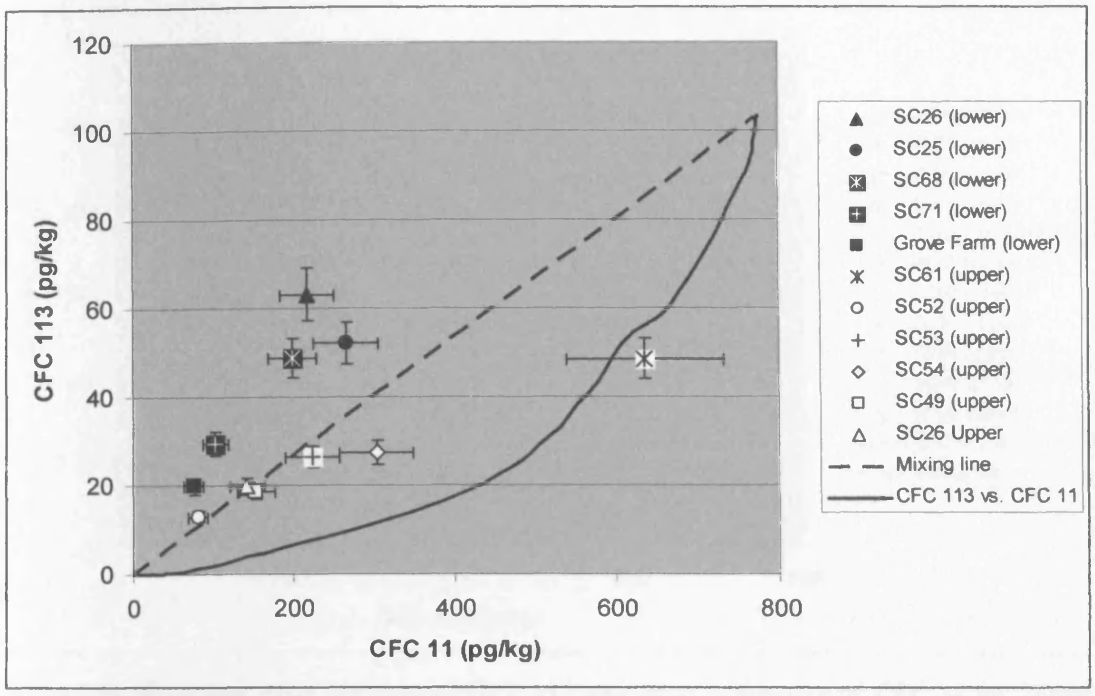

Figure 8.13 Historical trend diagram of CFC 113 plotted as a function of CFC 11 for Seamer Carr groundwaters.

Figure 8.13 also indicates differential behaviour between CFCs in the lower and the upper drift, with the upper drift waters plotting more closely to the envelope than the lower drift waters. This is contrary to what one would expect from a point further along the same flowpath (i.e. one would expect waters to become more depleted in CFC 11 and shift even further to the left as the traveled upward through the drift). However, restoring the data points to what would be their initial position on the trend line, it can be seen that the lower drift samples from SC25, SC26 and SC68 would be derived from later rainfall than the upper drift samples, whereas SC71 and the Grove Farm sample would be of roughly the same provenance.

The same type of analysis also resolves differences observed on Figure 8.14 (CFC 113 vs. CFC 12), as all lower drift groundwaters fall within or to the left of the envelope, with parts of the upper drift clearly affected by CFC 12 contamination. Should we return *these* back to a probable starting points (assuming no CFC 113 losses), again they cluster together around an average point below that exhibited by the lower drift samples. This then shows the expected pattern, in that an upward gradient through the drift will leave the older (lower concentration) waters above the younger (CFC-rich) waters. The two upper drift waters not conforming to this hypothesis are SC61 (north of the landfill) and SC52, which is in the upper drift but plots more closely to the lower drift facies.

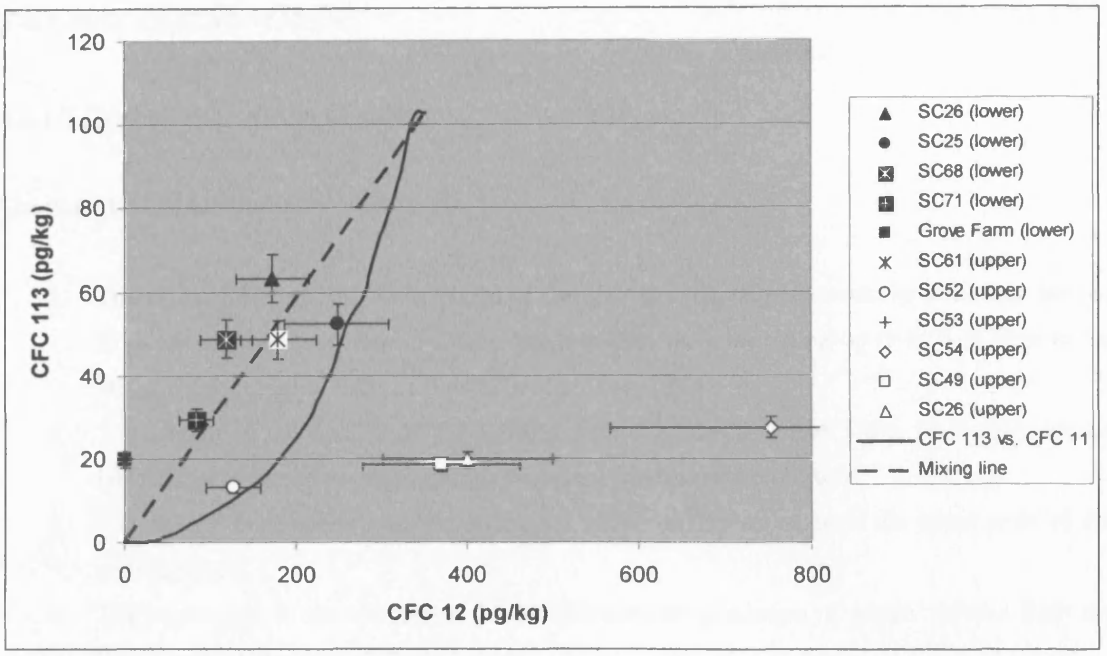

Figure 8.14 Historical trend diagram of CFC 113 plotted as a function of CFC 12 for Seamer Carr groundwaters.

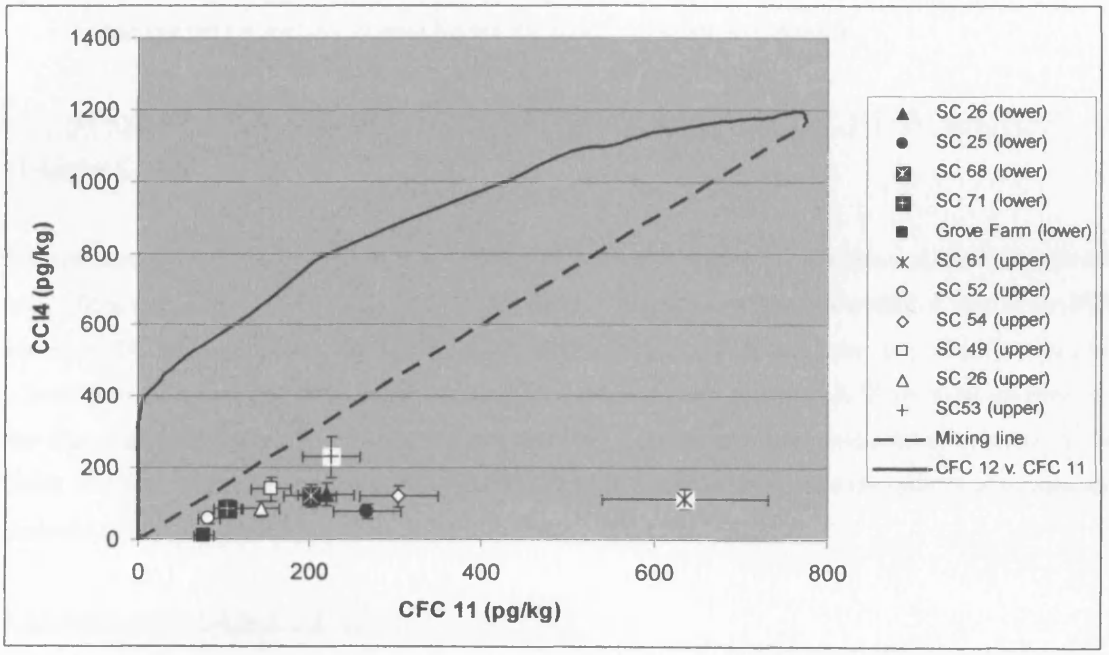

Figure 8.15 Historical trend diagram of CCl_4 plotted as a function of CFC 11 for Seamer Carr groundwaters.

Figure 8.15 shows that waters are depleted in CCl_4 with respect to CFC 11. This most probably reflects the greater degradability of CCl_4 (c. 100 times greater than CFC 11 according to Lee *et al* (1999)) rather than contamination with CFC 11 (as, from comparisons with CFCs 12 and 113, CFC 11 also appears to be degraded). This plot is therefore of little use for dating waters or identifying contamination (although obviously it shows that there is no CCl_4 contamination of any strength).

8.6 CHAPTER SUMMARY

8.6.1 SUMMARY OF MAIN FINDING

The main findings of the study are that:

1. The Black Dike and the River Hertford are both significantly impacted by pollution derived from the landfill. From the CFC data, leachate may be contributing up to 40% of flow in the Black Dike and up to 6.6% of flow in the River Hertford.
2. The impact of the landfill on the River Hertford is via the Black Dike. No impact on the Hertford is observed as a result of *groundwater* contaminant pathways.
3. The landfill is having a measurable impact on the quality of water in the upper parts of the drift aquifer.
4. The upper drift in the vicinity of the landfill contains a mixture of waters derived from the lower drift and the landfill itself.
5. The landfill is not significantly impacting water quality within the lower drift or the Corallian due to strong, upward, hydraulic gradients.
6. The New Dike may be weakly affected by contamination from the landfill, but this is less than that caused (probably) by runoff from the industrial estate to the north.

8.6.2 IMPLICATIONS FOR CONCEPTUALISATION OF THE PHYSICAL HYDROGEOLOGY AT SEAMER CARR

The conceptual model as derived from borehole and hydraulic head data provides a sensible framework with which to explain variability in CFC data. The data indicates that the lower drift is free of landfill-sourced CFC contamination. Therefore contaminant transport in groundwater is probably restricted primarily to the upper drift and, landfill-derived groundwater contamination is likely to be captured by the dike network, especially considering that both the temperature and conductivity profiles of the Black and New Dikes indicate greater groundwater (and leachate) influence on dike flow toward the southern end of the site.

8.6.3 BROADER SIGNIFICANCE OF THE STUDY

There is little published work regarding the use of CFCs as indicators of landfill contamination of ground and surface waters, although one study, of a range of halogenated organic compounds from a hazardous-waste-receiving site in Canada found CFC 113 (a DNAPL) to be the contaminant of greatest concentration and persistence. On other occasions CFCs have been used to identify groundwater contaminant plumes originating from non-landfill sources (e.g. Thompson and Hayes, 1979; Busenberg and Plummer, 1999). Other workers have focused on CFC concentrations in landfill gases (Brookes and Young, 1983; Foskett, 1994; Diepser and Stegmann, 1994; Allen *et al.*, 1997) and unsaturated soils influenced by the migration of landfill gas (Ward, 1996). There is little in the recent literature, with

most efforts in the field concentrating on the background levels of CFCs in aquifers and their application to age-dating groundwaters (see Chapters 3 for a review of work in this area). The most rigorous examples of the application of CFC measurements for the identification of landfill impacts on groundwater and surface water therefore remain the unpublished works of Bateman (1998) and Atkinson (2002). The current research has drawn upon these for insight into processes affecting CFC concentrations arising from landfill-impacted waters, and for methods of interpreting the raw data.

The research presented in this chapter emphasises the capability of the method to distinguish contaminant signals arising from landfill and non-landfill sources. This capacity is particularly important where there is more than a single possible source of CFCs. It also moves the methodology further into the mainstream by highlighting problematic issues that ought to be addressed in such studies. For example, it is clear that an accurate analysis of the leachate component in surface waters at Seamer Carr relies upon the establishment of a reliable leachate concentration. However, the clearly elevated and precisely located signals in impacted surface water offer a clear vindication of the methodological choice when compared to a typical indicator of landfill impacts (conductivity in this instance). This research also illustrates the importance of initial identification of a conceptual model of site hydrogeology. Such a model, together with knowledge of the physico-chemical properties and degradative potential of CFCs, provides a framework for understanding CFC distributions in and around landfills.

Much of the variability is, however, due to difficulties in maintaining an uncontaminated analytical system. Landfill leachate contains not only very high CFC concentrations, but an abundance of other halogenated compounds. It therefore appears to be best practice not to use the same analytical machinery for landfill samples and for 'clean' groundwater samples, although this has been unavoidable here. Undoubtedly improvements can be made in sample preparation to avoid some of these problems, although probably not without significant extra cost and effort.

Despite these problems and, furthermore, despite confusing factors of variable degradation and other differential subsurface behaviour, the CFC method is shown here to be capable of producing sensible and meaningful results useful to scientists, managers and regulators alike.

CHAPTER NINE

SUMMARY AND CONCLUSIONS

9.1 SUMMARY OF THE MAIN FINDINGS OF THIS RESEARCH

The main findings of this research fall into four categories. The first of these is development in interpretation of borehole dilution tests using an adaptation of existing methods together with recent modelling innovations. The second is related to the development of sulphur hexafluoride as a groundwater tracer in the vicinity of drinking water supply wells. The third is related to the field area and consists of improvements in the conceptualisation of Corallian limestone hydrogeology and the identification of relationships between the main public supply well at Irton and the aquifer, which are important for an understanding of water supply protection. This aspect of the findings also includes the use of alternative mathematical models for constraining hydrogeological conceptualisations in general and in particular the need to collect as much data as possible for the optimum interpretation. The fourth is the continuing development of CFCs and CCl_4 as hydrological tracers, and in particular as indicators of landfill impact, and the identification of an apparently oxidising aquifer as a sink for atmospheric CFCs. These themes are summarised below and placed within the context of their contribution to groundwater science.

9.2 BOREHOLE DILUTION TESTS AND GEOPHYSICAL LOGGING

Borehole dilution tests are straightforward experiments to perform and several were conducted on boreholes in both the confined and unconfined zones of the eastern Corallian. However, due to the widespread phenomenon of vertical hydraulic gradients within the aquifer, considerable deviation from the ideal condition of pure horizontal flow was observed. The condition of horizontal flow within the borehole has previously been considered central to the derivation of a Darcian flux from borehole dilution tests (e.g. Halevy *et al.*, 1967; Hall, 1991) due to the proportionality between the Darcian flux and the linear slope of tracer decay, on a logarithmic scale, over time. This linearity may be destroyed either by induced vertical mixing (which may be controlled through care in experimental methodology) or vertical water movements (flow) resulting from vertical hydraulic gradients. In the latter case loss of tracer becomes linear on an arithmetic scale.

The form of the raw data from the borehole dilution tests indicated strong preferential flow at certain levels and probable vertical flow within the boreholes. This was confirmed by geophysical logging of fluid parameters and flow in some of the boreholes experimented upon and is likely to be induced by

the presence of the borehole itself, connecting otherwise poorly connected fissures of differing hydraulic head. Nonetheless, using two independent methods of modelling the data it was still possible to derive and compare Darcian fluxes and volumetric flows within the aquifer. The variability encountered between boreholes was then explained by reference to the locations of the boreholes with respect to the confined and unconfined zones of the aquifer, and the proximity of the swallowholes, which was demonstrated to be an area of enhanced permeability within the aquifer.

The first modelling method employed was an adaptation of what was herein termed the 'standard' method; that is, one in which the slope of tracer decay in the borehole is related to the Darcian flux of the aquifer. It was shown that a procedure in which tracer mass was averaged over the entire borehole column, for each progressively later measurement time, produced theoretically acceptable results. This was on the basis of the observation that vertical flows within a borehole typically occur on a length scale (metres) less than the length of the borehole itself (tens of metres).

The second modelling method was an inverse method that attempted to reproduce visually the form of the borehole dilution test data by inputting flows into a spreadsheet model. The model was written especially to account for difficulties in deriving fluxes where vertical flow is problematic, and permits the borehole to be very precisely modelled when there is additional geophysical logging data. The geophysical data comprised fracture positions, volumetric flows and vertical groundwater velocities within the borehole. This was used to constrain tightly the preferential flow horizons and vertical flows (i.e. model inputs), after which the model was able to reproduce the form of the observed dilution accurately. This modelling procedure was thus independent of the former procedure (the 'standard' method) by assigning flow to reproduce observed results rather than deriving it from observed results. This independence was extremely important for a valid comparison of the two sets of processed data, which showed a convincing level of agreement when all results were plotted together. In other words; the independent methods exhibited agreement when comparisons were made between boreholes covering a wide geographical area. In contrast, individual locations showed either a greater or lesser extent of agreement between the two methods of analysis, thereby highlighting the dangers of inferring too much from local-scale results.

The borehole dilution tests illustrated differences in permeability at a regional scale, depending on position in either the confined or unconfined zones and on proximity to the Forge Valley swallowholes. Furthermore, both the dilution tests and the geophysical logging illustrated the dominance of fissure flow throughout most of the eastern aquifer. The geophysical logging also clearly illustrated differences in fissure frequency and spacing between the oolitic and calcareous grit members of the Corallian, with the oolitic limestones exhibiting twice the fracture frequency and half the fracture spacing of the grits (in particular the Lower Calcareous Grit). The information derived from the interpretation of the combined borehole dilution test and geophysical results was therefore of immediate practical use in the analysis of both the intermediate scale (10s to 1000s of meters) tracer testing and the regional (aquifer) scale CFC analyses. The development of understanding of the hydrogeology of the aquifer therefore relies fundamentally upon the results from these experiments,

which must be accounted for in any of conceptualisation of larger-scale processes affecting groundwater flow and both applied and environmental tracer transport.

Altogether, the results from the modelling as conducted in the two ways described has implications for the theory of borehole dilution testing analysis and enables the method to be more widely applied than hitherto thought possible (e.g. Leap and Kaplan., 1988; Hall, 1993; Hall, 1996; Ward *et al.*, 1998). This is true in aquifers where some vertical flow may otherwise have been considered to render the method ineffective. The borehole dilution test is a relatively cheap and simple method of obtaining groundwater data where more extensive experimentation, possibly in the form of tracer or pumping tests, is either impractical or prohibitively expensive in terms of finances and manpower (and which may be difficult to interpret) (Hall, 1996). Whilst the method cannot be claimed to be accurate in every single case, good correlations have been found between dilution testing and other methods of groundwater flux estimation (Newcomer *et al.*, 1996; Hall, 1996), and this relation is confirmed here through the regional picture developed on the basis of geographically distributed boreholes. The potential for the combination of this method with larger-scale experimental methods should not be overlooked. This aspect of the present work clearly meets the objectives of aquifer characterisation and support for the interpretation of more complex data, as defined in the introduction to this thesis.

9.3 APPRAISAL OF SF_6 AS A GROUNDWATER TRACER

The tracer injection system designed to saturate 500 L tank volumes with SF_6 was successful insofar as it achieved a concentration sufficiently high to mark a considerable body of water moving through the aquifer. It was unsuccessful, however, in retaining most of the gas, so that in effect it was not much better than openly sparging a large volume of water with the gas. However, the fact that the system was pressurised, and maintained an SF_6 headspace above the tracer solution, probably prevented some degassing of the SF_6 that *had* entered solution. Degassing was also prevented by the secondary tank discharging to the primary during injection, so as to prevent atmospheric contact with the tracer-containing water. Unfortunately the injection system leaked so that the intention of maintaining an SF_6 release to the atmosphere as low as possible was not realised, with 4 kg of the gas being released during the injection. Considerably more work would need to be done on this aspect of the experiment before attempting anything similar again. Furthermore, probable losses to the unsaturated zone upon injection and infiltration of the tracer meant that part of the quantitative aspect of the experiment was lost.

Nonetheless, the injection system worked sufficiently well for measurable (and high) concentrations of SF_6 to persist in water pumped at Irton for over six weeks following injection. A well-defined breakthrough curve was also measured at Derwentdale Farm North and positive results were recorded at Derwentdale Farm South, Cayton Station Road PWS and McCains. As one of the main objectives of the experiment had been to develop a tracer that could be used in public water supplies at concentrations high enough to permit close examination of the tailing characteristics of a BTC over a period of weeks, the experiment must be considered a success. However, interpretation of the results

has relied heavily upon previous tracer tests at the same locations, as well as additional borehole dilution testing, geophysical and hydrochemical information. More intensive sampling for SF_6 may have addressed some of these needs, although with only a single person performing the sampling and analysis this was impossible.

The analytical system performed sufficiently well for the purposes of the experiment, obtaining, in addition to SF_6, a measurement of CFCs 11 and 12 for each water sample taken. This must be considered an efficient use of resources. However, there was a small contaminant signal probably associated with the sample syringes so that optimum SF_6 detection limits were not attained. Detection limits and general functionality could be significantly improved with better sample storage and sample preparation techniques.

In terms of tracer performance, SF_6 suffered losses probably due to injection above the water table. Initially it was thought that this would not be a problem, but a considerable portion of the tracer remained unaccounted for and this is ascribed to volatilisation. Following that, however, the tracer performed well, clearly proving its potential to remain above detectable limits in a confined fissured aquifer for several weeks. Indeed, 44 days after injection the tracer was still detectable at the main target well nearly 2 orders of magnitude above the analytical detection limit. In terms of the dynamic range of the tracer, for this experiment a range between c. 20 $mgkg^{-1}$ of undiluted tracer concentration and an analytical detection limit of c. 3 $pgkg^{-1}$ (ppt) was achieved. This is a range of about 10 orders of magnitude. With a better analytical system SF_6 could be used with a potential dynamic range of 12 orders of magnitude.

There appear to be three main problems associated with use of SF_6 as an artificial groundwater tracer. The first of these is that the *environmental* application of utilising the existing (i.e. atmospherically-derived) dissolved gas as a hydrologic tracer is lost upon injection. This may not be such a problem in a rapidly-flushed aquifer such as the Corallian, but could destroy SF_6 dating potential completely. The second problem is that SF_6 requires elaborate injection and sampling equipment, and rigorous procedures, if it is to be constrained from entering the atmosphere in large quantities during an experiment, and from contaminating the sampling equipment or the field site (the latter did not appear to occur on this instance but is noted several times in the literature, see Chapter 3). The third concern is the global warming potential of the gas, which is higher than any other known gas, although obviously this is not a practical experimental problem.

Some important groundwork on SF_6 as a groundwater tracer was performed by Biggin (1991) in terms of sorption and degassing studies as well as groundwater transport of the tracer under laminar flow conditions in unconsolidated aquifers. Wilson and Mackay (1993) also examined sorption of the tracer in column experiments. However, tracing experiments in limestones and surface waters were less successful due to degassing of the tracer in karst conduits (Biggin, 1991; Strongman, 1994; Robinson, 1996). Other workers have also illustrated the difficulties associated with use of SF_6 as a groundwater tracer by severely contaminating their field sites and sampling wells (Dillon *et al.*, 1999; Corbett *et al.*,

2000a; Corbett *et al.* 2000b; Harden *et al.*, 2003). It is therefore clear that SF_6 needs to be treated with great respect and consideration before undertaking groundwater tracing experiments, but that this effort should be vindicated by the results, as this thesis clearly demonstrates.

9.4 TRACER TESTING, MODELLING AND REFINEMENTS IN HYDROGEOLOGICAL CONCEPTUALISATION

The objective of improving the conceptualisation of groundwater flow and potential contaminant transport in and around the Forge Valley – Irton area has been achieved through a piece-by-piece construction of a variety of empirical and theoretical conclusions. The chief empirical elements of this construction were evidence drawn from the following:

- Review of previous work in the area
- Local-scale geophysical logging and single-borehole dilution tests
- Intermediate-scale tracer testing over distances of between 20 and several thousand meters
- Aquifer-scale measurement of environmentally present (indigenous) groundwater tracers (CFCs)

The theoretical considerations consisted of all of those processes potentially operative within the aquifer and responsible for the nature and form of the empirical tracer observations. These were:

- Diffuse flow within a Darcian medium
- Hydrodynamic dispersion within a Darcian medium
- Hydrodynamic dispersion in pipe- or conduit flow
- Sorption of tracers
- Double porosity diffusion

Some of these theoretical considerations were stated in more concrete terms in the form of mathematical models. The models chosen to discriminate between potential processes were 1) A geohydrological dipole of unequal strength poles operating between the recharging swallowholes and the discharging Irton public supply well; 2) A double-porosity model of tracer transport in fractures (or conduits) and mass exchange with matrix porosity; and 3) Hydrodynamic dispersion of tracer plumes along single and multiple fractures/karst conduits.

Through the application and analysis of these individual components it was possible to test the conceptualisation of the aquifer and determine how rigorously each of the mathematically stated components could account for the degree of variation in the empirical observations made. From the results of these applications it was determined that, whilst a dipole model of flow was able to accurately predict the recessional slope of tracer decay at the main target well (facilitated only through the development of the SF_6 tracer method), it should not have exhibited such a close match to an additional sampling point some distance away. At this second sampling point, Derwentdale Farm

North, the recession after one week was fully explicable by reference only to a double porosity diffusion model. The double porosity diffusion model, however, was not able to account for the extent of tracer losses observed between the tracer injection and measurement points: this was only explicable with reference to the dipole model. It was therefore concluded that, following the first 24 hours, the dipole exhibited a strong control over recovery at Irton, but that arrivals following a week or so after injection exhibited a sufficient residence time for double porosity effects to assume control. The control over that tracer which *was* recovered within the first 24 hours (and really only over the first twelve hours or so) was shown to be hydrodynamic dispersion in one or two rapid-flow conduits (as shown by the close match between the advection-dispersion model and the peaks on the tracer breakthrough curves). Together this suite of models encompassed and accounted for all of the observed variability in the system, with each member of the suite solving part of the empirical problem.

That there are only a limited number of potential processes operable on contaminant pulses/plumes within an aquifer is obviously an important starting point for investigation into particular incidences of contaminant transport in fractured or karstic rocks. One of the major findings of this research is that the examination and either verification or elimination of potential processes can be rigorously addressed through studies drawing upon as wide a range of evidence as possible, collected over several scales of investigation. However, as this is not going to be possible in many situations, one of the more general insights gained is the fact that judicious analysis of existing or easily obtainable data (e.g. hydrochemical measurements, pumping tests, field observations etc.) can play an important initial role in the development of a conceptual model of a system. Such an approach was exemplified in the simple network model mooted prior to the more precise modelling efforts. An additional general point is that it is partly due to the limitations of the idealised cases, as represented by the mathematical models, that limits may be drawn around their contribution to the overall conceptualisation. In the same way as too much emphasis should not be placed upon any one data point in a series, neither should any precise model be expected to bear the weight of all observations.

With respect to implications for the management of water resources in fractured and/or karstic aquifers it is abundantly clear that various types of tracer test are capable of elucidating fundamental processes controlling contaminant transport. The degree of foresight and preparation that this permits should be more widely recognised by water companies when it comes to addressing the need to identify and manage source-protection-zones around public supply wells. Indeed, in terms of tracer test methodology, the final interpretation of the sensitive gas tracer SF_6 was shown to rely heavily upon other tracer test results performed using established dye tracers and sodium chloride (for dilution tests). Whilst SF_6 provides a tool for examination of processes controlling breakthrough curve tailing it is, after all, a difficult method to implement, and it was only through the application of fluorescent dyes that some simple but extremely important relationships between the pumping rate of the Irton well, the proportion of river water captured, and tracer first- and peak arrival times were also identified.

9.5 CFC RESULTS

The CFC and CCl_4 results from Corallian groundwater were interpreted with reference to historical equilibrium concentrations expected on the basis of assumptions regarding recharge temperature, elevation, atmospheric and vadose zone gas concentrations, and piston-flow and binary-mixing models. Despite considerable uncertainty in the data it was still possible to observe broadly similar patterns of CCl_4 and CFC 11 degradation throughout the aquifer, with occasional apparent CFC 113 degradation and contamination of all three CFCs, but not, seemingly, CCl_4.

The results showed a broad division into waters with lower CFC concentrations being produced from boreholes rather than springs, although with some boreholes exhibiting obvious similarities to river water. In this respect the conceptualisation of the aquifer built in earlier chapters is useful for interpreting the data, with apparent (model) groundwater ages of decades being rejected in favour of binary mixing between young waters and waters either old enough to contain zero background CFC or to have undergone partial loss of CFCs. End member waters were discriminated on the basis of borehole dilution and tracer test results and geophysical logging, as well as, in some cases, reference to lithological or hydrogeological differences in the situation of the spring or borehole. For example, the Augmentation borehole, immediately adjacent to the Forge Valley swallowholes, containing a known component of young water (from tracer testing) but with an apparent age of some decades, is more realistically described with a mixing model than a single age. On this basis proportions of modern waters were calculated for most sample locations. Interestingly the paradox of rapid tracer transport velocities and decade-old water from the same wells suggests that the matrix contribution to fissure waters is large. A further paradox lies in the degradation of CFC 11 in an oxidising aquifer. CCl_4 degradation is advanced in almost all waters sampled, but this is noted in the literature as a process occurring under aerobic conditions (e.g. Lee *et al.* 1999). Bateman (1998) also noted CFC 11 losses in both the Lincolnshire limestone and the English Chalk, together (tentatively) with the appearance of HCFC 21, the first degradation product of CFC 11, on several chromatograms. Peaks with an elution time corresponding to HCFC 21 were also noted during this project, the chromatographic column being the same as that used by Bateman (1998). CFC 12 (the least degradable CFC of the three) shows no evidence of degradation, so that CFC 11 losses are stated in comparison to this more conservative species. Hohener *et al.* (2003), in a review of the fate of CFCs in groundwater, note *no* records of CFC 11 degradation under aerobic conditions, so that it seems likely that there must be some consumption of CFC 11 (and CFC 113) in *anaerobic* environments within the aquifer, quite possibly in the matrix given the timescales involved. This finding suggests that double porosity limestone aquifers similar to the Corallian may be important sinks of atmospheric CFCs on a decadal timescale, a conclusion in agreement with those of Bateman (1998).

Seamer Carr landfill, by contrast, is a definite source of CFCs in ground and surface waters, although on balance it too probably acts as a net sink with respect to the amount of CFCs deposited in it because it is a largely anaerobic biodigestor. Indeed, CFC 11 degradation was observed on several chromatograms from the landfill study. The main findings are that the CFC impact of the landfill is

largely confined to the upper parts of the minor drift aquifer upon which it sits, and to surrounding surface water bodies. In particular, CFC atmospheric equilibrium ratio (AER) profiles of the Black Dike and the River Hertford are unequivocal in identifying a landfill source of contamination. However, the measurement of multiple CFCs highlights the methodological capability of distinguishing between different sources of contamination, as unidentified point-sources of CFC 113 are clearly evident both north of the landfill (probably somewhere on Eastfield industrial estate) and on the upper Hertford.

Little work has been done on the CFCs as indicators of landfill impact outside the UK, with only a single study reporting CFC 113 as one of a variety of halogenated organic compounds emanating from a hazardous waste site in Canada (Lesage *et al.* (1990) (although other workers note non-landfill-sourced contaminant plumes in groundwater). Within the UK, however, there is a wider variety of work including that of Ward *et al.* (1996), Bateman (1998) and Atkinson (2002), although only the latter two of these record groundwater concentrations. The present work, therefore, contributes to a growing body of knowledge regarding the behaviour of CFCs in and around landfill sites, and helps move the technique away from its experimental foundations and towards a position of routine analysis. More locally, the Seamer Carr study has helped to answer some fundamental questions regarding the impact of the landfill on local surface and groundwater bodies.

9.6 RECOMMENDATIONS AND SUGGESTIONS FOR FUTURE WORK

9.6.1 IN AND AROUND IRTON

Further work in the eastern Corallian is needed to confirm the relationships established between quantities and proportions of river water pumped at Irton and the pumping rate of the New Well, as those proposed here are based on few data. This would not necessarily involve further tracer testing as hydrochemical measurements taken at particular pumping rates (given time to establish a degree of equilibrium) ought to suffice and could probably be performed in-house by YWS Ltd.

In addition, the relationship between local Darcian flux values as determined from the modified 'standard' method and the simulation modelling method could be investigated further. The relationship illustrated indicates correlation between the two methods that could be improved (or disproved) by applying the method more widely. Furthermore, the degree to which the Darcian fluxes calculated by both methods correlate with fluxes and permeabilities determined from pumping tests and other investigative methods could also be examined over a range of aquifer types in order to clarify the role that borehole dilution testing has in field hydrogeology.

9.6.2 SF_6 METHODOLOGICAL DEVELOPMENT

Such an experiment as the one performed with SF_6 would be improved if more resources were available for its execution. The injection system could be considerably bettered and this should not

only increase tracer concentrations but ought to limit the release of SF_6 into the environment, a problem that could have later repercussion on an experiment in which SF_6 found its way from the atmosphere to sampling points via different routes from the one injected. It should also be emphasised that the applied use of this tracer leads to loss of future potential to use it as an environmental tracer, which may not be appreciated by other workers. The global warming potential of the gas should also be considered when using this technique. As noted, with an atmospheric lifetime of 3200 years (Ravishankara *et al.*, 1993), releases of the gas cannot be undone on the timescale of human civilisation. However, there is no doubt that it would be straightforward to adapt the system for injection of alternative gas tracers.

9.6.3 CFCs

CFC degradation products in groundwater have not been quantified, and are only identified on a circumstantial basis in this research. If HCFC 21 and other degradation products could be quantified it may be possible to reconstruct groundwater concentrations of the parent compounds. Such quantification could probably be performed during the same analysis procedures as are currently used for the CFCs themselves, providing the correct choice of analytical equipment and operational parameters were made. Studies into the role of the rock matrix on the degradation of otherwise recalcitrant organohalogens may also be worthwhile given the importance attached to many such compounds in groundwater supplies (EC Groundwater Directive 80.68/EEC). Indeed, with the frequency of CFC-contaminated waters and the frequency of multiple, unidentified, and often large additional peaks on chromatograms, a pesticide study of the Corallian aquifer in East Yorkshire may be overdue. It should also be recognised that some temporal patterns may emerge if sampling is conducted regularly over an extended period of time and that this may explain some of the variability observed between different sampling campaigns in this research.

Significant improvements in detection limits and reproducibility should be possible with more sophisticated analytical equipment. Such systems are well-described in the literature (see, for example, Plummer *et al.*, 2001). Despite significant efforts to decontaminate sampling and analytical equipment between runs, it is likely that carry-over of high CFC concentrations from one sample to another contributed significantly to noise in the data. Thus, for reasons of potential interference, studies that combine grossly-polluted and non-polluted field sites should be avoided, or separate apparatus should be used for the two categories of site.

REFERENCES

Aldous, P.J. and Fawell, J.K. (1986) The use of Fluorescein Sodium (Uranine) for groundwater tracing investigations in potable water supplies. WRc Environment, Medmenham Lab, Medmenham, Bucks.

Aldous, P.J., Fawell, J.K. and Hunt, S.M. (1987) The application and toxicity of Photine C when used as a groundwater tracer. WRc Environment, Medmenham Lab, Medmenham, Bucks.

ARUP (2000) 'Scheme Code PH-484-000 Irton WTW: Derwent Supply Feasibility Study, phase 2 report'. Report to Yorkshire Water Services Ltd.

Aspinwall and Co. (1994) Corallian limestone model, Report no. NR1704B. Report to the Environment Agency.

Aspinwall and Co. (1995) Corallian limestone model – Addendum report, Brompton Springs Model Extension. Report to the Environment Agency.

Aspinwall and Co. (1996) Seamer Carr landfill; evaluation of potential impacts on water resources – desk study.

Atkinson, T.C., Smith, D.I., Lavis, J.J. and Witaker, R.J. (1973) Experiments in tracing underground waters in limestones. *Journal of Hydrology*, **19**(4) 323-349.

Atkinson, T.C. and Davis, P.M. (2000) Longitudinal dispersion in natural channels: 1. Experimental results from the River Severn, UK. *Hydrology and Earth Systems Sciences*, **4**(3), 345-353.

Atkinson, T.C. (2001) The potential of artificial tracers for aiding groundwater protection and risk assessment. IN: Protecting groundwater; an international conference on applying policies and decision-making tools to land-use planning. *Conference proceedings. National groundwater and contaminated land Centre project NC/00/10.* Environment Agency, 2001.

Atkinson, T.C. and Barker, J.A. (2001) Characterising permeability, groundwater flow and contaminant attenuation in chalk catchments using tracer techniques. Proposal to NERC's Lowland Catchment Research Thematic Programme.

Atkinson, T.C., Barker, J.A., Ward, R.S., Low, R.G. (2001) Radon: An indicator of solute transport in doublr-porosity aquifers. *In: Seiler, K.P. and Wohnlich, S. (Eds.) New approaches to characterising groundwater flow (Proceedings of the 31st IAH congress, Munich, Vol. 1).* A.A. Balkema. p.p. 441 – 445.

Barker, I. & Courchee, R. (1982) Irton Pumping Test 1981: A groundwater and river flow investigation. *Unpublished technical document Yorkshire Water Authority* (now Yorkshire Water Services Ltd.).

Barker, J. A. (1985). *Memoirs of the 18th congress of the international Association of Hydrogeologists.* **1**: 250-269

Barker, J.A., Wright, T. and Fretwell, B. (2000). A pulsed double porosity method for double porosity solute transport modelling. *In: A. Dassargues (Ed.) Tracers and modelling in hydrogeology. IAH publication no. 262. International Association of Hydrological Sciences, p.p. 297-302.*

Bateman, A.S. (1998) Chlorofluorocarbons in groundwater. Unpublished PhD thesis University of East Anglia.

Bauer, M.R. and Yavitt, J.B. (1996) Processes and mechanisms controlling consumption of CFC11 and CFC12 by peat from a conifer swamp and black spruce-tamarack bog in New York State. *Chemosphere*, **32**(4) 759-768.

Bellanger, D. (1984) Groundwater velocity measurements using an electrical conductance borehole dilution device. Unpublished Masters Thesis, University of Waterloo. Cited in Palmer, C.D. (1993) Borehole dilution tests in the vicinity of an extraction well. *Journal of Hydrology*, **146**, 245 – 266.

Bohlke, J.K. and Denver, J.M. (1995) Combined use of groundwater dating, chemical, and isotopic analyses to resolve the history and fate of nitrate contamination in two agricultural watersheds, Atlantic coastal plain, Maryland. *Water Resources Research*, 31, 2319-2339.

Bohlke, J.K. (2004) TRACERMODEL1. Excel workbook for calculation and presentation of environmental tracer data for simple groundwater mixtures. *In: IAEA Guidebook on the use of chlorofluorocarbons in hydrology.* International Atomic Energy Agency, Vienna. In press.

Bottrell, S.H., Moncaster, S.J., Tellam, J.H., Lloyd, J.W, Fisher, Q.J., and Newton, R.J. (2000) Controls on bacterial sulphate reduction in a dual porosity aquifer system: the Lincolnshire Limestone aquifer, England. *Chemical Geology*, **169**(3-4) 461-470.

British Geological Survey (1998) Solid and Drift Geology map, sheet 54, 1:50 000, Scarborough.

Brouyère, S., A. Dassargues, R. Therrien, and Sudicky E.A. (2000) Modelling of dual porosity media: Comparison of different techniques and evaluation on the impact on plume transport simulations. In *Post Published Proceedings of MODELCARE'99, IAHS Publication no. 265*, ed. F. Stauffer, W. Kinzelbach, K. Kovar, and E. Hoehn, 22–27. Wallingford, Oxfordshire, UK: IAHS Press.

Bu, X. and Warner, M.J. (1995) Solubility of CFC 113 in water and seawater. *Deep Sea Research*, **42**(7) 1151-1161.

Bullister, J.L. and Wisegarver, D.P. (1998) The solubility of CCl4 in water and seawater. *Deep Sea Research*. **45** (8), 1285 – 1302.

Bullister, J.L., Wisegarver, D.P. and Menzia, F.A. (2002) The solubility of sulfur hexafluoride in water and seawater . *Deep Sea Research* Part I: Oceanographic Research Papers, **49**(1) 175-187

Burton, W.C., Plummer, L. N., Busenberg, E., Lindsey, B.D. and Gburek, W.R., (2002), Influence of fracture anisotropy on ground-water ages and chemistry, Valley and Ridge Province, Pennsylvania. *Ground Water* v. **40**, no. 3, p. 242-257.

Busenberg, E. and Plummer, L. N. (2000) Dating young groundwaters with sulphur hexafluoride: natural and anthropogenic sources of sulphur hexafluoride. *Water Resources Research*, **36**, 3011-3030.

Busenberg, E. and Plummer, L. N. (1992) Use of chlorofluorocarbons (CCl3F and CCl2F2) as hydrologic tracers and age dating tools: the alluvium and terrace system of central Oklahoma. Water Resources Research, **28**(9) 2257-2283.

Busenberg, E. and Plummer, L.N. (2004) USGS-CFC2004. USGS spreadsheet program for preliminary evaluation of CFC data. *In: IAEA guidebook on the use of chlorofluorocarbons in hydrology*. International Atmic Energy Agency, Vienna, in press.

Busenberg, E. Weeks, E.P., Plummer, L. N. and Bartholomay R.C. (1993) Age dating ground water by use of chlorofluorocarbons (CCl3F and CCl2F2) and distribution of chlorofluorocarbons in the unsaturated zone, Snake River Plain aquifer. Idaho National Engineering Laboratory, Idaho. USGS.

Carey, M.A. & Chadha, D. (1998) Modelling the hydraulic relationship between the River Derwent and the Corallian limestone aquifer. *Quarterly Journal of Geology and Engineering Geology*, **31**, 63 - 72.

Carl Bro. (2004) Final project proposal: Seamer Carr Landfill Site, Scarborough: Assessment of Environmental Impacts (incorporating Star Carr Wetland Project Proposals).

Chadha, D. (1968) Investigations into the hydrogeology of the eastern Vale of Pickering. *Unpublished MSc Thesis*. University of Leeds.

Chadha, D., Barker, I.C. & Courchee, R. (1977) Groundwater resources of the Corallian between Ebberston and Filey. *Yorkshire Water Authority internal report no. 627:13.* Now held by UK Environment Agency, York office.

Ciccioli, P., Cooper, W.T., Hammer, P.M. and Hayes, J.M. (1980) Organic solute-mineral surface interactions: a new method for the determination of groundwater velocities. *Water Resources Research*, **16**, 217-223.

Coats, K.H. and Smith, B.D. (1964). Dead-end pore volume and dispersion in porous media. *Society of Petroleum Engineering Journal*, **4**, 73-84.

Cook, and Herczeg, A.L., eds. (2000) *Environmental tracers in subsurface hydrology.* Kluwer Academic Publishers, Boston, 529 p.

Cook, P.G. and Solomon, D.K. (1995) Transport of atmospheric trace gases to the water table: implications for groundwater dating with chlorofluorocarbons and 85Kr. *Journal of Hydrology*, **191**, 245-265

Cook, P.G. and Solomon, D.K. (1997) Recent advances in dating young groundwater: Chlorofluorocarbons, 3H/3He and 85Kr. Water Resources Research, 31(2), 263-270

Cook, P.G., Solomon, D.K., Plummer, L.N., Busenberg, E.. and Schiff, S.L (1995) Chlorofluorocarbons as tracers of groundwater transport processes in a shallow, silty sand aquifer. *Water Resources Research*, 31(3), 425-434.

Cook, P.G., Solomon, D.K., Sanford, W.E., Busenberg, E., Plummer, L.N. and Poreda, R.J. (1996) Inferring shallow groundwater flow in saprolite and fractured rock using environmental tracers. *Water Resources Research*, 32(6), 1501-1509.

Corbett, D.R., Dillon, K. and Burnett, W. (2000a) Tracing groundwater flow on a barrier island in the north-east Gulf of Mexico. *Estuarine, Coastal and Shelf Science 51, pp. 227-242.*

Corbett, D.R., L. Kump, K.S. Dillon, W.C. Burnett, J.P. Chanton (2000) Fate of Wastewater-borne Nutrients under Low Discharge Conditions in the Subsurface of the Florida Keys, USA, *Marine Chemistry* **69**, 99-115.
Da Costa, J.A. and Bennett, R.R.. (1960) The pattern of flow in the vicinity of a recharging and discharging pair of wells in an aquifer having areal parallel flow. *Int. Ass. Sci. Hydrol. Publication* **52**, pp. 524 - 536, Commission of Subterranean Waters. (cited in Grove et al, 1970).
Debenham, L.S. (1971) Scarborough's water supply: The influence of water on the expansion and prosperity of Victorian Scarborough and on Later Events. *(Report to the Scarborough Borough Council Water Committee, 1971).* Held by Scarborough Public Library.
Deipser, A. (1998) Biodegradation of volatile CFCs, H-CFCs and VC in compost and marl. *Waste Management Research*, **16**, 330-341.
Deipser, A. and Stegmann, R. (1997) Biological degradation of VCCs and CFCs under simulated anaerobic landfill conditions in laboratory test digesters. *Environmental Science and Pollution Research*, **4**, 209-216.
Delaney, D. (2000) A conceptual model for groundwater flow and attenuation at Seamer Carr landfill site. M.Sc. thesis for Queen's University of Belfast.
Delin, G.N., Healy, R.W., Landon, M.K. and Bohlke, J.K. (2000) Effects of topography and soil properties on recharge at two sites in an agricultural field. *Journal of the American Water Resources Research Association.* **36**: 1401-1416.
Denovan, B. and Strand, S. (1992) Biological degradation of chlorofluorocarbons in anaerobic environments. *Chemosphere*, **24**, 935-940.
Dillon, K.S., Corbett, D.R., Chanton, J.P., Burnett, W.C., Furbish, D.J. (1999) The use of sulfur hexafluoride (SF6) as a tracer of septic tank effluent in the Florida Keys. Journal of Hydrology. **220**(3-4), pp 129-140.
Domenico, P.A. and Schwartz, F.W. 2nd Ed. (1998) Physical and Chemical Hydrogeology. Wiley. pp 506
Drinking Water Inspectorate (UK) (1999) List of substances, products and processes approved under regulations 25 and 26 for use in connection with the supply of water for drinking, washing, cooking and food production purposes. DWI. http://www.dwi.gov.uk/cpp/pdf/sos1999.pdf
Drost, W.D., Klotz, D., Moser, H., Neumaier, F. and Rauert, W. (1968) Point dilution methods of investigating groundwater flow by means of radioisotopes. *Water Resources Research.*, **4**, 125 – 146.
Drost, W.D. (1983) Single well techniques. *In: Tracer methods in isotope hydrology, 7-16.* IAEA-TECDOC-291. International Atomic Energy Agency, Vienna, Austria.
Dunkle Shapiro, S., Rowe, G., Schlosser, P., Ludin, A. and Stute, M. (1998) Tritium/Helium-3 dating under complex conditions in hydraulically stressed areas of a buried -valley aquifer. *Water Resources Research*, 34, 1165-1180.
Dunkle, S.A., Plummer, L.N., Busenberg, E., Phillips, P.J. Denver, J.M., Hamilton, P.A. Michel, R.L and Coplen, T.B. (1993) Chlorofluorocarbons (CCl3F and CCl2F2) as dating tools and hydrologic tracers in shallow groundwaters of the Delmarva peninsular, Atlantic Coastal Plains, United States. *Water Resources Research*, 29(12), 3837-3860.
Ekwurzel, B., Schlosser, P., Jr. W.M.S, Plummer, L.N., Busenberg, E., Michel, R.L., Weppernig, R. and Stute, M. (1994) Dating of shallow groundwaters: Comparison of transient tracers 3H/4H, CFCs and 85Kr. *Water Resources Research.* 30:1693-1708.
Elkins, J. (1999). Chlorofluorocarbons. *In: The Chapman & Hall Encyclopedia of Environmental Science*, edited by David E. Alexander and Rhodes W. Fairbridge, pp pp.78-80, Kluwer Academic, Boston, MA.
Entec UK Ltd. (2001) Corallian limestone model update. Report to the Environment Agency.
Environment Agency, (1997) Report on the microbial tracer exercise at West Ayton, 13 - 14 Oct. 1997. Unpublished technical document.
European Geophysical Services (1981) Report on boreholes logged in the Ayton area. Yorkshire Water Authority internal report.
European Geophysical Services (2002) Report on the CCTV survey and geophysical logging of observation boreholes drilled for the Osgodby Aquifer Storage and Recovery scheme at Irton, Yorkshire. Report to Yorkshire Water Services Ltd.
European Geophysical Services (2004) Report on the CCTV survey and geophysical logging of three boreholes at Ayton, Yorkshire. Report to UCL Dept. of Earth Sciences.
Fetter, C.W. (1998) Contaminant Hydrogeology, 2nd Ed. Prentice-Hall, pp. 500
Fisher, H.B. (1968) Dispersion prediction in natural streams. Journal of Sanitary Engineering, American Civil Society of Engineers. 94 (SA5):927-944. Cited in USEPA, 2002.
Ford, D. & Williams, P., (1989) Karst geomorphology and hydrology. Chapman and Hall.
Fox-Strangways, C.S. (1892) The Jurassic rocks of Britain, **Vol.1:** Yorkshire
Freeze, R.A. & Cherry, J.A. (1979) Groundwater. Prentice Hall. 604p

Gamlin, J.D., Clark, J.F., Woodside, G. and Herndon, R. (2001) Large-scale tracing of ground water with sulfur hexafluoride. Journal of Environmental Engineering **127**(2), pp 171-174.
Gaspar, E. (1987a) Modern Trends in Tracer Hydrology, **Vol 1**. CRC Press. pp 145.
Gaspar, E. (1987b) Modern Trends in Tracer Hydrology, **Vol 2**. CRC Press. pp 137.
Golder Associates (2000). Leachate management assessment, Seamer Carr landfill site, Scarborough.
Golder Associates (2001). Report on management of leachate at Seamer Carr landfill; summary of proposed scheme.
Gossett, J.M. (1987) Measurement of Henry's Law constants for C1 and C2 chlorinated hydrocarbons. *Environmental Science and Technology*, **21**(2), 202-208.
Gresswell, R.K (1958) Glaciers and glaciation. Hulton Educational Publications. 128pp
Gresswell, R., Yoshida., K. Tellam, J.H., and Lloyd, J. W. (1998) The micro-scale hydrogeological properties of the Lincolnshire Limestone, UK. *Quarterly Journal of Engineering Geology*, **31**: 181-197.
Grisak, G., Merritt, W.F. and Williams, D.W. (1977) A fluoride borehole dilution apparatus for groundwater velocity measurements. *Canadian Geotechnology Journal.* **14**: 554 – 561.
Grove, D.B., Beetem, W.A. and Sower, F.B. (1970) Fluid travel time between a recharging and discharging well pair in an aquifer having a uniform regional flow field. *Water Resources Research.* **6**,(5) 1404 - 1410.
Hahne, A., Volz, A., Ehhalt, D., Cosatto, H., Roether, W. and Weiss, W. (1978) Depth profiles of chlorofluoromethanes in the Norwegian Sea. *Pure and Applied Geophysics*, **116**, 575-582.
Haine, T.W.N. (1992) The use of transient tracers to study upper ocean processes. PhD thesis. University of Southampton.
Halevy, E. Moser, H., Zellhofer, O and Zuber, A. (1967) Borehole dilution techniques – a critical review. *In: Isotopes in hydrology.* Symposium Proceedings, Vienna, 1966. IAEA, Vienna, Austria, pp. 531 – 563.
Hall, S. H., S. P. Luttrell, and W. E. Cronin (1991) A method for estimating effective porosity and ground-water velocity. *Ground Water,* V. **29**, no. 2, pp. 171-174
Hall, S. H. (1993) Single-well tracer tests in aquifer characterization. *Ground Water Monitoring and Remediation,* V. **13**, no. 2, pp. 118-124.
Hall, S.H. (1996) Practical single-well tracer methods for aquifer testing. Workshop Notebook, Tenth National Outdoor Action Conference and Exposition, May 13-15, 1996, Las Vegas, Nevada. National Ground Water Association, Columbus, Ohio, USA. http://www.sibak.com/Library/0006.htm
Hann, M. J. and Lovelace, G. (2000). Hydrological survey Star Carr (engineers' report). Cranfield University.
Happell, J.D. and Wallace, D.W.R. (1998) Removal of atmospheric CCl_4 under bulk aerobic conditions in groundwater and soils. *Environmental Science and Technology*, **19**, 1244-1252.
Happell, J.D., Price, R.M., Top, Z. and Swart, P.K. (2003) Evidence for the removal of CFC-11, CFC-12, and CFC-113 at the groundwater–surface water interface in the Everglades. *Journal of Hydrology,* **279**(1-4) 94-105.
Harrison, I. (1973) The hydrogeology of the Vale of Pickering. Unpublished PhD thesis, University of Leeds.
Hayes, J.M. and Thompson, G.M. (1977) Trichlorofluoromethane in groundwater - A possible indicator of groundwater age. Water Resources Research Center, Technical report 90, Purdue University, NTIS Report PB 265 170, 25pp.
Hohener, P., Werner, D. Balsiger, C and Pasteris, G. (2003) Worldwide occurrence and fate of chlorofluorocarbons in groundwater. *Critical Reviews in Environmental Science and Technology,* **33**(1), 1-29.
Hoopes and Harleman (1964) Waste water recharge and dispersion in porous media. , Techn Rep No 75 Hydrodynamic Lab, MIT, Cambridge.
Huhn, O., Roether, W. Beining, P. and Rose, H. (2001) Validity limits of carbon tetrachloride as an ocean tracer. Deep Sea Research Part I: *Oceanographic Research* **48**, (9), 2025-2049
Hunter-Smith, R.J., Balls, P.W. and Liss, P.W. (1983) Henry's Law constants and the air-sea exchange of various low molecular weight halocarbon gases. *Tellus,* **35B**, 170-176.
Institute of geological sciences (1980). *British Regional Geology: Eastern England from the Tees to the Wash (2nd Ed.)* HMSO. 155 pp.
Intergovernmental Panel on Climate Change (IPCC), (2001) Climate Change 2001. Working Group 1: The Scientific Basis. Accessed at http://www.grida.no/climate/ipcc_tar 19/12/2004.
Johnston, C.T., Cook, P.G. Frape, S.K., Plummer, L.N. Busenberg, E. and Blackport, R.J. (1998) Ground water age and nitrate distribution within a glacial aquifer beneath a thick unsaturated zone. *Ground Water*, **36**(1), 171-180.
Kass, W. (1998) *Tracing technique in geohydrology* (English edition, first published in German 1992). A.A. Balkema. 580p.

Katz, B.G., Böhlke, J.K., and Hornsby, H.D. (2001) Timescales for nitrate contamination of spring waters, northern Florida, USA. *Chemical Geology*, **179**, 167-186.
Katz, B.G., Lee, T.M., Plummer, L.N. and Busenberg, E. (1995a) Chemical evolution of groundwater near a sinkhole lake, northern Florida 1: Flow patterns, age of groundwater, and influence of lake water leakage. *Water Resources Research*, **31**(6), 1549-1564.
Kendrick, R.I. (1979) Some aspects of network flow testing in the Corallian limestone of north Yorkshire. Unpublished MSc Thesis, University of Durham.
Key, B.D., Howell, R.D. and Criddle, C.S.(1997) Fluorinated organics in the biosphere. *Environmental Science and Technology*. **31**: 2245-2254.
Khalil, M.A.K. and Rasmussen R.A. (1989) The potential of soils as a sink of chlorofluorocarbons and other man-mad chlorocarbons. *Geophysical Research Letters*, **16**(7), 679-682.
Khalil, M.A.K. and Rasmussen R.A. (1990) Emissions of trace gases from Chinese rice fields and biogas generators: CH4, N2O, CO, CO2, chlorocarbons and hydrocarbons. *Chemosphere*, **20**, 207-226.
Kofod, M. and Isenbeck-Schroter, M. (2000) Degradation of CFC during riverbed infiltration. pp. 263-264 *in: Groundwater 2000*, Copenhagen, Denmark. (eds. P.L. Bjerg, P. Engesgaard and T.D. Krom).
Kumar, B. and Nachiappan, Rm. P. (2000) Estimation of alluvial aquifer parameters by a single-well dilution technique using isotopic and chemical tracers: a comparison. *In: Tracers and modelling in hydrogeology*. Ed. A. Dassargues. IAHS Publication 262, pp. 53-56.
Lapworth, H. (1927) The New Irton Water Scheme. (Printed as an Addenda to Richardson (1934). Held by Scarborough Public Library.
Leap. D. I., and P. G. Kaplan (1988) A single-well tracing method for estimating regional advective velocity in a confined aquifer: theory and preliminary laboratory verification. *Water Resources Research*, V. **23**, no. 7, pp. 993-998.
Lee, B.S., Bullister, J.L., and Whitney, F.A., (1999) Chlorofluorocarbon CFC11 and carbon tetrachloride removal in Saanich inlet, an intermittently anoxic basin. *Marine Chemistry*, **66**(Aug), 171-185
Lesage, S., Brown, S. and Hosler, K.R. (1992) Degradation of chlorofluorocarbon 113 under anaerobic conditions. *Chemosphere*, **26**(9), 1225-1243.
Lesage, S., Jackson, R.E., Priddle, M.W. and Riemann, P.G. (1990) Occurrence and fate of organic solvent residues in anoxic groundwater at the Gloucester landfill, Canada. *Environmental Science and Technology*, **24**, 559-566.
Lesage, S., McBride, R.A., Cureton, P.M. and Brown, S. (1993) Fate of organic solvents in landfill leachates under simulated field conditions and in anaerobic microcosms. *Waste Management and Research*, **11**, 215-226.
Lloyd, J.W, Greswell, R., Williams, G.M., Ward, R.S., Mackay, R. and Riley, M.S. (1998) An integrated study of controls on solute transport in the Lincolnshire Limestone. *Quarterly Journal of Engineering Geology*, **29**, 321-339.
Lovelock, J.E. and Lipsky, S.R.(1960) *Journal of the American Chemistry Society*, 82, 431.
Lovelock, J.E. (1971) Atmospheric fluorine compounds as indicators of air movements. *Nature*, **230**, 379.
Lovley, D.R. and Woodward, J.C. (1992) Consumption of freons CFC11 and CFC12 by anaerobic sediments and soils. *Environmental Science and Technology*, **26**, 925-929.
Maiss, M. and Brenninkmeijer, C.A.M., (2000) A reversed trend in emissions of SF_6 to the atmosphere?, p. 199-204. *In "Non-CO2 Greenhouse Gases: Scientific Understanding, Control and Implementation"*, J. Van Ham, A.P.M. Baede, L.A. Meyer, and R. Ybema (editors), Proceedings of the 2nd International Symposium, Noordwijkerhout, The Netherlands, 8-10 September 1999, Kluwer Academic Publishers, Dordrecht
Maiss, M., and C.A.M. Brenninkmeijer. (1998) Atmospheric SF6: Trends, sources, and prospects. *Environmental Science and Technology* 32:3077-3086.
Maloszewski, P. and Zuber, A. (1985) On the theory of tracer experiments in fissured rocks with a porous matrix. *Journal of Hydrology*. 79: *30,* 333-358
Marcus, Y. (1997) Solubilities of Buckminsterfullerine and Sulfur Hexafluoride in various solvents. *Journal of Physical Chemistry B*, 101, 8617-8623.
Mather, J.D. and Smith, D.B. (1972) Thermonuclear tritium - its use as a tracer in local hydrogeological investigations. Unpublished technical report to the Institute of Geological Sciences.
Millhouse, W. (1934) Scarborough Corporation Water Works. *Proceedings of the British Association of Water-Works Engineers*, 1934. (Held at Scarborough Public Library).
Milsom, J. & Rawson, P. (1989) The Peak Trough - a major control on the geology of the North Yorkshire coast. *Geological Magazine* **126**(6), 699 - 705.
Morrison, T.J. and Johnston, N.B. (1955) The salting out of non-electrolytes III; The inert gases and SF6. *Journal of the Chemical Society*, pp. 3655 - 3659.

Morton, (1938) The protection of the water-gathering grounds contributing to the Irton, Osgodby and Cayton Bay waterworks" Scarborough Corporation. Held by Scarborough Public Library.
Mottram, P., (2003) Tracer and borehole dilution testing of groundwater in the Brompton area, north Yorkshire. Unpublished undergraduate thesis, University College London.
Mroczek, E.K. (1997) Henry's Law constants and distribution coefficients of sulphur hexafluoride in water from 25oC to 230oC. *Journal of Chemical Engineering Data*, **42**(1), 116-119.
Mull, D.S. and Smoot, J.L. (1986) Groundwater flow characteristics described by quantitative dye tracing in karst terrane in the Elizabethtown area, Kentucky. *Proceedings of the 'Environmental problems in karst terranes and their solutions'* Conference, Bowling Green Kentucky. 407-422. Cited in USEPA (1988)
National Rivers Authority (1992) *Policy and Practice for the Protection of Groundwater. HMSO.*
National Rivers Authority (1995a) *Guide to groundwater vulnerability mapping in England and Wales.* HMSO.
National Rivers Authority (1995b) *Guide to groundwater protection zones in England and Wales.* HMSO
Neale, S. (2001) Karst groundwater protection in England and Wales – an update *In: Protecting groundwater; an international conference on applying policies and decision-making tools to land-use planning.* Conference proceedings. National groundwater and contaminated land Centre project NC/00/10. Environment Agency, 2001.
Newcomer, D. R., S. H. Hall, and V. R. Vermuel (1996) Use of improved hydrologic testing and borehole geophysical logging methods for aquifer characterization. *Ground Water Monitoring and Remediation.*
Ordnance Survey (2000). Scarborough, Bridlington and Filey. 1:50 000 Landranger 101.
Oster, H., Sonntag, C. and Munnich, K.O. (1996) Groundwater age dating with chlorofluorocarbons. *Water Resources Research*, **32**(10), 2989-3001.
Oxley, D. (2002) A hydrogeochemical analysis of the Corallian limestone aquifer, north Yorkshire, England. Unpublished undergraduate dissertation, University of East Anglia.
Ozyurt, N.N. and Bayari, C.S. (2003) LUMPED: a Visual Basic code of lumped-parameter models for mean residence time analyses of groundwater systems. *Computers and Geosciences*, **29**, 79-90.
Palmer, C.D. (1993) Borehole dilution tests in the vicinity of an extraction well. *Journal of Hydrology*, **146**, 245 – 266.
Plummer, L.N. and Busenberg, E. (1999) Chlorofluorocarbons: Tools for dating and tracing young groundwater. Chapter 15 (pp 441-478) *in: Environmental Tracers in Subsurface Hydrology* (eds. P.Cook and A. Herczeg), Kluwer.
Plummer, L.N., Busenberg, E, McConnell, J.B., Drenkard, S., Schlosser, P. and Michel, R.L. (1998a). Flow of river water into a karstic limestone aquifer 1: Tracing the young fraction in groundwater mixtures in the Upper Floridan Aquifer near Valdosta, Georgia. *Applied Geochemistry*, **13**(Nov), 995-1015.
Plummer, L.N., Busenberg, E, Drenkard, S., Schlosser, P., Ekwurzel, B., Weppernig, R., McConnell, J.B. and Michel, R.L. (1998b) Flow of river water into a karstic limestone aquifer 2: Dating the young fraction in groundwater mixtures in the Upper Floridan Aquifer near Valdosta, Georgia. *Applied Geochemistry*, 13, 1017-1043.
Plummer, L.N., Busenberg, E., Böhlke, J.K., Nelms, D.L., Michel, R.L., and Schlosser, P. (2001) Groundwater residence times in Shenandoah National Park, Blue Ridge Mountains, Virginia, USA: a multi-tracer approach. *Chemical Geology*, **179**, 93-111.
Plummer, L.N., Michel, R.L., Thurman, E.M. and Glynn, P.D. (1993) Environmental tracers for age-dating young groundwaters. *In Regional Ground-Water Quality* (ed. W.M.Alley), p.255-294. van Nostrand Reinhold.
Poole, C. (2003) *The essence of chromatography.* Elsevier. 925pp.
Rademacher, L.K., Clark, J.F. and Boles, J.R. (2002) Groundwater residence times and flow paths in fractured rock determined using environmental tracers in the Mission Tunnel; Santa Barbara County, California, USA. *Environmental Geology*, **43**, 557-567.
Randall, J.H. and Schultz, T.R., (1976) Chlorofluorocarbons as hydrologic tracers: a new technology. *Hydrology Water Resources*, Arizona, Southwest, **6**, 189-195
Randall, J.H., Schultz, T.R. and Davis, S.N. (1977) Suitability of fluorocarbons as tracers in groundwater resources evaluation. *Technical report to Office of Water Research and Technology*, U.S. Department of the Interior, NTIS PB 277 488, 37pp.
Ravishankara, A.R., Solomon, S., Turnipseed, A.A. and Warren, R.F. (1993) Atmospheric lifetimes of long-lived halogenated species. *Science.* **259**: 194-199.
Reeves, M.J. (1973) Groundwater chemistry (of the Corallian aquifer); a report to the Yorkshire River Authority. Held by Yorkshire Water Services, report ref. COR/GEN/015.

Reilly, T.E., Plummer, L.N., Phillips, P.J. and Busenberg, E. (1994) The use of simulation and multiple environmental tracers to quantify groundwater flow in a shallow aquifer. *Water Resources Research*, **30**(2) 412-433.
Richardson, H. (1934). Scarborough Water Works. (Printed in the *Proceedings of the British Association of Water-Works Engineers*, 1934). Held by Scarborough Public Library.
Robinson, J.N. and Barker, J. (1999) A fractured/fissured approach to groundwater protection zones. *Research and Development Project Record W6/020/1*. Environment Agency 1999.
Scanlon, B.R., Mace, R.E., Barrett, M.E. and Smith, B. (2003) Can we simulate regional groundwater flow in a karst system using equivalent porous media models? Case study, Barton Springs Edwards aquifer, USA. *Journal of Hydrology,276,(1-4) 137-158.*
Scheutz, C., Winther, K. and Kjeldson, P. (2000) Removal of halogenated organic compounds in landfill gas by top-covers containing zero-valent iron. *Environmental Science and Technology,* **34**, 2557-2563.
Schultz, T.R. (1979) *Trichloromethane as a groundwater tracer for finite-state models.* Ph.D thesis, University of Arizona.
Schultz, T.R., Randall, J.H., Wilson, L.G. and Davis, S.N. (1976) Tracing sewage effluent recharge. *Ground Water*, **14**(6) 463-471.
Scott, R.P.W. (1996) *Chromatographic Detectors.* Marcel Dekker, New York.
SECOR (1998) *Seamer Carr landfill site: Hydrogeological desk study and data review.*
SECOR (1999) *DRAFT. Seamer Carr landfill site: Regulation 15 Risk Assessment.*
Semprini, L. Hopkins, G.D., McCarty, P.L. and Roberts, P.V. (1992) In-situ biotransformation of carbon tetrachloride and other halogenated compounds resulting from biostimulation under anoxic conditions. *Environmental Science and Technology*, **26**, 2454-2461.
Severinghaus, J.P., Keeling, R.F., Miller, B.R., Weiss, R.F., Deck, B., and Broecker, W.S., (1997) Feasibility of using sand dunes as archives of old air, *Journal of Geophysical Research* **102**, 16783-16792
Shapiro, S.D., Rowe, G., Schlosser, P., Ludin, A. and Stute, M. (1998) Tritium/3He dating under complex conditions in hydraulically stressed areas of a buried-valley aquifer. Water Resources Research. **34**(5), 1165-1180.
Shapiro, S.D., Schlosser, P., Smethie, W.M. and Stute, M. (1997) The use of 3H and tritiogenic 3He to determine CFC degradation and vertical mixing rates in Framvaren Fjord, Norway. *Marine Chemistry*, **59**, 141-157.
Smart, P.L. (1981) Variation of conduit flow velocities with discharge in the Longwood to Cheddar Rising system, Mendip Hills. *Proceedings of the 8th International Congress of Speleology.* **1**, 333-337. Cited in USEPA (1988).
Southern Science Ltd. (1994) Preliminary assessment of the hydrogeology of swallowholes on the rivers Rye and Riccal. Report to the Environment Agency.
Spurlock, F. Burow, K. and Dubrovsky, N. (2000) Chlorofluorocarbon dating of herbicide-containing well-waters in Fresno and Tulare counties, California. *Journal of Environmental Quality.* **29**, 474-483.
Stanton, W.I. and Smart, P.L. (1981) Repeated dye traces of underground streams in the Mendip Hills, Somerset. *Proceedings of the University of Bristol Speleological Society.* **16**(1) 47-48. Cited in USEPA (1988)
Straw, A. & Clayton, K. (1979) *The Geomorphology of the British Isles; Eastern and Central England.* Methuen & Co. 247p.
Szabo, Z. Rice, D.E. Plumier, L.N., Busenberg, E., Drenkard, S. and Schlosser, P. (1996) Age dating of shallow groundwater with chlorofluorocarbons, tritium/helium 3 and flowpath analysis, southern New Jersey coastal plain. *Water Resources Research.* **32**(4), 1023-1038.
Tate, T.K., Robertson, A.S. and Gray, D.A. (1970). The hydrogeological investigation of fissure flow by borehole logging techniques. *Quarterly Journal of Engineering Geology and Hydrogeology.* **2**, 195-215.
Thompson, G.M. (1976) *Trichloromethane, a new hydrologic tool for tracing and dating groundwater.* Ph.D. thesis, Indiana University.
Thompson, G.M. and Hayes, J.M. (1979) Trichlorofluoromethane in groundwater - a possible tracer and indicator of groundwater age. *Water Resources Research*, **15**(3), 546-554.
Thompson, G.M., Hayes, J.M. and Davis, S.N. (1974) Fluorocarbon tracers in hydrology. *Geophysical Research Letters* **1**(4), 177-180.
United States Environmental Protection Agency, (1988) Application of dye-tracing techniques for determining solute transport characteristics of ground water in karst terranes. Technical document EPA904/6-88-001. 103p.

United States Environmental Protection Agency, (2002) The QTRACER2 program for tracer-breakthrough curve analysis for tracer test in karstic aquifers and other hydrologic systems. EPA/600/R-02/00

Upstill-Goddard, R.C. and Wilkins C.S. (1995) The potential of SF_6 as a geothermal tracer. *Water Resources*, **29**(4), 1065-1068.

United States Geological Survey, Reston Laboratory web pages (http://water.usgs.gov/lab)

Wallace, D.W.R., Being, P. and Putzka, A. (1994) Carbon tetrachloride and chlorofluorocarbon in the south Atlantic Ocean 19° S. *Journal of Geophysical Research (Oceans)*, **99**, 7803 – 7819.

Ward, R.S., Williams, G.M. and Hills, C.C. (1996) Changes in major and trace components of landfill gas during subsurface migration. *Waste Management Research.* **14**, 243 – 261.

Ward, R.S., Williams, A.T., Barker, J.A., Brewerton, L.J. and Gail, I.N. (1998) Groundwater Tracer Tests: A review and guidelines for their use in British Aquifers. *British Geological Survey Report WD/98/19*

Warner, M.J. and Weiss, R.F. (1985) Solubilities of chlorofluorocarbons 11 and 12 in water and seawater. *Deep-sea research*, **32**(12), 1485-1497.

Waters-Marsh, P. (1984) *Tracer investigation of Bogg Hall karst, Kirbymoorside, North Yorkshire.* Unpublished MSc Thesis. University of East Anglia.

Watson, A.J., Upstill-Goddard, R.C. and Liss, P.S. (1991) Gas exchange in rough and stormy seas measured with a dual tracer technique. *Nature*, **349**, 145-147.

Watson, S. J. (2004) *Solute transport and hydrodynamic characteristics in the chalk at Timanstone, Kent.* Unpublished PhD thesis. University College London.

Weeks, E.P., Earp, D.E. and Thompson, G.M. (1982) Use of atmospheric fluorocarbons F11 and F12 to determine diffusion parameters of the unsaturated zone in the southern High Plains of Texas. *Water Resources Research*, **18**(5), 1365-1378.

Weppernig, R., Stute, M. (1994) Dating of shallow groundwater: comparison of the transient tracers 3H/3He, chlorofluorocarbons and 85Kr. *Water Resources Research*, **30**(6), 1693-1708.

Wilhelm, E., Battino, R. and Wilcock, R.J. (1977) Low pressure solubility of gases in liquid water. *Chemical Review*, **77**, 219-262.

Willard, H.H., Merritt, J., Dean, J.A. and Settle, J. (1988) *Instrumental methods of analysis.* Wadsworth Publishing Company.

Wilson, G.B., Andrews, J.N. and Bath, A.H. (1990) Dissolved gas evidence for denitrification in the Lincolnshire Limestone groundwaters, eastern England. *Journal of Hydrology*, **113**, 51-60.

Wilson, R.D. and Mackay, D.M. (1993) The use of sulphur hexafluoride as a conservative tracer in saturated sandy media. *Ground Water*, **31**, 719-724.

Wilson, R.D. and Mackay, D.M. (1996) SF_6 as a conservative tracer in saturated media with high intergranular porosity or high organic carbon content. *Ground Water*, **34**, 241-249.

Yorwaste. (2000). Operational Plan (map), Seamer Carr landfill site.

Yorwaste (1995) Geology, hydrogeology and hydrology of Seamer Carr landfill and the proposed extension area.

APPENDIX 1

A SHORT HISTORY OF SCARBOROUGH'S WATER SUPPLY[38]

Black Douglas the Scot razed Scarborough to the ground in 1318. However, this antisocial behaviour led to the construction of the town's first piped water supply.

The area had been inhabited for several centuries prior to the depredations of Black Douglas, archaeological evidence indicating that the Romans (c. 370AD) had been using water from a well sunk in the Corallian on Castle Hill (Figure A1.1). (Which, incidentally, at c. 0.08km^2 must be a strong candidate for the Corallian's smallest catchment.) Nevertheless, subsequent inhabitants of the town, requiring more water than Castle Hill could supply, took it upon themselves to dig more wells, most of which were in the drift. The water from these wells is reported to have weighed an ounce per gallon more than the Castle Hill water, obviously indicating greater dissolved solids (and probably some not-quite-so-dissolved solids too).

When the Franciscan monks arrived in 1239 these wells were found to be satisfactory. However, by 1283 they had decided it would be better to have their own supply, and commissioned a conduit to be extended from springs outside the town. However, bureaucracy being what it is, this scheme was not put into effect until 26 years later when pure necessity, in the bearded form of Black Douglas, had shoved the rebuilding of the town down their throats.

Thus, in 1319, three conduits were built between the town and Corallian springs to the south-west (in Falsgrave). These supplied three wells in the town, and were found to be sufficient for the next twenty years, when the needy Franciscans completed a fourth conduit so as to avoid sharing their supply with the townsfolk. These conduits have periodically surfaced during later constructions in the town, and are noted to have been made of stone slabs some two feet (0.6m) beneath the surface. That they were exceptionally leaky was not a matter of urgent importance, as between 1349 and 1400 the Black Death killed half the population. However, once the townsfolk had got back on their feet, they installed lead pipework to address the problem, thus securing a steady supply until it was found, once again, that there wasn't enough to 'go around'.

[38] This section a short synopsis of lengthier articles by Lapworth (1927), Millhouse (1934), Richardson (1934) and Debenham (1971).

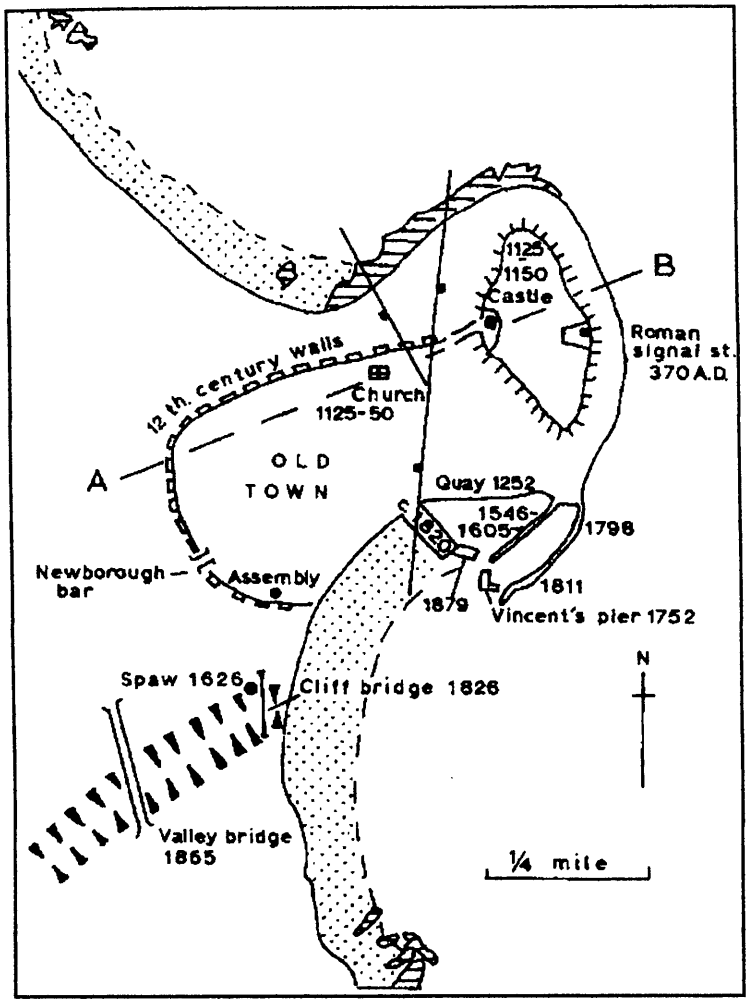

Figure A1.1 Scarborough Castle Hill showing two major faults (the 'Y' shape) and some less important local features.

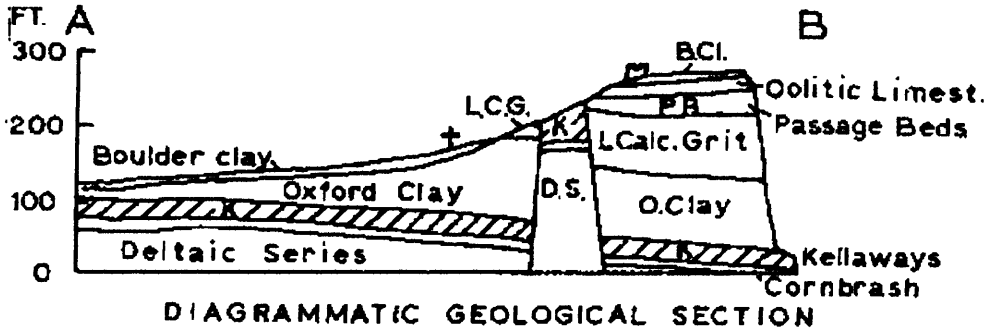

Figure A1.2 Cross section (A-B) through Scarborough castle Hill as shown on Figure 2.29.

This was three centuries later, a testament to the efficacy of lead piping. In the meantime the Franciscans had been kicked out by Henry VIII (1539), leaving the supply in secular hands. By the mid- to late-seventeenth century Scarborough was becoming known for its 'Spaw' (spa) waters, although its popularity did not really burgeon for another hundred years. In 1781 the Scarborough Corporation, a public body, petitioned parliament for funds to improve the supply. But, by 1801, nothing having been done, the Scarborough Mercury was scooping fistfights in the queues at the wells.

Some improvements were brought about in the distribution systems, but the supply was still predominantly from the three springs at Falsgrave, each tapping a different level in the limestone, with a couple of additional smaller sources. Conditions remained unsatisfactory for another twenty years, until the modern era arrived at Scarborough in the shape of a certain Mr. William Smith.

Amongst his many achievements, Smith was able to list, at 200 000 gallons (about $900m^3$) 'the largest covered receptacle in England', a reservoir built to prevent the various spring sources previously tapped from running to waste. And that was not all, for by his own account he seems to have constructed some sort of piezometer (perhaps the first in British hydrogeology) during his further investigations into the potential for damming water within the Corallian at (probably) Falsgrave. His investigations bore some fruit, as through these measures he succeeded in raising the groundwater level by 14ft (4.25m), thus capturing much winter rainfall for summer use.

Smith's work, however, was not sufficient to counter the ever-more rapidly growing demand. Scarborough's population was to triple in the first half of the 19th century, and the seasonal demand increased in tandem. The only obvious solution to the town's problems was provided by *Capitalism* which, represented by Scarborough Water Company, bought a spring-driven mill at Cayton Bay and converted it to a pumping station, in 1845. This was supplemented by the sinking of Osgodby well, 10ft in diameter and with three adits, in 1872 and, once the Company had been transferred to public ownership, a further well sunk at Irton (1882). The Irton New Well was drilled in 1927 to double production, with further wells being drilled at Filey (1957) and Cayton Carr (1971). Figure 2.29 shows the increase in production, all of it from the Corallian, between 1845 and 1992.

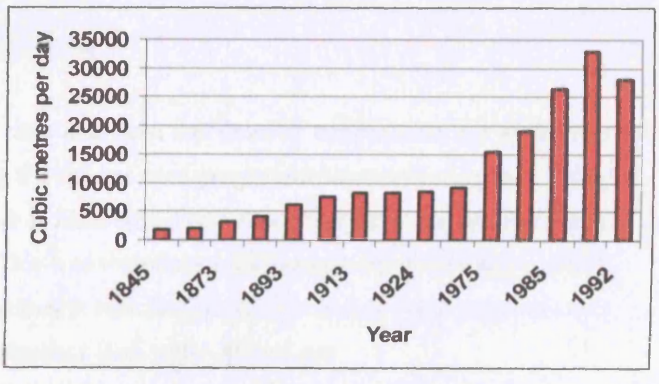

Figure A1.3 The growth of Scarborough's water supply, 1845 – 1992.

With the growth of the water supply, so too the awareness of pollution. The first (poorly) recorded tracer test between the Forge Valley swallows and Irton was in 1908, and the Scarborough Corporation, in 1938, produced a report entitled "The protection of the water-gathering grounds contributing to the Irton, Osgodby and Cayton Bay waterworks" (Morton, 1938). See Chapter 2 for more exciting details!!!

APPENDIX TWO

GAS CHROMATOGRAPHY, ORDER OF ANALYSIS

Method for water samples.

1) Ensure gas flow rates and oven and detector temperatures are at the correct settings, and that the computer controlling the GC has been programmed correctly to receive a sample.
2) Affix glass syringe to three-way Luer-Lok at top of purge tower.
3) Flush Luer-Lok with a few mL of sample.
4) Flush purge tower with a few mL of sample.
5) Drain purge tower.
6) Immerse trapping loop in liquid nitrogen until temperature is maintained at -185°C.
7) Inject 50-60mL of sample into purge tower, close Luer-Lok and remove syringe.
8) Allow sample to purge for 10 minutes.
9) Switch 6-way sampling valve to sampling position.
10) Remove liquid nitrogen bath and replace with boiling water bath
11) Contemporaneously with 10), press button to start data acquisition and temperature programme.

Method for standard analysis

1) Ensure gas flow rates and oven and detector temperatures are at the correct settings, and that the computer controlling the GC has been programmed correctly to receive a sample.
2) Ensure purge tower is filled with a completely purged water sample (purged for a few tens of minutes or longer). This is to reproduce actual sample conditions more closely.
3) Ensure correct volumetric standard loop is attached to 6-way standard valve.
3) Flush volumetric standard loop with standard gas
4) Immerse trapping loop in liquid nitrogen until temperature is maintained at -185°C.
5) Stop standard gas flow through volumetric standard loop.
6) Switch 6-way standard valve to flush purge gas through volumetric standard loop, and subsequently through filled purge tower and through cold trap.
7) Repeat steps 3, 5 and 6 until the desired volume of standard has been flushed through the cold trap.
8) Follow steps 9) – 11) as for water sample analysis.

APPENDIX 3

BOREHOLE LOGS FROM OSGODBY ASR BOREHOLES

The following three geophysical borehole logs were provided to the author in photocopy and bitmap format by YWS Ltd, but not in the original PDF format. Larger reproduction has been attempted but the quality remains poor. The logs are described in more detail in Chapter 5. Note that the order of presentation is OBH 2, then 4, then 5.

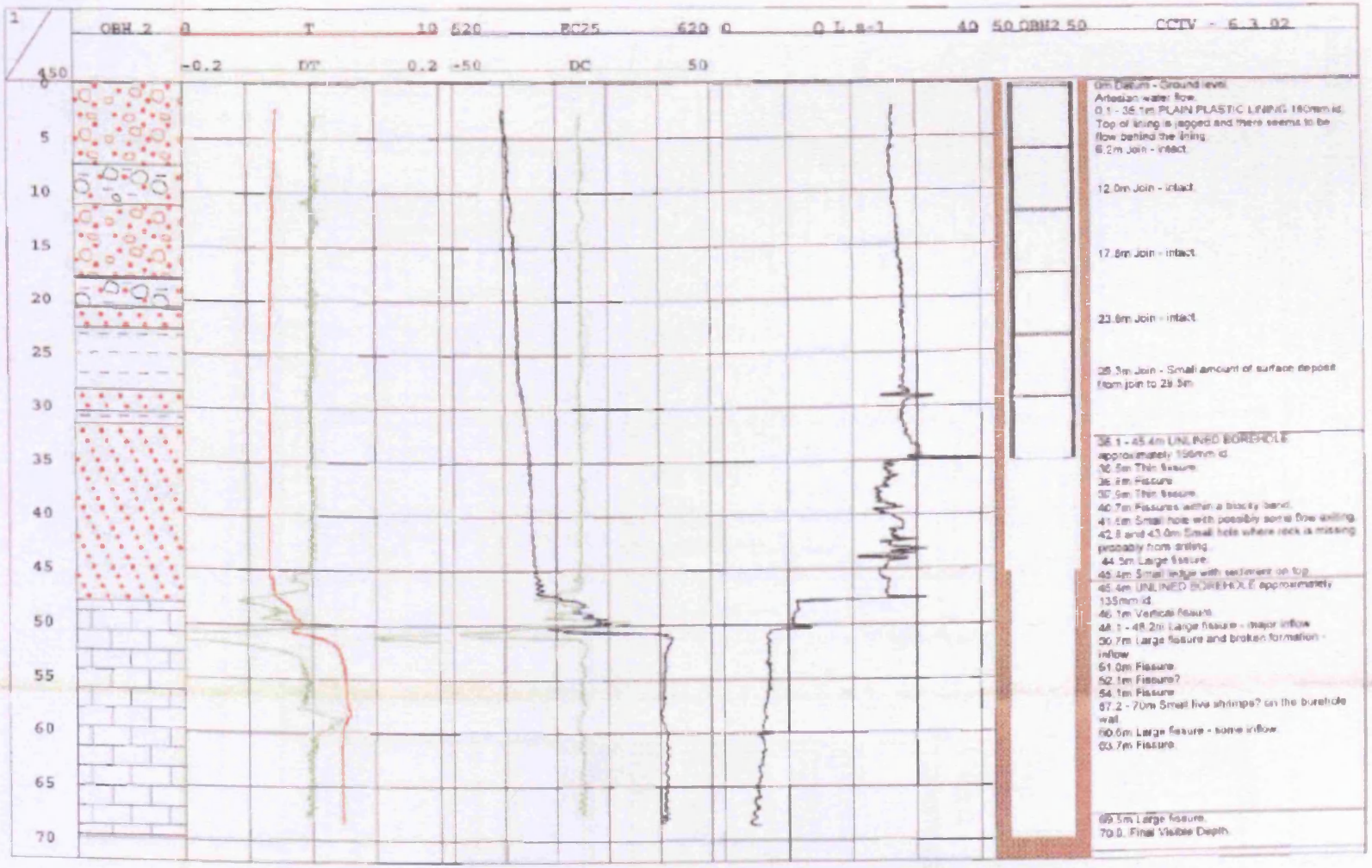

Figure A3.1 Geophysical log of OBH 2 showing Temperature, differential temperature, Electrical conductivity normalised to 25° C and differential conductivity, fluid flow, construction and fissure details.

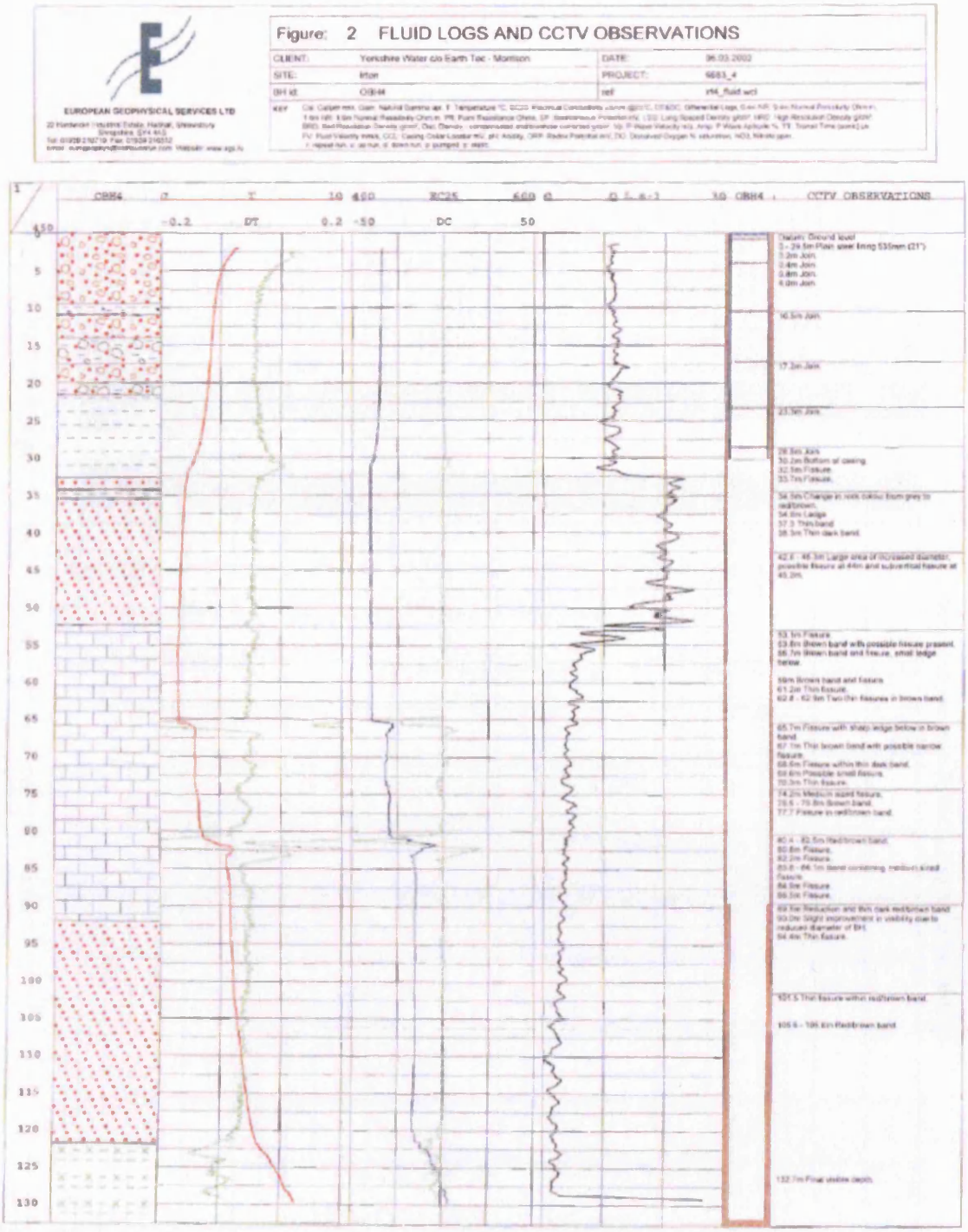

Figure A3.2 OBH 4 Geophysical borehole log

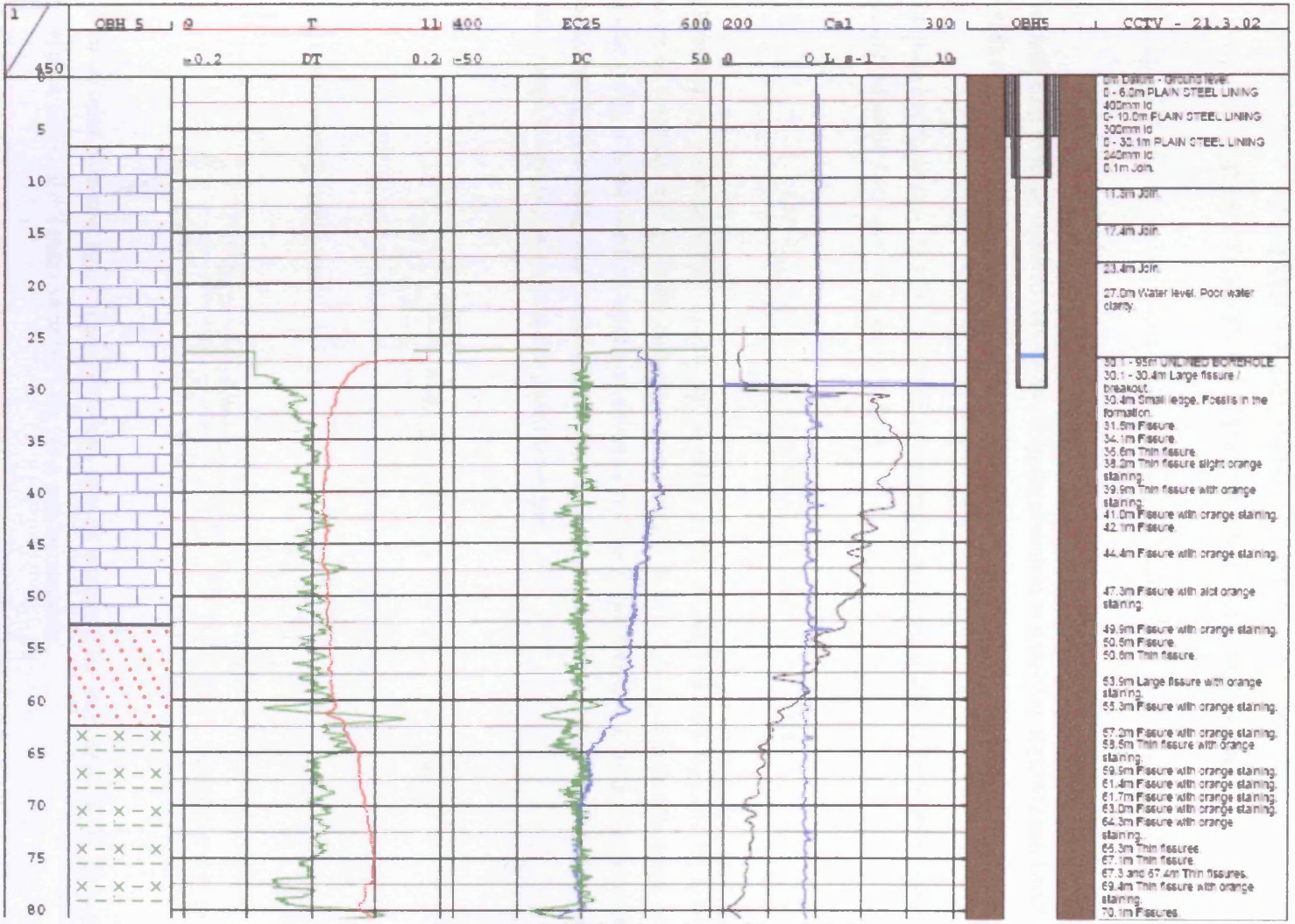

Figure A3.3 OBH 5 Geophysical borehole log

APPENDIX FOUR

BOREHOLE DILUTION TEST ANALYSIS: DERIVATION OF THE 'STANDARD' METHOD.

The following series of equations are based on theory presented in Halevy *et al* (1967) and Drost *et al* (1968).

The change of tracer mass in a borehole over time is equivalent to the difference between the mass flux into and out of the borehole. This may be written:

$$\Pi r^2 L_{SAT} \Delta C = q L_{SCRN} \alpha D (Cb - C) \Delta t \qquad \text{A4.1}$$

Where r is the borehole radius, L_{SAT} is the saturated length of borehole (m), L_{SCRN} is the screened length of borehole (m), ΔC is the change in concentration (g/m^3), q is the specific discharge of the aquifer (m/d), α is the width of aquifer contributing to flow in the borehole, D is the diameter of the borehole (m), Cb is background concentration (g/m^3), C is the concentration at any time t (m^3/d) and Δt is the change in time (d). Integrating this equation we get:

$$\Pi r^2 L_{SAT} \int_{C0}^{C} \frac{dC}{Cb - C} = q L_{SCRN} \alpha D \int_{t0}^{t} dt \qquad \text{A4.2}$$

This, upon rearrangement gives:

$$q = \frac{\Pi r^2 L_{SAT}}{\alpha 2 r t L_{SCRN}} \ln\left(\frac{Cb - C}{Cb - C0}\right) \qquad \text{A4.3}$$

As, for an open borehole, $L_{SAT} = L_{SCRN}$ and alpha may be taken as 2 for most cases where there is no gravel pack (see Ogilvi's equation below), Eq. A4.4 may be rewritten:

$$\ln\left(\frac{Cb - C}{Cb - C0}\right) = \frac{4qt}{\Pi r} \qquad \text{A4.5}$$

However, as we plot $\ln\left(\frac{C-Cb}{C0-Cb}\right)$ and not $\ln\left(\frac{Cb-C}{Cb-C0}\right)$ it is necessary to multiply both sides by -1 to complete the analysis, that is:

$$\ln\left(\frac{C-Cb}{C0-Cb}\right)=\frac{-4qt}{\Pi r} \qquad \text{A4.6}$$

So that the slope of the line plotted, A,

$$A = -\frac{4q}{\Pi r} \qquad \text{A4.7}$$

And thus:

$$-q = \frac{\Pi rA}{4} = 0.785rA \qquad \text{A4.8}$$

Assuming a porosity it is possible to calculate an average linear velocity according to v = q/ne. Ogilvi's equation (cited in Halevy, 1967) for calculating α is:

$$\alpha = \frac{4}{\left[1+\left(\frac{r1}{r2}\right)^2\right]+\frac{K2}{K1}\left[1-\left(\frac{r1}{r2}\right)^2\right]} \qquad \text{A4.9}$$

Where r1 and r2 are the inner and outer well radii respectively, and K1 and K2 the hydraulic conductivity of the well screen and the aquifer, respectively, from which it can be seen that when r1 = r2, α = 2.

APPENDIX FIVE

A SPREADSHEET SIMULATION OF A BOREHOLE DILUTION TEST

This appendix is based on a document provided by John Barker, UCL.

An advection-dispersion model of a borehole dilution test (BHDT) has been implemented within Microsoft Excel (BH_DIL#.XLS where # represents the version number). The code was primarily designed for simulation, to give insights into the types of behaviour that might be seen during a BHDT. However, if used with careful judgement, the code can also be used to interpret real data via manual calibration.

Conceptual model and mathematical description

The model for borehole dilution is one of steady-state flow, controlled by inflows and outflows, and transient advective-dispersion of solute in one dimension. The following diagram provides the basic notation.

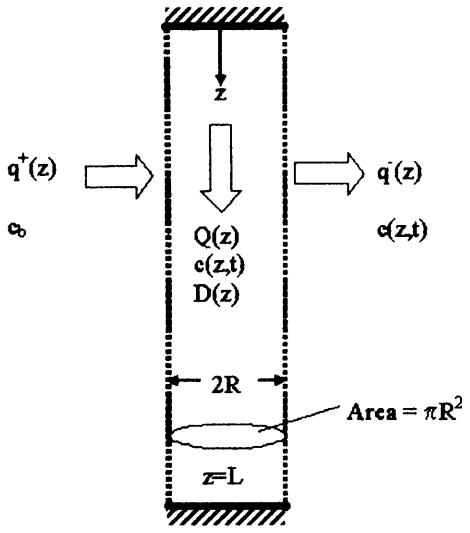

Figure A5.1 Basic notation describing the borehole dilution model.

We regard the vertical volumetric flux in the borehole to be a function of the fluxes in and out:

$$\frac{dQ(z)}{dz} = q^+(z) - q^-(z) \qquad \text{(A5.1)}$$

We assume zero flow through the top and bottom of the system:

$$Q(0) = Q(L) = 0 \qquad \text{(A5.2)}$$

We assume perfect mixing across the borehole so at any depth we have a single concentration $c(z,t)$. This is assumed to be governed by the advection-dispersion equation in the form:

$$A\frac{\partial c(z,t)}{\partial t} + \frac{\partial Q(z)c(z,t)}{\partial z} = A\frac{\partial}{\partial z}\left[D(z)\frac{\partial c(z,t)}{\partial z}\right] + q^+(z)c_b - q^-(z)c(z,t) \qquad \text{(A5.3)}$$

From left to right, the terms represent: rate of change of mass, net vertical advective flux, vertical dispersive flux, lateral flux in, and lateral flux out.

$D(z)$ represents a dispersion coefficient which is considered a function of Q and hence of z. This has been assumed to take the form:

$$D(z) = \alpha v(z)^P$$
$$v(z) = \frac{|Q(z)|}{\pi R^2} \qquad \text{(A5.4)}$$

So α can be regarded as a generalized dispersivity, which will have dimensions dependent on the power, P. (The normal case is when P=1.) The validity of Equation (A5.4) need to be tested and the parameters determined by fitting the model to data: point tests provide particularly suitable data.

The second term in Equation (A4.3) can be expanded and then use made of Equation (A5.1) to give:

$$A\frac{\partial c(z,t)}{\partial t} + Q(z)\frac{\partial c(z,t)}{\partial z} = A\frac{\partial}{\partial z}\left[D(z)\frac{\partial c(z,t)}{\partial z}\right] + q^+(z)\left[c_b - c(z,t)\right] \qquad \text{(A5.5)}$$

Numerical Implementation

We discretize the system in two ways that must not be confused.

Physical sectioning of the borehole

Firstly we consider the borehole to comprise sections which can be as small as a fracture or as large as the distance between two fractures. A single section is defined as having uniform lateral fluxes, in and out, and a constant initial concentration.

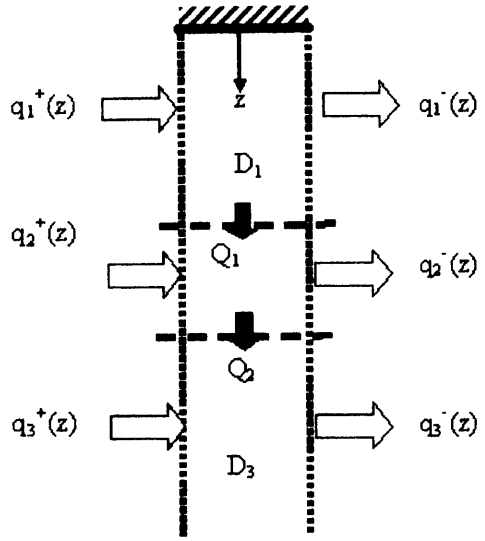

Figure A5.2 Physical sectioning of the borehole.

The vertical fluxes at the section boundaries are readily obtained as:

$$Q_n = Q_{n-1} + \left(q^+_{n-1} - q^-_{n-1}\right)\left(z_n - z_{n-1}\right) \qquad \text{(A5.6)}$$

Within each section we interpolate to obtain the flux at any depth, z:

$$Q(z) = Q_{n-1} + \left(q^+_{n-1} - q^-_{n-1}\right)\left(z - z_{n-1}\right) \qquad \text{(A5.7)}$$

Numerical discretization

The numerical solution is achieved using a simple finite-difference approach with a constant time step:

$$\Delta t = t_j - t_{j-1} \qquad \text{(A5.8)}$$

and spatial step:

$$\Delta z = z_i - z_{i-1} \qquad \text{(A5.9)}$$

Note the use of subscripts (n, i and j, respectively) to distinguish the three discretizations: 'physical', 'numerical depth', 'numerical time'. Concentration is represented thus:

$$c_i^j = c(z_i, t_j)$$

Values on the spatial discretization grid are obtained from values on the physical grid by linear interpolation. The discretization of Equation (5) employed is the fully-implicit scheme:

$$A\frac{c_i^{j+1}-c_i^j}{\Delta t}+Q_i\frac{c_i^{j+1}-c_i^{j-1}}{2\Delta z}=\frac{A}{\Delta z}\left[D\left(z_i+\frac{\Delta z}{2}\right)\frac{c_{i+1}^{j+1}-c_i^{j+1}}{\Delta z}-D\left(z_i-\frac{\Delta z}{2}\right)\frac{c_i^{j+1}-c_{i-1}^{j+1}}{\Delta z}\right]+q_i^+\left[c_b-c_i^{j+1}\right] \tag{A5.10}$$

This can be manipulated into the form

$$A_ic_{i-1}^{j+1}+B_ic_i^{j+1}+C_ic_{i+1}^{j+1}=R_i^j \tag{A5.11}$$

for the i[th] spatial numerical depth. The left hand side concentrations are all at time t_{j+1} and the three coefficients (A_i, B_i, C_i) are time independent. The right-hand term, R_i^j, contains concentrations at the previous time t_j.

Such a set of equations (one for each depth, z_i) can be recognized as a 'tridiagonal' system and is accurately solved by a routine based on the Thomas algorithm. The result is the full set of concentrations, at the numerical discretization intervals, all the way down the borehole at time t_{j+1}, based on the values of concentration at time t_j. Thus the code advances in time. Of course the initial concentrations must be specified and those must be provided within the same spatial intervals as the lateral fluxes.

Implementation

The model has been implemented in Excel with the solution of the numerical equations and other computations, such as interpolation, written in Visual Basic.

APPENDIX 6

BOREHOLE DILUTION TEST SIMULATION MODEL INPUTS

Top	Bottom	qin	qout	Q
0	1	0.5	7.5	0
1	2	0.5	0.5	-7
2	3	0.5	0.5	-7
3	4	0	0	-7
4	5	0	0	-7
5	6	0	0	-7
6	7	0	0	-7
7	8	4	4	-7
8	9	4	4	-7
9	10	4	4	-7
10	11	4	4	-7
11	12	4	4	-7
12	13	4	4	-7
13	14	4	4	-7
14	15	0	50	-7
15	16	0	0	-57
16	17	0	0	-57
17	18	0	0	-57
18	19	0	0	-57
19	20	0	0	-57
20	21	0	0	-57
21	22	0	0	-57
22	23	0	0	-57
23	24	0	0	-57
24	25	0	0	-57
25	25.2	0	0	-57
25.2	25.4	0	0	-57
25.4	25.6	490	0	-57
25.6	25.8	0	0	41
25.8	26	0	0	41
26	26.2	0	0	41
26.2	26.4	0	0	41
26.4	26.6	0	0	41
26.6	26.8	0	0	41
26.8	27	0	0	41
27	28	0	0	41
28	29	0	0	41
29	30	0	0	41
30	31	0	40	41
31	32	0.5	0.5	1
32	33	0.5	0.5	1
33	34	0.5	0.5	1
34	35	0.5	1.5	1

Augmentation borehole model inputs

Top	Bottom	qin	qout	Q
0	0.2	0.75	0.75	0
0.2	0.4	0.75	0.75	0
0.4	0.6	0.6	0.6	0
0.6	0.8	0.6	0.6	0
0.8	1	0.6	0.6	0
1	1.2	0.6	0.6	0
1.2	1.4	0.6	0.6	0
1.4	1.6	0.6	0.6	0
1.6	1.8	0.6	0.6	0
1.8	2	0.6	0.6	0

Brompton Dale Deep borehole model inputs

Top	Bottom	qin	qout	Q
0	0.5	0	0.9	0
0.5	1	0	0	-0.45
1	1.5	0	0	-0.45
1.5	2	0.2	0	-0.45
2	2.5	0	0	-0.35
2.5	3	0	0	-0.35
3	3.5	0	0	-0.35
3.5	4	0	0	-0.35
4	4.5	0	0	-0.35
4.5	5	0	0	-0.35
5	5.5	0	0	-0.35
5.5	6	0	0	-0.35
6	6.5	0	0	-0.35
6.5	7	0.7	0	-0.35

Derwent Ford borehole model inputs

Top	Bottom	qin	qout	Q
0	0.5	0	1	0
0.5	1	0	0	-0.5
1	1.5	0	0	-0.5
1.5	2	0	0	-0.5
2	2.5	0	0	-0.5
2.5	3	0	0	-0.5
3	3.5	0	10	-0.5
3.5	4	0	0	-5.5
4	4.5	0	0	-5.5
4.5	5	0	0	-5.5
5	5.5	0	0	-5.5
5.5	6	0	0	-5.5
6	6.5	0	0	-5.5
6.5	7	0	0	-5.5
7	7.5	0	0	-5.5
7.5	8	11.2	0	-5.5
8	8.5	0	0	0.1
8.5	9	0	0	0.1
9	9.5	0	0	0.1
9.5	10	0	0.2	0.1
10	16	0	0	0

Tetherings Plump borehole model inputs: vertical flow model

Top	Bottom	qin	qout	Q
0	0.5	0.25	0.65	0
0.5	1	0.25	0.25	-0.2
1	1.5	0.25	0.25	-0.2
1.5	2	0.25	0.25	-0.2
2	2.5	0.25	0.25	-0.2
2.5	3	0.25	0.25	-0.2
3	3.5	2	2	-0.2
3.5	4	2	2	-0.2
4	4.5	2	2	-0.2
4.5	5	2	2	-0.2
5	5.5	2	2	-0.2
5.5	6	2	2	-0.2
6	6.5	2	2	-0.2
6.5	7	2	2	-0.2
7	7.5	2	2	-0.2
7.5	8	2.6	2	-0.2
8	8.5	0	0.2	0.1
8.5	9	0	0	0
9	9.5	0	0	0
9.5	10	0	0	0
10	16	0	0	0

Tetherings Plump borehole model inputs: horizontal flow model

Top	Bottom	qin	qout	Q
0	1	3.5	0	0
1	2	0	0	3.5
2	3	0	0	3.5
3	4	0	0	3.5
4	5	0	0	3.5
5	6	0	0	3.5
6	7	0	0	3.5
7	8	0	0	3.5
8	9	0	0	3.5
9	10	0	0	3.5
10	11	0	0	3.5
11	12	0	0	3.5
12	13	0	0	3.5
13	14	0	0	3.5
14	15	0	0	3.5
15	16	0	0	3.5
16	17	0	0	3.5
17	18	0	0	3.5
18	19	0	0	3.5
19	20	0	0	3.5
20	21	0	0	3.5
21	22	0	0	3.5
22	23	0	0	3.5
23	24	0	0	3.5
24	25	0	0	3.5
25	26	0	0	3.5
26	27	0	0	3.5
27	28	0	3.5	3.5

Wykeham Village Hall borehole model inputs

Top	Bottom	qin	qout	Q
0	0.2	0	2	0
0.2	0.4	0	0	-0.4
0.4	0.6	0	63	-0.4
0.6	0.8	0	0	-13
0.8	1	0	0	-13
1	1.2	0	0	-13
1.2	1.4	0	0	-13
1.4	1.6	0	0	-13
1.6	1.8	0	0	-13
1.8	2	69	0	-13
2	2.2	0	0	0.8
2.2	2.4	0	0	0.8
2.4	2.6	0	4	0.8

Brompton Dale Shallow borehole model inputs

Top	Bottom	qin	qout	Q
0	0.5	0.5	1	0
0.5	1	0.5	0.5	-0.25
1	1.5	0.5	0.5	-0.25
1.5	2	0.5	0.5	-0.25
2	2.5	0.5	0.5	-0.25
2.5	3	8.5	0	-0.25
3	3.5	0	0	4
3.5	4	0	0	4
4	4.5	0	0	4
4.5	5	0	0	4
5	5.5	0	0	4
5.5	6	0	40	4
6	6.5	0	0	-16
6.5	7	0	0	-16
7	7.5	0	0	-16
7.5	8	0	0	-16
8	8.5	0	0	-16
8.5	9	0	0	-16
9	9.5	18	0	-16
9.5	10	0	0	-7
10	10.5	0	0	-7
10.5	11	0	0	-7
11	11.5	14	0	-7
11.5	12	0	0	0

Swallowholes Borehole model inputs.

APPENDIX 7

BOREHOLE DILUTION TESTS AND TRACER TEST DATA

The following tables give data from the borehole dilution tests and tracer tests conducted as part of this research.

Depth mbfl	Background conductivity mS/cm	Temp Centigrade	Conductivity mS/cm				
			0 Minutes	20 Mins	60 mins	150 mins	1125 mins
5	0.52	8.8	1.76	1.61	1.65	1.56	0.92
6	0.52	8.8	1.76	1.74	1.67	1.54	0.92
7	0.52	8.9	1.81	1.77	1.65	1.5	0.89
8	0.52	8.9	1.78	1.77	1.61	1.43	0.88
9	0.52	9	1.77	1.77	1.55	1.31	0.85
10	0.53	9	1.75	1.72	1.47	1.25	0.83
11	0.53	9.1	1.66	1.58	1.38	1.19	0.78
12	0.54		1.65	1.55	1.23	1.11	0.77
13	0.69	9.2	1.63	1.46	1.17	1.04	0.76
14			1.89	1.43	1.22	1.04	0.73
15	0.67	9.4	1.79	1.58	1.18	1	0.73
16	0.69		1.63	1.46	1.11	0.93	0.72
17	0.7	9.5	1.33	1.29	0.95	0.86	0.73
18	0.7		1.42	1.1	0.93	0.81	0.73
19	0.7	9.5	1.56	1.02	0.87	0.75	0.71
20	0.58	9.4	1.78	1.18	0.79	0.56	0.58
21	0.57	9.4	1.62	1.3	0.73	0.54	0.56
22	0.56	9.4	1.57	1.27	0.67	0.54	0.53
23	0.58	9.4	1.68	1.16	0.65	0.55	0.54
24	0.59	9.5	1.52	1.23	0.62	0.56	0.56
25	0.6	9.5	1.35	1.13	0.6	0.59	0.56
26	0.68	9.5	2.04	0.81	0.67	0.67	0.57
27	0.68	9.5	2.04	0.8	0.67	0.67	0.67
28	0.68	9.6	2.03	0.74	0.67	0.67	0.67
29	0.68	9.6	1.92	0.69	0.67	0.67	0.67
30	0.68	9.6	1.75	0.68	0.67	0.67	0.67
31	0.68	9.6	1.57	0.68	0.67	0.67	0.67
32	0.68	9.6	1.27	0.67	0.67	0.67	0.67
33	0.68	9.6	1.04	0.67	0.67	0.67	0.67
34	0.68	9.6	0.74	0.67	0.67	0.67	0.67
35	0.68	9.6	0.7	0.67	0.67	0.67	0.67
36	0.68	9.6	0.7	0.67	0.67	0.67	0.67
37	0.68	9.6	0.7	0.67	0.67	0.67	0.67
38	0.68	9.6	0.73	0.67	0.67	0.67	0.67
39	0.68	9.6	0.81	0.67	0.67	0.67	0.67
40	0.68	9.6	1.11	0.68	0.67	0.67	0.67
41	0.68	9.6	1.51	0.68	0.68	0.68	0.68
42	0.68	9.6	1.6	0.68	0.68	0.68	0.68
43	0.68	9.7	1.66	0.68	0.7	0.69	0.68
44	0.68		1.83	1.68	1.72	1.49	0.68
45	0.68		1.97	1.87	1.8	1.51	0.77
46	0.68	9.7		2.06	1.75	1.48	0.77

Table A7.1 Augmentation Borehole BHDT results

Depth mbfl	Background conductivity mS/cm	Conductivity mS/cm						
		1 min	8 mins	35 mins	78 mins	120 mins	220 mins	940 mins
28.8	0.63	8.3	10.7	10.42	10.14	9.9	9.63	7.65
28.3			10.72	10.39	10.09	9.88	9.62	7.53
28	0.63	13	10.8	10.39	10.07	9.76	9.55	7.51
27	0.63	5	5.5	5	4.2	5.45	5.6	7.47
26	0.55	1.27	0.95	0.81	0.59	0.53	0.51	0.71
25	0.55	1.17	0.92	0.78	0.56	0.54	0.52	0.52
24	0.47	0.86	0.87	0.71	0.55	0.52	0.49	0.52
23	0.47	1.07	0.96	0.85	0.55	0.53	0.49	0.48
22	0.47	1.02	0.95	0.86	0.55	0.53	0.49	0.48
21	0.56	0.99	0.95	0.85	0.55	0.55	0.51	0.49
20	0.69	1	0.95	0.83	0.92	0.82	0.73	0.68
19	0.69	0.98	0.9	0.86	0.97	0.83	0.8	0.68
18	0.7	0.98	0.87	0.78	0.92	0.81	0.81	0.68
17	0.66	2.48	2.04	1.7	1.32	1.24	0.99	0.75
16	0.66	2.03	1.97	1.7	1.31	1.18	0.98	0.75
15	0.64	2.14	2.02	1.69	1.3	1.22	1.04	0.76
14	0.64	2.53	2.36	1.98	1.54	1.62	1.38	0.86
13	0.64	3.35	3.03	2.49	2.08	2.11	1.84	1.11
12	0.64	3.47	3.36	2.99	2.55	2.57	2.12	1.28
11	0.64	3.51	3.42	3.28	2.89	2.97	2.6	1.51
10	0.64	3.42	3.41	3.38	3.15	3.23	2.86	1.7
9	0.64	3.52	3.43	3.43	3.31	3.33	3.06	1.8
8	0.64	3.44	3.42	3.42	3.38	3.4	3.2	1.95
7	0.64	3.38	3.4	3.41	3.39	3.41	3.29	2.04
6	0.64	3.38	3.42	3.42	3.38	3.37	3.33	2.15
5	0.64	3.5	3.43	3.37	3.33	3.32	3.34	2.21
4	0.64	2.88	3.15	3.2	3.27	3.28	3.32	2.23

Table A7.2 Swallowholes Borehole BHDT results.

Depth mbfl	Background conductivity mS/cm	Conductivity mS/cm					
		1 min	20 mins	45 mins	85 mins	190 mins	370 mins
46.6	0.54	4.83	3.41			2.49	0.62
46	0.54	4.45	2.85	2.87	2.87	2.45	0.61
45	0.54	2.86	2.87	2.88	2.87	2.35	0.58
44	0.54	2.8	2.92	2.87	2.86	2.27	0.58
43	0.54	2.97	2.96	2.79	2.56	2.11	0.56
42	0.54	2.96	2.81	2.52	2.51	1.84	0.56
41	0.54	2.99	2.82	2.58	2.53	1.51	0.56
40	0.54	2.8	2.83	2.52	2.5	1.25	0.56
39	0.54	2.85	2.85	2.53	2.47	1.01	0.56
38	0.54	2.8	2.86	2.53	2.43	0.86	0.56
37	0.54	2.8	2.79	2.49	2.37	0.78	0.55
36	0.54	2.91	2.47	2.53	2.33	0.73	0.55
35	0.54	2.83	2.47	2.51	2.29	0.69	0.55
34	0.54	2.69	2.51	2.47	2.25	0.66	0.55
33	0.54	2.34	2.5	2.45	2.14	0.63	0.55
32	0.54	2.52	2.55	2.36	2.28	0.63	0.55
31	0.549	2.73	2.68	2.48	2.08	0.62	0.55
30	0.549	2.92	2.69	2.56	1.17	0.61	0.55
29	0.549	2.76	2.68	2.56	1.45	0.6	0.55
28	0.549	2.63	2.56	2.56	1.13	0.59	0.55
27	0.549	2.77	2.5	2.55	0.98	0.59	0.55
26	0.549	2.68	2.53	2.42	0.85	0.59	0.55
25	0.549	2.4	2.54	2.04	0.79	0.58	0.55
24	0.549	2.51	2.36	1.69	0.73	0.58	0.55
23	0.549	2.62	2.01	1.34	0.69	0.57	0.55
22	0.549	2.64	1.67	1.07	0.66	0.57	0.55
21	0.549	2.4	1.35	0.92	0.64	0.57	0.55
20	0.549	2.19	1.07	0.84	0.63	0.57	0.55
19	0.549	1.82	1.03	0.79	0.64	0.57	0.55
18	0.549	1.79	1.14	0.76	0.71	0.6	0.55
17.5	0.549	1.91		0.81	0.75		0.55

Table A7.3 Wykeham Village Hall Borehole BHDT results.

Depth mbfl	Background conductivity mS/cm	Conductivity mS/cm						
		10 min	20 mins	40 mins	125 mins	260 mins	445 mins	next am
46.6	0.54	7.6	5.07	9.35	5.05	10	7.63	7.8
46	0.54	3.2	3.25	3.26	3.37	3.43	3.46	3.48
45	0.54	3.42	3.29	3.32	3.33	3.44	3.42	3.38
44	0.54	3.65	3.44	3.41	3.38	3.45	3.42	3.39
43	0.54	3.45	3.42	3.43	3.42	3.46	3.43	3.39
42	0.54	3.42	3.43	3.45	3.44	3.48	3.44	3.39
41	0.54	3.47	3.47	3.48	3.46	3.42	3.45	3.39
40	0.54	3.36	3.48	3.44	3.39	1.33	3.37	3.27
39	0.54	2.89	3.16	2.6	2.36	0.61	1.23	1.92
38	0.54	0.92	0.76	0.77	0.65	0.6	0.62	0.59
37	0.54	0.8	0.74	0.69	0.63	0.6	0.59	0.56
36	0.54	0.76	0.73	0.69	0.62	0.6	0.59	0.56
35	0.54	0.76	0.74	0.67	0.61	0.61	0.58	0.56
34	0.53	0.79	0.88	0.68	0.62	0.61	0.59	0.56
33	0.49	0.75	1.13	0.72	0.65	0.7	0.61	0.57
32	0.49	1.5	1.72	1.11	0.9	0.84	0.76	0.66
31	0.48	2.23	2.72	1.57	1.2	0.14	0.98	0.75
30	0.48	2.65	2.23	2.06	1.5	1.32	1.21	0.88
29	0.48	2.71	2.47	2.26	1.77	1.6	1.39	1.04
28	0.48	2.71	2.64	2.557	2.2	1.82	1.57	1.19
27	0.48	2.72	2.71	2.67	2.37	2.02	1.82	1.28
26	0.48	2.77	2.73	2.74	2.46	2.18	2	1.43
25	0.48	2.82	2.76	2.76	2.57	2.35	2.1	1.51
24	0.48	2.75	2.74	2.76	2.68	2.48	2.25	1.6
23	0.48	2.71	2.74	2.77	2.72	2.58	2.35	1.74
22	0.48	2.74	2.75	2.77	2.75	2.66	2.47	1.83
21	0.48	2.83	2.78	2.77	2.76	2.71	2.55	1.94
20	0.48	2.73	2.74	2.77	2.74	2.74	2.61	2.02
19	0.48	2.66	2.69	2.7	2.71	2.74	2.65	2.1
18	0.48	2.73	2.68	2.68	2.68	2.74	2.68	2.19
17	0.48	2.52	2.66	2.63	2.65	2.7	2.67	2.25
16	0.48	2.49	2.58	2.61	2.61	2.66	2.67	2.31
15	0.48	2.65	2.57	2.6	2.6	2.66	2.66	2.37
14	0.48	2.73	2.6	2.6	2.6	2.65	2.66	2.41
13	0.48	2.53	2.59	2.61	2.6	2.66	2.66	2.46
12	0.48	2.56	2.6	2.62	2.62	2.66	2.66	2.49
11	0.48	2.66	2.63	2.64	2.61	2.66	2.66	2.53
10	0.48	2.73	2.65	2.65	2.64	2.67	2.67	2.55
9	0.48	2.67	2.66	2.67	2.65	2.68	2.66	2.57
8	0.48	2.59	2.65	2.67	2.66	2.68	2.67	2.58
7	0.48	2.69	2.66	2.67	2.65	2.68	2.67	2.6
6	0.48	2.73	2.66	2.67	2.64	2.68	2.66	2.6
5	0.48	2.65	2.65	2.66	2.63	2.67	2.65	2.61
4	0.48	2.62	2.64	2.63	2.6	2.65	2.62	2.6
3	0.48	2.65	2.61	2.59	2.55	2.53	2.58	2.6
2	0.48	2.54	2.44	2.5	2.48	2.43	2.52	2.59
1.2	0.48	1.76	2.22	2.37	2.41	2.49	2.5	

Table A7.4 Tetherings Plump Borehole BHDT results

Depth mbfl	Background conductivity mS/cm	Conductivity mS/cm					
		1 min	5 mins	15 mins	50 mins	110 mins	330 mins
25	0.6	2.68	2.58	2.58	2.68	2.57	1.92
26	0.6	2.08	2.21	2.3	2.56	2.49	1.68
27	0.6	3.03	2.97	2.94	2.78	2.07	1.56
28	0.6	3.07	2.99	2.89	2.78	2	1.31
29	0.6	3	3.1	3.05	2.74	1.92	1.07
30	0.6	3.2	2.69	3.63	2.34	1.32	0.81
31	0.6	2.35	1.81	2.8	3.18	1.6	0.69

Table A7.5 Derwent Ford Borehole BHDT results

Depth mbfl	Background conductivity mS/cm	Conductivity mS/cm						
		1 min	20 mins	44 mins	71 mins	136 mins	257 mins	1275 mins
6	0.257	0.297	0.27	0.289	0.282	0.282	0.278	0.288
10	0.248	0.263	0.271	0.264	0.264	0.266	0.267	0.272
12	0.248	0.271	0.272	0.272	0.271	0.268	0.267	0.27
14	0.249	0.423	0.408	0.434	0.42	0.426	0.427	0.41
14.5	0.249	0.567	0.58	0.562	0.564	0.55	0.533	0.511
15	0.249	0.716	0.615	0.539	0.532	0.506	0.488	0.475
15.2	0.393	0.743	0.614	0.547	0.529	0.504	0.486	0.47
15.4	0.46	0.743	0.573	0.536	0.521	0.499	0.481	0.469
15.6	0.464	0.723	0.549	0.519	0.514	0.496	0.478	0.469
15.8	0.466	0.657	0.533	0.516	0.509	0.493	0.478	0.469
16	0.466	0.638	0.527	0.516	0.509	0.493	0.478	0.469
16.2	0.466	0.615	0.525	0.514	0.509	0.493	0.478	0.469
16.4	0.466	0.601	0.526	0.512	0.51	0.493	0.478	0.469
16.6	0.466	0.595	0.523	0.512	0.509	0.494	0.478	0.469
16.8	0.466	0.594	0.521	0.512	0.511	0.494	0.478	0.469
17	0.466	0.585	0.511	0.514	0.498	0.494	0.478	0.468
17.2	0.466	0.648	0.571	0.532	0.533	0.517	0.49	0.47
17.4	0.466	0.795	0.654	0.617	0.612	0.553	0.502	0.475
17.6	0.466	0.922	0.789	0.682	0.708	0.602	0.518	0.478

Table A7.6 Brompton Dale Shallow Borehole BHDT results

Depth mbfl	Background conductivity mS/cm	Conductivity mS/cm						
		1 min	15 mins	32 mins	67 mins	115 mins	175 mins	267 mins
6	0.242	0.247	0.246	0.246	0.246	0.247	0.247	0.247
10	0.243	0.247	0.247	0.247	0.246	0.247	0.248	0.249
20	0.245	0.252	0.254	0.255	0.257	0.263	0.268	0.276
30	0.287	0.309	0.308	0.31	0.316	0.325	0.327	0.357
40	0.46	0.535	0.531	0.522	0.512	0.494	0.486	0.481
41	0.463	0.57	0.579	0.563	0.537	0.509	0.499	0.487
42	0.468	0.613	0.612	0.599	0.565	0.527	0.51	0.496
43	0.461	0.658	0.645	0.633	0.589	0.54	0.524	0.507
44	0.463	0.708	0.692	0.67	0.605	0.559	0.532	0.511
44.2	*0.462*	0.735	0.7	0.672	0.608	0.564	0.532	0.511
44.4	*0.462*	0.74	0.708	0.681	0.614	0.561	0.531	0.512
44.6	*0.462*	0.752	0.723	0.682	0.616	0.563	0.535	0.514
44.8	*0.462*	0.745	0.735	0.69	0.621	0.57	0.537	0.512
45	0.461	0.758	0.741	0.695	0.624	0.574	0.539	0.516
45.2	0.466	0.856	0.76	0.697	0.637	0.579	0.54	0.517
45.4	0.465	0.856	0.763	0.708	0.656	0.62	0.548	0.52
45.6	0.45	0.809	0.795	0.735	0.706	0.664	0.571	0.554
45.8	0.45	0.815	0.795	0.736	0.716	0.665	0.57	0.555
46	0.45	0.814	0.795	0.736	0.716	0.665	0.57	0.555
46.2	0.449	0.814	0.795	0.736	0.716	0.665	0.57	0.555
46.4	0.449	0.813	0.795	0.736	0.715	0.665	0.57	0.555
46.6	0.449	0.813	0.795	0.736	0.715	0.665	0.57	0.554
46.8	0.449	0.812	0.795	0.736	0.715	0.664	0.569	0.554
46.95	*0.449*	0.81	0.794	0.735	0.714	0.663	0.569	0.553

Table A7.7 Brompton Dale Deep Borehole BHDT results

Time 21st May 2002	Mins after injection	Concentration ppt	Concentration minus background
11.5	110	2627	0
12.12	132	2619	-8
12.3	150	2620	-7
12.45	165	2623	-4
13.03	183	2618	-9
13.13	193	2621	-6
13.24	204	2635	8
13.3	210	2675	48
13.42	222	2949	322
13.55	235	3407	780
14.1	250	3773	1146
14.3	270	3665	1038
14.45	285	3491	864
15	300	3454	827
15.1	310	3418	791
15.24	324	3275	648
15.4	340	3105	478
16	360	2932	305
16.2	380	2850	223
16.4	400	2759	132
16.57	417	2731	104
17.22	442	2702	75
17.41	461	2684	57
18	480	2675	48
18.2	500	2667	40
19.02	542	2647	20
19.32	572	2648	21
20	600	2637	10
20.35	635	2638	11
21	660	2632	5
21.36	696	2628	1
22	720	2632	5
23	780	2630	3
2.45	1005	2632	5
7	1260	2633	6
8	1320	2635	8
9	1380	2640	13

Table A7.8 May 21st 2002 swallowholes to Irton Fluorescein tracer test data measured at Irton New Well

Date	Hours after injection	Background concentration (ppt)	Measured Concentration (ppt)	Photine (ppt)	Passive detector score
09-Jul	0	8.997	9.107	0.11	0
10-Jul	24	8.997	9.356	0.359	0
11-Jul	48	8.997	9.627	0.63	0
12-Jul	72	8.997	15.94	6.943	3
13-Jul	96	8.997	9.092	0.095	0

Table A7.9 July 9th 2002 Seavegate Gill to McCains Photine tracer test data measured at McCains.

		Hours following tracer injection				
	Background	6	24	48	72	96
Augmentation 25m	0	5	4	3	3	1
Augmentation 35m	0	4	3	1	0	0
Augmentation 45m	0	4	3	1	0	0
Irton	0	0	0	0	0	0
Derwentdale Farm North	0	0	0	0	0	0
Wykeham	0	0	0	0	0	0
Tetherings Plump	0	0	1	1		0
Seavegate Gill	0	0	0	0	1	0

Table A7.10 14th April 2003 Passive cotton-wool detector results for Photine injected in to the Swallowholes borehole.

Date	Time	time after injection minutes	SF6 Picograms per kilogram
31/07/2004	14	1662	0.717511389
01/08/2004	14	3112	1.195979197
02/08/2004	13	4507	1.214469749
03/08/2004	13	5952	2.527306505
04/08/2004	12	7342	1.040380857
05/08/2004	9	8562	1.455048468
06/08/2004	14	10332	0.899915921
07/08/2004	10	11517	0.561404896
08/08/2004	13	13117	0.898179308
09/08/2004	13	14602	0.177843767
11/08/2004	16	17642	1.244647678
16/08/2004	15	24792	0.803625888
19/08/2004	14	29007	1.205519677
24/08/2004	15	36307	0.538434606
03/09/2004	12	50522	1.650326742

Table A7.11 SF_6 measured at Cayton Carr House Lane borehole

Date	Time	time after injection minutes	SF6 Picograms per kilogram
31/07/2004	14	1647	1.106071173
01/08/2004	14	3099	2.314475679
02/08/2004	13	4490	5.580405813
03/08/2004	13	5937	4.184603166
04/08/2004	13	7362	1.174364711
06/08/2004	14	10317	0.769959693

Table A7.12 SF_6 measured at Cayton Station Road borehole

Date	Time	time after injection minutes	SF6 Picograms per kilogram
	10	0	0.585505234
	13	169	2547.544081
	13	204	30740.93147
	14	244	194807.3823
	15	277	483058.9748
	15	307	750136.431
	16	352	468672.2891
	16	382	434666.4575
	17	412	200054.9048
	17	437	138937.4651
	18	481	106745.9709
	19	511	37282.55448
	19	543	26826.51361
	20	612	16198.9907
	22	687	13087.98435
31/07/2004	0	845	7859.862192
	2	947	7396.126281
	5	1157	4755.977407
	9	1381	7681.32528
	14	1675	1826.349337
	18	1906	2554.595369
	21	2077	1472.072774
01/08/2004	8	2748	1650.063757
	12	3012	1701.768067
	19	3397	1511.101246
02/08/2004	9	4263	82.56012279
	16	4694	923.9324887
03/08/2004	9	5672	658.5100919
	14	5984	988.9873811
	20	6339	1017.331544
04/08/2004	9	7136	752.9646178
	13	7392	650.3337412
05/08/2004	9	8577	489.1548553
	19	9180	427.9391828
06/08/2004	14	10302	417.3824466
07/08/2004	11	11547	320.0387334
08/08/2004	13	13127	199.2213918
09/08/2004	14	14607	200.6109023
10/08/2004	13	15987	61.95868686
11/08/2004	12	17367	144.9603468
13/08/2004	12	20247	159.3364373
16/08/2004	20	25047	121.5843496
19/08/2004	13	28947	123.1617288
24/08/2004	17	36387	82.19773604
29/08/2004	10	43167	70.95418592
03/09/2004	12	50487	56.18374373
12/09/2005	15	63657	42.958

Table A7.13 SF6 measurements made at Irton following injection to the Forge Valley swallowholes at c. 11am on the 30th of July, 2004.

Date	Time	time after injection minutes	SF6 Picograms per kilogram
01/08/2004	14	3137	0.631213986
02/08/2004	14	4552	3.899522114
03/08/2004	14	5967	0.480936416
03/08/2004	21	6387	1.310462565
04/08/2004	9	7112	0.852773606
04/08/2004	13	7377	0.772949823
05/08/2004	9	8547	0.496579173
05/08/2004	13	8837	0.866004456
05/08/2004	18	9120	0.550173638
06/08/2004	10	10083	0.592335559
07/08/2004	10	11532	0.883274216
09/08/2004	13	14582	0.20590437
11/08/2004	16	17622	0.587385046
16/08/2004	15	24777	0.748071949

Table A7.12 SF_6 measured at McCains borehole

Date	Hour	Minute	Minutes after injection	SF6 pg/kg
30/07/2004	12	50	137	301.671
	19	4	511	580.092
31/07/2004	0	25	832	5733.615
	2	38	965	30278.547
	5	35	1142	90696.921
	9	50	1397	87095.781
	14	41	1688	58987.815
	18	31	1918	18300.575
	18	31	1918	16782.532
	21	25	2092	6816.056
01/08/2004	8	37	2764	1422.415
	8	37	2764	2347.245
	13	0	3027	654.926
	19	25	3412	778.593
02/08/2004	9	55	4282	849.070
	17	23	4730	774.474
03/08/2004	9	20	5687	241.328
	20	25	6352	395.453
04/08/2004	14	5	7412	247.285
05/08/2004	9	53	8600	203.396
	19	50	9197	154.648
06/08/2004	15	30	10377	141.473
09/08/2004	14	20	14627	127.368
11/08/2004	12	25	17392	90.414
16/08/2004	14	40	24727	59.653
19/08/2004	13	0	28947	43.084
24/08/2004	15	10	36277	22.552
29/08/2004	10	15	43182	17.863
03/09/2004	11	55	50482	14.563
09/09/2005	12	45	59172	20.161

Table A7.13 SF_6 measured at Derwentdale Farm North borehole

Date	Hour	Minute	Mins after injection	SF6 pg/kg
31-Jul	14	50	1697	1.983
31-Jul	18	40	1927	0.491
03-Aug	20	35	6362	1.498
06-Aug	15	20	10367	1.312
08-Aug	17	25	13372	0.504
11-Aug	12	50	17417	0.594
16-Aug	15	10	24757	1.327
19-Aug	13	10	28957	1.427
24-Aug	15	20	36287	2.000
03-Sep	12	20	50507	16.089
05-Sep	15	50	53597	13.833
09-Sep	13	0	59187	33.710

Table A7.14 SF6 measured at Derwentdale Farm South borehole.

Date	Hours	Mins	Minutes after injection	ppt
30/07/2004	11	8	0	0
30/07/2004	13	22	134	50
30/07/2004	13	57	169	1097
30/07/2004	14	37	209	2326
30/07/2004	15	10	242	2240
30/07/2004	15	40	272	1058
30/07/2004	16	25	317	522
30/07/2004	16	55	347	349
30/07/2004	17	25	377	200
30/07/2004	17	50	402	150
30/07/2004	18	34	446	124
30/07/2004	19	4	476	95
30/07/2004	19	36	508	67
30/07/2004	20	45	577	53
30/07/2004	22	0	652	67
30/07/2004	24	38	810	37
30/07/2004	26	20	912	17
30/07/2004	29	50	1122	10
30/07/2004	33	34	1346	44
30/07/2004	38	28	1640	5

Table A7.15 Fluorescein measured at Irton 30/7/2004

BH	Jan-97	Feb-97	May-97	Jul-97	Sep-97	Oct-97	Nov-97	Dec-97	Feb-98	Mar-98	May-98	Jun-98
HA5	24.75		24.77	24.81	24.78	24.81	24.79	24.83	24.85	25.01	24.95	24.95
HA9	24.4		24.38	24.4	24.4	24.4	24.4	24.42	24.5	24.56	24.51	24.5
HA10	24.07		24.05	23.99	24.09	24.09	24.06	24.12	24.16	24.25	24.19	
SC10	25.11	25.11	25.09	25.01	25.15	25.07	25.12	25.13	25.04	24.81	24.88	24.54
SC25 LOWER	25.65	25.65	25.29	25.6	25.69	25.62	25.58	25.67	25.7	25.8	26	25.61
SC26 UPPER	24.06	24.06	24.03	24.01	23.98	24.05	24.05	24.01	24.02	23.98	24.04	23.81
SC26 LOWER	24.14	24.14	24.06	24.12	24.06	24.13	24.05	24.14	24.11	24.31	24.34	24.12
SC32	25.69		25.66	25.7	25.64	25.62	25.68	25.66	25.63	25.62	25.7	25.61
SC33	25.89		25.85	25.82	25.82	25.87	25.88	25.86	25.83	25.89	25.95	25.96
SC35	26.08		26.01	26.09	26.04	26.03	26.03	26.03	25.99	26.07	26.13	26.06
SC49	23.69	23.69	23.69	23.71	23.63	23.72	23.68	23.65	23.61	23.62	23.67	23.55
SC52	23.6	23.6	23.61	23.6	23.53	23.66	23.58	23.61	23.6	23.79	23.82	23.74
SC53	23.59	23.59	23.57	23.62	23.64	23.64	23.59	23.61	23.65	24.03	24.04	23.9
SC54	23.45	23.45	23.43	23.42	23.37	23.48	23.44	23.42	23.51	23.78	23.78	23.61
SC57	27.06		27	26.98		27.02	27.03	26.99	27.02	26.94	27.03	26.85
SC58	26.77		26.78	26.75		26.75	26.75	26.78	26.74	26.8	26.83	26.77
SC59	27.16	27.16	27.13	27.17	27.16	27.17	27.14	27.17	27.13	27.13	27.14	26.96
SC60	27.58		27.56	27.58	27.56	27.6	27.58	27.77	27.79	27.94	27.88	27.29
SC61	26.74		26.69	26.74	26.73	26.74	26.71	26.75	26.8	26.86	26.84	26.85
SC62	27.67		27.56	27.56	27.56	27.55	27.58	27.65	27.7	27.8	27.8	27.73
SC63	27.34		27.35	27.32	27.38	27.44	27.37	27.39	27.52	27.6	27.55	27.37
SC64	27.17		27.16	27.21	27.17	27.21	27.15	27.14	27.2	27.24	27.25	26.94
SC65	27.29		27.28	27.26	27.38	27.3	27.31	27.43	27.51	27.61	27.58	26.94
SC68 UPPER		24.58	23.62	23.67					23.69		23.64	23.62
SC68 LOWER		24.58	23.85	23.87					23.89		23.85	23.88
SC69 UPPER	23.36	23.36	23.38	23.59	23.43	23.42	23.41	23.43	23.49	23.54	23.59	23.53
SC69 LOWER	23.85	23.85	23.97	24.26	24.02	24.01	24	23.99	23.94	24.09	24.13	24.03
SC70 UPPER	24.37	24.37	24.41	24.38	24.46	24.45	24.44	24.42	24.55	24.67	24.73	24.68
SC70 LOWER	24.33	24.33	24.37	24.34	24.34	24.36	24.38	24.38	24.45	24.51	24.59	24.46
SC71 UPPER		25.97	24.82	24.71	24.85	24.78	24.83		24.83	24.84	24.88	24.82
SC71 LOWER		25.97	25.06	24.82	25.09	25.06	25.07	25.04	24.94	25	25.04	24.96
SC72 UPPER	25.34	25.34	25.22	25.28	25.19	25.23	25.25	25.19	25.07	25.09	25.16	25.11
SC72 LOWER	25.38	25.38	25.43	25.35	25.37	25.47	25.45	25.43	25.38	25.32	25.37	25.34
SC73 UPPER	25.59	25.59	25.69	25.89	25.66	25.73	27.71	25.69	25.86	26.03	26.09	26.06
SC73 LOWER	25.95	25.95	26	26.26	25.98	26.03	26.02	26.06	25.98	26.46	26.49	26.46

Appendix 8a Seamer Carr groundwater level data compiled from (compiled from SECOR (1998), Delaney (2000), Golders (2000) and additional data supplied by Yorwaste Ltd. (personal communication).

Borehole	Avg. Leachate level 1993 - 2002 maOD
SC36	27.17
SC37	27.22
SC40	26.00
SC41	31.40
SC42	27.60
SC45	27.98
SC46	27.62
SC47	27.94
SC48	27.42
SC50	28.26
SC51	28.64
SC76	29.75
SC77	30.53
SC78	28.25
SC79	30.08
SC80	28.46
SC81	30.25
SC82	30.29
SC83	27.58
SC84	29.46
SC85	29.58
SC86	29.14

Appendix 8b Leachate levels for waste monitoring boreholes, Seamer Carr landfill. Compiled from data given by Golder Associates (2000), SECOR (1998), Delaney (2000), Golders (2000) and additional data supplied by Yorwaste Ltd. and the Environment Agency (personal communication).